Bacterial and Fungal composition of *Sorghum bicolor*: A Metagenomics and Transcriptomics analysis using Next-Generation Sequencing

by

KEDIBONE MASENYA

submitted in accordance with the requirements for
the degree of

DOCTOR OF PHILOSOPHY

in the subject

LIFE SCIENCES

at the

UNIVERSITY OF SOUTH AFRICA

SUPERVISOR: DR D.J.G. REES

CO-SUPERVISOR: PROF. M. TEKERE

September 2020

DECLARATION

Name: Kedibone Masenya
Student number: 56600126
Degree: Doctor of Philosophy in Life Sciences

Thesis title: **Bacterial and Fungal composition of *Sorghum bicolor*: A Metagenomics and Transcriptomics analysis using Next- Generation Sequencing**

I declare that the above thesis is my own work and that all the sources that I have used or quoted have been indicated and acknowledged by means of complete references.

I further declare that I submitted the thesis to originality checking software and that it falls within the accepted requirements for originality.

I further declare that I have not previously submitted this work, or part of it, for examination at Unisa for another qualification or at any other higher education institution

SIGNATURE

23 September 2020
DATE

DEDICATION

I dedicate this thesis

To my mom, Ms Rebecca Masenya

For her steadfast support, love, advice and encouragement which have been invaluable to me

Philippians 1:6

Being confident of this very thing, that he who began a good work in you will complete it until the day of Christ Jesus.

ACKNOWLEDGEMENTS

My utmost sincere gratitude goes to God the Creator and the Almighty, to whom I owe my very existence, for being with me and keeping me safe from conception to date. This PhD has been very challenging yet an incredible journey and many people have made this trip enjoyable and possible.

A big thank you to my supervisor Dr DJG Rees, for his supervision, meticulous editorial skills and for introducing me to next generation sequencing and bioinformatics. Thank you for giving me the opportunity to do this degree and for the resources. Dr RE Pierneef for his great expertise that greatly assisted me at different stages of my research and mentorship. Prof Tekere her guidance and patience throughout this research.

To Agricultural Research Council- Biotechnology Platform (ARC-BTP) staff and students, especially the big lab, I thank you for your continued support. I will also like to thank Dr Minique De Castro aka Ouma for her valued contributions and continued encouragement throughout this PhD, Dr Thulani Makhalanyane for his meticulous editorial skills.

I would also like to thank my family members; this would not have been possible without you, my mom, who constantly reminded me that she didn't raise a quitter and for loving me immensely. My sister Mokgadi and my brother Mathi, my niece Lehlogonolo and my nephews, Thato and Nyaku, for encouragement and continued support. Thank you for understanding in all those times I needed to come home and be with you and it was just impossible. I would like to offer special thanks to my late brother Given, who, although now no longer with us, has supported me throughout the PhD journey .

All my friends and well-wishers, I am grateful for the humour, productive and inspiring conversations we had. Finally, my sincere gratitude goes to Agricultural Research Council – Professional Development Programme (ARC-PDP), National Research Foundation (NRF) and UNISA for financial assistance.

ABSTRACT

Sorghum crop has become attractive to breeders due to its drought tolerance, and many uses including a human food source, animal feed, industrial fibre and bioenergy crop. Sorghum, like any other plant, is a host to a variety of microbes that can have neutral, negative or positive effects on the plant. While the majority of microorganisms are beneficial, pathogens colonize plant tissues and overwhelm its defence mechanisms. This colonization is a direct threat to the sorghum productivity. The development of microbiome-based approaches for sustainable crop productivity and yield is hindered by a lack of understanding of the main biotic factors affecting the crop microbiome. Metabarcoding has proven to be a valuable tool which has been widely used for characterizing the microbial diversity and composition of different environments and has been utilized in many research endeavours. This study analyses the relationship between the microbiota and their response to natural pathogen infection in sorghum disease groups (R, MR, S and HS) and identifies the most dominant pathogen in the highly susceptible disease group. The study also, assesses the spore viability through the use of the automated cell counter and confirms *Fusarium graminearum* (dominant pathogen linked to the HS disease group) through sequencing of the marker genes, to subsequently characterize pathways likely to be involved in pathogen infection resistance. To achieve the objectives, a combination of 16S rRNA (V3/V4 regions) and ITS (ITS1/ITS4) of the internal transcribed spacer regions were amplified and sequenced using NGS technologies to study the microbiota in response to natural infection. Additionally, comparative transcriptional analysis of sorghum RILs in response to *Fusarium graminearum* infection was conducted through RNA-Seq.

Upon natural infection, the foliar symptoms assessment of the RILs was conducted and four disease groups; resistant (R), moderately resistant (MR), susceptible (S) and highly susceptible (HS) were designated. The results of the present metabarcoding study indicate that resistant sorghum leaves (R group) supported a large diversity of fungal and bacterial microbes. The genera *Methylorubrum*, *Enterobacter* and *Sphingomonas* with reported plant growth promoting traits were more abundant and highly enriched in the R and MR group, with members of the latter genus significantly enriched in the R group. The resistant fungal group had a majority of OTUs showing similarity to well-known plant growth-promoting fungal

genus including *Papiliotrema* (*Tremellaceae* family), which are known biocontrol agents. The yeast *Hannaella* was also highly linked with the resistant plants. Some *Hannaella* species are known to produce indole acetic acid (IAA) for promoting plant growth.

Metabarcoding was also used to assess the major potential disease-causing taxa associated with the highly diseased group. It identified fungal pathogenic species, that have not previously been identified as pathogens of sorghum such as *Ascochyta paspali* and *Ustilago kamerunensis* (which are known pathogenic fungi of grass species) and were associated with the susceptible disease groups (S and HS). These analyses revealed the potential sorghum fungal pathogen *Epicoccum sorghinum*, and was highly linked with the S disease group. It further expanded the identification of a reportedly economically importance species causing sorghum related diseases *Fusarium graminearum* (anamorph *Gibberella zeae*). This species has also been identified in this study to be highly associated with the RILs showing major disease symptoms.

Fusarium graminearum a significant pathogen in winter cereals and maize has been associated with stalk rot of sorghum and sorghum grain mould. The presence of *Fusarium graminearum* in sorghum can be a toxicological risk, since this species has the potential to produce mycotoxins. It was further shown that natural pathogen infection results in distinct foliar microbial communities in sorghum RILs. The co-occurrence taxa represented by Tremellomycetes and Dothiomycetes fungal classes and *Bacillaceae* and *Sphingomonadaceae* bacterial family had more central roles in the network. The modules which are located centrally on the network have been expected to play important 'topological roles' in interconnecting pairs of other fungal and bacterial taxa in the symbiont–symbiont co-occurrence network. These taxa having a central role, are considered to be keystone microbes, and have been suggested to be drivers of microbiome structure and functioning. The results of bacterial and fungal community composition, community co-occurrences further suggested the importance of keystone taxa which may disproportionately shape the structure of foliar microbiomes. The foliar disease symptom assessments revealed that sorghum RIL 131 was highly diseased and RIL 103 did not show any visible disease symptoms and were subsequently used for transcriptomic analysis.

Gene expression patterns were studied between the identified RIL that did not show visible symptoms (resistant RIL no 103) and the RIL that showed major disease symptoms (susceptible RIL no 131). *Fusarium graminearum* the dominant potential pathogen found in this study to be associated with the highly susceptible plants was used to inoculate RILs at seedling stage in a greenhouse and samples were collected in triplicates at 24 hours post infection (hpi), 48 hpi, 7 days post infection (dpi) and 14 dpi. Prior to that, ITS and UBC genes confirmed the identity of *Fusarium graminearum*, and the automated haemocytometer confirmed the cell/spore viability. Using RNA-Seq analysis it was shown that the resistant RIL had defence related pathways from early response (24- 48 hpi) to late response (7-14 dpi). And the more the infection progressed, the more the defence related genes were up-regulated in terms of fragments per kilobase of exon model per million reads mapped (FPKM) and False Discovery Rate (FDR ≤ 0.05) values.

Transcriptome time series expression profiling was used to characterize the plant response to *Fusarium graminearum* with the Dirichlet Process Gaussian Process mixture model software (DPGP) in susceptible and resistant RILs. The susceptible RIL (number 131) transcriptional response upon *Fusarium graminearum* infection presented differences of the closely related clustered expression profiles across all timepoints in both RILs. Group 2 exclusively clustered the genes encoding the sesquiterpene metabolism pathway, which is one of the major physiological change occurring in response to fungal infection and has been previously reported to produce the mycotoxins associated with Fusarium head blight (FHB) of cereals. This pathway presented an increase from the initial infection phase to the late infection phase in group 4, the genes encoding starch sucrose, metabolism and cyanoamino acid pathways presented a pattern that had a sharp decline from 48 hpi -14 dpi (at a later stage of infection). This could suggest that, as the time progresses in the susceptible RIL the pathways which are important in plant defence declines at a late infection stage. Group 3 presented a pattern increase of the 5-lipoxygenase (LOX 5) gene expressed from 48 hpi-14 dpi timepoints. The loss and silencing of LOX5 function have in the past described to be linked with enhanced disease resistance. In this study the LOX5 was expressed and this could suggest that LOX5 might have a function as a susceptibility factor in disease caused by *Fusarium graminearum* in sorghum RILs. CBL-interacting protein kinase 6 (CIPK6) gene was also associated with this

group. This gene has been associated with negative regulation of immune response to *Pseudomonas syringae* in *Arabidopsis* as plants overexpressing CIPK6 were more susceptible to *Pseudomonas syringae*.

Transcriptional response of a resistant RIL (number 103) to infection with *Fusarium graminearum* presented an increase in genes encoding metabolic and biosynthesis of metabolites pathways in group 1 and group 4 at early infection phase and a sharp decline in the late infection phase. An increase in the genes encoding pathways in earlier infection state could suggest the establishment of a beneficial energy balance for defence. Additionally, genes encoding phenylpropanoid (PAL), galactose and glycolysis pathway were amongst the genes increased at early stages of infection in group 1. Sugar can play a significant role in resistance to fungal pathogens through phenylpropanoid metabolism stimulation, and previous studies showed that the phenylpropanoid pathway could play a role in resistance of wheat to *Fusarium graminearum* and deoxynivalenol.

Overall, this study represents a first step in understanding the molecular mechanisms involved in resistance to *Fusarium graminearum*. This analysis has also identified the reported beneficial microbes and defence related genes and pathways. Together, the current findings suggest that different 'resident' consortia found in naturally infected and uninfected sorghum plants may be viable biocontrol and plant-growth promoting targets. Cultivation studies may shed light on the nature of the putative symbiotic relationships between bacteria and fungi. These results have consequences for crop breeding, and the analysis of microbial diversity and community composition can be useful biomarkers for assessing disease status in plants. The transcriptome and metabarcoding data generated will help guide further research to develop novel strategies for management of disease in sorghum RILs through the integrative approach considering both beneficial microbes and defence related genes. This provides the baseline information and will positively impact in the development of *Fusarium graminearum* resistant genotypes in future through the integration/incorporation of beneficial microorganisms (bacteria and fungi) and resistant genes in breeding strategies.

Keywords: Sorghum; Microbiome; Metabarcoding; Network, RIL; Next generation sequencing; Differential gene expression; Transcriptomics

RESEARCH OUTPUTS

Research articles

Masenya, K.; Tekere, M.; Thompson, G.; Makhalanyane, T., Pierneef, R., Rees, J. (2020). Pathogen infection influences a distinct microbial community composition in sorghum RILs. International Plant and Soil Journal. Accepted for publication.

Masenya, K.; Pierneef, R., Tekere, M., Rees, J (2020). Gene expression patterns in susceptible and resistant recombinant inbred line (RILs) in response to *Fusarium graminearum* infection across different time-points (2020). In preparation.

Conference presentations

Masenya, K.; Tekere, M.; Thompson, G.; Rees, J. Metagenomic analysis of bacteria harbored in sorghum leaf tissue. Agricultural Research Council Professional Development Conference, Pretoria, South Africa. 04-06th September 2018

Masenya, K.; Tekere, M.; Thompson, G.; Rees, J. Metagenomic signatures of bacteria harbored in sorghum leaf tissue. International Congress of Plant Pathology (ICPP), Boston, Massachusetts, USA, 29 July-03 August 2018.

Masenya, K.; Tekere, M.; Rees, J. Metagenomics Analysis of Bacteria in Sorghum Using Next Generation Sequencing. ICBMB 2017: 19th International Conference on Biotechnology and Molecular Biosciences Cape Town, South Africa. November 02-03, 2017

TABLE OF CONTENTS

LIST OF FIGURES

CHAPTER 2

CHAPTER 3

CHAPTER 4

CHAPTER 5

LIST OF TABLES

CHAPTER 2

CHAPTER 3

CHAPTER 4

CHAPTER 5

APPENDICES: LIST OF TABLES

CHAPTER 3

CHAPTER 5

LIST OF ABBREVIATIONS

ANOVA	Analysis of variance
ARC	Agricultural Research Council
BAM	Binary alignment map
BCA	Biological control agent
BLAST	Basic local alignment search tool
bp	Base pair
DEPC	Diethyl pyrocarbonate
DGEs	Differential gene expression
DNA	Deoxyribonucleic acid
dpi	Days post infection
ET	Ethylene
FAO	Food and Agriculture Organization
FAOSTAT	Food and Agriculture Organization of the United Nations Statistical Database
FHB	Fusarium head blight
GTF	General transfer format
hpi	Hours post infection
HS	Highly susceptible
IAA	Indole acetic acid

JA	Jasmonic acid
KEGG	Kyoto Encyclopedia of Genes and Genomes
KO	KEGG Orthology
MAMPS	Microbe associated molecular pattern
MR	Moderately resistant
NGS	Next generation sequencing
NMDS	Non-metric multidimensional scaling
PCR	Polymerase chain reaction
PNA	Peptide-nucleic acid
PTI	Pattern-triggered immunity
R	Resistant
RILS	Recombinant inbred lines
RLKS	Receptor-like kinase
RNA	Ribonucleic acid
RNA-SEQ	Ribonucleic acid sequencing
S	Susceptible
SA	Salicyclic acid
SAGL	Southern African Grain Laboratory
SAM	Sequence Alignment Map

SMRT	Single-molecule real-time sequencing
SNP	Single nucleotide polymorphism
SOLiD	Sequencing by oligonucleotide ligation and detection
TAE	Tris base, acetic acid and EDTA
TBE	Tris base, boric acid and EDTA
UBC	Ubiquitin C
UNISA	University of South Africa
USDA	United States Department of Agriculture.
ZEA	Zearalenone
TCB-B	1,2,3-trichlorobenzene

CHAPTER 1

General Introduction

1.1 CHAPTERS OUTLINE

This work is divided into 6 chapters. Each of the chapters are separately introduced and a reference list is provided at the end of all chapters.

Chapter 1: Introduction

This chapter will provide a general introduction and motivation for the study. The aims and objectives of the study are stated.

Chapter 2: Literature review

In this chapter literature related to the project is reviewed. A brief overview of sorghum taxonomy, importance, domestication and breeding. Plant created micro-environments will be reviewed extensively. A brief overview of plant microbe interactions will be reviewed looking specifically at bacterial/fungal interactions with plants. Both beneficial and non-beneficial plant microbe interactions will be reviewed. *Fusarium graminearum* will be reviewed. This will be followed by a broad description of metagenomic projects studying phyllosphere fungal and bacterial communities specifically. In the subsequent section, detailed information on next-generation sequencing will be introduced, followed by Illumina sequencing technology description specifically looking at sequencing the 16S rRNA and ITS gene in plants, transcriptomics and the bioinformatic analysis of next-generation sequencing data.

Chapter 3: Bacterial and fungal composition of sorghum in asymptomatic and symptomatic sorghum RILS

This chapter will describe the fungal and bacterial composition associated with *Sorghum bicolor* in order to determine whether the diversity is increasing or decreasing on both asymptomatic (resistant) and symptomatic (susceptible) sorghum RILS in response pathogen infection. The study also presents an assessment of the bacterial and fungal pathogenic taxa predominantly found in both the pathogen infected and the asymptomatic plants and the identification of the pathogenic taxa highly associated with the symptomatic plants.

Chapter 4: Molecular identification of *Fusarium graminearum* and cell viability

The confirmation of the species identity of the *Fusarium graminearum* of the strains used in this study, using molecular techniques; and the cell /spore viability conducted with the automated cell counter are presented.

Chapter 5: Comparative gene expression

This chapter presents the comparative transcriptome analyses of resistant and susceptible sorghum inbred lines in response to the fungal pathogen (*Fusarium graminearum*). The assessment of whether *Fusarium graminearum* induces specific defence-related genes is presented through an analysis of differential gene expression using whole transcriptome analysis with RNA-Seq.

Chapter 6: General discussion and conclusions

In this chapter the final conclusion and further prospects of this study is discussed.

1.2 GENERAL INTRODUCTION

Sorghum (*Sorghum bicolor*) is the fourth most important cereal crop cultivated in South Africa, after maize, wheat and barley (Beukes et al., 2017; Lateef et al., 2015). Climate change has sparked a renewed interest in sorghum, as it is a robust plant species that can tolerate drought, soil toxicities and a wide range of temperatures (Medraoui et al., 2007). It has remained a basic staple food for many rural communities. This is particularly the case in the more drought prone parts where this hardy crop offers better household food security (Mundia et al., 2019). Additionally this crop is a promising target for forage, grain, and as a potential energy plant for biofuel production (Gleadow et al., 2016). On a global scale, sorghum is the fifth most important cereal crop after wheat, rice, maize and barley (FAOSTAT 2018). For the past 21 years sorghum recorded an increase in production/yield from 18 million tons in 21 million hectares (ha) to 29 million tons in 29 million ha (FAOSTAT 2018). A sharp production decline was observed in South Africa with the production of 223 thousand tons in the harvested area of 98 thousand ha in the past 21 years to 115 thousand tons in the area harvested of 29 thousand ha (1999-2018). The production decline trend in sorghum was caused by abiotic components like drought (SAGL). Additionally, a major reason for South African sorghum production decline is that yield levels have failed to increase, and producers shifted to more profitable crops like soybeans and corn (USDA 2019). Sorghum plant production constraints/decline was not only caused by abiotic factors, biotic components that includes microbial communities play a crucial role in plant ecosystems (Mendes et al., 2013). Microbial communities also play a pivotal role in the functioning of plants by influencing their physiology and development (Guazzaroni et al., 2018).

Sorghum, like any other plant, interacts with a broad range of microorganisms. These microbes include bacterial and fungal communities residing on or inside various plant organs, of which those associated with leaf and roots surface are best characterized (Bulgarelli et al., 2013). These microorganisms have neutral, beneficial or detrimental effects on plant development and health (Rosselli and Squartini, 2015). The positive interactions provide an environment that benefit the plant host by increasing stress tolerance, nutrient acquisition, pathogen resistance and also aid in phytoremediation of environmental pollutants (Dar et al., 2019; Kumar and

Verma, 2019; Mia et al., 2014). Plants are however not only colonized by beneficial microbes, they are also susceptible to several fungal and bacterial pathogens that result in pre and post-harvest deterioration including the production of potentially harmful mycotoxins.

Fusarium head blight (FHB) is one of the fungal diseases caused mainly by *Gibberella zeae* (Schwein) Petch (Anamorph: *Fusarium graminearum* Schwabe). *Fusarium graminearum*, the dominant pathogen contributing towards sorghum grain mould has been previously isolated from sorghum (Funnell-Harris et al., 2017; Funnell-Harris et al., 2013; Burgess et al., 2002; Trimboli and Burgess, 1985). Various mycotoxin-producing *Fusarium* species have been isolated from sorghum grain in South Africa (Beukes et al., 2017). These unfavourable plant microbe's interaction may also lead to genotypes that appear to be susceptible to the local and endemic pathogenic strains and the susceptibility varies depending on the host genotype (Fall et al., 2019). There are also several genotypes that are resistant to diseases (TeBeest et al., 2004). The ratings for disease resistance and severity for selected high-yielding and popular grain sorghum genotypes have been delineated into resistant (R), moderately Resistant (MR), susceptible (S) and highly susceptible (HS) groupings (TeBeest et al., 2004). Phenotypic observation of sorghum genotype based on the disease severity is essential, as the use of resistant genotypes may be the most cost-effective means of managing diseases and can be important component for ensuring food security (Haussmann et al., 2000).

Additionally, insights into the bacterial and fungal communities associated with various diseases should be essential components of food and energy security programs, as they open the possibility to develop new environmentally-friendly strategies for agricultural sustainability (Wei and Jousset, 2017). Traditionally, estimates of microbial diversity were based solely on culturable microorganisms. However, microscopic observations and mathematical modelling estimate that 99% of microbes are unculturable under standard laboratory conditions (Vorholt, 2012; Schloss et al., 2009; Schloss and Handelsman, 2006; Stach and Bull, 2005). Next-generation sequencing (NGS)-based tools have allowed for profiling of microbial communities on an unprecedented scale (Zhou et al., 2018; Vernikos et al., 2015). NGS sequencing of the taxonomically informative 16S rRNA gene and ITS provides

a powerful tool for investigating bacterial and fungal diversity in plant species (Sanschagrin and Yergeau, 2014; Porter and Golding, 2011).

This study used sorghum recombinant inbred lines (RILs) of the F9 generation, created by crossing two inbred lines followed by repeated selfing to create a set of inbred lines whose genomes are a mosaic of the parental genomes (Shiringani et al., 2010). The genetic material of all the microbes (microbiomes) of these RILs and the relationship to plant health has not been examined. Metabarcoding technique which uses short genetic sequences to identify individual taxa will increase the understanding of the foliar microbiomes of sorghum RILs and its link to natural infection. The use of this technique will also assist in identifying the reported economically important pathogen taxa associated with sorghum RILs.

Fusarium graminearum was linked with the HS disease group in this study, and will be subsequently used for the gene expression analysis. This pathogenic taxa is an important sorghum production biotic constraint worldwide due to its ability to produce mycotoxins. It is a major disease problem on cereal crops, as it can influence the yield and lead to economic losses. However, management of sorghum mycotoxins is difficult and a better understanding of pathogen aggressiveness as well as surveillance is needed for improved control. *Fusarium graminearum* disease severity varies depending on the host genotype resistance (Fall et al., 2019). Gene expression analysis of the pathogen-host interaction could possibly enhance understanding of the resistant process and provides valuable information about the resistant process of *Fusarium graminearum* in sorghum. Recent studies investigating the mechanisms underlying the host defence response against *Fusarium graminearum* using comparative transcriptome analysis in susceptible and resistant maize and wheat genotypes, have been undertaken (Brauer et al., 2019; Yuan et al., 2019). The studies concluded that the susceptible wheat genotype displayed higher auxin accumulation during infection relative to resistant genotypes, and in maize the differentially expressed genes (DEGs) associated with pathogenesis-related protein 1 (PR1) and regulation of salicylic acid were significantly enriched during *F. graminearum* infection, suggesting that these DEGs play dominant roles in maize resistance to *Fusarium graminearum*. The studies proved that RNA sequencing (RNA-Seq) technology has been very useful in conducting transcriptomics studies.

1.3 JUSTIFICATION OF THE STUDY

One of the major challenges of the 21st century will be to create sustainable crop production and environmentally sound systems. Enhanced production will be required to provide sufficient food for the increasing human population, which is predicted to reach a plateau of 9 billion people by 2050 (Gerland et al., 2014). Sorghum is one of the main staples for the food insecure people. It is attractive to breeders due to its drought tolerance, bioenergy potential, and use as human food and animal feed. It is also a versatile crop that can be grown as grain and sweet-stem crop. Globally, grain sorghum is an important staple food crop and sweet-stem sorghum is to a greater extent considered as a promising biofuel feedstock (Vanamala et al., 2018). Sorghum hosts microbes that can have neutral, negative or positive effects on the plant. While the majority of microorganisms are beneficial, some are pathogens that colonize leaves and overwhelm the plant defence mechanisms, as the result, the full potential of sorghum productivity has not been realised due to an array of biotic constraints (Mengistu et al., 2016). Plant pathogens represent major and constant constraint to food production, with global crop losses estimated to be 20% – 30% principally in food-deficit areas (Savary et al., 2019). This presents a direct threat to the sorghum productivity, yet not much is known about microbial diversity, and the interplay between associated bacteria and fungi in leaves remains unexplored. Recent reports, using metagenomic analysis, have revealed potential key taxa associated with the rhizosphere and seed of sorghum (Kuramae et al., 2020; Hara et al., 2019; Kinge et al., 2019; Xu et al., 2018; Guo, 2016). However, none of these studies assessed the aerial region of the plant, which is suggested to be one of the primary entry sites for pathogens (Cernava et al., 2019). This knowledge deficit is broadly true for plants where, in contrast to the rhizosphere, substantially less is known regarding the effects of plant-microbe associations on foliar diseases.

Additionally, emerging and re-emerging plant pathogens challenge the ability to ensure plant health and growth worldwide (Köberl et al., 2011). There is an increasing demand for ecologically compatible agricultural strategies. Plant biotechnology contributes to the development of numerous crop varieties with greater drought, better nutritional value and enhanced disease resistance. Unfortunately, beneficial plant microbe interactions were often ignored in breeding strategies although plant associated microbes fulfil important ecosystem

functions for soils and plants (Berg et al., 2017; Berg and Smalla, 2009). Overall, it is necessary that agricultural productivity be substantially increased within the next few decades and as a result, agricultural practice is heading toward a more environmentally friendly and sustainable approach. Understanding these microbial interactions is thus important in plant diseases management.

Fusarium graminearum is one of the major biotic constraints affecting sorghum productivity and it has been found in this study to be highly associated with the susceptible disease group (Choi et al., 2013; Quazi et al., 2010; Tarekegn et al., 2006; Menkir et al., 1996). It affects the three most important crops grown in South Africa (GRAINSA, 2017). It causes ear rot in maize, it is a major contributor in the grain mould of sorghum and causes Fusarium head-blight in wheat (Beukes et al., 2017). However, it has been indicated that sorghum only acts as an asymptomatic host of *F. graminearum* (Pena et al., 2019; Burgess et al., 2002), but it has the potential to produce 15-acetyldeoxynivalenol (15-ADON), deoxynivalenol (DON), nivalenol (NIV), zearalenone (ZEA) and 3-acetyldeoxynivalenol (3-ADON) (Yerkovich et al., 2017). In addition, the pathogenicity of *Fusarium graminearum* to sorghum was shown in other studies (Van Rooyen, 2019; Bodoči et al., 2013) where it had the highest pathogenicity on sorghum grain, followed by *Fusarium solani*, *Fusarium verticillioides* and lastly *Fusarium subglutinans.* The susceptibility of grain sorghum to colonization by *Fusarium graminearum* was assessed on sorghum seedlings and it was found that this pathogen can initiate host infection at initial growth phases and progressively colonize adjacent tissues as an endophyte. The results also showed that stem as well as roots tissues are susceptible to infection. This pathogen causes diseases that results in reduced yield due to abortion of florets, reduced seed filling market and quality values, endosperm deterioration and surface discoloration embryo (Nida et al., 2019; Kange et al., 2015; Audilakshmi et al., 2011). Production losses due to mycotoxins range from 30% to 100% depending on time of flowering, cultivar, and prevailing weather conditions during flowering to harvesting (Das and Padmaja, 2016). The International Crops Research Institute for the Semi-Arid Tropics (ICRISAT), has projected US$ 130 million as total losses due to grain mould in the semi-arid tropical areas of Africa and Asia. The United States of America (USA) and India have seen losses of 50 - 80 million dollars (Gosal and Wani, 2018).

This study will add knowledge to what is currently available about the role and effects of fungal and bacterial communities in sorghum and how these communities change under biotic stress conditions. Understanding the dynamics of the phyllosphere bacterial and fungal composition may allow us to modify these communities to increase resistance against foliar pathogens and also allow successful colonization and growth of beneficial or commensal bacteria and fungi (Copeland et al., 2015). To date there has not been a feasible way to control mycotoxins caused by *Fusarium graminearum*. The best way to remove/limit mycotoxins from contaminated food crops is to be able to control *Fusarium graminearum*. Assessing whether *Fusarium graminearum* induces specific defence-related genes will add knowledge in ways to control *Fusarium graminaerum* in sorghum. This will be done by characterizing the transcriptome time series gene expression profiling in response to *Fusarium graminearum* infection in resistant and susceptible recombinant inbred lines (RILS) through the use of RNA-Seq technique.

1.4.1 AIM

- To identify the fungal and bacterial populations on/within sorghum leaves that are naturally infected with various pathogens through the use of metabarcoding, and to identify the pathogenic taxa highly associated with susceptible plants
- To identify the resistance genes and pathways that are associated with *Sorghum bicolor* response to the identified taxa associated with diseased RILs (*Fusarium graminearum*) through the use of transcriptomics (RNA-Seq).

1.4.2 OBJECTIVES

The objectives of the study were

- To determine the fungal and the bacterial community structure changes in sorghum RILs in response to natural pathogen infection using metabarcoding;
- To characterize the fungal and bacterial taxa associated with disease groups (R, MR, S and HS) in response to natural pathogen infection;
- To identify the most dominant pathogen in diseased sorghum RILs

- To confirm *Fusarium graminearum* through marker genes, analyse cell/spore viability, and characterize pathways likely to be involved in pathogen infection resistance through RNA-Seq.

CHAPTER 2

Literature Review

2.1 LITERATURE REVIEW

2.1.1 Sorghum taxonomy and importance

Sorghum (*Sorghum bicolor* (L.) Moench) is one of the main staple foods for the world's most food insecure people (Mekbib, 2007). This crop was first described in 1753 by Linnaeus under the name of *Holcus*. Later, Moench distinguished the genus sorghum from the genus holcus (Clayton, 1961). The present official taxonomic concept of the sorghum genus and species concur with the one recognized by Moench. All the distinct names given by several taxonomists are therefore taken as synonym to *S. bicolor* (L.) Moench. *Sorghum bicolor* belongs to the genus *Sorghum*, *Poaceae* family, of the *Andropogoneae* tribe (Von Mark and Dierig, 2014). The *S. bicolor* species include all cultivated sorghum species as well as wild and semi wild plants which are regarded as weeds (Mutegi et al., 2011).

Sorghum is a grassy non-halophyte, which is both salt and drought tolerant, and it is considered a promising crop for semi-arid regions (do Nascimento et al., 2014). It is classified into two major classes: grain sorghum and sweet-stem sorghum. Sweet-stem sorghum is well adapted to temperate and sub-tropical regions (Reddy et al., 2007). It is a fast growing C4 crop with high photosynthetic efficiency, high sugar accumulation in the stalks and have a high potential for biomass production (Almodares and Hadi, 2009). The total soluble sugars of the juice in the stalk can vary from 7-24% depending on the sweet-stem sorghum variety. Sweet-stem sorghum is a multi-purpose crop which can be cultivated for the simultaneous grain production from its panicle (for food, mainly porridges and flat breads); sugary juice from its stalk (for making ethanol and syrup); and green leaves and bagasse (as an organic fertilizer, for paper manufacturing and an excellent fodder for animals) (Mengistu et al., 2016). In contrast to other bioenergy feedstocks sorghum produces other valuable by-products and food products.

Grain sorghum ranks fifth among the world's cereal crops in area sown after wheat, rice, maize and barley (dos Santos et al., 2017). Its drought tolerance makes it a strategic crop for sustainable grain production because of climate change and increasing food demand (Hadebe et al., 2017). It is rich in starch similar to maize, and has important agronomic advantages, such as ability to grow in a wide range of soil types and climates (Ramírez et al., 2016). However, limited research has been conducted on its performance for bioethanol since it generally shows

lower ethanol yield compared to maize and its lower susceptibility to hydrolysis, especially after heat moisture treatments (Perez-Carrillo et al., 2012). It has been reported that the key factors that affect the performance and efficiency of ethanol fermentation of grain sorghum include, the amount of extractable proteins, content of phenolic compounds (tannins), protein-starch interactions, starch content, amylose-amylopectin ratio, viscosity of the sorghum grain suspensions and starch digestibility (Ramírez et al., 2016).

2.1.2 Sorghum domestication and production

Sorghum was domesticated in arid areas of north-eastern Africa. After its domestication, the agricultural usage of sorghum spread across Africa and into the continent of Asia through traditional trade routes. The world sorghum production for the 2018/2019 season ~~stands~~ was at 58.4 million tons (SAGL, 2019). The three largest sorghum producers in the world are Africa 41%, America 38% and Asia 17% (FAOSTAT 2018) between 1999 to 2018 (Figure 2.2A). In 2018 Africa had an increase in sorghum production (Figure 2.2B) with 50%. The production of sorghum in South Africa increased in the mid-eighties when over 300,000 hectares were planted. However, the production declined dramatically as producers shifted to more profitable crops like soybeans and corn (Figure 2.1). Since 2010 the average area planted in South Africa declined to 86,000 hectares (ha) and reached 28,800 ha in 2018, due to drought conditions. A major reason for South African sorghum production decline is that yield levels have failed to increase as yield levels of soybeans and corn, leading to less competitive gross margins (USDA 2019). Unless there is a change in technology that, could improve sorghum, productivity, producers will continue to shift to more profitable crops and the decreasing trend in hectares planted with South African sorghum will continue. However, the area planted to sorghum in South Africa improved in 2017 to 48,500 ha, a 75 percent increase from the previous season. Limpopo province producers drove the increase in sorghum plantings to levels of around 20,000 ha, after only 5,000 ha of sorghum was planted in 2017 (USDA 2019). The overall world sorghum crop production of the 2018 season was 59 million tons, with the harvested area of 42 million hectares of land (FAOSTAT 2018; SAGL 2019) Figure 2.1.

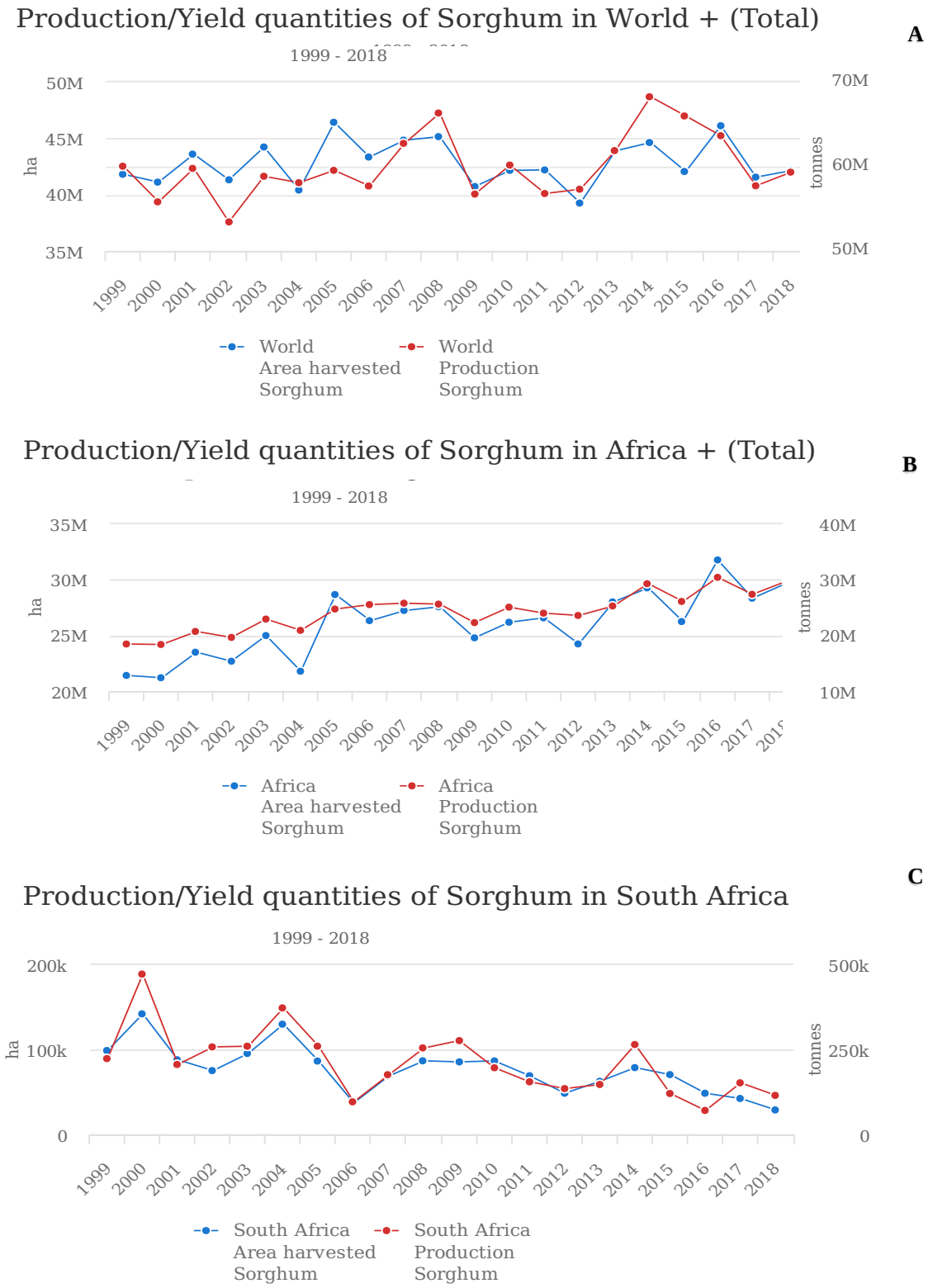

Figure 2.1: The sorghum production in tons and the area harvested in hectares between 1999-2018 of sorghum (A) world (B) Africa and (C) South Africa. Figure adapted from (FAOSTAT, 2018). The sorghum production trend is indicated by a red trend, and the area harvested is indicated by the blue trendline.

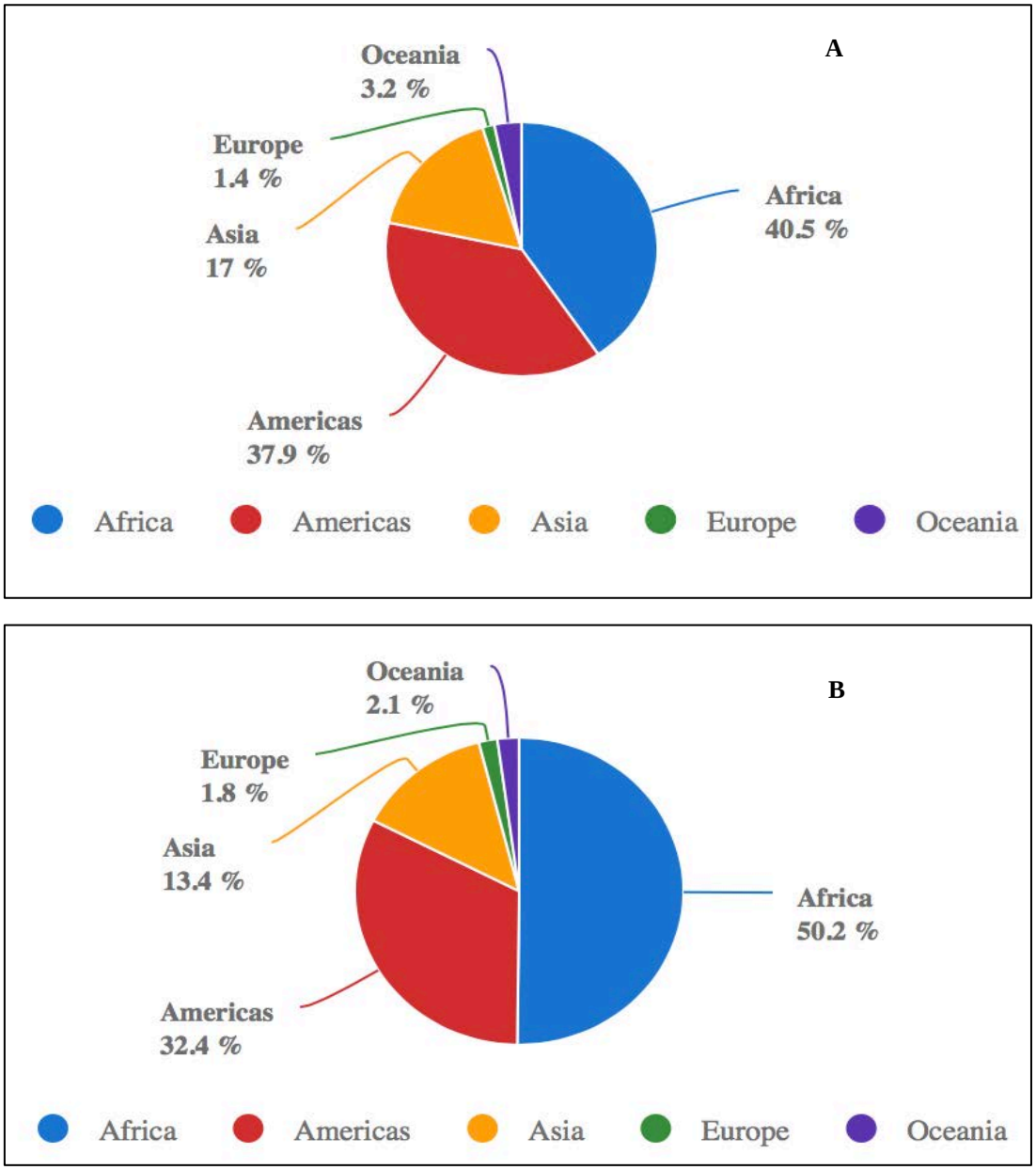

Figure 2.2: The total percentage of sorghum (Adapted from FAOSTAT 2018). (A) The total percentage of sorghum production (tonnage) accumulated between 1999 to 2018 (B) showing production accumulated in 2018.

2.1.3 Sorghum breeding, RILs and germplasm

Breeding efforts are essential because productivity of sorghum is threatened by abiotic and biotic constraints (Motlhaodi, 2016; Reddy et al., 2007). The major goal of the breeding programs is to improve the productivity of the crop (Reddy et al., 2007). The sorghum productivity is mainly determined by quantitative traits such as stem sugar related characteristics and grain yield (Shiringani et al., 2010). Additionally, other breeding objectives for sorghum are pests and host plant resistance to pathogens, and currently drought adaptation (Chisi, 2010). Sorghum breeders worldwide aim at improving various characteristics of the crop that can result in commercialization. Although for many years the main trait was grain yield, interest has now shifted from grain to stalk to manipulate biofuel-feedstock related traits. Substantial crop improvement has been achieved by breeding in the last decades (Lenaerts et al., 2019).

For any crop improvement program, germplasm has shown to be the most important raw material, and yet the possible extinction of this invaluable resource is a reality the world has to face (Mengesha and Rao, 1982). Currently, the main aim is to have in hand the important raw material required for improvement of crop, and sorghum is a crop endowed with one of the highest levels of genetic diversity (Visarada and Aruna, 2019). There are close to a quarter million accessions of sorghum collected and maintained by national and international genebanks, worldwide. The two biggest sorghum germplasm holders are the International Crops Research Institute for the Semi-Arid Tropics (ICRISAT) and the US Department of Agriculture (USDA) (Singh and Upadhyaya, 2015). The majority of collections in the United State gene bank are from India, Mali, Yemen, Sudan and Ethiopia (http: www.arg-grin.gov/cg).

About 16% of the world sorghum collection (235,711 accessions) is conserved at ICRISAT, genebank in India (Wang et al., 2016; FAO 1998). A main repository for sorghum germplasm in the world is, ICRISAT with a total of 37,949 accessions from 92 countries. These accessions comprise 458 wild and weedy relatives, 99 cultivars, 4,814 advanced breeding lines and 32,578 landraces (Upadhyaya et al., 2014) of the total collection. The germplasm maintained at ICRISAT consists of five basic races: durra, kafir, caudatum, guinea and bicolor (Figure 2.3)

and their 10 hybrid races based on spikelet morphology and panicle (Raemaekers, 2001; Harlan, 1975). However, three races predominantly represent the collection: durra, caudatum and guinea, of the 10 hybrid races, only three, durra-bicolor, guinea-caudatum and durra-caudatum are common. Zimbabwe, Uganda and India have all the ten hybrid and five basic races (Reddy et al., 2007). Caudatum and its hybrid races are adequately represented in Sudan and durra, guinea-caudatum and their hybrid races in Ethiopia. The guinea race collections are mostly from Zambia, Togo, Tanzania, Sierra Leone, Mozambique, Mali, Malawi, India Gambia, Burkina Faso and Benin. The Southern African Development Community (SADC) countries such as South Africa, Botswana, Swaziland, Lesotho and Zimbabwe have contributed only kafirs and their hybrid races. However, kafirs races are photoperiod insensitive at ICRISAT, Patancheru, India (Upadhyaya et al., 2014). The durras are from Russia, Yemen, Pakistan, Cameroon, India, Somalia, Niger and Ethiopia and caudatums are from Sri Lanka, Namibia, Central African Republic, Uganda, Sudan, Rwanda, Kenya and Burundi. The ICRISAT taxonomic collection is poor in some cultivated and transplanted sorghum. Furthermore ICRISAT is divided into base and active collections, over 30,000 sorghum accessions has been conserved in the Svalbard Global Seed Vault, Norway (Upadhyaya et al., 2014). Additionally, genome mapping, molecular marker development and tagging of agronomically important traits have been taken well into consideration and whole genome resequencing determined a large number of single nucleotide polymorphisms (Mace et al., 2013; Morris et al., 2013).

Breeding programs of sorghum globally are working towards enhanced varieties with drought tolerance, better quality, agronomic traits and disease-resistance (Sallam et al., 2019; Serba et al., 2017). The regions within genomes containing genes related with a specific quantitative trait are known as quantitative trait loci (QTLs). Molecular breeding approaches are increasingly being adopted to identify genomic regions and develop genetic linkage maps influencing traits of importance in sorghum. Sorghum genome mapping based on DNA markers commenced in the early 1990s and many sorghum genetic linkage maps were published in the last decade, initially based on RFLP markers (Djè et al., 1999; Tao et al., 1993). RAPDs (Dahlberg et al., 2002; Ayana et al., 2000), ISSRs (Yang et al., 1996), SSRs (Djè et al., 1999), AFLPs (Ritter et al., 2007; Menz et al., 2004) and Diversity Array

Technology (DArT) markers (Sánchez-Sevilla et al., 2015). Genetic linkage maps are an important requirement for studying the inheritance of quantitative and qualitative traits, to develop markers for molecular breeding, comparative genomic and map-based gene cloning studies. Nested Association Mapping (NAM), are the multi-parent cross populations which are developed to circumvent spurious associations and assist in increasing the rare alleles 's detection strength in crops (Hu et al., 2018). The NAM mapping simultaneously exploits both the advantages of association mapping and linkage analysis. It takes advantages of both historic and recent combination of events in order to have the advantages of either association mapping /linkage analysis (Sivakumar et al., 2019; Yu et al., 2008). Association mapping and linkage analysis are two generally used methods to dissect the genetic architecture of complex traits as complementary approaches. Association mapping offers high resolution with either prior candidate gene information/ high marker coverage genome scan, while linkage analysis often characterize broad chromosome regions of interest with relatively low marker coverage (Kushwaha et al., 2017; Thornsberry et al., 2001). Combination of the two approaches will provide integrated mapping strategy which will advance mapping resolution without needing excessively dense marker maps. Recombinant inbred lines (RILs) serve as a powerful tool for genetic mapping. A RIL is formed when two inbred lines are crossed followed by selfing to create a new inbred line whose genome is a mosaic of the parental genomes (Broman, 2005). Briefly, the parental cross from two highly bred lines is used to generate the F1 generation. Crossing two members of the F1 generation produce the F2 generation. Then the individuals from the F2 population are selfed in a single-seed descent strategy that results in highly homozygous lines by the F7-9 generation. RILs have a number of advantages for genetic mapping; multiple invasive phenotypes may be obtained on the same set of genomes, one can phenotype multiple individuals from each strain to reduce environmental, individual and measurement variability

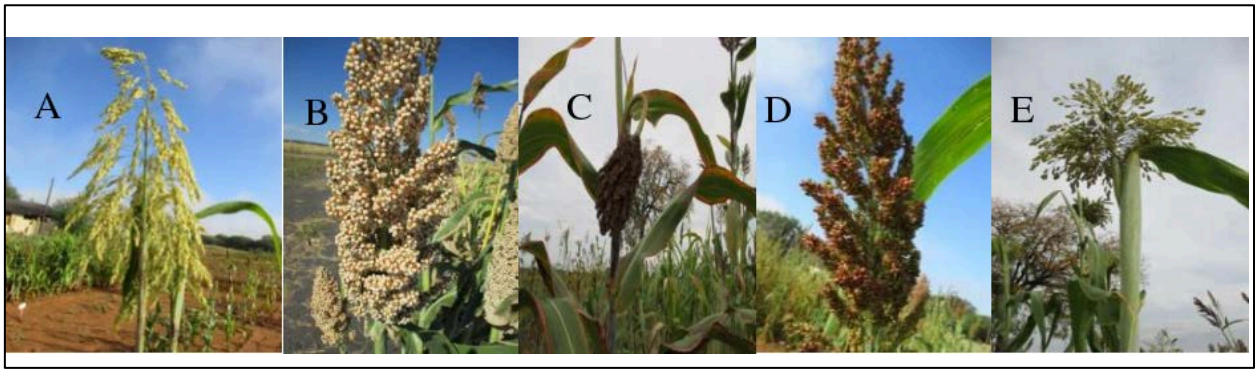

Figure 2.3: Morphological variability in sorghum germplasm indicating different races. A- Guinea; B-Caudatum; C- Durra; D- Kafir; E- Bicolor Adapted from (Motlhaodi, 2016).

2.2 Sorghum genome

Sorghum is a C4 monocot and a genetic model for C4 grasses due to its small genome. The nuclear DNA content of sorghum is 732.2 MB with 34,129 loci and 47,121 transcripts that encodes proteins (McCormick et al., 2018). A sorghum genome transcriptome atlas of gene expression was constructed from 47 RNA-Seq profiles of growing and developed tissues of stems, roots, seed, panicles and leaves collected during the juvenile, vegetative and reproductive stages (McCormick et al., 2018). The genome is a diploid with a haploid complement of 10 chromosomes; it is viewed as a diploid from the perspective of genome organization (Luo et al., 2016). It is three times smaller than the pearl millet and maize genome, and 20 times smaller than the wheat genome. The original sorghum reference genome sequence was based on approximately 8.5 fold depth paired-end Sanger sequence reads from genomic libraries with 100 fold variation in the inserts size (Paterson et al., 2009). Gene annotation analysis incorporating RNA-Seq showed that a high number of genes have not been annotated in sorghum version 1 and many annotations were not complete (Olson et al., 2014).

2.3 Overview of plant microbe interactions in plants

Sorghum, like any other plant, interacts with a broad range of microorganisms. Plants host a remarkable diversity of microorganisms known as the plant microbiota (Bulgarelli et al., 2012; Knief et al., 2012; Lundberg et al., 2012). Plants live in association with diverse microbes, which thrive on the plant above in the phyllosphere and below ground in the rhizosphere (Knief, 2014). Figure 2.4 represents the general overview of plant microbes' interactions. The leaf microbiota is diverse and comprises many different genera of filamentous fungi, bacteria,

algae, yeasts, and, less frequently, nematodes and protozoa (Rossmann et al., 2017). These large numbers of diversified microbes interact with one another and form complex interaction networks. The plant-associated (symbiotic) and free-living diazotrophic bacteria are ubiquitous in soil (Rico et al., 2014), but barely much has been established with regards to their contribution associated with the phyllosphere. Plant microbe interactions are regarded to be dynamic and can have neutral, beneficial, or detrimental effects on the development of plant health (Rosselli and Squartini, 2015).

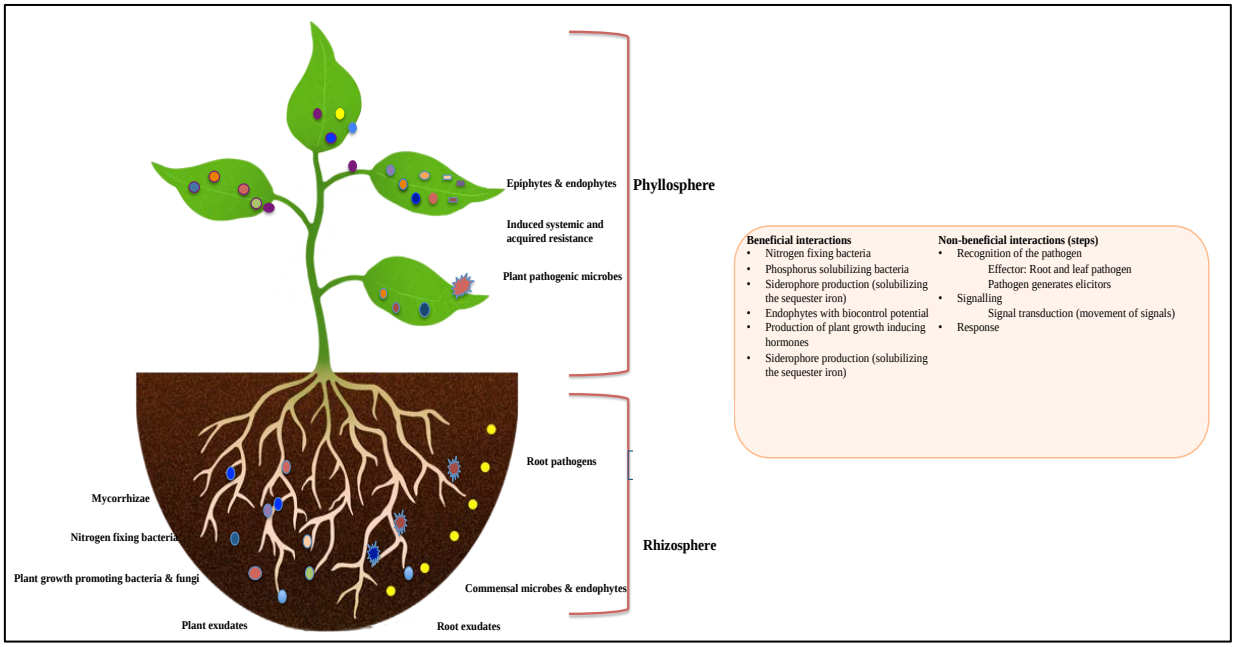

Figure 2.4: Plant microbe's interactions (beneficial and non-beneficial interactions) in the rhizosphere and phyllosphere.

2.4 Beneficial interactions

Plant associated microbes isolated from phylloplane and rhizoplane surfaces are known as epiphytes, while those found within the interior tissues of the plant are known as endophytes (Andrews and Harris, 2000). Endophytes inhabit tissues without causing harm to the plant. The majority of the diverse plant-colonizing microbes induce systemic resistance against pathogens and utilize a plant growth promoting effect (Esitken et al., 2010). Plant growth promoting microbes isolated from *S. bicolor* and other crops has reported biocontrol activities (Mishra et al., 2017; do Nascimento et al., 2014). Producers became increasingly dependent on agrochemicals as a dependable approach of crop protection, assisting with their economic

stability operations as agricultural production intensified over the past few decades (Ravisankar and Nithya, 2018). However, constant use of chemical inputs causes development of pathogen resistance to the applied agents and their non-target environmental impacts (Gao and Xu, 2014). Furthermore, the consumer demand for pesticide-free food and the increasing cost of pesticides, particularly in less-affluent regions of the world, has led to a search for substitutes for these products. There are also a proportion of diseases for which chemical solutions are few, non-existent or ineffective (Gerhardson, 2002). Biological control is thus being regarded as a supplemental or an alternative approach of reducing the chemicals use in agriculture (Welbaum et al., 2004; Postma et al., 2003).

A substantial proportion of the plant-associated microorganisms are known for their antagonistic activity against other microbes including pathogens (Berg et al., 2013) because of their ability to produce hormones. This functional group of antagonists is a valuable resource in the ongoing development of biological control agents (BCAs) that are supplied in agriculture to suppress pathogens. The use of a mixture of compatible biocontrol agents with multiple mechanisms of action, can be effective under a wider range of climatic conditions, thus reducing some of limitations of biocontrol activity in the field. Such mixtures can potentially have synergistic effects, which may result in higher level of protection and wider spectrum of diseases that can be controlled (Corrêa et al., 2014; Guetskyl et al., 2002).

2.4.1 Overview of plant growth promoting direct mechanisms

2.4.1.1 Nitrogen fixing bacteria

Fixed nitrogen is regarded as one of the major limiting nutrients in plant development, as plants cannot directly assimilate molecular nitrogen (Gopalakrishnan et al., 2015). The biological process responsible for the reduction of molecular nitrogen into ammonia is referred to nitrogen fixation and a wide variety of microbes belonging to the bacterial domain have the capacity to colonize the phyllosphere and interact with plants. These microorganisms are capable of transforming atmospheric nitrogen into fixed nitrogen usable by plants. These organisms affect more than 90% of all nitrogen fixation (Puri et al., 2018).

2.4.1.2 Phosphorus solubilizing bacteria

Phosphorus is less available in most soils than any other macronutrients; this is a factor constraining the productivity of plants and therefore requires the application of substantial doses of phosphate fertilizers to increase productivity of plant (Rathinasabapathi et al., 2018). This essential element plays a significant role in energy transfer reactions, respiration and photosynthesis. One way of improving the endogenous phosphorus sources effectiveness is to use microbes that exude substances capable of facilitating with the solubilization of insoluble phosphates (Rathinasabapathi et al., 2018). Inorganic forms of phosphorus are solubilized by a group of heterotrophic micro-organisms excreting organic acids that dissolve phosphatic minerals and phosphate solubilization through a large number of saprophytic fungi and bacteria. A rhizobia bacterium is known to nodulate legumes and has the greatest solubilization potential (Marra et al., 2012). Phosphorus solubilizing bacteria mainly *Bacillus, Pseudomonas* and *Enterobacter* and fungi *Talaromyces aurantiacus* and *Aspergillus neoniger* are very effective in increasing the plant available phosphorus in soil, along with the growth and yield of crops (Zhang et al., 2018a; Dash and Dangar, 2017; Hayat et al., 2017).

2.4.1.3 Siderophore production (solubilizing the sequestered iron)

Under aerobic conditions most iron in soil is available in the insoluble form and is not readily available to plants, even though is needed for major physiological processes such as photosynthesis, nitrogen fixation, and respiration in the plant (Morrissey and Guerinot, 2009). To meet their requirement microbes have developed special mechanisms to facilitate the iron siderophore complexes uptake through a specified outer membrane receptor protein and chelate insoluble iron through siderophores release (Golonka et al., 2019). The involvement of *Pseudomonas* spp. in the production of siderophores has been well documented (Besset-Manzoni et al., 2018; Luján et al., 2015). Mycorrhizal (symbiotic fungi) has been reported to produce siderophore (Hanudin et al., 2017).

2.4.1.4 Production of hormones inducing plant growth

In the processes of plant growth gibberellins, indole acetic acid (IAA), cytokinins and ethylene plays a significant role. These hormones can be synthesized by the plant itself or by their associated microbes for instance *Burkholderia phytofirmans* and hemibiotrophic or

necrotrophic fungi produce IAA (Kurepin et al., 2015; Ludwig-Müller, 2015). Additionally, plant associated microbes can influence the plant hormonal balance (Nihorimbere et al., 2011). Ethylene has shown that the balance is most important for the hormonal effect, at low levels. it can promote plant growth in several plant species (Ravanbakhsh et al., 2018). When present in high levels this compound can be a chlorosis, senescence and leaf abscission hormone. In this case, the high level of plant ethylene that is formed can significantly exacerbate the effects of the stress (that triggered the ethylene response) (Glick, 2014). Bacteria are capable of reducing the ethylene through the interaction of plant growth promoting bacteria containing ACC (1-aminocyclopropane-1-carboxylate) deaminase (Liu et al., 2015). Aminocyclopropane-1 carboxylic acid (ACC) is a precursor of ethylene in plants (Vo et al., 2016). ACC deaminase producing microbes are able to degrade this substance, so the uptake by and the level in the root is reduced (Ravanbakhsh et al., 2018). Thus making the bacteria to eventually increase root-growth by lowering the endogenous ACC levels (El-Tarabily et al., 2019; Glick, 2005). Because ethylene has been established as a stress hormone, bacteria producing ACC deaminase have a potential to safeguard the plant against abiotic and biotic stress (Raghuwanshi and Prasad, 2018; Saleem et al., 2007).

2.5 Non-beneficial interactions

Non-beneficial interactions between the host plant and the pathogens have been classified into either predation or parasitism (Ngah et al., 2018). Parasitic/pathogenic microbes occur when microbes utilize the resources of plants such as nutrients and water at the expense of the growth of the plant, development and health (Fatima and Senthil-Kumar, 2015). Depletion of the plant's resources increases its susceptibility to diseases, reduces its fitness and can thus lead to the host death (Abdullah et al., 2017). Sorghum yield and quality are also constrained by many environmental factors including certain diseases. Sorghum serves as a host for over 100 pathogens (bacterial, fungal, and viral pathogens) that infect different plant parts with more fungal diseases colonizing the crop in comparison to bacterial and viral diseases (Klein et al., 2001). The most important pathogenic microbes and their key symptoms are listed in Table 2.1.

Table 2.1: Fungal and bacterial pathogens of sorghum (adapted from Frederiksen and Odvody, 2000; TeBeest et al., 2004; Das, 2019).

Sorghum diseases	Bacteria/fungi	Symptoms	Occurrence
Fungal leaf blight	*Exserhilum turcicum*	Large cigar-shaped lesion oriented lengthwise along the leaf	Is favoured by temperatures that are moderate (18° to 27°C) and rain or heavy dews
Charcoal rot	*Macrophomina phaseolina*	Presence of black sclerotia and a stringy, dry appearance of the stem near the soil line	Late season as plants near maturity
Bacterial leaf spot	*Pseudomonas syringae*	Water soaked spot lesions on leaves	Warm regions especially during the rainy season
Bacterial leaf streak	*Xanthomonas campestris* pv. *holcicola*	Water soaked tissue between veins that later turn brown with red margins.	Appears during warm temperatures as early as the second leaf stage of the seedling.
Bacterial leaf stripe	*Burkholderia Pseudomonas andropogonis* *Pseudomonas sorghicola*	Characterized by long narrow stripes that can vary from red to black	Occur in mid-season, especially during warm and humid weather
Sorghum smut **Loose-smut** **Covered-smut**	*Sporisorium sorghi* *Sporisorium cruenta*	Characterized by infection of rachis spikelet in a panicle malformed (loose smut), a long	wet periods present severe disease symptoms

Head-smut **Long-smut**	*Tolyposporium ehrenbergii* *Sporisorium reilianum*	sorus enclosed by a whitish thick membrane (long smut), sorus enclosed with a grayish-white membrane (head smut), sorus that is not easily ruptured (covered smut)	
Fungal, zonate, gray, rough, oval, target leaf spot	*Gloeocercospora sorghi* *Cercospora sorghi* *Ascochyta sorghi* *Ramulisporasorghicola* *Bipolaris sorghicola*	Zonate- circular bands with straw-colour zones that resembles a bull's eye; Gray-narrow rectangular lesions turn gray with age, delimited by veins; Oval- sandpaper roughness lesions with margins which are defined; Rough- small, water-soaked spots with red border and straw center; Target-cylindrical spots with irregular margin and straw center (target)	Potentially occur in warm and high rainfall conditions
Anthracnose	*Colletotrichum sublineolum*	Small, circular, elliptical, or elongated spots	Wet and humid weather encourages rapid development of the disease

Sorghum ergot	*Claviceps sorghi*, *Claviceps africana*	Characterized by spots and have margins that are wide and red, orange, purple, or tan with straw-coloured center	Problematic at any time that grain sorghum is stressed after bloom and into the fill period
Grain moulds	*Fusarium* spp. *Alternaria alternate* *Phoma sorghina* *Curvularia lunata*	orange, pink, or white seeds found on heads infected	Disease can be severe in wet periods.
Downy mildew	*Peronosclerospora sorgi*	Characterized by a white, downy pathogen growth on the leaves lower surfaces and seedling stunting	High relative humidity is required to allow conidia production, infection
Rust	*Puccinia purpurea*	Presence of reddish-brown pustules first on lower leaves then on younger leaves	High relative humidity

2.6 *Fusarium graminearum* (*Gibberella zeae*) in sorghum

Gibberella zeae (anamorph *Fusarium graminearum*) is a devasting mycotoxin-producing pathogen of grain crops (GRAINSA, 2017). It can influence the yield and also lead to major economic losses, causing adverse implications for society, especially in poor communities. It is a major cause of diseases on cereal crops, as it can influence the yield and lead to economic losses. It is a hemi-biotrophic pathogen which has been previously isolated from sorghum grain (Funnell-Harris et al., 2017; Funnell-Harris et al., 2013; Burgess et al., 2002). It forms part of the *Fusarium* species complex that causes grain mould disease, sorghum production major constraint throughout the world (Beukes et al., 2017; Funnell-Harris et al., 2017). Sorghum grain mould is caused by complex fungal pathogens, which infect the developing caryopsis and proceed through grain development. Infection before and after the physiological seed maturity is promoted by temperatures of 25 to 35°C, rainy weather and/or by prolonged periods of humid (> 85 to 90% relative humidity) throughout grain development (Little et al., 2012; Navi, 2006; Tarekegn et al., 2006). *Fusarium* spp., *Curvularia lunata, Phoma sorghina,* and *Alternaria alternata,* are widely known grain mould causing fungal species (Nida et al., 2019; Mpofu and McLaren, 2014). *Fusarium graminearum* was identified as the dominant species causing grain mould in sorghum (Nida et al., 2019; Menkir et al., 1996) followed by *Fusarium thapsinum,* previously referred as *Fusarium verticillioides* until the acceptance of the name change from *Fusarium moniliforme* to *Fusarium verticillioides* (Nida et al., 2019; Katile et al., 2010; Summerell et al., 2003). Fusarium grain mould is the major component of sorghum grain mould disease complex (Das, 2019; Das et al., 2012).

2.6.1 Economic importance

Fusarium graminearum affects the three most important crops grown in South Africa (GRAINSA, 2017). It causes ear rot in maize, grain mould in sorghum and Fusarium head-blight in wheat (Beukes et al., 2017; Mavhunga, 2013). Production losses due to mycotoxins range from 30% to 100% depending on time of flowering, cultivar and prevailing weather conditions during flowering to harvesting (Shiri et al., 2017; Das and Padmaja, 2016; Thakur et al., 2006). Yield losses on highly susceptible sorghum lines can reach 100% (Prom et al., 2017). Substantial economic losses are due to the impact on seed quality and yield. It is

challenging to accurately estimate losses caused by the disease since it involves the assessment of losses from production to marketing and down to utilization of the seed or grain (Hundekar et al., 2016). The International Crops Research Institute for the Semi-Arid Tropics (ICRISAT), has projected US$ 130 million as total losses annually due to mycotoxins infected products in the semi-arid tropical areas of Africa and Asia. The United State of America (USA) and INDIA has experienced US$ 50 -80 million loss (Gosal and Wani, 2018). Sorghum *Fusarium graminearum* related diseases results in reduced yield due to abortion of florets and reduced seed filling, market values and quality are affected due to endosperm deterioration and surface discoloration embryo (Nida et al., 2019; Kange et al., 2015; Audilakshmi et al., 2011). GRAIN SA (2015), have reported that there has been an increase in the occurrence of *Fusarium graminearum* species causing *Fusarium* species complex in South African crops. Other than reduced grain quality, the ability of *Fusarium* species in producing the mycotoxins that contaminate grain, is of concern for livestock and humans (Pinotti et al., 2016).

2.6.2 Control measures

The most prominent traditional ways to control grain mould is categorized into physical methods, de-contamination through enterosorption, biological decontamination and chemical inactivation (Ismail et al., 2018). Once a product that is contaminated has reached a processing facility, segregation and clean-up are the initial control options through electronic sorting and hand-picking, however, some mycotoxins will not be entirely destroyed at processing temperatures as they are chemically stable (Waliyar et al., 2008). The use of hydrated sodium calcium aluminosilicates (HSCAS) additives in feeds that are contaminated has proven to also be efficient in preventing atoxicosis (Ismail et al., 2018). Furthermore, biological methods have been used as alternatives for mycotoxin decontamination. Despite all the mentioned measures, demonstrating efficient decontaminating properties biological methods usually rely on compounds that are produced specifically by selected microbes (Čolović et al., 2019). Chemical inactivation through ammoniation has proved to be useful, like other failed measures, ammoniation has been shown to be less effective against other mycotoxins contamination (Ditta et al., 2018). The transcriptomics (discussed in details in section 2.18) approach have led to better understanding of pathogen resistance mechanisms in plants (Kazan and Gardiner, 2018; Gkarmiri et al., 2015). Not many studies on sorghum gene-expression in

response to grain mould infection has been conducted. The gene expression study that was conducted, aimed at determining whether resistant and susceptible lines differed in response to sorghum grain mould causing pathogens using real-time reverse transcriptase-polymerase chain reaction (Katile et al., 2010). This study suggested that sorghum cultivars respond differently to grain mould causing taxa, and the resistant cultivar showed a greater induction of pathogenesis-related (PR) proteins. PR proteins have shown evidence in playing a role in preventing fungal colonization (Prom et al., 2017; Katile et al., 2010). Furthermore, studies on sorghum response to *Fusarium* infection has been widely conducted using genome wide association mapping studies to identify resistant loci (Cuevas et al., 2019; Nida et al., 2019).

2.7 Plant immune response to pathogens

Plants have developed complex disease resistance mechanisms against diverse pests and pathogens. The plant surface ‘s main purpose is to provide a protective barrier that can block the attack caused by microbial pathogens (Andersen et al., 2018). This defence is mounted by chemical and structural modifications to plant tissues specific to individual plant taxa. This include the production of a broad range of antimicrobial compounds and waxes, including terpenes, phenolics and tannins, that select for different types of microbial populations (Savoia, 2012). Innate immunity is triggered by the immune receptors activation and the initial line of innate immunity is triggered by the pathogen-associated molecular patterns (PAMPs) detection through pattern-recognition receptors (Nürnberger and Kemmerling, 2018). In plants, MAMPs are perceived by receptor-like proteins or cell-surface receptor-like kinases (RLKs) to mount pattern-triggered immunity (PTI) (Nürnberger and Kemmerling, 2018). However the pathogenic microbes are able to overwhelm pattern triggered immunity through the production of virulence effectors (Hwang et al., 2015). Many pathogenic microbes are able to deliver effector proteins into host cells to favour pathogen survival, multiplication and mediate effector-triggered susceptibility (Bertuzzi et al., 2019).

In plant-pathogen interaction, plants exploit signalling pathways for disease control, with plant hormones, jasmonic acid (JA), ethylene (ET) and salicylic acid (SA) (Bertuzzi et al., 2019). These signalling pathways induce expression of several defence-related genes in the presence of pathogens (Andersen et al., 2018). SA signalling is commonly involved in the activation of plant defence against pathogens that have a biotrophic phase in their life cycle, followed by

the establishment of systemic acquired resistance (Rodriguez-Moreno et al., 2018; Grant and Lamb, 2006). In contrast to SA, ET and JA are usually associated with defence against necrotrophic pathogens (Beckers and Spoel, 2006). Some pathogens display both necrotrophic and biotrophic phases of growth, designated hemi-biotrophs, and results in more complex circumstances (Sun et al., 2016; Bari and Jones, 2009). However, these signalling pathways may be utilized by pathogen for their host pathogenesis. The phytotoxin coronatine, secreted by *P. syringae* mimics jasmonates and activates JA signalling in *P. syringae*-infected plants (Geng et al., 2014; Uppalapati et al., 2007) for its pathogenesis fitness. These interactions take place in the different plant-created microenvironments, that provide habitats distinctive for microorganisms colonization (Morgan et al., 2005).

2.8 Plant created microenvironments

Fungi and bacteria are inhabitants commonly found on both the internal tissues and the surfaces of most plants and have diverse effects on the host plant development. Microbial communities have the ability to colonize internal plant tissues without causing any disease damage and play a very significant role in the growth of host plants (Ryan et al., 2008). Yaish et al. (2015) study on the date palm tree, revealed through molecular characterization that majority of the species belonged to *Bacillus* and *Enterobacter* genera and these species have a potential to promote plant growth and development. Some microorganisms can act as plant pathogens that can pose unique problems for disease control. The plant-microbe interactions in different microenvironments that are plant-influenced will be discussed broadly in section 2.8.1-2.8.3. The current study focuses on the diversity of phyllosphere (leaf) microorganisms associated with *S. bicolor*; therefore, the establishment of phyllosphere communities, including their significance to plant life will be discussed in greater detail. Plant created microenvironments include the endosphere, phyllosphere, and rhizosphere (Compant et al., 2011).

2.8.1 Endosphere

Some of the rhizosphere or endophytic microbes colonize the internal tissues (endosphere) without causing adverse effects to the host plant (Chebotar et al., 2015). These microbes are endophytes and are selected naturally to colonize the endosphere in the tissue between plant cells. Some endophytes are seed borne while others come through horizontal transfer (Frank

et al., 2017). The endophytes are generally regarded as plant symbionts, which can offer a variety of benefits to the plant (Chang et al., 2014). Metagenomic studies on sugar beet revealed the diversity and stability of endophytic bacteria, where 13 classes were retrieved, with Alphaproteobacteria being the dominant class followed by Acidobacteria, Gemmatimonadates and Actinobacteria (Tsurumaru et al., 2015). These endophytes have reported plant growth promoting traits (Shi et al., 2014). Fungal endophytes of perennial reeds were characterized to determine if the symbiosis of fungi could contribute to the invasiveness through their effects on seed germination and seedling growth. The results suggested that many endophyte taxa are seed borne and can increase seed germination and seedling growth (Shearin et al., 2018).

2.8.2 Rhizosphere

Within the soil system, there is the rhizosphere, the immediate surrounding of the plant root. It is a microbial hotspot regarded to be one of the most dynamic interfaces on earth (Philippot et al., 2013). The rhizosphere microbial community composition is comprised of a complex food web that utilizes the plant nutrients. This is a main driving force in the rhizosphere microbial diversity regulation and activity (Mendes et al., 2014). Studies on apple orchard rhizosphere soil bacteria have revealed that the most prevalent bacterial phyla were Proteobacteria, Actinobacteria and Acidobacteria (Franke-Whittle et al., 2015). The bacterial and fungal communities has been studied in olive root system and *Canalisporium*, *Aspergillus*, *Minimelanolocus* and *Macrophomina* were the main fungal genera present (Fernández-González et al., 2019).

2.8.3 Phyllosphere

The aerial parts of living plants including leaves, buds, stems, fruits and flowers provide a habitat for microorganisms termed the phyllosphere (Aleklett et al., 2014). This microbial habitat is one of the largest microbial habitats on earth, with leaf surfaces area estimated to exceed 10^8 km^2 globally (Morris et al., 2002). The phyllosphere represents a niche with great agricultural and environmental importance (Whipps et al., 2008a). Bacteria and fungi are the most common microbes in this habitat and therefore most focus of most studies (Deveau et al., 2018). The phyllosphere is the microenvironment, which is characterized by the most nutrient

deficient, habitat of microbes due to very small amounts of exudate released by the plant, and it is exposed to rain and wind environmental factors (Kwak et al., 2014). The impermeable, nutrient deficient and leaf surfaces is covered with water resistant cuticle that impedes the colonization of microbes. However, microbes are transferred from the atmosphere to the phyllosphere by vectors such as animals and insects (Gordon and Olson, 2013). Large numbers of bacteria and fungi were reported from different roots, plant tissues, nodules, flowers, leaves and sprouts of legumes, and they can promote plant establishment under adverse conditions, accelerate seedling emergence and improve plant growth (Chang et al., 2014). The beneficial microorganisms having mutualistic relationships that promote plant growth and enhance disease resistance in the phyllosphere plays an integral part in agriculture (Farrar et al., 2014). Phyllosphere bacterial communities of tropical trees were dominated by a core microbiome of taxa including, Alpha-, Beta-, and Gammaproteobacteria, Actinobacteria and Sphingobacteria (Kembel et al., 2014). This is in contrast to Dees et al. (2015) study on the phyllosphere of *Lactuca sativa* and *Diplotaxis tenuifolia*, where the 16S rRNA sequences identified were attributed to only four phyla, with the most dominant being Proteobacteria followed by Actinobacteria, Acidobacteria and Bacteroidetes. The existence of a complex fungal consortium supported a high phyllosphere fungal diversity of olives suggesting a significant impact on olive productions. Even though substantial studies have been conducted in other phyllosphere of other crops, recent reports, using metagenomic analysis, have revealed potential key taxa associated with the rhizosphere and seed of sorghum (Kuramae et al., 2020; Hara et al., 2019; Kinge et al., 2019; Xu et al., 2018; Guo, 2016). However, none of these studies assessed the aerial region of the plant, which is suggested to be one of the primary entry sites for pathogens (Cernava et al., 2019). This knowledge deficit is broadly true for plants where, in contrast to the rhizosphere, substantially less is known regarding the effects of plant-microbe associations on foliar diseases. Figure 2.5 represents the phylogenetic tree of major lineages of bacteria based on 16S rRNA sequence comparisons and phylum classification of fungi based on internal transcribed sub-regions (Tedersoo et al., 2018).

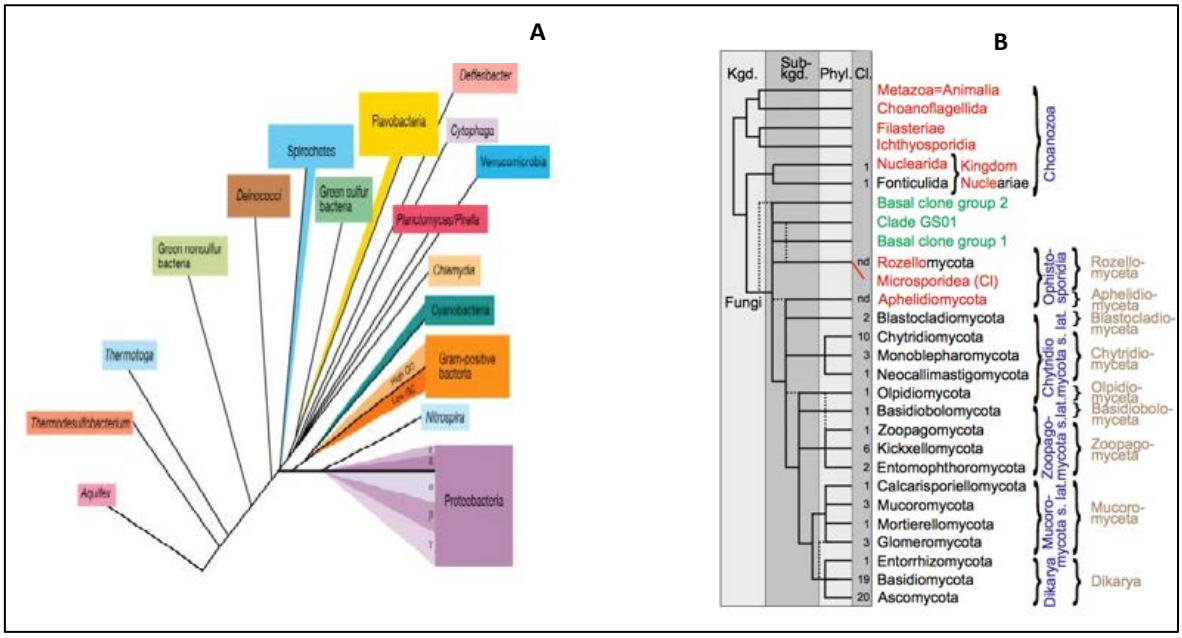

Figure 2.5: A: Major phyla of bacteria and fungi, based on 16S rRNA and ITS region: **A** represents the bacterial 16S rRNA **B:** Fungal phylum-level classification. Numbers behind branches indicate the classes. Names in red indicate traditionally considered taxa under the Zoological nomenclature; names in green indicate undescribed major clades with unofficial names; names in blue indicate taxonomic super- and sub-ranks and old classification (Tedersoo et al., 2018).

2.9 Diversity of plant associated microbes

Leaf tissues are mostly colonized by both soil-borne and air-borne bacteria (Vorholt, 2012) and are ubiquitous global habitats that harbour diverse microbial communities. It is estimated that on the global scale, the phyllosphere spans more than 10^8 km^2 and is colonized by up to 10^{26} bacterial cells (Vorholt, 2012). Belowground and aboveground interactions exert critical control on the composition and function of terrestrial ecosystems yet the fundamental relationships between microbial diversity and plant diversity remain elusive (Lindow and Brandl, 2003). Current understanding of the drivers of plant bacterial associations on leaves has been based on studies of individual host species and individual bacterial strains (Kembel et al., 2014). Different plant species possess different characteristic bacterial phyllosphere communities (Kim et al., 2012; Knief et al., 2012). Lambais et al. (2014) reported that leaf characteristics, such as composition, cuticle structure, leaf age, volatile organic compounds emissions and chemical composition might be related to bacterial communities interspecies

differences. The phyllosphere is a common niche for synergism between microbial diversity and plant (Yadav, 2017).

2.10 Synergistic microbial interactions

Plants in natural environments establish multiple interactions with various different microbes throughout their lifetime. Despite their potentially paramount importance for plants, these extremely complex microbiota have remained largely uncharacterized (Schenk et al., 2012). Historically, to understand the mechanisms underlying the development of plant diseases, molecular pathology research has largely focused on the direct interaction's characterization between plant pathogens and their hosts, missing from this disease triangle is the impact of other microbes on pathogen establishment. The earliest reports (in the 1800s) with regard to communities of microbes as disease causal agents are ascribed to Pasteur, who noticed that synergistic interactions of different microorganisms could cause a disease. The emergence of studies comprising synergistic interactions that involves multispecies has proved to be fundamental in the proper understanding of diseases caused by microorganisms (Lamichhane and Venturi, 2015; Short et al., 2014), as the consortia and interactions of multispecies are likely to be involved in the aggravation and disease establishment. Plants engage in multiple biotic interactions that either reduce (parasitic) or enhance plant performance. These multiple biotic interaction affects their survival, growth and reproduction and consequently influences the primary productivity of natural ecosystems, agricultural yield and the evolution of plant traits. A review by Amor et al. (2017) suggests that introduced populations interact with different parasites, mutualists and competitors under different abiotic conditions. Studying this multitrophic is important, as an infection by only one microorganism might not result in disease symptoms that are severe whereas the synergistic interactions resulting from co-infection with other taxa of microbes might result in the development of harsh disease. Moreover, such plant interactions can be of fundamental significance for evolution, microbial pathogenesis understanding and development of effective disease control strategies.

Microbiome based approaches development for productivity and sustainable crop yield is hindered by a lack of understanding of the main biotic factors shaping the crop microbiome (Hamonts et al., 2018). Understanding the microbe-microbe interactions on crops may provide a future source of targets for intervention and disease control (Snelders et al., 2018). Schenk et al. (2012) suggested that a better understanding of detrimental and beneficial interactions between plants and microbes might offer opportunities that are unprecedented to increase the productivity of crops.

2.11 Variables affecting the microbial community structure in the phyllosphere

Microbial communities in the phyllosphere is shaped by different factors, including, microbial interactions, environmental cues, plant phenotypes and genotypes (Vorholt, 2012). It was discovered that the leaf microbial community at the start of the season is strongly influenced by the microbiota of the soil but, with season progression, it becomes less diverse, and transitions to have a higher fraction of shared leaf-specific taxa between all samples (Copeland et al., 2015). The effect on microbial colonization of leaves is seasonally driven rather than solely driven by leaf maturity (Dees et al., 2015). Williams et al. (2013) also suggested that microbial diversity in the phyllosphere differs between seasons of planting. The phyllosphere microbial community composition can be affected by environmental factors, such as temperature, UV radiation, water availability, geographic location, nitrogen fertilization and air pollution, as well as by biotic factors, such as plant species. Plant location rather than plant species could have a significant influence on the phyllosphere community as plants growing close to each other often get infected to similar microbial inocula (Williams et al., 2013; Vorholt, 2012; Redford et al., 2010; Whipps et al., 2008b). Additionally, the phyllosphere is an open system and microbes can invade plant leaves by migration from the soil, atmosphere, other plants, animals and insects (Gu et al., 2010a). Other factors that influence microbial diversity in the phyllosphere are leaf age and irrigation (Williams et al., 2013).

2.12 Metagenomics

Handelsman et al.(1998) first coined the term metagenomics in 1998 by proposing to clone environmental DNA fragments into BAC vectors. The majority of the planet's biological diversity is comprised of uncultured microbes. The two of the three domains of life are

represented by microorganisms, however standard techniques cannot culture about 99% of the microorganisms (Riesenfeld et al., 2004). Therefore, culture-independent techniques are important in understanding the population structure, genetic diversity and ecological roles of the majority of microorganisms (Singh et al., 2009). As such, the advent of high-throughput next-generation sequencing (NGS) has brought classical environmental studies to another level and revolutionized the microbial ecology field (Oulas et al., 2015).

This type of technology has led to the introduction of the metagenomics field defined as the direct genetic analysis of genomes recovered from an environmental sample with no prior need for clonal cultures (Riesenfeld et al., 2004). Figure 2.6 shows research techniques used to fully characterize metagenomes. The term is currently and widely applied to studies performing certain genes of interest amplification (marker gene amplification metagenomics), but originally, it was only used for sequence-based and functional analysis of the collective microbial genomes contained in an environmental sample (full shotgun metagenomics).

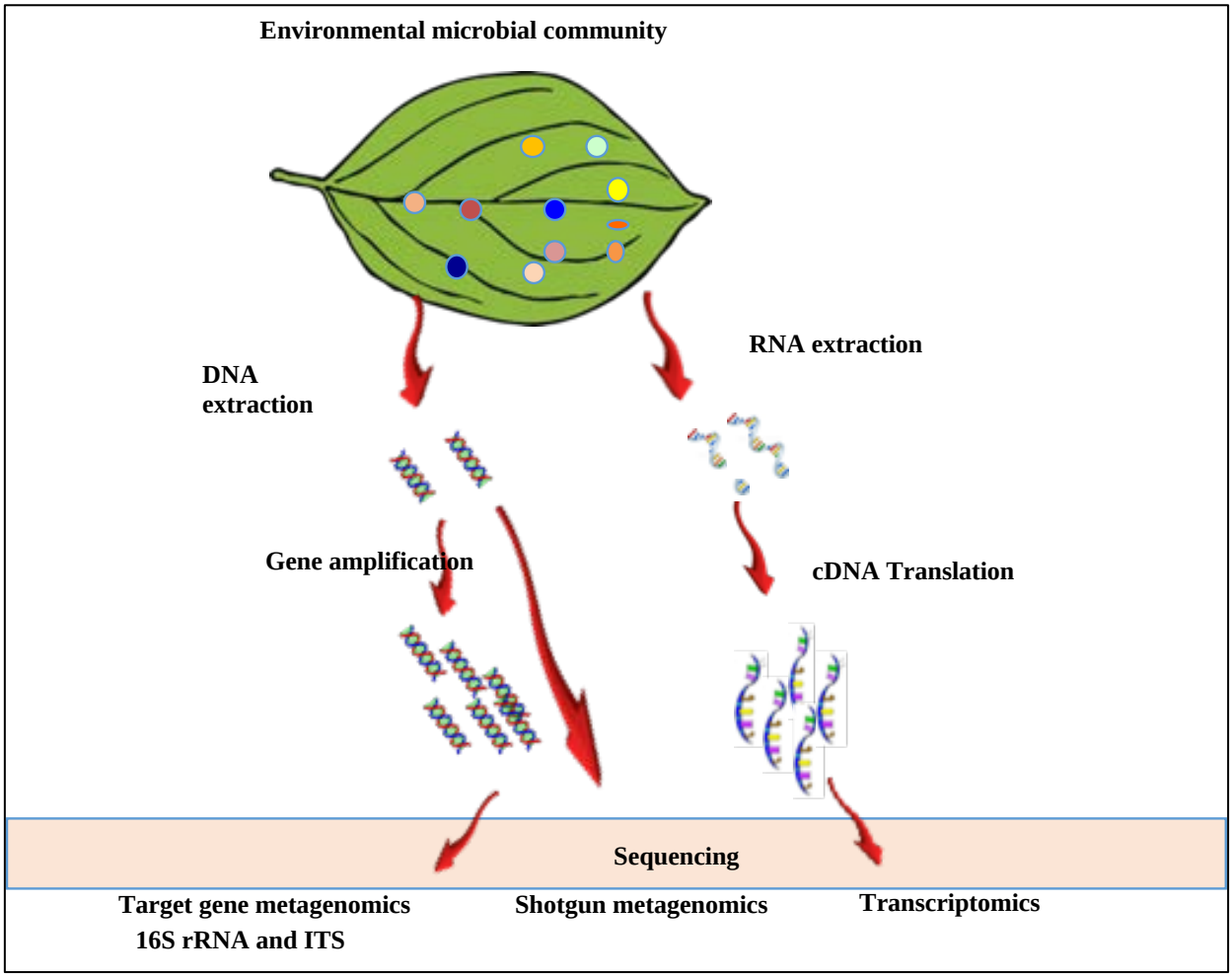

Figure 2.6: Metagenomics (metabarcoding and deep sequencing) and transcriptomics research techniques for microbes and gene expression studies in plants (Gubb and Matthiesen, 2010)

2.13 Traditional metagenomic studies

Metagenomic molecular approaches have been classified into two major categories; partial community or whole community analysis, depending on their capability to reveal microbial diversity function and structure (Rastogi et al., 2013). The partial community strategies include PCR based methods where the total RNA/DNA isolated from the environmental sample is used as a template for microorganisms characterization. The generated PCR product includes a combination of microbial gene signatures from all organisms present in the sample. In microbial ecology 16S rRNA gene amplification from environmental samples has been extensively used for partial community analysis. The PCR products amplified from

environmental DNA are analysed primarily by clone libraries, genetic fingerprinting and/or sequencing (Yadav, 2017; DeSantis et al., 2007). The whole community analysis offers a more genetic diversity comprehensive view compared to PCR-based molecular techniques targeting only a few or single genes. These approaches analyse all the genetic information present in total DNA extracted from a pure culture/ an environmental sample (Rastogi and Sani, 2011).

2.14 Next-generation sequencing (NGS) technology and bioinformatic analyses

While the metagenomic techniques explained above are highly effective in the characterization of microbial diversity, the process of cloning is costly and laborious. Next-generation sequencing (NGS) opens the possibility to conduct microbial communities studies through directly sequencing the environmental genetic material (Hugerth and Andersson, 2017; Hall, 2007), circumventing the need for cloning. There is a potential to discover new organisms that are highly divergent from those already known as they do not rely on known sequence information and are not biased towards any specific microbial group (Snyder et al., 2009). Since the advent of NGS technologies with the commercialization of 454 pyrosequencing in 2005, Illumina sequencing in 2007, and other high-throughput technologies, the genome sequencing cost has dropped significantly. NGS have impressively accelerated biological science research during the past years by allowing the production of large volumes of sequence data to an extremely lower price per base, contrarily to traditional sequencing methods (Knief, 2014). These sequencing technologies are fast high-throughput techniques for DNA sequencing and thus more appropriate for metagenomic sequencing than conventional Sanger sequencing (Cardenas and Tiedje, 2008). The Roche 454 was the first high-throughput sequencing technology successfully applied for the analysis of biodiversity (Liu, 2009), and has now been discontinued by Roche. The Illumina technology is very efficient in performing comparatively high sequencing depth despite having short read lengths, and has greatly reduced per base costs (Loman et al., 2012; Caporaso et al., 2011). Illumina currently produces a suite of sequencers (NextSeq 500, MiSeq and the HiSeq series 2000, 2500, 3000 and 4000 and Novaseq series 5000 and 6000 Systems) optimized for a variety of turnaround times and throughputs. The HiSeq and MiSeq are the most established platforms. This technology has been used for sequencing the amplicon of fungal and bacterial marker genes to characterize phyllosphere and rhizosphere microbial communities.

The recent and on-going developments in the genomics field allow researchers to address plant microbe biology questions that were not conceivable in the past years. However, a shift towards the Illumina platform is currently noticeable and in particular the MiSeq instrument is fitting for such studies as it produces reads with a length (300bp) comparable to those of the first 454 instruments at much lower cost (Allali et al., 2017; Caporaso et al., 2011). The HiSeq NGS platform aids in recovering enough rRNA reads from metagenome as it differs markedly in scale with the MiSeq platforms. HiSeq 2500 produces 600 Gb in a standard run, in contrast to MiSeq, which produces 1.5 Gb per day (Caporaso et al., 2012). Nevertheless, the amount of sequence data obtained through MiSeq runs will in many cases be adequate to obtain a sequencing depth that provides statistically significant answers to research questions.

Since the development of the next generation sequencing technologies, there has been a continuous improvement in NGS technologies with the third generation sequencing promising to further revolutionize the genomics research (van Dijk et al., 2014). The three commercially available third-generation DNA sequencing technologies are the Oxford Nanopore Technologies sequencing platform, Pacific Biosciences (PacBio) Single Molecule Real Time (SMRT) sequencing, the Illumina Tru-seq Synthetic Long-Read technology and the 10x Genomics Chromium (Edwards et al., 2019). The PacBio SMRT technology is the most established of these sequencing technologies, and was commercially introduced in 2010 (Kang et al., 2019; Roberts et al., 2013).

2.15 Metabarcoding

The development of DNA barcoding represents a significant advance in the molecular microbial identification. This technique relies on the sequencing of one or more short DNA fragments from standardized regions of the genome in identification of species (Abdelfattah et al., 2018; Hebert et al., 2003). The barcode genes are defined as any fragment of DNA that contains significant divergence and species-level genetic variability (Bingpeng et al., 2018). The oligonucleotides used to amplify the standardized region of the genome should generate short amplicons so as to be compatible with current, NGS technologies (Nilsson et al., 2019; Kress and Erickson, 2008). Furthermore, the barcode genes must possess conserved flanking

sites that may be utilized to design universal PCR primers, to provide a wide taxonomic application.

The ability for microbial communities characterization from any kind of matrix and sample has had a great impact on plant-associated microbes studies and use epiphytic, endophytic, and soil-borne (Hassani et al., 2018). The evolutionary information inferred by specific marker genes, have previously allowed hidden microbial worlds investigation, more especially in microbial ecology (Boon et al., 2014; Moreira and López-García, 2002). The opportunities provided by NGS were rapidly embraced in prokaryotic and fungal ecology (Bálint et al., 2014).

The ever-increasing metagenomic studies, conducted by metabarcoding technology and analytical software, have characterized microbial communities from complex environmental samples, and provided new information about their response to environmental factors (Rausch et al., 2019). The availability of NGS platforms makes it possible to study bacterial and fungal diseases complexes using this metagenomic approach (Ruppert et al., 2019). There have been a number of studies, on the use of NGS analysis of fungi infecting crop plants (Bai et al., 2018; Hong et al., 2015; Gu et al., 2010b; Al Rwahnih et al., 2009). Another study using NGS analysis of 16S rRNA Leveau and Tech (2010) showed that the bacterial community on leaves differed, both in size and structure, from that found/occurring on grape leaves.

2.16 Sequencing 16S rRNA gene in bacteria

The 16S ribosomal RNA (16S rRNA) gene is a well-suited marker for amplicon metagenomics phylogenetic surveys aiming to study the bacterial community, as this gene shows enough polymorphism in enabling the discernment between different taxonomic groups (Klindworth et al., 2013). The 16S rRNA gene is universally present in all bacteria and contains regions with either high or low sequence variability (Bukin et al., 2019). It is the most commonly used molecular marker in microbial ecology. NGS sequencing techniques has advanced the application of 16S rRNA profiling (Hamady et al., 2008). NGS technologies, including the Illumina sequencers, use 16S rRNA amplification primers targeting hypervariable regions,

although it is still arguable which regions are best for species profiling (de la Cuesta-Zuluaga and Escobar, 2016).

The 16S rRNA gene contains nine hypervariable regions (V1–V9) that demonstrate differential and considerable sequence diversity among different bacteria (Chakraborty et al., 2010). Although no single hypervariable region is able to distinguish among all bacteria, regions, V2, V3 and V6 provide the maximum discriminating power and contain maximum heterogeneity for analysing bacteria (Chakravorty et al., 2007). However, Kembel et al. (2012) argued that the 16S rRNA marker might not be a convenient, since it has copy numbers that are variable, with some taxa having up to 15 copies of this gene. As a consequence, there might be taxa overrepresentation in the final set of sequences and that could lead to community structure estimations that are biased. However, the use of 16S rRNA gene marker advantages outweigh this inconvenience and that is why amplicon sequencing it is widely used in surveys.

2.16.1 Challenges sequencing 16S rRNA gene in plant microbes

One of the main obstacles when using 16S amplicons metagenomics for evaluating the plant-associated microbial community and diversity is the amplification of eukaryotic organelle DNA by most primers. The chloroplast and mitochondria genomes from the plant, and bacterial 16S rRNA sequences of bacteria are homologous and this homology makes bacterial rRNA gene amplification and sequencing difficult. This will then result in most of the sequence data being from plant sequences, which is of no interest to the study. This is true for studies aimed at assessing endophytic microbial diversity, as the extraction of DNA is performed directly from plant tissues, resulting in an increased plant DNA content in the extract. Zarraonaindia et al. (2015) presented that the chloroplast sequences posed the biggest problem on *Vitis vinefera*, since they can make up to 98% of the sequences obtained using the Illumina MiSeq sequencer, in contrast to mitochondrial sequences which do not seem to pose a significant problem.

Chloroplast sequences are most closely related to nitrogen–fixing unicellular Cyanobacteria (Kembel et al., 2014). It is typically possible to distinguish between bacterial DNA sequences and eukaryotic organelle DNA sequences, but it does complicate the bacterial community analysis (Bulgarelli et al., 2013). The utilization of sequence-specific peptide nucleic acid

(PNA) clamps, which bind to, and block host-derived DNA amplification has been conducted. PNA oligos are polymers of purine and pyrimidine bases connected via peptide bond and are artificially synthesized. Due to their specificity of the sequence, PNAs are designed to bind host organellar sequence variants of a target region and efficiently block their PCR amplification (Figure 2.7). Universal PNA clamps have been suggested to being able to obstruct/block host plant-derived mitochondrial (mPNA) and plastid (pPNA) sequences at the V4 16S rRNA locus (Fitzpatrick et al., 2018). PNA clamps suppress the mitochondrial and plant host plastid 16S contamination and reduce the bias and produce sequencing results that are more accurate through PNA clamping. PNA clamping occurs when the PNA probes have strong specificity to its target DNA and binding affinity, and are not being recognized by DNA polymerase as a primer. However, these universal PNAs efficacy was tested only in the *Arabidopsis thaliana* model plant (Fitzpatrick et al., 2018; Lundberg et al., 2012). Another set of blocking primer based on the technique described was established to reduce non-target plant DNA amplification when performing metagenomic research on microbial endophyte communities. Compared to a standard PCR in an Illumina-based study of *Sorghastrum nutans* leaves, bacterial amplification efficacy was increased 300-fold (Arenz et al., 2015).

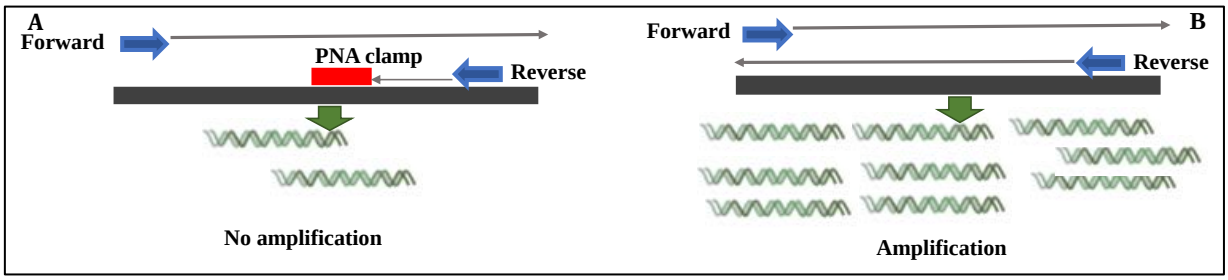

Figure 2.7: Indicates how the PNA clamp suppresses the amplification of the host DNA. The presence of the PNA clamp suppresses the amplification of the host DNA, resulting in no amplification of the host DNA. B The absence of the PNA clamp resulted in the amplification of the host DNA.

Another primary challenge faced in plant-associated metagenomic studies is the recovery of good-quality DNA (mDNA) that can allow reliable downstream analyses using PCR-based technique. There is a couple of studies that evaluated different mDNA extraction procedures to retrieve endophytic bacterial diversity and quality DNA (Wust et al., 2016; Maropola et al., 2015). Their study concluded that commercial kits retrieved higher quality mDNA when compared to classical DNA extraction protocols. Maropola et al. (2015) study forms a baseline for the current study.

2.16.2 The internal transcribed spacer region (ITS) sequencing

Fungal analyses have relied on traditional phenotypic and morphologic features, which were the main criteria for fungal classification for a long time (Cuadros-Orellana et al., 2013). However, due to the phenotypic overlap between different taxa, the existence of intermediate forms and the instability of morphological traits, these traditional approaches alone does not allow for reliable fungal classification at lower taxonomic levels (Feau et al., 2009) even at the light of modern molecular techniques (Cuadros-Orellana et al., 2013). Methods that relies on parallel sequencing of short DNA fragments amplified by PCR have been widely used (Schoch et al., 2012).

Target-gene amplicon sequencing application is the most exhausted high-throughput sequencing in microbial ecology. The fungal genetic marker internal transcribed spacer (ITS) has been proposed to be the official fungal primary barcode (Coissac et al., 2016; Fajarningsih, 2016; Das and Deb, 2015). It is a non-coding region that is highly polymorphic, with enough taxonomic units and has the ability to separate sequences into species level (Fajarningsih, 2016). It is located in the ribosomal RNA operon and has a length ranging from 450 to 750 bp (De Beeck et al., 2014). The advantage of using ITS as DNA barcoding is that it has been used in many studies and has updated reference sequences that exists in the NCBI database (Samson et al., 2019). The most commonly used oligonucleotides for sequence-based fungal classification at the species level are ITS1, ITS2, ITS3 and ITS4 (Gardes and Bruns, 1993; White et al., 1990). These oligonucleotides pairs have been used in many mycological research branches and are popular tools in fungal community research (Tedersoo et al., 2018; Amend et al., 2010; Jumpponen et al., 2010; Buée et al., 2009).

2.17 Meta-barcoding bioinformatic analyses

Bioinformatic analysis of plant microbiome and gene expression studies demands the use of tools that effectively analyses the large amount of data produced from deep and amplicon sequencing for gene expression patterns and overview of taxonomic classification. Various tools are available for analysis of 16S rRNA gene sequencing data and include, Quantitative Insights Into Microbial Ecology (QIIME) (Caporaso et al., 2012), MOTHUR, and Metagenomics - Rapid Annotation using Subsystems Technology (MG-RAST) (Meyer et al., 2009). These pipelines are self-contained and are widely used for amplicon metagenome analyses. Additionally, they can be utilized to process 16S rRNA gene sequences from quality control to taxonomic classification and are three of the most cited and generally used pipelines in 16S rRNA gene sequences analysis (Plummer et al., 2015). The comparison between the diversity and taxonomic compositions generated by MG-RAST and QIIME using samples from the gastro-intestine was investigated (D'Argenio et al., 2014). The study did not find any significant changes in the alpha diversity measures or microbial compositions; however it was concluded from the study that QIIME produced compositional assignments that are more accurate, primarily due to the inability to classify large number of reads by MG-RAST. Plummer et al. (2015) did the similar investigation comparing the MOTHUR, QIIME and MG-RAST pipelines. The pipelines detected the similar abundances at phylum level. Pipeline difference was observed with regard to genera taxonomic assignments from the *Enterobacteriaceae* family, particularly *Klebsiella* and *Enterobacter.*

2.18 Gene expression and Bioinformatics

While high-throughput sequencing has enabled the use of metagenomic DNA for taxonomic classification (Tett et al., 2012). However, a metagenome contains relatively few rRNA genes reducing the taxonomic assignments strength and also it doesn't allow the functional annotation in a host. Other techniques are necessary to identify which genes are actually being expressed through transcriptomics. Transcriptomics, is a method where total RNA from the environment is sequenced to reveal active community members and metabolic pathways in a sample. This is technically much less challenging than enrichment of mRNA and avoids PCR biases. The incorporation of transcriptomics and metagenomics will therefore extensively assess/identify the plant microbiome taxa and the genes expressed upon pathogen infection.

Historically, mRNA expression has been conducted by qPCR or microarray based approaches. However, the two technologies have not been reliable in evaluating novel alternative splicing isoforms (Shendure, 2008). The inexpensive and rapid sequencing capacity offered by next-generation sequencing instruments has become the main choice to measure gene expression levels. Reconstruction of novel and known transcripts at single-base level, with broad dynamic range, and not limited by signal saturation and reproducibility levels that are high are key advantages offered by RNA-Seq over hybridization-based technologies (Roy et al., 2011; Bullard et al., 2010; Shendure, 2008). RNA-Seq is an NGS based technology for profiling the RNA that enables the measurement and comparing gene expression patterns at unprecedented resolution based on next-generation sequencing (Finotello and Di Camillo, 2015). RNA-Seq is the standard method for transcriptome analysis generating a huge volume of data. However, its interpretation is not straightforward and accurate data analysis involves choices of tools and several different steps (Kukurba and Montgomery, 2015). Subsequently, the advent of RNA-Sequencing (RNA-Seq) technologies, introduced various statistical analysis tools for differential gene expression (DGE) (Hrdlickova et al., 2017). Twenty five (25) pipelines performance for testing differentially expressed genes in RNA-Seq data were recently evaluated and no single tool uniformly performed better than the others (Assefa et al., 2018). Cuffdiff also forms part of the pipelines utilized to test for differentially expressed genes, test the statistical significance of observed changes and is used to quantify transcript abundance measured by fragments per kilobase of transcript per million fragments mapped (FPKM) (Li et al., 2018). A basic reference based data analysis pipeline consists of pre-processing (remove sequences with low quality to get better alignment), alignment of the raw reads with the reference genome, assembly of the transcripts and detection of differentially expressed genes (Yalamanchili et al., 2017).

2.19 Pathway and cluster analysis

The data generated from RNA-Seq is extremely large and user-friendly tools to analyze it have been developed (Tagliaferri et al., 2014). The analysis of transcriptomics data requires access to statistical methods that are robust, data analysis tools to identify patterns and transcripts correlating with the experimental phenotypes. MultiExperiment Viewer (MeV) is a Java-based application allowing analysis of advanced gene expression data (Howe et al., 2011). This

softwares could be used for gene expression analysis, and includes, hierarchical clustering, t-tests, k-means clustering, EASE and analysis of variance (ANOVA) (Howe et al., 2011).

Clustering methods for RNA-Seq data time series partitions genes into disjoint clusters based on expression response similarity. K-means clustering (Tavazoie et al., 1999), hierarchical clustering (Eisen et al., 1998) and self-organizing maps (Tamayo et al., 1999) are clustering methods, that evaluate similarity response using Euclidean distance or correlation. These clustering approaches assume that adjacent time points expression levels are independent, which is not valid for time series transcriptome data (Ramoni et al., 2002). A couple of these approaches demand for post hoc analyses and model selection to dictate the number of clusters that are most appropriate. The Dirichlet Process Gaussian Process mixture model (DPGP) has been developed to circumvent the problem that the other clustering methods presents in measuring gene expression levels across time (McDowell et al., 2018). DPGP has compared favourably to time series data clustering methods that currently exists. It is the most accessible, publicly-available software package and it is robust to non-Gaussian marginal observations (McDowell et al., 2018).

Although the statistical approaches on DEGs provides valuable information regarding the changes across phenotypes, they alone cannot describe the complex mechanisms that are involved in the given condition (Nguyen et al., 2019). The most common tools used to address this is to search the knowledge contained in various pathway databases such as Kyoto Encyclopedia of Genes and Genomes (KEGG) (Kanehisa et al., 2004), Reactome (Fabregat et al., 2018), BioCarta (Adriaens et al., 2008), NCI-PID WikiPathways (Schaefer et al., 2009) and PANTHER (Thomas et al., 2003). The analysis of pathway approaches use databases and the given gene expression data to identify the significantly impacted pathways in a given condition (Conesa et al., 2016).

2.20 CONCLUSION

In summary, over the last three decades, since the first studies using the concept of metagenomics, extraordinary advances in permitting measurement of population diversity levels *in situ* and allowing the prediction of functions encoded by microbial communities in the field have been achieved. The phyllosphere is an economically and scientifically important microenvironment in which to conduct microbial ecology studies and is also suggested to be one of the entry site for pathogens. It has been discussed in details as this plant microenvironment has more to contribute to the microbial ecology field, plant pathology and plant genomics. The phyllosphere also contribute in providing more efficient and less environmentally harmful means of plant protection. *Sorghum bicolor* has emerged as an essential food security crop, as well as biofuel production, that is both salt and drought tolerant, and its review with regards to domestication, taxonomy and importance has been discussed in details. Next Generation Sequencing (NGS) has revolutionized the research on bacterial and fungal compositions in plants, and high-throughput sequencing is now at a state that it is very good for analysing ITS and 16S rRNA sequences for fungal and bacterial community. When conducting these studies, it is imperative that metagenomic information overload be transformed into biological understanding. It was reviewed in this chapter that bacteria and fungi can synergistically interact to stimulate plant development through a range of mechanisms that include inhibition of fungal plant pathogens and improved nutrient acquisition. These interactions can be of significance in maintaining soil fertility and plant health, within sustainable low-input agricultural cropping systems that depends on biological processes rather than agrochemicals. Metagenomics through barcoding has proved to be an efficient microbial ecology tool, to determine who is there. However, it cannot determine the genes expressed in response to biotic/abiotic stress inflicted upon the host. Existing functional screening metagenomic methods usually have low rates of gene target identification. Therefore, the construction of an alternative tool that is able to detect enzymatic activities/other target gene output is required. This challenge lead to the introduction of transcriptomics, where total RNA from the environment is sequenced revealing active functional annotation and

metabolic pathways. This greatly come into play to be able to circumvent the inability of metabarcoding in revealing functional annotation, and has been discussed in details. Incorporating meta-barcoding (describing the taxonomic classification) and transcriptomics approaches (functional approaches) will improve the understanding on the taxa making up a community and also predict the functional roles in the ecosystem. Bioinformatic softwares have been developed that can deal with both microbial community analyses and gene expression studies. In conclusion, by combining the collective information in overcoming the previously described challenges. Shedding light on the “hidden” world of uncultured microorganisms and its inherent enzymatic treasures shall make it possible to integrate emerging concepts in the plant pathology and genomics field. Collective intelligence from a plethora of experts is imperative in bringing biotechnological solutions and answering central biological questions in a myriad of different fields in this review. This will therefore, expand the knowledge currently present in a myriad of areas.

CHAPTER 3

Identification of bacterial and fungal populations on/within sorghum leaves that are naturally infected with various diseases through the use of metabarcoding

3.1 INTRODUCTION

The past three decades of research using model plant systems (*Nicotiana tabacum* and *Arabidopsis thaliana*) have revealed a variety of plant adaptations, which have evolved in response to both biotic and abiotic environmental stressors (Ritpitakphong et al., 2016; Lundberg et al., 2012; Ryu et al., 2007). Recently, studies have shown that both healthy and asymptomatic plants co-exist with diverse assemblages of microorganisms including protists, archaea, fungi and bacteria (Lebreton et al., 2019; Hassani et al., 2018). These microorganisms have collectively been shown to influence plant growth and productivity (Stone et al., 2018; Almario et al., 2017; Buée et al., 2009; Lindow and Brandl, 2003). Plant-associated microorganisms positively influence plant health by increasing nutrient acquisition, stress tolerance and pathogen resistance (del Carmen Orozco-Mosqueda et al., 2020; Finkel et al., 2019; Jones et al., 2019; Tsolakidou et al., 2019; Schirawski and Perlin, 2018; Mia et al., 2014). Yet, the understanding of the interplay between microbiomes and plants remains rudimentary and has largely focused on model plant species (Berendsen et al., 2018; Edwards et al., 2015; Aleklett et al., 2014).

Understanding the interaction between microbiomes and plants is central to the elucidation of the response to biotic and abiotic stress in agriculturally important crops. To ensure food security, it is essential to optimize the reliability of production pipelines by minimizing environmental impacts (Saad et al., 2020; Wille et al., 2019). Integrating insights regarding beneficial plant microbiomes to enhance plant growth and disease resistance will contribute to increased agricultural production which will ultimately contribute to food security (Busby et al., 2017; Mounde, 2015; Pascale et al., 2020; Sivakumar et al., 2020).

While the vast majority of microorganisms are beneficial to plant growth, plant pathogens may colonize leaves and overwhelm the innate plant defence mechanisms in order to cause diseases. This colonization by fungal and bacterial pathogens is a direct threat to the productivity and sustainability of sorghum production (Chala et al., 2019; Bandara et al., 2017; Kelly et al., 2017). Sorghum is a versatile crop that can be grown as grain and sweet crop. However the full potential of sorghum productivity has not been realised due to an array of biotic and abiotic

constraints (Mengistu et al., 2016). Plant pathogens represent a constant and major food production constraints, with global crop losses estimated to be 20%– 30% principally in food-deficit areas (Savary et al., 2019).

Elucidating the composition of the sorghum microbiome and relating this to its effects on plant health may provide important cues to potential strategies for pathogen management. The few studies available on the sorghum microbiome have been mainly based on culture-dependent methodologies, which are known to miss 99% of microbial communities (Sanmartín et al., 2018; Tripathi et al., 2018; Mihajlovski et al., 2015). Recent reports, using metagenomic analysis, have revealed potential key taxa associated with the rhizosphere and seed of sorghum (Kuramae et al., 2020; Hara et al., 2019; Kinge et al., 2019; Xu et al., 2018 Guo, 2016). However, none of these studies assessed the aerial region of the plant, which is suggested to be one of the primary entry sites for pathogens (Cernava et al., 2019). This knowledge deficit is broadly true for plants where, in contrast to the rhizosphere, substantially less is known regarding the effects of plant-microbe associations on foliar diseases.

Regardless of sorghum recombinant lines (RILs) being suited to all proposed approaches for renewable fuel production i.e., from starch, sugar, and/or cellulose (Xie et al., 2018), less is known with regard to their leaf microbial structure. *Sorghum bicolor* and *Sorghum propinquumis* have been used for early-generation genetic analysis by single-seed descent and differs in traits related to plant architecture, growth and development, reproduction, and life history (Kong et al., 2013). The F2 generation sorghum inbred lines produced from this are the widest euploid cross that can be made with the cultigen (*S. bicolor*) by conventional means. The interspecific populations from these lines offer opportunities to genetically dissect a wide range of traits related to plant domestication and crop productivity, some of which have begun to receive attention (Feltus et al., 2006; Chittenden et al., 1994). The opportunities offered by comparison of *S. bicolor* and *S. propinquum* have led to much effort to develop genomics resources, including a detailed genetic map (Bowers et al., 2003).

Sorghum recombinant lines used in this study are useful models, however, the microbiomes of these RILs and the relationship to plant health has not been examined. To increase the understanding of the foliar microbiomes of sorghum RILs and its link to natural infection,

bacteria and fungi associated with asymptomatic and symptomatic plants using 16S ribosomal ribonucleic acid (rRNA) gene and internal transcribed spacer (ITS) region sequencing, respectively were characterized. In addition to revealing the relative abundance patterns of bacteria and fungi the significant differential abundance of taxa in asymptomatic and symptomatic sorghum RILs was assessed. Adding to revealing the fungal and bacterial relative and differential taxa abundance patterns the co-occurrence dynamics and diversity measures of fungi and bacteria were examined.

3.2 MATERIALS AND METHODS

3.2.1 RIL material

The mapping population was originally derived by selfing a single F1 plant from *S. bicolor* grain (M71) and sweet sorghum (SS79) and advanced to the F9 generation by single seed decent (Shiringani et al., 2010) to produce a mapping population of 187 F9 recombinant inbred lines (RILs). These RILs were mapped for quantitative traits such as grain yield and stem sugar-related traits for biofuel yield of sorghum. The F9 generation seeds used in this study were collected from the Agricultural Research Council (ARC) - Grain Crops Institute, Potchefstroom, South Africa (see RIL information Appendix Table 3A.1).

3.2.2 Cultivation of sorghum RILs

The sorghum RIL seeds were cultivated in a mixture of autoclaved vermiculite and perlite medium in pots sterilized with 70% ethanol at the ARC - Biotechnology Platform (ARC-BTP), Onderstepoort, South Africa. A pot experiment was carried out in a net-house which was used to reduce the damage caused by insects, wind and the hail in the crop. The net-house was used to mimic nature and is naturally ventilated and climate controlled (natural temperature and light). The RILs were subjected to the same planting conditions and were left to grow until the matured grain filling developmental stage (120 days old plant) to allow the plants to be naturally colonized by pathogenic and commensal microbes. Moisture was maintained by watering to weight every 2–3 days. To assess the role of sorghum leaf microbial community structure in sorghum disease manifestation, 45 leaf samples (1^{st}/ 2^{nd} leaf below the flag leaf - emerged final leaf) from individual RILs at the grain filling stage (maturity) were retrieved. The foliar symptoms (Table 3.1) were scored according to the method described by TeBeest et al. (2004). The pathogen susceptibility of the RILs was based on foliar symptoms after allowing for natural infection by pathogens. The scale used presented visual foliar symptoms of four models that denoted, resistant (R), moderately resistant (MR), susceptible (S) and highly susceptible (HS) disease groups under natural infection. The symptoms and lesions on the leaf area of the R group was (1-10%) with MR, S and HS symptoms and lesions represented by 11-30%, 31->50% and 51->75%, of the leaf area, respectively.

3.2.3 Sampling

Leaf samples were collected from 45 individual RILs based on the even distribution of phenotype (foliar symptoms) across all disease groups. The number of samples collected for the resistant group (R) were (n = 11), moderately resistant (MR) (n = 10), susceptible (S) (n = 12) and highly susceptible (HS) (n=12) were confirmed with the Chi-square test in Excel. Table 3.1. The leaves were harvested by hand (using gloves and forceps which was pre-sterilized with 70% ethanol for each leaf sampled). The leaf samples were kept in sterile bags in a -4°C ice box and were stored in a −80 °C freezer until further processing (this was to ensure that DNA is of good quality for further processing).

3.2.4 DNA extraction, PCR amplification and sequencing

Leaf material was crushed using the Savant Fastprep^{TM} FP120 Cell Disruptor (Thermofisher Scientific), followed by total DNA extraction using the Chemagic DNA Plant Kit (Chemagen, Perkin Elmer) as detailed in the manufacturers protocol. For bacterial amplification, primers with a PNA-PCR clamp added to block the amplification of host DNA were used to amplify the 16S rRNA gene V3-V4 region (Lundberg et al., 2012; Herlemann et al., 2011). For fungi taxon-specific primers, ITS1 and ITS4 regions were amplified as described previously (Gardes and Bruns, 1993). Amplicons were purified using the MinElute® PCR Purification Kit (Qiagen). The concentration and quality of the purified PCR product was evaluated using the Qubit Fluorometer (Invitrogen). The amplicon library was normalized and prepared for sequencing following the Illumina MiSeq 16S rRNA gene library preparation guide (Illumina 2016). Sequencing was done by utilizing the MiSeq Illumina Sequencer (Illumina, San Diego, CA) with a MiSeq Reagent Kit v3 to generate 2 × 300 paired end reads at the ARC Biotechnology Platform.

3.2.5 Bioinformatics analyses

3.2.5.1 Operational Taxonomic Unit (OTU) Assignment

Analysis of bacterial and fungal communities was performed using the Quantitative Insights Into Microbial Ecology (Qiime2) version 2019.10 (Caporaso et al., 2010) with demux plugins (https://github.com/qiime2/q2-demux) (Amir et al., 2017). Forty-five samples of 16S and ITS sequencing data were received in the fastq file format and included forward and reverse paired-end reads. MiSeq 2500 generated ITS and 16S rRNA data was de-multiplexed at the sequencing facility. The forward and reverse reads, were combined into one "qza" file in the conda environment and then imported into Qiime2 using the Casava 1.8 pipeline (paired-end).

The length of nucleotides to trim and truncate, for the subsequent Deblur qiime denoise analysis was obtained from the demux.qzv visualization. The demux.qzv visualization showed the quality scores of the reads, which allowed for the removal of reads with lower than Phred33 scores. Deblur plugin was used to remove chimeric sequences and sequence variant calling of the Illumina-amplicon sequences.

Taxonomic assignments were performed using qiime feature-classifier classify-sklearn in which a pre-trained Naïve-Bayes classifier SILVA 138 database (Yilmaz et al., 2014) was used for bacterial taxonomic classification. For fungal ITS taxonomy analysis, a UNITE database (https://unite.ut.ee/) was used. Compositional and taxonomic analyses were conducted by using feature-classifier plugins, i.e. composition (Mandal et al., 2015) and taxa (https://github.com/qiime2/q2).

Sequences were binned according to similarity, resulting in operation taxonomic units (OTUs), followed by the generation of a representative sequence for each OTU (Schloss and Handelsman, 2005). The resulting representative sequences, hereinafter referred to as OTUs, were used for downstream taxonomic assignment and diversity metrics. The feature table was then used to generate a phylogenetic tree with the "phylogeny fasttree" command (Price et al., 2010). The complete list of commands and the system details are listed in Appendix C.

3.2.5.2 Exploratory analyses

Exploratory analyses were performed in R v.3.5.1 and Bioconductor v.3.0 (Gentleman et al., 2004). Briefly, Rarefaction curves were computed using phyloseq. The two alpha diversity indices were computed (Simpson and Shannon) to measure diversity by accounting for dominance and richness in phyloseq. These indices were obtained using the plot_anova_diversity function of the microbiomeSeq package (Heruth et al., 2016). β-Diversity was visualized using PCoA ordinations generated with the Bray–Curtis distance metric. Ordinations were created with the phyloseq and ggplot2 (v2.1.0) packages. Pair-wise analysis of variance (ANOVA) of diversity measures were computed using microbiomeSeq (McMurdie and Holmes, 2013), with plot_anova_diversity function. β-Diversity was measured using PERMANOVA with the betadisper function from the microbiomeSeq package (Heruth et al., 2016; Oksanen et al., 2007). Taxonomic classification data was normalised and visualised using phyloseq and microbiomeSeq package. Differential abundance plots between the disease groups were obtained through the use of DESeq2 R package (Love et al., 2014) with p-value cutoff of 0.05. Networks interactions were done using the R package Sparse InversE Covariance estimation for Ecological Association and Statistical Inference (SpiecEasi) (Kurtz et al., 2015), with neighbourhood selection (MB method). The complete list of R packages and scripts are listed in Appendix C.

3.3 RESULTS

3.3.1 Foliar assessments reveal discrete pathogen groups which were evenly distributed (Chi-square tests).

The results from foliar assessments delineated the grouping of RILs into the following disease groups: resistant (R) (n = 11), moderately resistant (MR) (n = 10), susceptible (S) (n = 12) and highly susceptible (HS) (n=12) (Table 3.1). Comparisons of the distribution of disease groups were generated between R, MR, S and HS using Chi-square tests. These analyses showed that the number of samples per disease group was evenly distributed.

Table 3.1: The samples from individual RILs of which manual foliar disease rating was done based on visual symptoms of the leaves collected according to a rating scale described by TeBeest et al. (2004).

Severity scale	Symptoms and lesions	Disease reaction	No of samples	Visual symptoms
2 3	1-5% leaf area 6-10 % leaf area	Resistant (R)	11	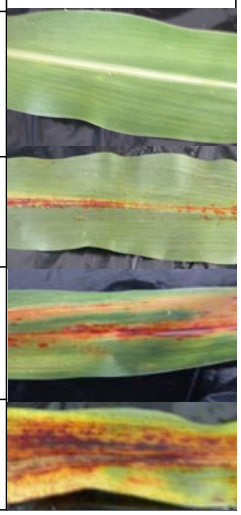
4 5	11-20 % leaf area 21-30 % leaf area	Moderately resistant (MR)	10	
6 7	31-40 % leaf area 41-50 % leaf area	Susceptible (S)	12	
8 9	51-75% leaf area > 75% leaf area	Highly susceptible (HS)	12	

3.3.2 Rarefaction curves for samples used in this study (phyloseq)

The illustrated rarefaction curves primarily determines the minimum sample size and also indicates the number of OTUs with a given depth of sequencing. The bacterial and the fungal rarefaction reached the near plateau phase depicting satisfying sampling depth (Figures 3.1A and 3.1B respectively).

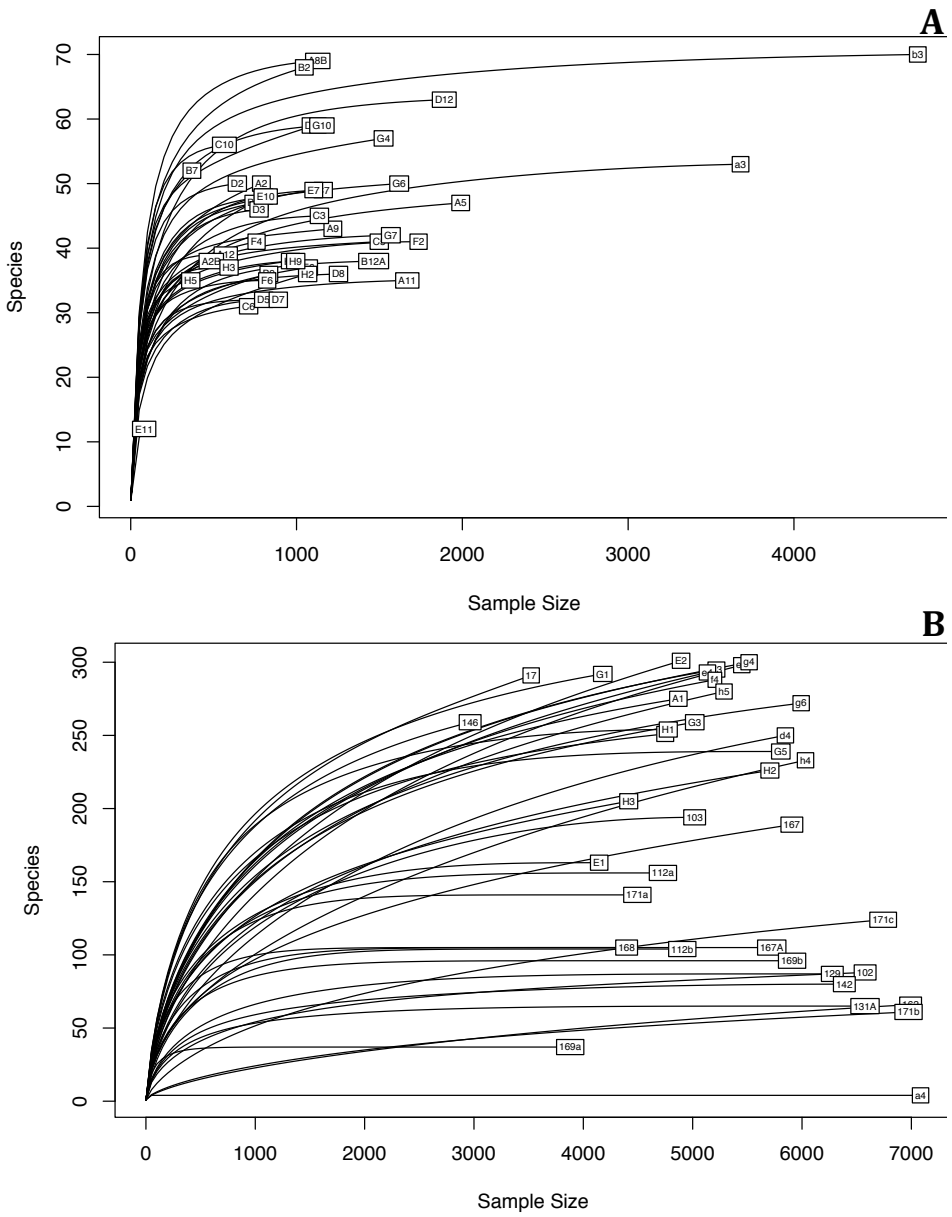

Figure 3.1: Curve showing the number of individual (A) Bacterial and (B) Fungal OTUs identified in a given rarefaction. The rarefaction curves were generated using vegan, with an OTU defined at 97% similarity.

3.3.3 Bacterial and fungal alpha diversity of sorghum leaves (microbiomeSeq package)

Estimates of indices measuring richness (Shannon) and dominance (1-Simpson index), showed that the bacterial alpha-diversity differences resulted in HS disease group significantly harbouring high bacterial species richness (Shannon), compared to R group (ANOVA, p-value = 0.034; df = 19) Figure 3.2A. However, diversity measures which account for dominance (1-Simpson index) suggest that HS samples were dominated by fewer species (ANOVA, p-value = 0.05; df = 19). The R group was significantly more diverse (ANOVA, p-value = 0.05; df = 19) consistent with low 1-Simpson index values compared to the other disease groups, based on species dominance (Figure 3.1B). The Shannon index of the S disease group was associated with high species richness compared with the R group (ANOVA, p-value = 0.026; df = 18). The diversity measures for the MR group did not show any significant difference with the other disease groups (see Appendix C for detailed statistics on fungal and bacterial alpha diversity measures).

Similarly, the fungal alpha-diversity differences between disease groups were statistically significant. The HS disease group had a significantly higher Shannon–Weaver index compared to the R group (ANOVA, p-value = 0.034; df = 19) Figure 3.1B. Fungal population diversity measure 1-Simpson index indicated a significant difference between HS and R (ANOVA, p-value = 0.05; df = 19). Indices measuring dominance (1-Simpson index) suggest that the fungal populations on HS plants were less diverse compared to those on R plants. A significant difference in the Shannon–Weaver index between S and R (ANOVA, p-value = 0.0136; df = 18) was observed, with S disease group indicating higher species richness. The MR group did not show any significant difference in 1-Simpson index diversity. However, in terms of the Shannon index, the MR group was associated with high species richness.

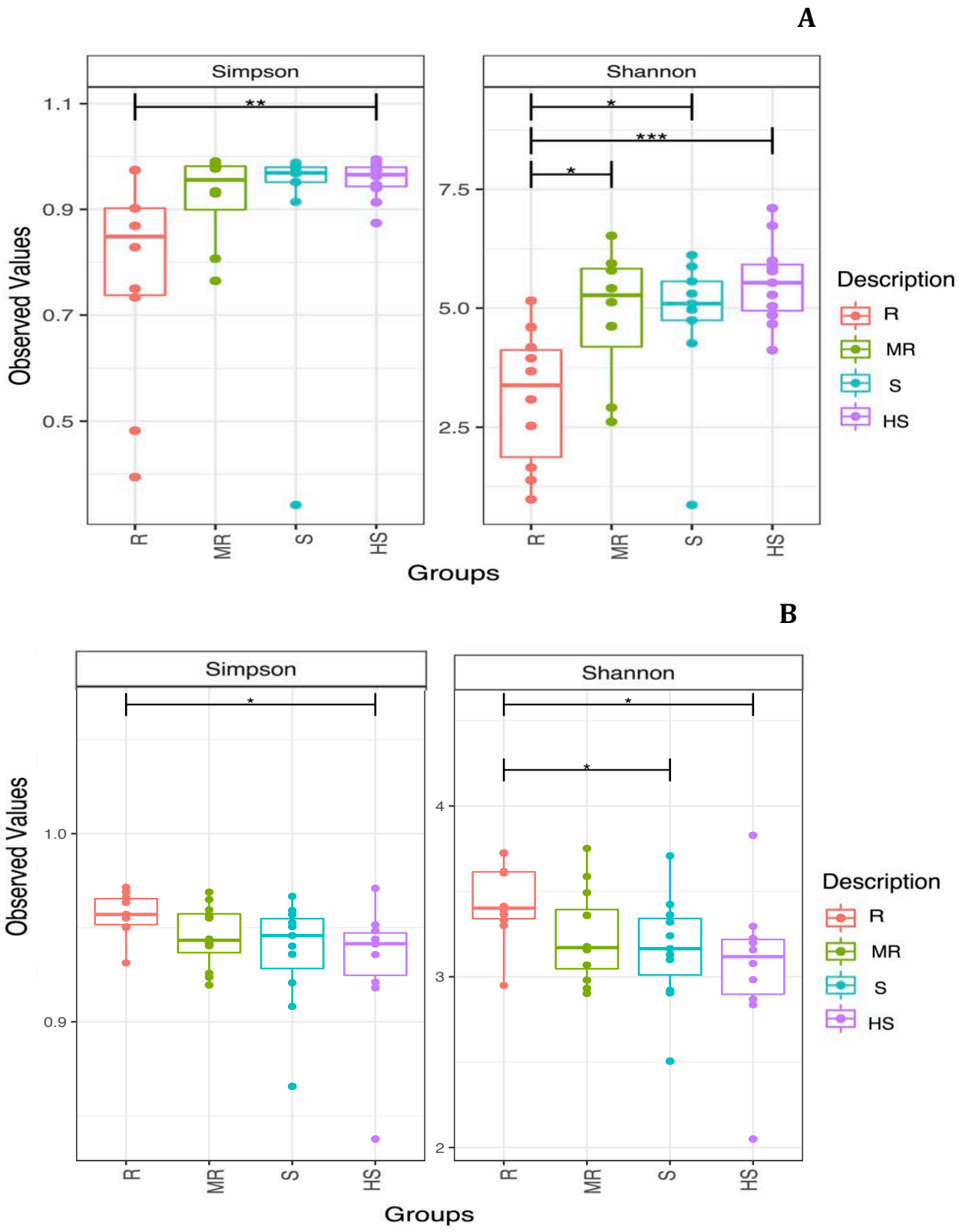

Figure 3.2: (A) Bacterial (B) Fungal alpha diversity metrics based on Shannon's and 1-Simpson's diversity indices on disease groups R, MR, S and HS. The box plots represent

the observed bacterial and fungal values based on richness, and dominance of different disease groups. The lines represent the interquartile range and asterisks above the boxplots represents statistically significant differences at (p-value < 0.05) plotted using the plot_anova_diversity function within MicrobiomeSeq R package. For 1-Simpson index box (**p-value = 0.05; df= 19 between HS and R), for Shannon index box plot (*** p-value = 0.034, df= 19 between HS and R), (* p-value = 0.013; df = 18 between R and S) in Fungi. For bacterial alpha diversity 1-Simpson index box (* p-value = 0.05; df = 19 between HS and R), for Shannon index box plot (*p-value = 0.034; df = 19 between HS and R), (* p-value = 0.026; df =18 between R and S)

3.3.4 Beta-diversity and disease severity (microbiomeSeq package)

Bacterial abundance variation, beta- dispersion revealed a significant difference between the R and S group ($P_{PERMDISP}$ = 0.04; df = 18) Figure 3.3A. Permutation analysis of variance (PERMANOVA) and corresponding r-squared revealed that microbial communities were significantly differentiated across all the disease groups, with (R^2=0.16, $P_{PERMANOVA}$ = 0.001; df = 41) for bacteria and (R^2= 0.216, $P_{PERMANOVA}$ = 0.001; 41). PCoA showed a cluster for each disease group and the differences between the clusters were tested for significance using PERMANOVA (Figure 3.3B). Beta-dispersion, used to measure variances in fungal abundance revealed the significant differences in the microbial community dispersion (within-group variation in beta-diversity) between MR and HS ($P_{PERMDISP}$ = 0.002; df = 18) and R and HS ($P_{PERMDISP}$ = 0.005; df = 19). See supplementary statistics details for fungi and bacteria in Appendix Table 3A.5 and Appendix Table 3A.6 respectively.

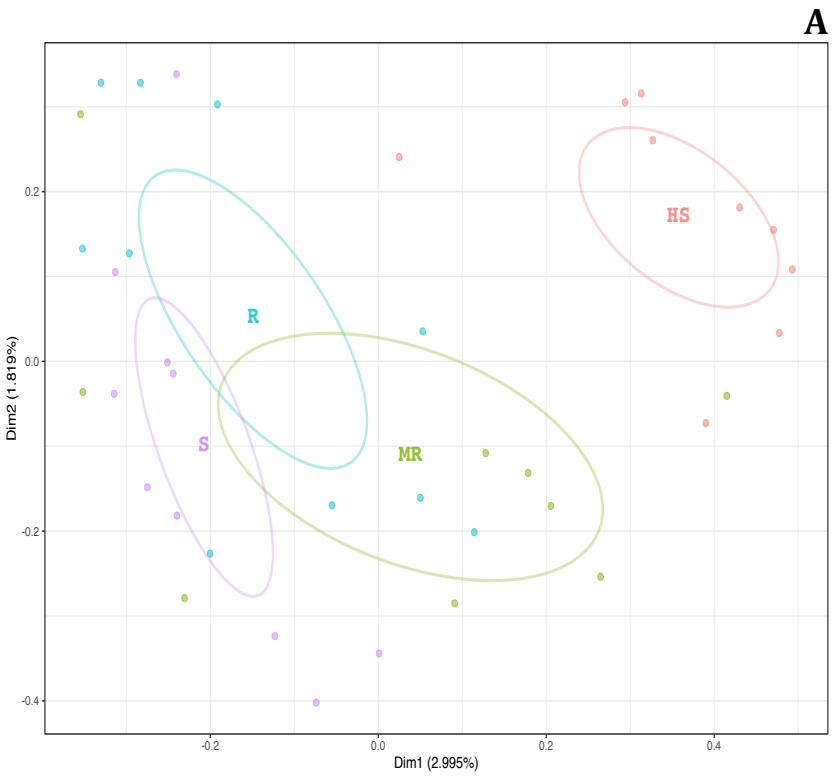

PERMANOVA
R^2= 0.216
p-value= 0.001 ***

BETA-DISPERSION
HS-MR p-value=2e-03 **
HS-R p-value=5e-03 **

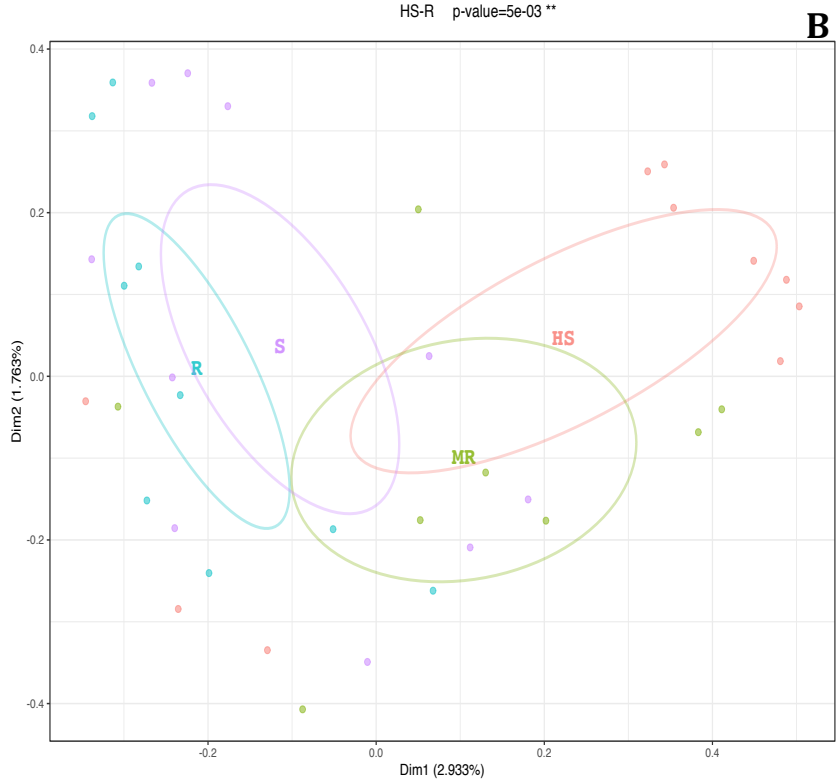

PERMANOVA
R^2= 0.16
p-value= 0.001 ***

BETA-DISPERSION
R-S p-value=4e-02 *

Figure 3.3: Beta diversity of (A) Bacterial and (B) Fungal communities represented via Principal Coordinates Analysis (PCoA) based on Bray-Curtis distance from the PERMANOVA analysis (betadisper function) across disease groupings (R, MR, S and HS). Groupings is based on the categorical factors depicted with ellipses representing the standard error around the centroid.

3.3.5 Bacterial and fungal composition of sorghum leaves (microbiomeSeq)

The impact of microbial communities on sorghum RILs after exposure to natural infection by pathogens was assessed in this study. The bacterial and fungal composition observed consisted of both disease-causing and reported beneficial taxa. Analysis of bacterial abundance, revealing the composition of commensal and pathogenic bacteria of sorghum RILs across all disease groups at the family and genus levels is shown in (Figures 3.4A; 3.4B and Table 3.2). The known pathogen *Pantoea* (~ 10%) were exclusively associated with the HS disease group. The S disease group had a higher relative abundance of the genera *Siccibacter* and the pathogenic genus *Cronobacter* (~ 5% for both genera). It was found that Proteobacteria and Firmicutes had the highest relative abundances among all the disease groups. The dominant families across all disease groups were *Erwiniaceae*, *Bacillaceae*, *Enterobacteriaceae* and *Pseudomonadaceae* with members of the genera, *Bacillus* and *Pseudomonas* highly dominant across all the disease groups. Among all disease groups, sequences assigned to members of the genera *Bacillus* and *Kosakonia* were found at high relative abundances in both R and HS disease group. The relative abundance of *Bacillus* sequences in both R and HS were evenly distributed (~ 10%). Similarly, an even distribution of relative abundance of *Kosakonia* sequences was observed in the R and HS disease group. These taxa were followed by members of the genus *Sphingomonas* which were highly abundant and evenly distributed (~ 10%) in the R and MR group. Bacterial sequences were assigned to 246 OTUs, of which 81 of the OTUs corresponded to 32.9% and were shared amongst all disease groups. The HS disease group harboured the highest proportion of unique OTUs (21) corresponding to 8.5%, while MR and S had the lowest number of unique OTUs (14), corresponding to 5.7%. Disease groupings S and HS shared 5 OTUs that corresponded to 5.3% of bacterial OTUs with only 5 OTUs corresponding to 2% shared between the R and MR groups (Figure 3.6A).

The most dominant fungal pathogenic species, for the plants designated as HS, was the well-known phytopathogen members of the family *Nectriaceae* and genus *Gibberella* (40%).

Members of the genus *Epicoccum* (family *Didymellaceae*), were exclusively found in the R and S disease groups and accounted for over 5% relative abundance. In addition to these genera, members of families *Didymellaceae* (*Ascochyta* genus) and *Ustilaginaceae* (*Ustilago* genus) were found in the susceptible disease groups albeit in lower abundance (<5%). Furthermore, members of the families *Didymellaceae* (*Didymella* genus) and *Massarinaceae* (*Sclerostagonospora* genus), were also amongst the potential pathogenic taxa found across all disease groups, although in low percentages (Figures 3.4C and 3.4D). Table 3.3 further highlights the known potential sorghum pathogenic taxa and the pathogenic taxa not commonly found in sorghum.

The dominant phyla were Ascomycota and Basidiomycota respectively, which in total comprised over 55% of the OTUs. Chytridiomycota, Kickxellomycota, Glomeromycota, Mucoromycota and Rozellamycota were detected at much lower relative abundances, cumulatively 9% of fungal OTUs. Unassigned fungi encompassed less than 13% of OTUs. The most substantial differences were observed among the different disease groups, with a higher relative abundance of OTUs found in the HS samples. Members of the family, *Pleosporaceae*, *Bulleribasidiaceae*, *Tremellaceae* with taxa in the genera *Phoma* (30%), *Didymella* (30%) and *Papiliotrema* (20%) dominated the samples designated as the R group (Figures 3.3A and 3.3B). The S and HS disease groups had a high proportion of fungal OTUs, which agrees with results from Shannon diversity analyses (Figure 3.2B). The R and MR groups had the same fungal composition, with, the relative abundance of genera identified as *Papiliotrema*, *Phoma* and *Cladosporium* high in the R group. Similarly, the S and HS disease groups had the same microbial composition with a high relative abundance (more than 20%) of *Gibberella* genus in the HS disease group, while *Epicoccum* was more abundant in the R group and S disease group. Surprisingly, our analyses showed that the sorghum fungal community had more OTUs (478) compared to the bacterial OTUs (246) Appendix Tables 3A.2 and 3A.3. The majority of these fungal OTUs (301) were shared and corresponded to 63% of all OTUs distributed among all the disease groups. The HS disease group had the highest proportion of 11 unique fungal OTUs which corresponded to 2.3%. The distribution of fungal OTUs in HS relative to R group is shown in Figure 3.6B.

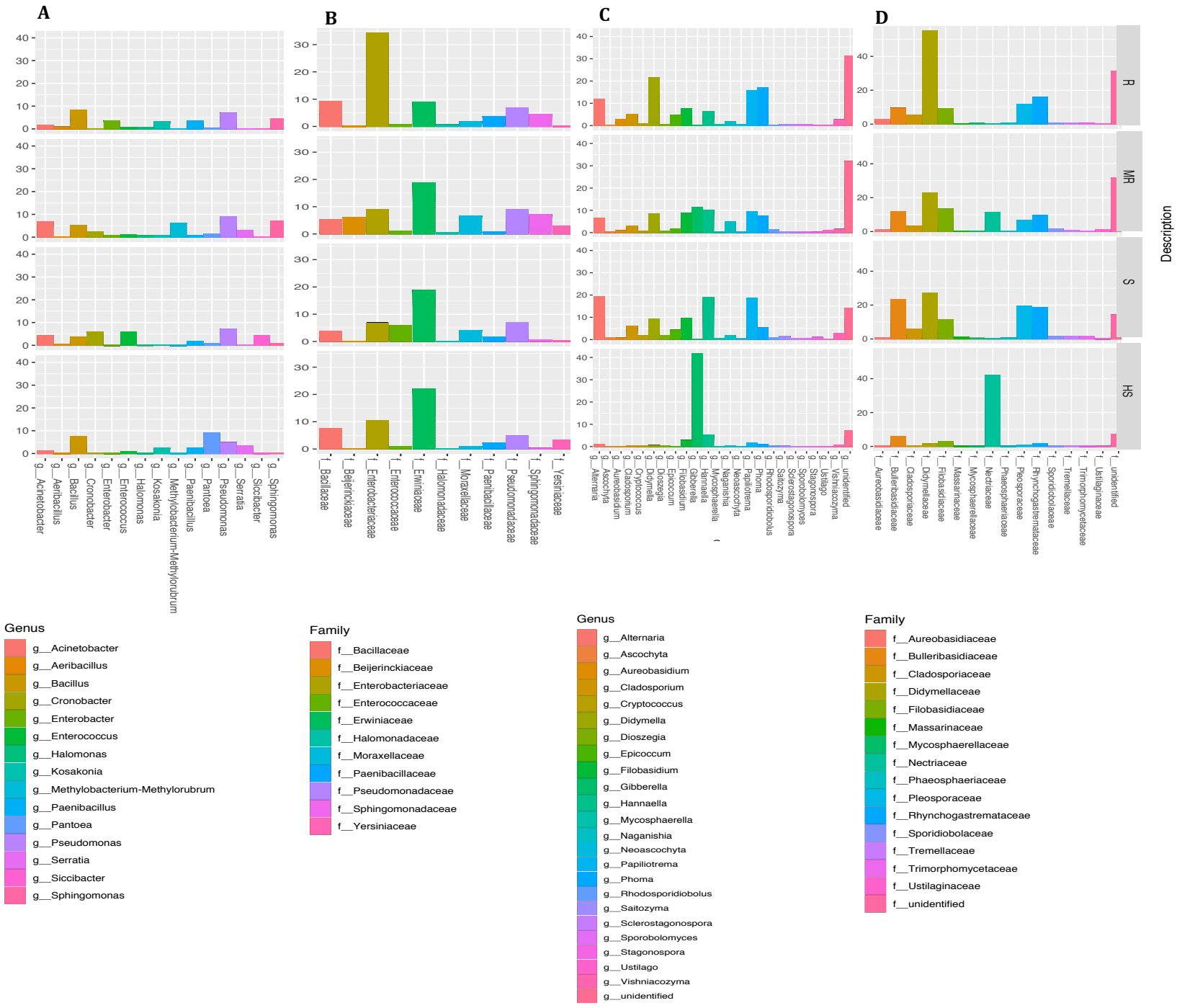
A
B
C
D
R
MR
S
HS
Description
g__Acinetobacter
g__Aeribacillus
g__Bacillus
g__Cronobacter
g__Enterobacter
g__Enterococcus
g__Halomonas
g__Kosakonia
g__Methylobacterium-Methylorubrum
g__Paenibacillus
g__Pantoea
g__Pseudomonas
g__Serratia
g__Siccibacter
g__Sphingomonas
f__Bacillaceae
f__Beijerinckiaceae
f__Enterobacteriaceae
f__Enterococcaceae
f__Erwiniaceae
f__Halomonadaceae
f__Moraxellaceae
f__Paenibacillaceae
f__Pseudomonadaceae
f__Sphingomonadaceae
f__Yersiniaceae
g__Alternaria
g__Ascochyta
g__Aureobasidium
g__Cladosporium
g__Cryptococcus
g__Didymella
g__Dioszegia
g__Epicoccum
g__Filobasidium
g__Gibberella
g__Hannaella
g__Mycosphaerella
g__Naganishia
g__Neoascochyta
g__Papiliotrema
g__Phoma
g__Rhodosporidiobolus
g__Saitozyma
g__Sclerostagonospora
g__Sporobolomyces
g__Stagonospora
g__Ustilago
g__Vishniacozyma
g__unidentified
f__Aureobasidiaceae
f__Bulleribasidiaceae
f__Cladosporiaceae
f__Didymellaceae
f__Filobasidiaceae
f__Massarinaceae
f__Mycosphaerellaceae
f__Nectriaceae
f__Phaeosphaeriaceae
f__Pleosporaceae
f__Rhynchogastremataceae
f__Sporidiobolaceae
f__Tremellaceae
f__Trimorphomycetaceae
f__Ustilaginaceae
f__unidentified

Figure 3.4: The relative abundance of taxa in sorghum disease groups. (A) Bacterial genera across disease groups (R, MR, S and HS), (B) The relative abundance of bacterial family across different disease groups (C) Fungal genera relative abundance across disease groups. (D) The relative abundance of fungal family across different disease groups. Each bar represents a disease group, the colour distinguishes the taxon in each group. *Gibberella*, *Pantoea* and *Serratia* genera indicated an increasing trend in relative abundance in the HS disease group, while *Alternaria* and *Cronobacter* showed an increase in relative abundance trend across all disease groups. *Papilliotrema* and *Sphingomonas* indicated an increase trend in the R and MR group, with *Methylorubrum* showing an increase in relative abundance trend in the R group.

Table 3.2: Plant pathogenic bacteria inhabiting sorghum and other cereal plants across various disease groups (R, MR, S and HS).

Potential pathogenic taxa	**Disease group**	**Percentage (%) of samples**	**Recorded symptoms**	**Reference**
Pantoea	HS	10	Bacterial leaf spot of sorghum	(Lana et al., 2012; Cota et al., 2010)
Serratia	S	<10	Cucurbit Yellow Vine Disease	(Besler and Little, 2017)
Pseudomonas	R. MR, S, HS	<10	Bacterial leaf stripe of sorghum	(Kaplin et al., 2017)

Table 3.3: Plant pathogenic fungi inhabiting sorghum and other cereal plants across various disease groups (R, MR, S and HS).

Potential pathogenic taxa	Disease group	Percentage (%) of samples	Recorded symptoms	Reference
Epicoccum	S	<10	Grain mould of sorghum	(Oliveira et al., 2017a)
Mycosphaerella	R, MR, S, HS	<5	Charcoal rot in sorghum	(Bandara et al., 2018, 2017; Quaedvlieg et al., 2013; Das et al., 2012)
Sclerostagonospora Anamorph *Leptosphaeria*	MR, S, HS	<5	Blackleg and leaf blotch in sorghum, wheat and maize	(Ma et al., 2019; Quaedvlieg et al., 2013; Fitt et al., 2006)
Ascochyta	R, MR, S, HS	<5	Leaf spots	(Xu et al., 2019; Jayashree and Wesely, 2018; Tivoli and Banniza, 2007)
Didymella	R MR S	>20 10 10	Leaf spot and leaf blight	(Moral et al., 2018)
Ustilago	S	<10	Leaf smut disease	(Kruse et al., 2018; Omayio et al., 2018)
Gibberella	HS MR	>40 >10	Stalk rot and Sorghum complex disease	(Nida et al., 2019; Kelly et al., 2017; Gilbert and Fernando, 2004)

Phoma	R MR S HS	>10 <10 5 <5	Mycotoxins in sorghum	(Bennett et al., 2018; Oliveira et al., 2017b)
Alternaria	R MR S HS	>10 <10 20 <5	Leafspot	(Astoreca et al., 2019; Wei et al., 2020)

3.3.6 Potential fungal and bacterial species (microbiomeSeq)

Because the taxonomic assignments for the microbes particularly at species rank cannot be accurately annotated due to the amplicon studies relatively short sequences, the species will be reported as potential/ possible species (Meola et al., 2019). The potential bacterial species presented the members of the species *Mixta gaviniae* which was highly associated with the HS disease group. While the species *Paenibacillus wenxiniae* and *Bacillus clausii* were highly linked with the R group (relative abundance <10%) Figure 3.5A.

The most dominant fungal potential species (relative abundance >50%) for the plants designated as HS, was the well-known potential phytopathogen *Gibberella zeae.* Potential species *Epicoccum sorghinum* (family *Didymellaceae*), a sorghum pathogen, was exclusively found in the HS plants. In addition to these known potential sorghum pathogens, members of the species *Ascochyta paspali* and *Ustilago kamerunensis*, both potential grass species pathogens, were found in the susceptible disease groups. Furthermore, members of the *Didymella glomerata* and *Sclerostagonospora phragmiticola* species, were also amongst the potential species found across all disease groups, though in low percentages Figure 3.5B.

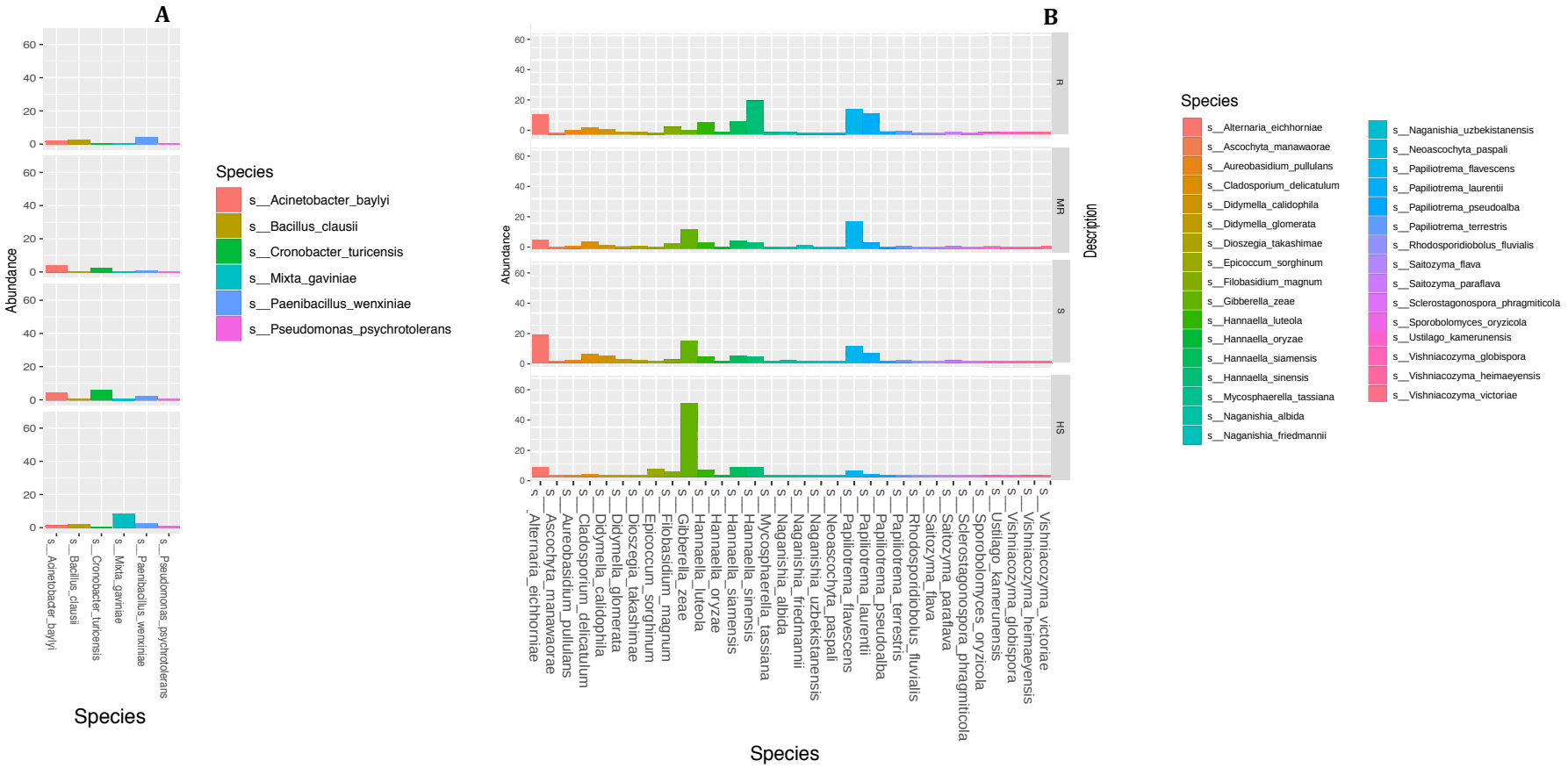
A
Abundance
Species
s__Acinetobacter_baylyi
s__Bacillus_clausii
s__Cronobacter_turicensis
s__Mixta_gaviniae
s__Paenibacillus_wenxiniae
s__Pseudomonas_psychrotolerans
B
Abundance
Description
R
MR
S
HS
Species
s__Alternaria_eichhorniae
s__Ascochyta_manawaorae
s__Aureobasidium_pullulans
s__Cladosporium_delicatulum
s__Didymella_calidophila
s__Didymella_glomerata
s__Dioszegia_takashimae
s__Epicoccum_sorghinum
s__Filobasidium_magnum
s__Gibberella_zeae
s__Hannaella_luteola
s__Hannaella_oryzae
s__Hannaella_siamensis
s__Hannaella_sinensis
s__Mycosphaerella_tassiana
s__Naganishia_albida
s__Naganishia_friedmannii
s__Naganishia_uzbekistanensis
s__Neoascochyta_paspali
s__Papiliotrema_flavescens
s__Papiliotrema_laurentii
s__Papiliotrema_pseudoalba
s__Papiliotrema_terrestris
s__Rhodosporidiobolus_fluvialis
s__Saitozyma_flava
s__Saitozyma_paraflava
s__Sclerostagonospora_phragmiticola
s__Sporobolomyces_oryzicola
s__Ustilago_kamerunensis
s__Vishniacozyma_globispora
s__Vishniacozyma_heimaeyensis
s__Vishniacozyma_victoriae
Species
s__Alternaria_eichhorniae
s__Ascochyta_manawaorae
s__Aureobasidium_pullulans
s__Cladosporium_delicatulum
s__Didymella_calidophila
s__Didymella_glomerata
s__Dioszegia_takashimae
s__Epicoccum_sorghinum
s__Filobasidium_magnum
s__Gibberella_zeae
s__Hannaella_luteola
s__Hannaella_oryzae
s__Hannaella_siamensis
s__Hannaella_sinensis
s__Mycosphaerella_tassiana
s__Naganishia_albida
s__Naganishia_friedmannii
s__Naganishia_uzbekistanensis
s__Neoascochyta_paspali
s__Papiliotrema_flavescens
s__Papiliotrema_laurentii
s__Papiliotrema_pseudoalba
s__Papiliotrema_terrestris
s__Rhodosporidiobolus_fluvialis
s__Saitozyma_flava
s__Saitozyma_paraflava
s__Sclerostagonospora_phragmiticola
s__Sporobolomyces_oryzicola
s__Ustilago_kamerunensis
s__Vishniacozyma_globispora
s__Vishniacozyma_heimaeyensis
s__Vishniacozyma_victoriae

Figure 3.5: The relative abundance of potential species in sorghum disease groups. (A) Bacterial species across disease groups (R, MR, S and HS) (B) The relative abundance of fungal species across different disease groups. Each bar represents a disease group, the colour distinguishes the taxon in each group.

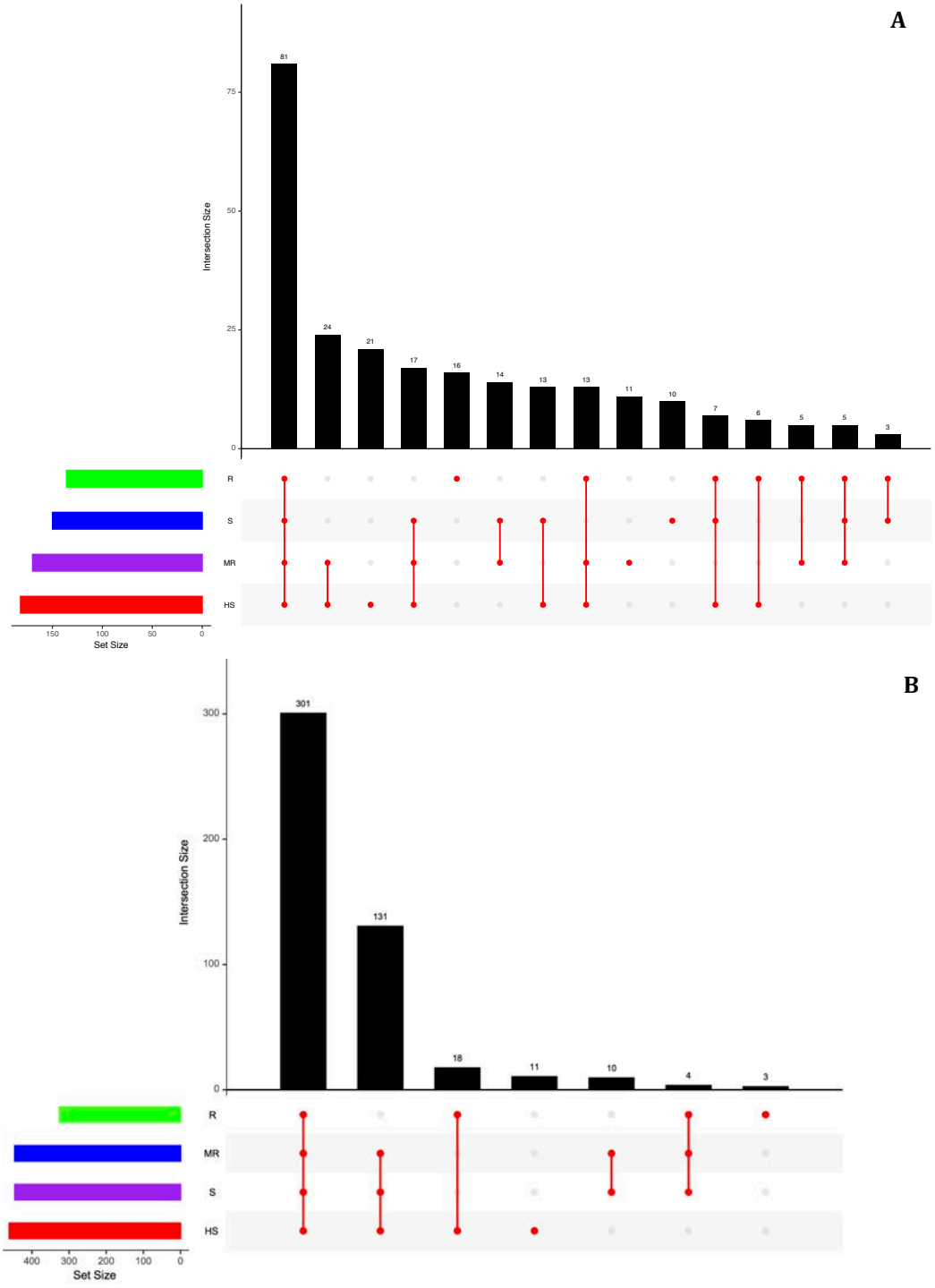

Figure 3.6: (A) Upset plot showing shared and unique bacterial OTUs across disease groups (B) Upset plot showing shared and unique fungal OTUs across disease groups. The total size of each disease group is represented on the left barplot. The overlapping red lines indicates the number of OTUs across all disease groups and connecting bar indicates multiple

disease groups. The bar chart placed on top of the matrix represents the number of the OTUs across all disease groups.

3.3.7 Differential taxa abundance (DESeq2 R package)

Differential abundance analyses were conducted to determine the taxa that showed significant abundance between the R and HS disease group (differential abundance was done in these groups as they showed significant differential abundance). Differentially abundant taxa were determined with a log2 fold change ≥ 0 cut-off and an p adjusted-value of ≤ 0.05. The relative difference in abundance was expressed as log2 fold change, with more represented differentially abundant taxa expressed at a log2 fold change of > 0 and the less represented differentially abundant taxa expressed at a log2 fold change < 0 with p adjusted< 0.05. The bacterial analyses showed 15 differentially abundant genera between the two disease groups and included *Methylorubrum, Aeribacillus, Pantoea, Serratia, Halomonas, Enterobacter, Kosakonia, Sphingomonas, Acinotobacter, Paenibacillus, Enterococcus, Siccibacter, Pseudomonas, Bacillus* and *Cronobacter*. Members of the genera *Pantoea* and *Serratia* were significantly enriched in the HS disease group while *Methylorubrum* and *Aeribacillus* were highly enriched in the R group (Figure 3.7A). Eleven (11) fungal genera, *Gibberella, Epicoccum, Alternaria, Papiliotrema, Phoma, Aerobasidium, Cladosporium, Filobasidium, Ascochyta* and *Didymella* showed significant differential abundance in the HS disease group, while *Hannaella* genus was significantly enriched in the R group (Figure 3.7B).

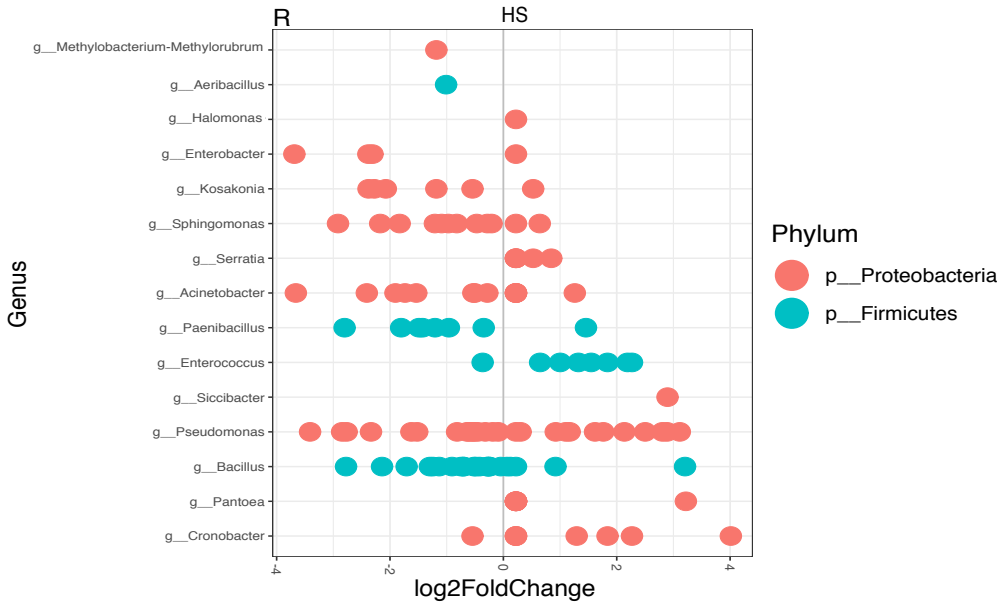
R
HS
g__Methylobacterium-Methylorubrum
g__Aeribacillus
g__Halomonas
g__Enterobacter
g__Kosakonia
g__Sphingomonas
g__Serratia
g__Acinetobacter
g__Paenibacillus
g__Enterococcus
g__Siccibacter
g__Pseudomonas
g__Bacillus
g__Pantoea
g__Cronobacter
Genus
-4
-2
0
2
4
log2FoldChange
Phylum
p__Proteobacteria
p__Firmicutes

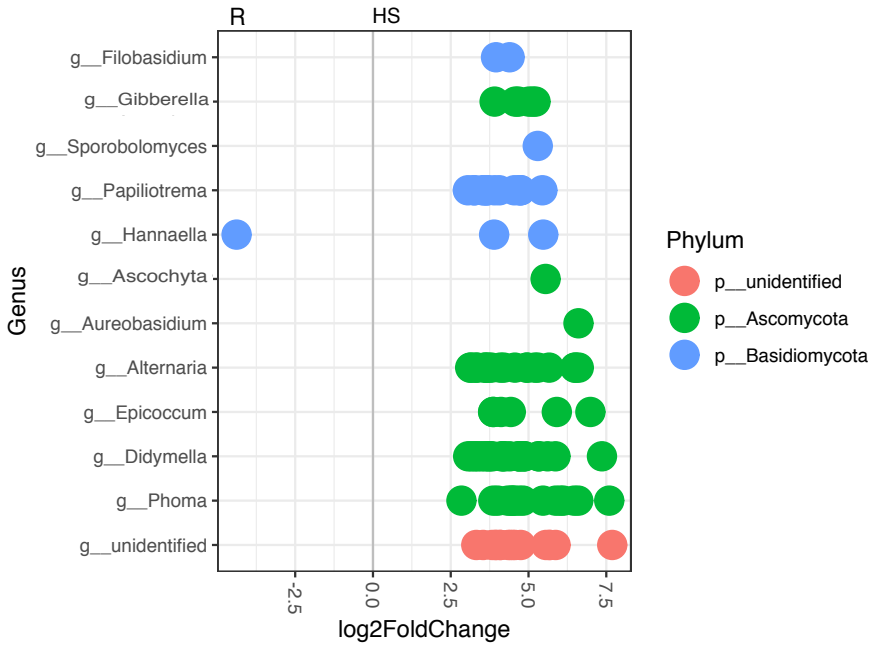
R
HS
g__Filobasidium
g__Gibberella
g__Sporobolomyces
g__Papiliotrema
g__Hannaella
g__Ascochyta
g__Aureobasidium
g__Alternaria
g__Epicoccum
g__Didymella
g__Phoma
g__unidentified
Genus
-2.5
0.0
2.5
5.0
7.5
log2FoldChange
Phylum
p__unidentified
p__Ascomycota
p__Basidiomycota

Figure 3.7: Differential abundance between the examined disease groups (R and HS). (A) Bacterial genera and phyla (B) Fungal genera and phyla. The log2 fold change as measured by DESeq2 is plotted for each fungal and bacterial genus significantly associated with R and HS disease groups at p values < 0.05.

3.3.8 Inference of Microbial Ecological Networks across all the disease groups (SpiecEasi)

To elucidate co-occurrences and co-exclusion of key microorganisms in the networks, bacterial and fungal interactions were investigated with SPIEC-EASI. The bacterial network revealed positive correlations between taxa (85% hubs/edges) represented by members of the class Alphabacteria, Gammabacteria and *Bacilli* at q-value < 0.05 (Figures 3.8A and 3.8B). The negative correlation was indicated by only 15% of the hubs/edges networks, (Appendix Table 3A.5). The abundant bacterial class (*Bacillaceae* and *Sphingomonadaceae*), showed co-association patterns. The bacterial families, *Bacillaceae* and *Sphingomonadaceae* tended to have more central roles in the network than OTUs from the *Pseudomonadaceae*, *Methylobacteriaceae* and *Enterobacteriaceae*, which were peripheral and were not co-associated with other taxa (Figures 3.8A and 3.8B). The OTUs that were most highly connected (nodes with high degree) and that connect different parts of the network (nodes with high betweenness centrality) were from the member of the family *Bacillaceae* and *Sphingomonadaceae*.

The co-occurrence relationships dominated the inferred fungal networks. Similar to fungal networks, the inferred networks in bacteria were dominated by co-occurrence relationships.
The fungal network revealed co-occurrence (positive correlations) between taxa (89% hubs/edges) represented by members of the class *Cystobasidimycetes, Dothiomycetes, Microbotryomycetes, Sordiomycetes, Tremellomycetes* and *Ustilaginomycetes* (Figures 3.8C and 3.7D; Appendix Table 3A.5) at q-value < 0.05. The co-exclusion (negative correlation) was indicated by only 11% of the hubs/edges networks, represented by the key fungal taxon *Agaricomycetes* (Figure 3.8C; Appendix Table 3A.5). The abundant fungal classes, *Tremellomycetes* and *Dothiomycetes*, showed co-interaction patterns.

The *Tremellomycetes* and *Dothiomycetes* classes tended to have more central roles in the network than OTUs from *Sordiomycetes*, which were peripheral and were not co-associated with other taxa (Figures 3.8C and 3.8D). The OTUs that were most highly connected (nodes with high degree) and that connect different parts of the network (nodes with high betweenness centrality) were *Tremellomycetes* and *Dothiomycetes* classes.

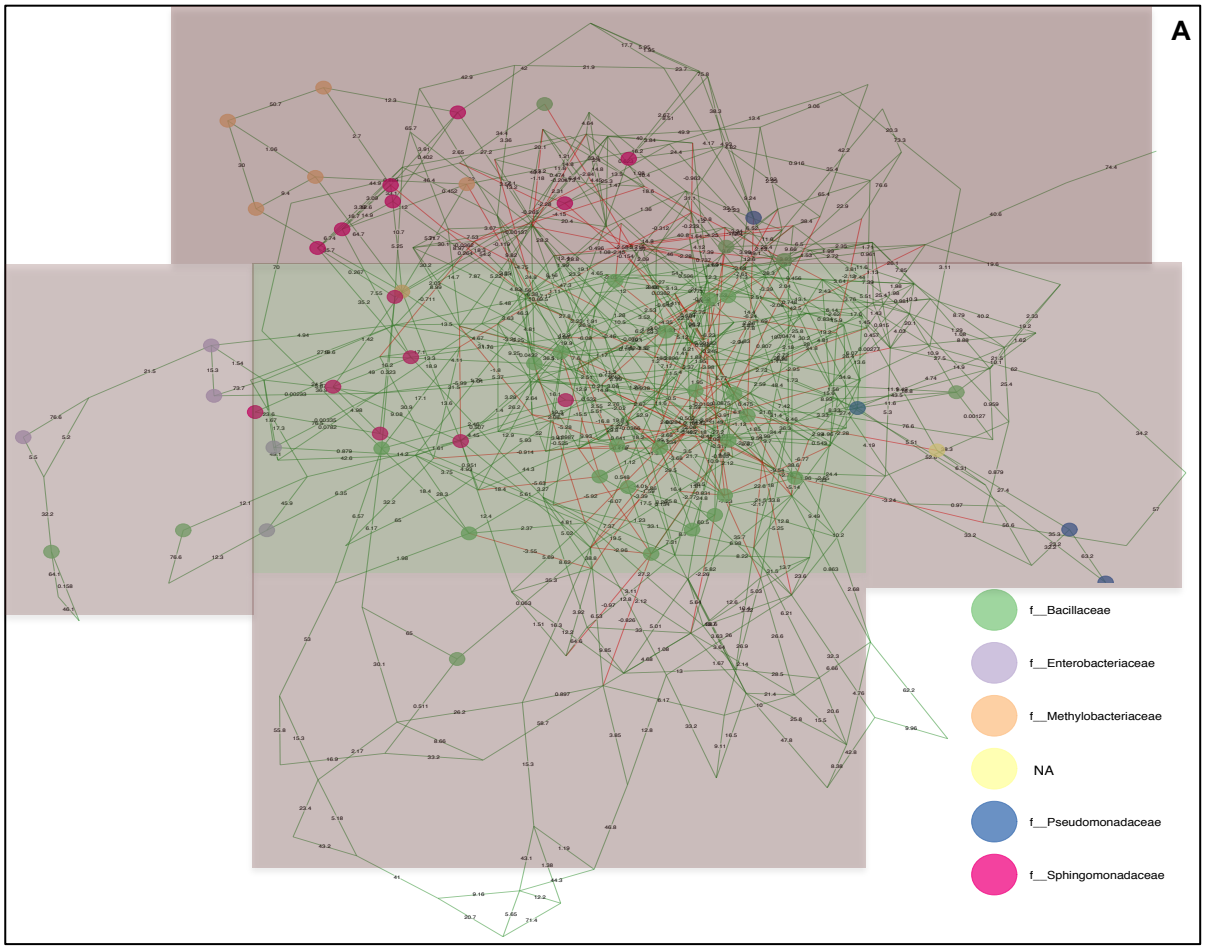
A
f__Bacillaceae
f__Enterobacteriaceae
f__Methylobacteriaceae
NA
f__Pseudomonadaceae
f__Sphingomonadaceae

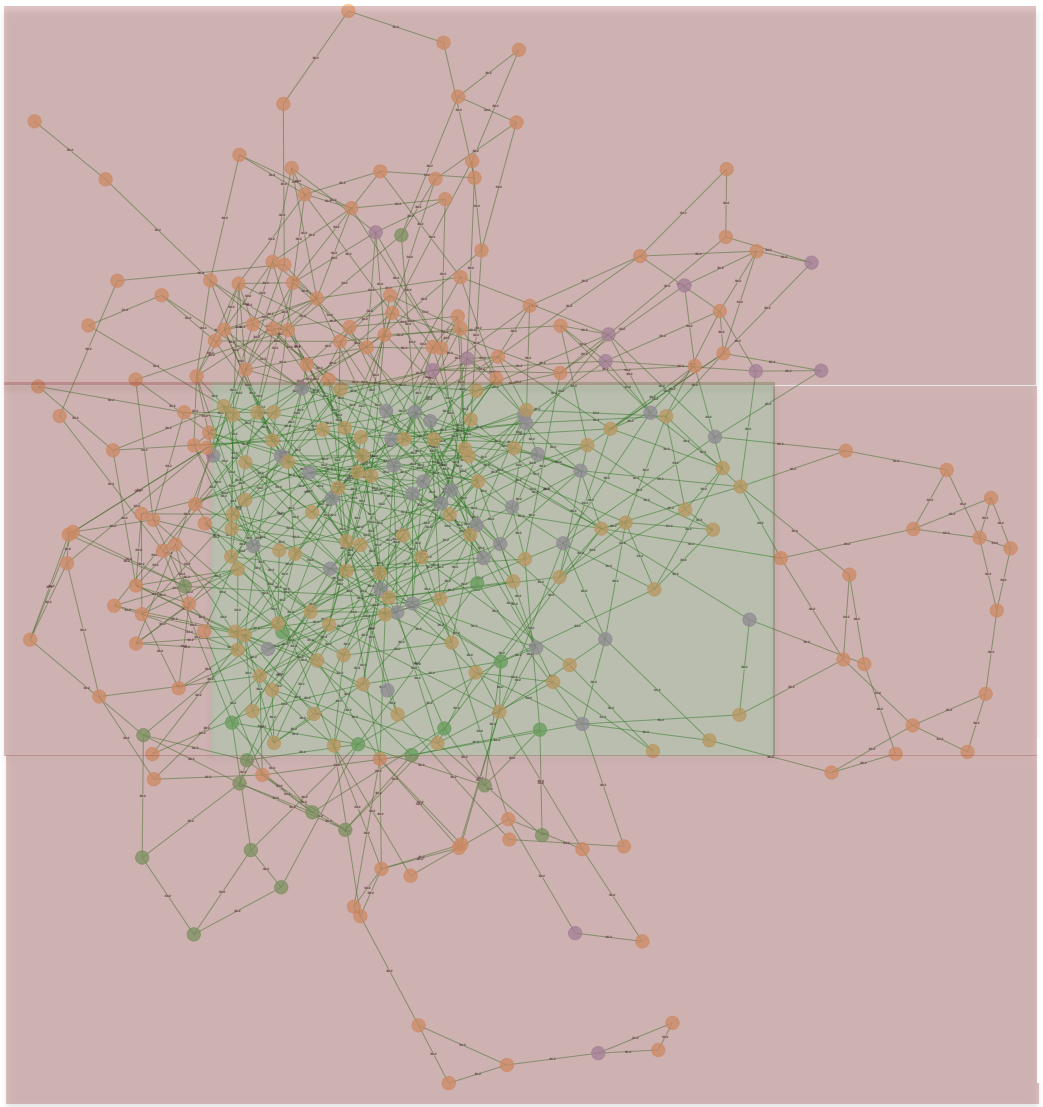

B

c__Alphaproteobacteria

c__Bacilli

c__Gammaproteobacteria

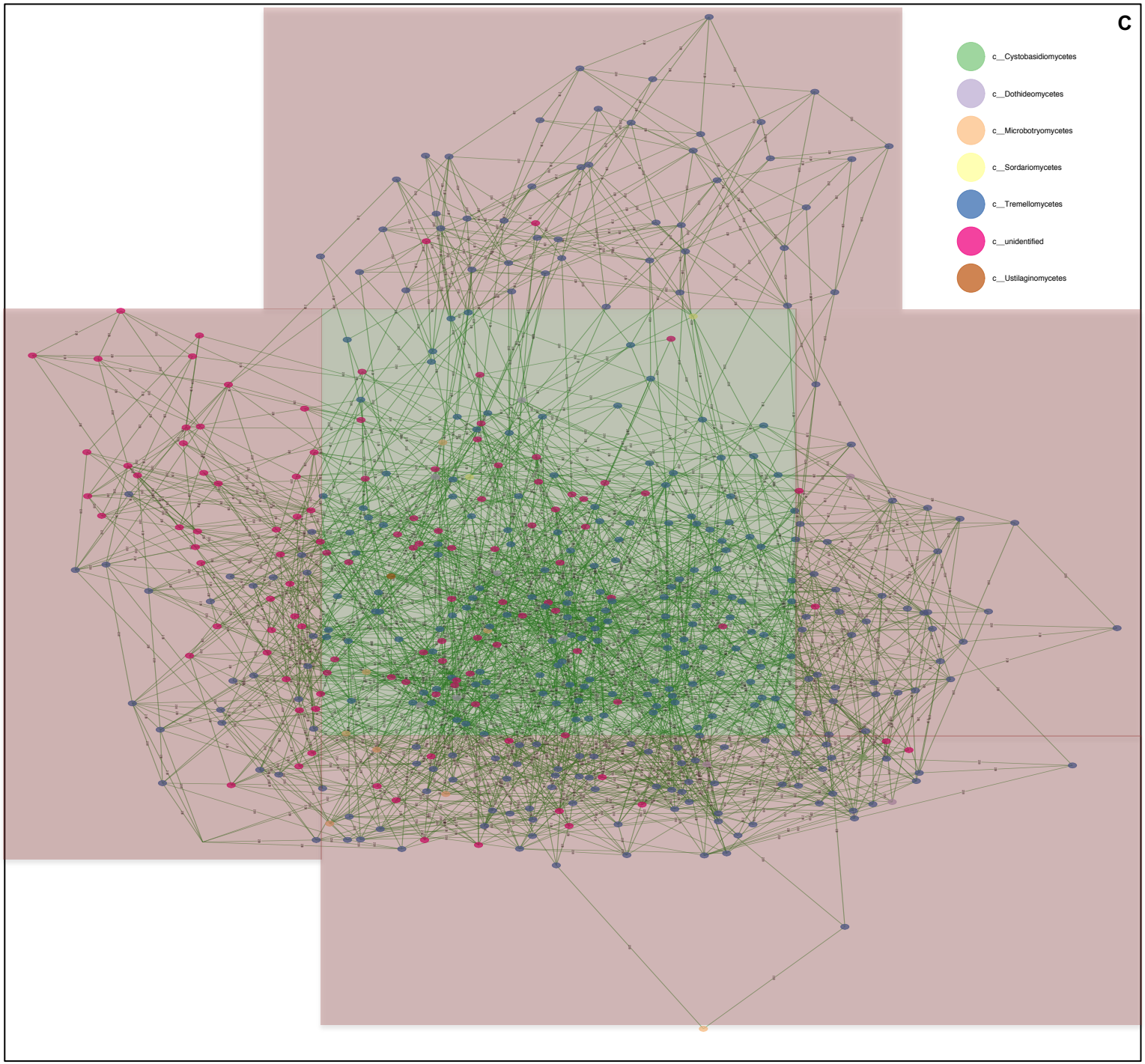
C
c__Cystobasidiomycetes
c__Dothideomycetes
c__Microbotryomycetes
c__Sordariomycetes
c__Tremellomycetes
c__unidentified
c__Ustilaginomycetes

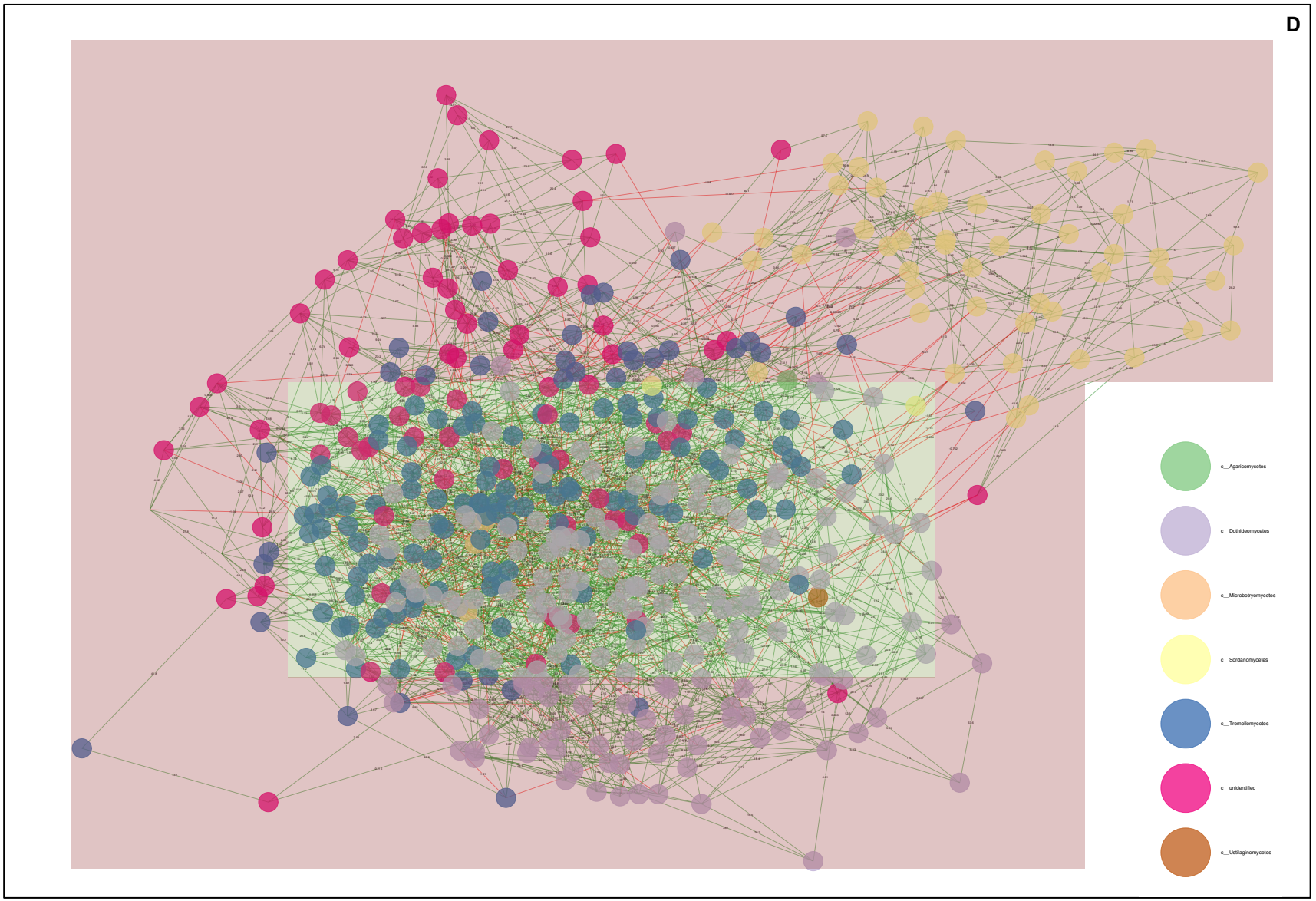
D
c__Agaricomycetes
c__Dothideomycetes
c__Microbotryomycetes
c__Sordariomycetes
c__Tremellomycetes
c__unidentified
c__Ustilaginomycetes

Figure 3.8: Ecological Networks across all the disease groups in (A) Bacterial family (B) Fungal family. Nodes indicating co-occurrence relationships (central- represented by a green colour and peripheral taxa- represented by a pink colour) across all the disease groups (C) Bacterial class (D) Fungal class. The R package SPIEC-EASI was used for networks construction. Network visualizations with OTU nodes were coloured according to class lineage. Nodes correspond to OTUs and edges represent significant co-association between the two OTUs. Edges are coloured by sign (co-occurrence: green represented by beta > 0; co-exclusion: red represented by beta < 0 pulsar.params = 0.05).

3.4 DISCUSSION

The community dynamics of microbial assemblages linked to the rhizosphere of plants are increasingly well documented. Unfortunately, little is currently known regarding the composition and community dynamics of the foliar microbiome (Peñuelas and Terradas, 2014). This study provides novel insights into the leaf microbial structure and diversity of sorghum RILs. The current results suggest that previous studies may have underestimated the effects of natural infection in selecting the microbial communities in sorghum plants, as there is evidence of studies on naturally coexisting soil and rhizosphere microbial consortia (Zegeye et al., 2019; Nemergut et al., 2013). The strong correlation between the diseased groups and the sorghum microbiota was found after natural infection. This observation suggests that naturally occurring pathogens may considerably shape the structure of microbiota, favouring some taxa.

Rarefaction curves used to measured observed OTUs with a given depth of sequencing, permitted direct comparisons of samples of different sample sizes (Kim et al., 2017). The metabarcoding sequencing depth of the bacterial and fungal OTUs was sufficient for the analysis and sampling depth. However, it is important to note that to investigate and determine species level identification of microbiota using NGS it is not possible because Miseq can capture only about 200 bp. Therefore, full length 1500 bp makes a reliable species identification. The samples used in this study were not rarefied because of well-established statistical theory, that discourage the samples to be rarefied (McMurdie and Holmes, 2014).

The investigation of natural infection variation uncovered a remarkable amount of heritable genetic variation among RILs. The variance expressed has a clear quantitative basis, with clear boundaries between a “resistant” and a “susceptible” group of RILs but no clear boundaries between the “resistant and moderately resistant” and “susceptible and highly susceptible”. Similarly, *Arabidopsis thaliana* accession ‘s response to natural infection resulted in the same variation in a group of ecotypes (Kover and Schaal, 2002).

The results of alpha diversity analysis, displayed clear contrasts between disease groups, which supports this hypothesis. The beta diversity analysis indicated a distinction between the RILs displaying disease symptoms and those that did not show disease symptoms (S; HS and R; MR samples). The alpha and beta-diversity metrics showed that the RIL microbiome assemblage was associated with the severity of the disease symptoms. Alpha diversity analyses (Shannon index) indicated that fungi and bacteria were richer in highly susceptible leaves. However, the HS group had lower fungal and bacterial diversity (dominance index) than the resistant plants, while the R group was more diverse (dominance index) relative to the other disease groups. Similarly, there were significant fungal and bacterial variation (beta diversity) between the RILs that showed disease symptoms (S and HS disease groups) and those that did not show disease symptoms (R and MR groups). Similar to the current study, vines with moderate pierce disease symptoms displayed higher microbial diversity (dominance index) than severely symptomatic vines (Deyett and Rolshausen, 2019). The current data could suggests a plant-driven microbial response to the pathogen infection as plants are known to drive microbial assemblage in order to cope with biotic stresses and increase environmental fitness (Deyett and Rolshausen, 2019; Berendsen et al., 2018; Turner et al., 2013). This data highlights a plant-driven microbial response to the pathogen infection. In contrast, in severely symptomatic vines, the toxic environment (e.g., occlusion of xylem vessel with tyloses and decrease of hydraulic conductivity; Deyett et al., 2019) is not conducive to microbial survival. A similar result was also observed in a soil microbiome where soil surrounding healthy tobacco plants harboured more diverse microbial communities, based on soil samples collected around bacterial wilt affected plants (Yang et al., 2017). Other reports have also shown that plants with a microbial community that is diverse were less susceptible to pathogen attack than those with less complex microbial communities (Berg et al., 2017; Shade, 2017; Yang et al., 2017; van Elsas et al., 2012). This is likely due to increased competition for available resources among potential pathogens and other microorganisms in the less diverse community (Shade, 2017). The results suggest that highly diverse plant microbiomes could decrease the chance of disease outbreak as pathogens are likely to be outcompeted (Berg et al., 2017; Shade, 2017; Yang et al., 2017).

The largest number of unique OTUs were associated with the susceptible disease group in both bacterial and fungal datasets. This is consistent with previous studies which have shown that diseased hosts tend to harbour more unique OTUs when compared to healthy hosts (Rosenzweig et al., 2012). The fungal communities associated with the highly susceptible disease group was the most complex. Zhang and colleagues (2018) recently reported an increase in the fungal community richness (Shannon index) and linked this to increased disease pressure. Another report revealed that soils with Fusarium wilt were colonized by more richer bacterial communities (richness) and also harboured significantly different community structure compared to healthy soils (Zhou et al., 2019). The current results on the leaf microbiome demonstrate similar patterns and possibly suggest that plant diseases may affect shifts in the phyllosphere of fungal and bacterial communities on sorghum leaves.

Taxonomic assignments for fungal taxa, up to genus level, was dominated by a considerable portion of fungi classified as known pathogens of sorghum. Genera such as *Cladosporium, Alternaria* and *Sporobolomyces* found in this study are frequent filamentous fungi colonizing the phyllosphere as epiphytes and endophytes and is in agreement with previous observations (Kinge et al., 2019; Rana et al., 2019; Glushakova and Chernov, 2004; Inácio et al., 2002; Arnold et al., 2000). Fungal families *Nectriaceae* and *Didymellaceae* classified as *Gibberella* and *Epicoccum*, respectively were assigned, and significantly linked to the HS and (HS and S) disease groups, respectively. These genera are pathogenic taxa and have been previously reported to be a major causative genera in sorghum grain mould disease (de Oliveira et al., 2018; Kelly et al., 2017; Oliveira et al., 2017a). Sorghum grain mould disease is a major limitation to sorghum production (Kinge et al., 2019; Sharma et al., 2011), and the *Gibberella* genus has been reported to be the dominant species causing grain mould in sorghum (Nida et al., 2019; Menkir et al., 1996). Interestingly, members of the genus *Epicoccum* were also associated with the resistant group, albeit in low levels. Fungi belonging to the genus *Epicoccum* are ubiquitous ascomycetes frequently isolated from healthy and diseased grapevine (Del Frari et al., 2019; Bruez et al., 2014; Hofstetter et al., 2012; Pancher et al., 2012). However, there are different references to the *Epicoccum* genus, not ascribed to a species, that have been reported from healthy grapevine cuttings (Halleen et al., 2003), pruning wounds (Úrbez-Torres and Gubler, 2011) and mature grapevine plants (Choueiri et al., 2014;

Kuntzmann et al., 2010). These fungi have been thought to be endophytes or saprophytes in grapevine but their role on healthy or diseased plants, where they can co-inhabit with different grapevine trunk diseases pathogens, has not been investigated (Del Frari et al., 2019). The members of the genera *Ascochyta* (*Didymellaceae* family) and *Ustilago* (*Ustilaginaceae* family) causing sorghum leaf stripe disease and leaf smut, respectively, were also associated with the HS and S disease groups (Xu et al., 2019; Jayashree and Wesely, 2018; Kruse et al., 2018; Omayio et al., 2018; Tivoli and Banniza, 2007). It was also detected that *Didymella* (*Didymellaceae* family) which was highly significant in the R group, *Alternaria* and *Sclerostagonospora* anamorph *Leptosphaeria* (*Massarinaceae* family), which are known to cause sorghum blackleg, leaf spot and leaf blight (Ma et al., 2019; Moral et al., 2018; Quaedvlieg et al., 2013; Fitt et al., 2006) were significantly associated with MR, S and HS. Interestingly, members of the genera *Didymella* and *Alternaria* were highly associated with the R group. This was expected, as members of these genera has been shown to exhibit plant growth capabilities (Turbat et al., 2020; Zhou et al., 2018). Additionally, members of genus *Phoma* (*Didymellaceae*), previously reported as having the ability to produce mycotoxins in sorghum (Bennett et al., 2018; Oliveira et al., 2017b) was highly associated with all the disease groups. Members of the *Phoma* genus were significantly associated with the R group and was unsurprising as this genus has both biocontrol and plant growth capabilities (Saldajeno et al., 2012).

The resistant fungal group had a majority of OTUs showing similarity to well-known plant growth-promoting fungal genus including *Papiliotrema* (*Tremellaceae* family), which are known biocontrol agents (Schisler et al., 2019). Members of the genus *Alternaria*, from the *Pleosporaceae* family, were also detected in high relative abundances in the resistant group and have previously been demonstrated to possess bio-herbicide traits (Poudel et al., 2016).

Members of the family *Bulleribasidiaceae* and *Hannaella* yeast were also detected at high relative abundances in resistant plants. *Hannaella* yeasts are frequently observed in the phyllosphere of various plant species (Edwards et al., 2015; Nasanit et al., 2015; Nutaratat et al., 2014; Caporaso et al., 2012). Some *Hannaella* species are known to produce indole acetic acid (IAA) (Kaewwichian et al., 2015; Sun et al., 2014). The IAA producing microorganisms are reported to be efficient bio-fertilizer inoculants used for promoting plant growth (Mehmood et al., 2018), although another study has suggested that yeasts may not necessarily promote

plant growth (Sun et al., 2014). Therefore, it remains unclear how *Hannaella* yeasts interact with other yeasts, bacterial or fungal species in or on plant leaves. The precise mechanisms used to influence plant performance and host-genotype specifically also remain unclear.

Pantoea, a sorghum bacterial pathogen causing leaf spot, was significantly and exclusively associated with the HS disease group. *Pseudomonas*, bacterial pathogens causing leaf blight in sorghum, was associated with all the disease groups including R, MR, S and HS. The presence of *Pseudomonas* in the R group suggests that it embodies an attractive biocontrol agent because of their catabolic adaptability and their capacity to produce a wide range of antifungal metabolites as previously reported (Gómez-Lama Cabanás et al., 2018; Panpatte et al., 2016; Praveen Kumar et al., 2012). Members of the *Serratia* genus, causing cucurbit yellow vine disease on cucurbits, sunflower, alfalfa were associated with the S disease group (Besler and Little, 2017). These pathogens are known to colonize several monocotyledonous plants but have not previously been found on sorghum leaves (Moral et al., 2018; Quaedvlieg et al., 2013). This finding is perhaps not unusual as some pathogenic fungi have very broad host ranges and may infect numerous different plant species (Prospero and Cleary, 2017; Bolton et al., 2006). Some fungi may also have very narrow host ranges and the pathogen-response of the plant may vary, determining the presence or absence of detectable symptoms (Yuan and Gao, 2015). However, not much is known regarding the host specificity of pathogens infecting agriculturally important plants like sorghum.

The taxonomic assignments for the majority of fungal species were classified at a considerable portion as either potential or possible fungal species. These so-called potential microbial taxa include taxa which could not be accurately annotated, particularly at lower taxonomic ranks. This is a common issue in microbial classification studies and is due to several issues including the relatively short sequences generated from amplicon studies and possibly due to insufficient representative curated sequences in the databases used for classification (Meola et al., 2019). Nevertheless, fungal species were potentially classified as *Gibberella zeae* and *Epicoccum sorghinum* species, respectively, which were linked to the HS and S disease groups, respectively. These species are potential pathogenic taxa and have been previously reported to be major causative species in sorghum grain mould disease (de Oliveira et al., 2018; Kelly et

al., 2017). *Gibberella zeae* (anamorph *Fusarium graminearum*) was previously reported to be the dominant species causing grain mould in sorghum (Nida et al., 2019). The potential pathogenic species *Ascochyta paspali* and *Ustilago kamerunensis* causing leaf stripe disease and head smut, respectively, in *Paspalum dilatatum* and *Pennisetum purpureum* grass species (from the same *Poaceae* family as sorghum) were also associated with the HS and S disease groups (Omayio et al., 2018). Interestingly, a newly identified potential pathogenic *Mixta gaviniae* species of the genus *Erwiniaceae* family was highly associated with the HS disease group (Palmer et al., 2018).

For the analysis of bacterial composition, it was found that Proteobacteria and Firmicutes were had the highest relative abundances among all the disease groups. Previous studies showed that phyllosphere bacterial communities were dominated by the phyla Proteobacteria followed by the Actinobacteria, Bacteroidetes and Firmicutes (Knief et al., 2010; Müller et al., 2016). Many genera that includes *Bacillus*, *Methylorubrum*, *Pantoea*, and *Pseudomonas* have been reported from the phyllosphere environment of different crop plants (Aquino et al., 2019; Dobrovol'skaya et al., 2017; Luo et al., 2012; Meena et al., 2012; Mukhtar et al., 2010). It was shown that bacterial pathogens were present at considerably lower proportions compared to fungi. While, sorghum serves as host to over 100 pathogens, previous studies suggest that fungi are more likely to colonize plants in comparison to bacterial pathogens (Akinrinlola et al., 2018; Zheng et al., 2016). Interestingly, the susceptible disease group had a higher relative abundance of members of the family *Bacillaceae*, which are usually associated with healthy plants and have the ability to promote plant growth (Das et al., 2012; Klein et al., 2001). However, members of this family also contain other plant pathogens such as *Bacillus pumilus*, a ginger rhizome rot pathogen (Yuan and Gao, 2015). In addition, members of this family may survive unfavourable conditions, such as droughts or invasion by pathogens (Zheng et al., 2016). This may explain the high relative abundances of the *Bacillaceae* family in the susceptible disease group.

The genera *Methylorubrum*, *Enterobacter* and *Sphingomonas* were more abundant and highly enriched in the R and MR group, with members of the latter genus significantly enriched in the R group. *Enterobacter* and *Sphingomonas* have been previously reported to exhibit plant

growth-promotion traits (Schlemper et al., 2018; Knief et al., 2010) Little is known regarding the phylogenetic taxa and functional attributes of the recently classified *Methylorubrum* genus (Grossi et al., 2020; Green and Ardley, 2018). However, members of this genus are abundant in the phyllosphere and have the ability to promote growth in some plants (Koskimaki et al., 2015; Bulgari et al., 2011; Schreiner et al., 2010; Sagaram et al., 2009). Members of this family have also been shown to associate with plants which displayed resistance to disease (Schisler et al., 2019; Wallace et al., 2018; Zhang et al., 2018b; Rakotoarisoa et al., 2015; Trivedi et al., 2010).

Microbial taxa that frequently co-occur with other taxa form networks, which potentially play a key role within the microbiome. The current findings showed that the OTUs represented by Tremellomycetes and Dothiomycetes classes had more central roles in the network than OTUs from the Sordiomycetes, which were peripheral. The bacterial networks *Bacillaceae* and *Sphingomonadaceae* had more central role in the network. The modules which are located centrally on the network have been reportedly expected to play important 'topological roles' in interconnecting pairs of other fungal and bacterial taxa in the symbiont–symbiont co-occurrence network (Layeghifard et al., 2017; Toju et al., 2016). Both the fungal and bacterial network data suggest that the dominant taxa in terms of microbial community composition are essential in structuring the co-association network. These dominant taxa, are considered to be keystone microbes, and have been suggested to be drivers of microbiome structure and functioning (Hamonts et al., 2018; Layeghifard et al., 2017).

Conclusion

To the best of our knowledge, this is the first study to assess both the fungal and bacterial composition in the leaves of sorghum RILs. It is shown that natural pathogen infection results in distinct foliar microbial communities in sorghum RILs. The results of bacterial and fungal community composition, community co-occurrences further suggest the importance of keystone taxa which may disproportionately shape the structure of foliar microbiomes. The current data provides a baseline for testing hypothesis related to the importance of keystone taxa in foliar microbiota. Cultivation studies may shed light on the nature of the putative symbiotic relationships between bacteria and fungi.

The analysis of microbial diversity and community composition in this study could suggest that different ‘resident’ consortia found in sorghum plants may be viable biocontrol and plant-growth promoting agents. These results can also be useful biomarkers for assessing disease status in plants, and therefore contribute towards crop breeding.

CHAPTER 4

Sequencing of marker genes and cell viability assessment of *Fusarium graminearum* (*Gibberella zeae*)

4.1 INTRODUCTION

Fusarium graminearum, was significantly associated with the highly susceptible plants in the current study. It was not surprising to observe the characterization of *Fusarium graminearum* (*Gibberela zeae*), as it has been previously reported in other studies. This pathogen was isolated in sorghum residues from the Krasnodar region of the Northern Caucasus (Burgess et al., 2002; Francis and Burgess, 1977). Menkir et al. (1996) found significant levels of the *Gibberella* disease in sorghum and incidence of *Gibberella zeae* was positively correlated with Sorghum Grain Mould (SGM) damage scores.

Fusarium graminearum, is a cause of major disease of cereal crops, and can influence the yield and lead to economic losses (Beukes et al., 2017). It is the dominant pathogen causing head blight disease of wheat, and has occasionally been isolated from sorghum (Burgess et al., 2002; Trimboli and Burgess, 1985). *Fusarium graminearum* showed the highest pathogenicity on sorghum grain when compared to other *Fusarium* species (Quazi et al., 2010). This species has the potential to produce zearalenone (ZEA, 15-acetyldeoxynivalenol (15-ADON), deoxynivalenol (DON), nivalenol (NIV) and 3-acetyldeoxynivalenol (3-ADON) (Yerkovich et al., 2017) which can negatively influence the health of people and animals when heavily mycotoxin contaminated food based products of sorghum are ingested over a long period (Pinotti et al., 2016). Studies on infection of sorghum seedlings by *Fusarium graminearum* indicated that this pathogen can infect the sorghum host at early growth stages and gradually colonize adjacent tissues (Van Rooyen, 2019; Bodoči et al., 2013). GRAINSA, 2017, Schoeman and Greyling-Joubert (2017) have reported that there has been an increase in the occurrence of *Fusarium graminearum* in South African crops.

Traditional diagnostic methods for identification and detection of *Fusarium graminearum* in culture or in infected grains were based on morphological features. This process is laborious and it can often be challenging to differentiate between species that are similar. Molecular methods are more sensitive, faster and are also employed in *Fusarium* species identification. PCR with primers targeting the internal transcribed sequence (ITS) between ribosomal DNA (Schilling et al., 1996) for the detection and identification of *Fusarium graminearum* has been used extensively. However, sequences in the ITS regions have shown to be highly variable in fusaria (O'Donnell, 1992), as several species of *Fusarium* morphological features closely

resemble those of *F. graminearium* (Aoki et al., 1999). The most commonly used primers in fungal ecology for sequence-based fungal identification at species level are ITS1, ITS2, ITS3 and ITS4 (De Beeck et al., 2014; White et al., 1990). In this chapter, molecular methods were used to confirm *Fusarium graminearum* with ITS (ITS1 and ITS4 regions) and UBC primer sets ($UBC85F_{410}$-$UBC85R_{410}$) specific to the *Fusarium graminearum*, and also to check the cell/spore viability of the identified species through an automated cell counter.

4.2 MATERIALS AND METHODS

4.2.1.1 Fungal isolation (mycelia production and harvest)

The isolate was originally derived from wheat grain and was received from the Agriculture department at University of South Africa (UNISA). *Fusarium graminearum* was grown separately in Petri plates containing potato dextrose agar (PDA) medium in triplicate. Plates were incubated at 25°C for 10–14 days. Fungal conidia were harvested by flooding the plates with 10 ml sterilized water and then the agar surface was scraped with a spatula to dislodge the conidia. The conidial suspensions were filtered through four layers of sterile cheesecloth into two separate beakers and diluted with sterile water at various concentrations from 1×10^6 to 2×10^4 conidia/ml.

4.2.1.2 Determination of cell viability

Cultivated spore (harvested from a media) viability and count was conducted using a LUNA-II™ automated cell counter (Logos Biosystems inc, USA) following the manufacturer's instructions. Briefly, a cell count was performed by mixing 10 µl of the cell sample with 10 µl of trypan blue stain, 10 µl of the mixed cell sample was loaded into the inlet of one chamber of the counting slide. The slide was inserted into the slide port of the cell counter. The cell count was read generating results for total, live, dead cell concentrations and viability.

4.2.2 *Fusarium graminearum* confirmation

4.2.2.1 Isolation of DNA

Fungal DNA was isolated using the CTAB method with minor modifications. Fresh fungal mycelium grown from 6 days old mycelia was transferred to a 2 ml plastic tube, and 500 µl lysis buffer (Macherey-Nagel) was added. The mycelium was crushed using the Savant Fastprep™ FP120 Cell Disruptor for 20 s and incubated for 60 min at 60 °C. The total volume of 140 µl 1.4 M NaCl and 65 µl of 10% CTAB was added. Following, incubation at 60 °C for 10 min, 452.5 µl SEVAG was added and incubated for 30 min at 4 °C. After 10 min centrifugation at 14000 x g, the supernatant was transferred to a fresh tube and 440 µl isopropanol was added, mixed and centrifuged for 10 min at 14000 x g.

4.2.2.2 DNA purification and concentration quantification

The supernatant was then discarded and the pellet was washed twice with cold 70% ethanol. The pellet was dried and dissolved with 25 µl elution buffer (10 mM Tris-Cl, 1 mM EDTA, pH 8.0). A volume of 1 µl RNase A (20 mg/ml) was added to DNA samples, mixed and incubated at 37 ºC for 1 h. The concentration of the DNA was determined using Qubit 2.0 fluorometer.

4.2.2.3 PCR amplification, gel electrophoresis and concentration quantification

Fusarium graminearum species isolated in triplicates were confirmed using two primer sets ITS1 and ITS 4 and UBC85F410 and UBC85R410 (DeLeon-Rodriguez et al., 2013; Group et al., 2009; Schilling et al., 1996). Each PCR reaction contained DNA template (~10-20 ng), 10 µM of each primer (Integrated DNA Technologies, USA), 2.0 mM $MgCl_2$; 0.2 mM of each dNTP; and 1.25 U Taq DNA polymerase (Thermo Scientific Co., USA) and PCR grade water to a final volume of 25µl. The reaction was carried out on a G STORM Thermal cycler (Gene Technologies, UK). The thermal cycling conditions used were, initial denaturation at 95 °C for 1 min, followed by 30 cycles of denaturation for 30 s at 94 °C, and the annealing phase at 55 °C for 60s (ITS1 and ITS 4) and 61 °C for 30s (UBC85F410 and UBC85R410) and extension at 70°C for 20 s; a final extension was performed at 72 °C for 10 min. PCR amplicons concentration was quantified using a Qubit® fluorometer. The quality of the amplicon was viewed with agarose gel electrophoresis. Briefly, the cast gels were equilibrated in the running buffer 1xTBE (Tris base: Boric acid: EDTA at 10 V/cm for 30 min). A RiboRuler RNA ladder was used as molecular size marker (RiboRuler, Fermentas).

4.2.2.4 PCR product sequencing

Sanger sequencing of PCR products was conducted at Inqaba Biotec (Gauteng, South Africa). PCR purified products of the (ITS1 and ITS 4) and (UBC85F410 and UBC85R410) gene of the strains were analyzed for nucleotide. sequence determination by using the ABI PR1SM 3500XL DNA Sequencer (Applied Biosystems) at Inqaba Biotechnical Industrial (Pty) Ltd, Pretoria, South Africa, according to the manufacturers protocol.

4.2.2.5 Quality control and sequence assembly

Sequencing data was obtained in the AB1 file format and was visualized and edited using SnapGene software (GSL Biotech, Chicago, IL, USA). Subsequent, to the conversion of the file from ABI format to fastq, the quality of the sequenced data was assessed using the FastQC v0.10.1 tools (Andrews, 2010). CLC-Workbench was used to assemble the resultant sequences and consensus sequences were submitted to BLASTn on NCBI (www.ncbi.nlm.nih.gov/BLAST) to retrieve known sequences that are homologous as references for species identification.

4.2.2.6 Phylogenetic analysis and sequence alignment

The molecular evolutionary genetics analysis package (MEGA v.7.0) (Tamura et al., 2011) was used for phylogenetic analysis and multiple sequence alignments. Non-parametric maximum likelihood (ML) bootstrapping with heuristic searches of 10,000 replications was performed to assess branch support in phylogenetic trees generated. The percentage values of 97% or larger were regarded as evidence that the groupings were of the same species. Sequences amplified from *Fusarium graminearum* with fungal ITS primer set and UBC primer set were aligned separately with the voucher sequences to estimate the similarities between the samples through NCBI blast (www.ncbi.nlm.nih.gov/BLAST). Alignments were further visualised with the GenBank datasets using CLC Bio Genomics workbench v9.0.

4.3 RESULTS

4.3.1 *Fusarium graminearum* pathogen viability

The conidial suspensions resulted in live cells being more than the dead cells in terms of cell number and concentration (3.45×10^5) Figure 4.1. The pathogen viability was at 65% which was enough to initiate pathogen infection (Table 4.1).

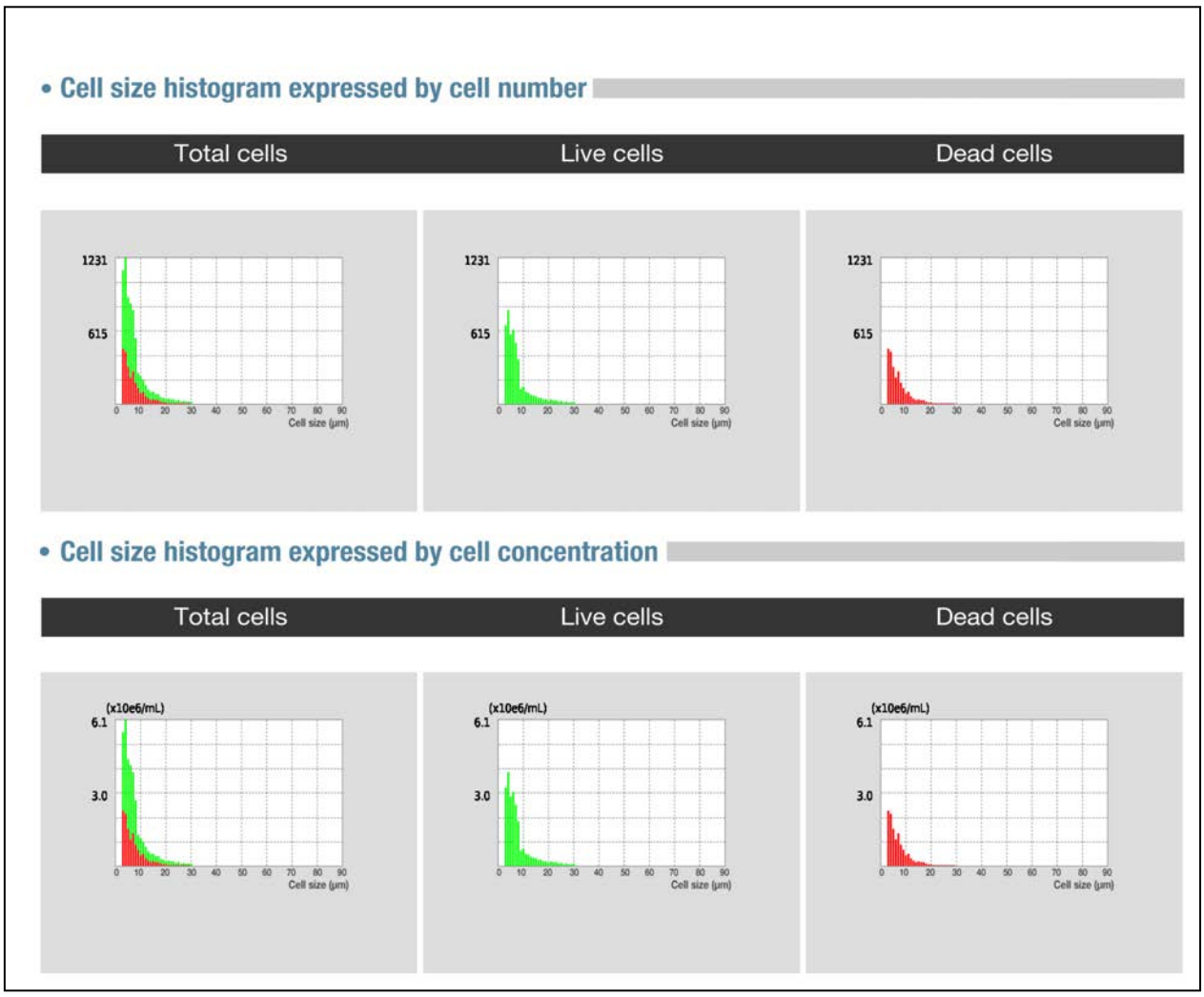

Figure 4.1: Cell size histogram expressed by cell number and cell concentration measuring total cells (red and green colour), live cells (green colour) and dead cells (red colour). The pathogen viability concentration was at 65% which was enough to initiate pathogen infection.

Table 4.1: The total number of live and dead cell as measured by the automated cell counter. The cell viability of the pathogen was 65% represented by the number of live cells.

Total cell concentration	3.47 x 10^7 cells/mL
Live cell concentration	2.25 x 10^7 cells/mL
Dead cell concentration	1.22 x 10^7 cells/mL
Viability	65%
Average cell size	8.8 μm
Total cell number	7057
Live cell number	4580
Dead cell number	2477

4.3.2 Molecular characterization and phylogenetic analyses of *Fusarium graminearum*

4.3.2.1 PCR amplification

The identification and confirmation of *Fusarium graminearum* through molecular analysis was indicated. The amplification of the ITS and the UBC regions of the *Fusarium graminearum* resulted in the ~500 bp expected product (Figures 4.2A and 4.2B), which was subsequently confirmed through Sanger sequencing.

4.3.2.2 Quality control and sequence alignment

The analysis showed the higher quality reads (most reads above Phred scores 20) of the UBC+ITS data (Figures 4.3A and 4.3B). ITS and UBC primer sets generated consensus sequences subjected to BLASTn and resulted in a retrieval of known homologous sequences with a percentage similarity of 97-100. The sequence alignment of different GenBank species (NCBI) showing sequence similarities with the ITS consensus sequences of the isolates used in this study, presented that these regions are highly variable as shown in alignments with sequences from other *Fusarium* spp. (Figure 4.4).

4.3.2.3 Phylogenetic analyses

The ITS consensus sequences were further aligned with the *Fusarium graminearum* voucher species with unique accession numbers (MN017275- MN017277) and the evolutionary tree derived from the maximum likelihood analysis for the primer sets ITS set clustered with *Fusarium graminearum* voucher sequences and this is shown in Figures 4.5 and 4.6. For the UBC primer sets (which are *Fusarium graminearum* species specific) the isolates DNA sequences showed similarity (97%) to GenBank species *Fusarium graminearum* (HG970333.1) only, in contrast to ITS which has shown to be highly variable. It was confirmed that *Fusarium graminearum* aligned with the consensus sequences, as shown in Figure 4.7. Sequences with UBC primer sets also aligned and clustered with *Fusarium graminearum* voucher species (accession numbers, MT723845-MT723847) Figures 4.8 and 4.9, confirming the similarity and identity of *Fusarium graminearum*. The UBC and ITS primer set exclusively clustered with *Fusarium graminearum* voucher species with unique GenBank accession

number (MT723845-MT723847; MN017275- MN017277 respectively) at 99-100% sequence identity. While the Fusaria species in the NCBI database were highly variable (Figure 4.10).

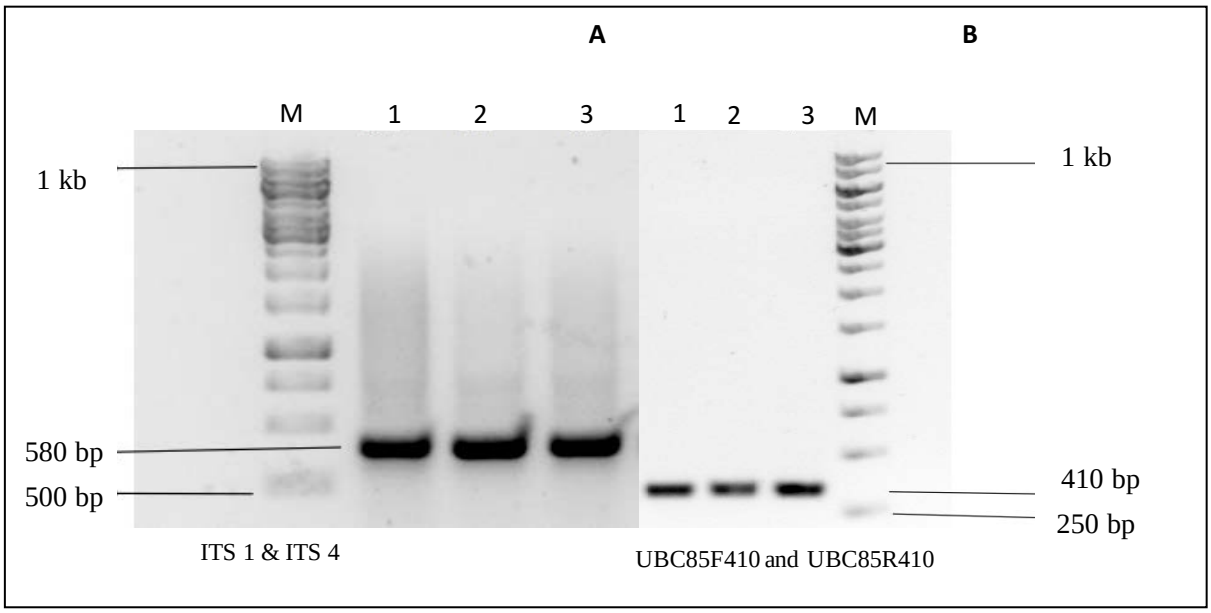

Figure 4.2: Agarose gel amplified DNA of *Fusarium graminearum*. M. indicates the 1kilobase (kb) molecular marker lane. Lanes 1-3 represents amplified ITS1 and ITS 4 regions of *Fusarium graminearum* in 3 replicates (A) targeted ITS regions, (B) Agarose gel amplified DNA of *Fusarium graminearum*. M. indicates the 1 kb molecular marker lane. Lanes 1-3 represents the amplified UBC85F10 & UBC85R410 regions of *Fusarium graminearum* in 3 replicates

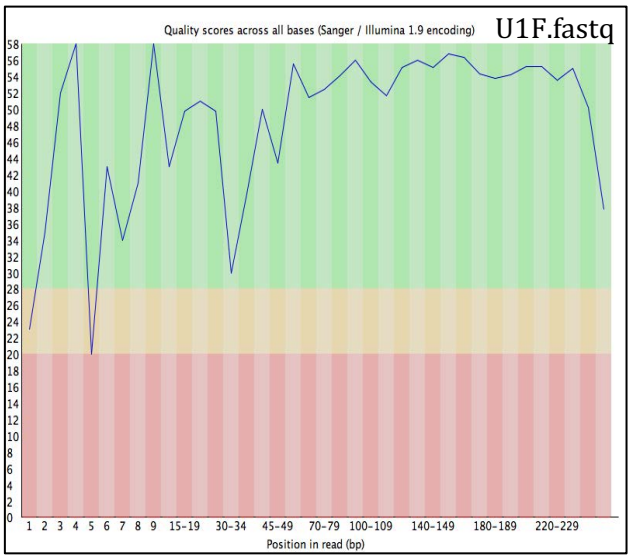
Quality scores across all bases (Sanger / Illumina 1.9 encoding)
U1F.fastq
Position in read (bp)

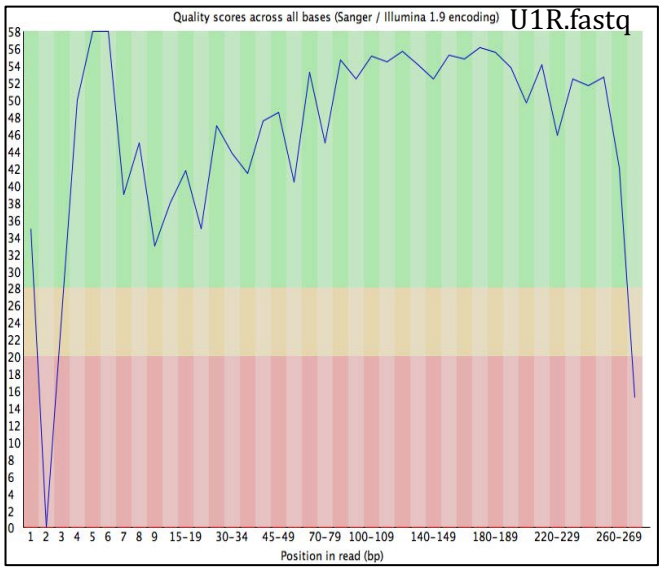
Quality scores across all bases (Sanger / Illumina 1.9 encoding)
U1R.fastq
Position in read (bp)

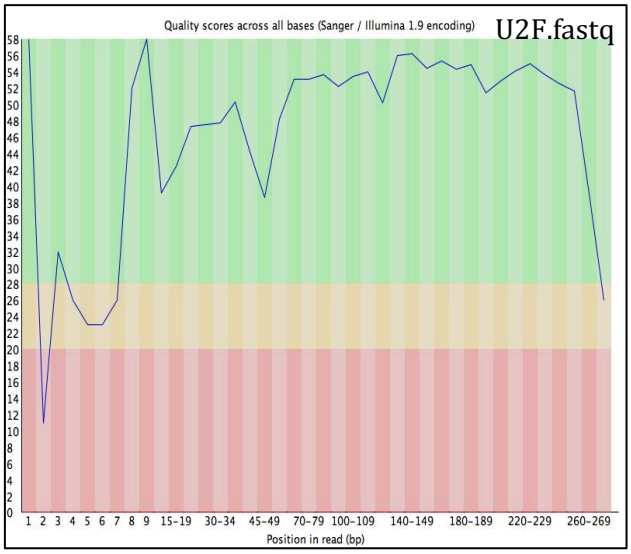
Quality scores across all bases (Sanger / Illumina 1.9 encoding)
U2F.fastq
Position in read (bp)

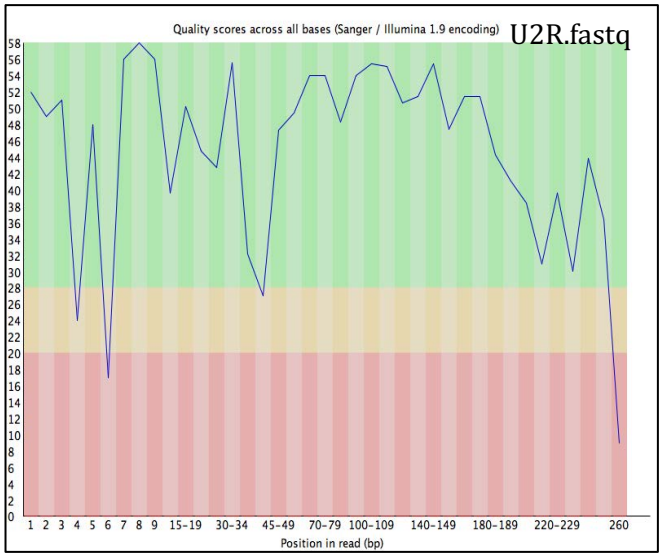
Quality scores across all bases (Sanger / Illumina 1.9 encoding)
U2R.fastq
Position in read (bp)

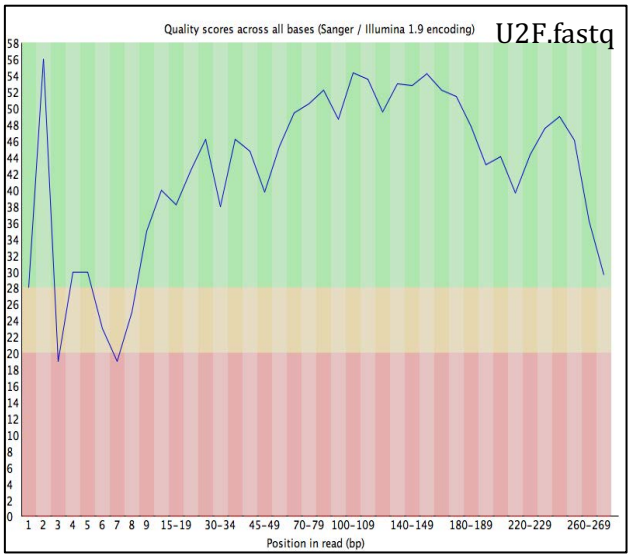
Quality scores across all bases (Sanger / Illumina 1.9 encoding)
U2F.fastq
Position in read (bp)

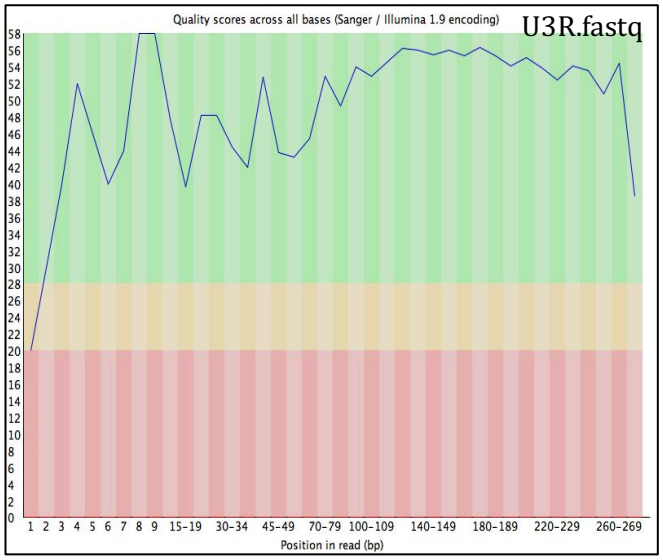
Quality scores across all bases (Sanger / Illumina 1.9 encoding)
U3R.fastq
Position in read (bp)

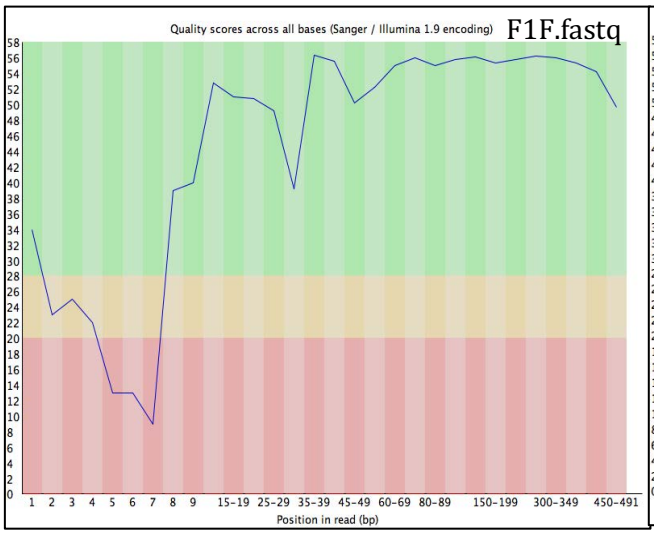
Quality scores across all bases (Sanger / Illumina 1.9 encoding)
F1F.fastq
Position in read (bp)

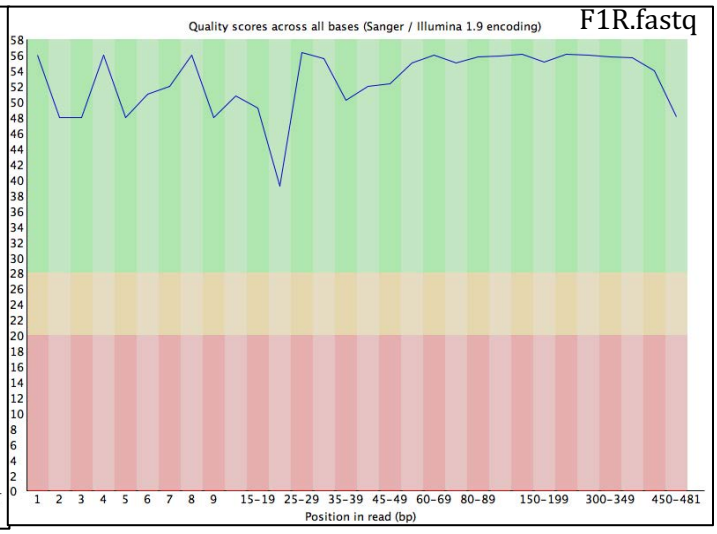
Quality scores across all bases (Sanger / Illumina 1.9 encoding)
F1R.fastq
Position in read (bp)

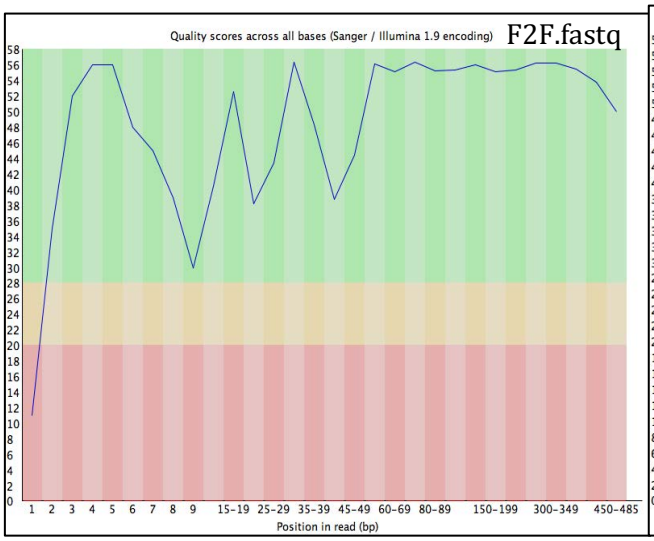
Quality scores across all bases (Sanger / Illumina 1.9 encoding)
F2F.fastq
Position in read (bp)

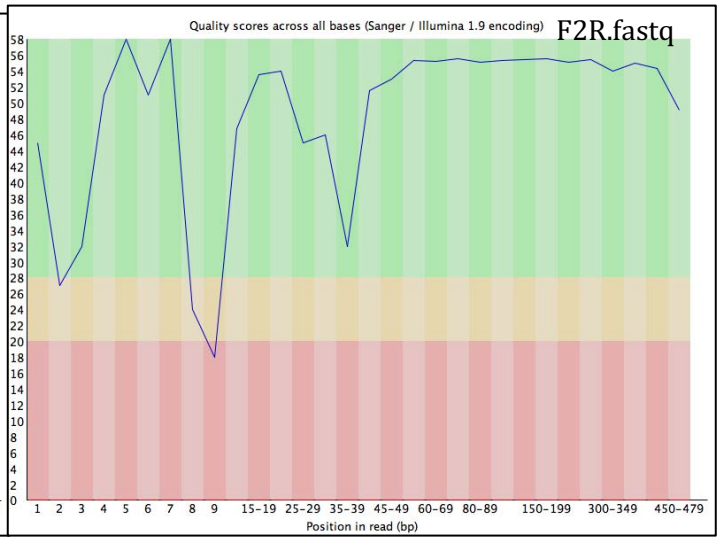
Quality scores across all bases (Sanger / Illumina 1.9 encoding)
F2R.fastq
Position in read (bp)

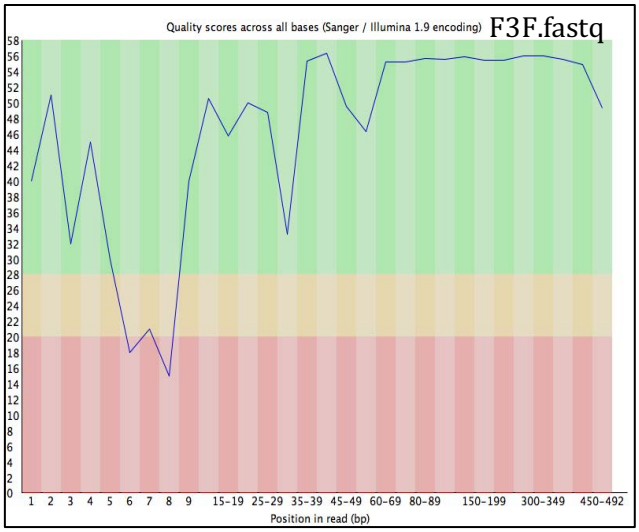
Quality scores across all bases (Sanger / Illumina 1.9 encoding)
F3F.fastq
Position in read (bp)

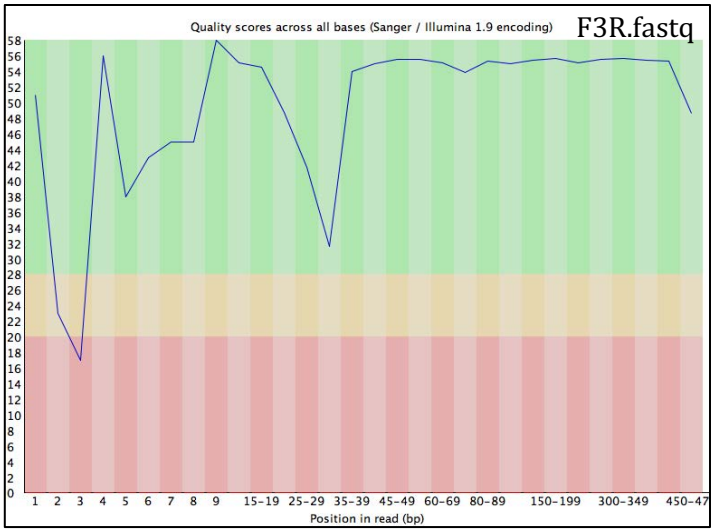
Quality scores across all bases (Sanger / Illumina 1.9 encoding)
F3R.fastq
Position in read (bp)

Figure 4.3: Sanger base quality reads used to create a consensus sequence (assembly) checked and analysed by FastQC v0.10.1 tools (Andrews, 2010) (A) reads generated by the UBC primer set (B) reads generated by the ITS primer set. The analysis showed the higher quality reads (most reads above Phred scores 20) of the UBC+ITS data.

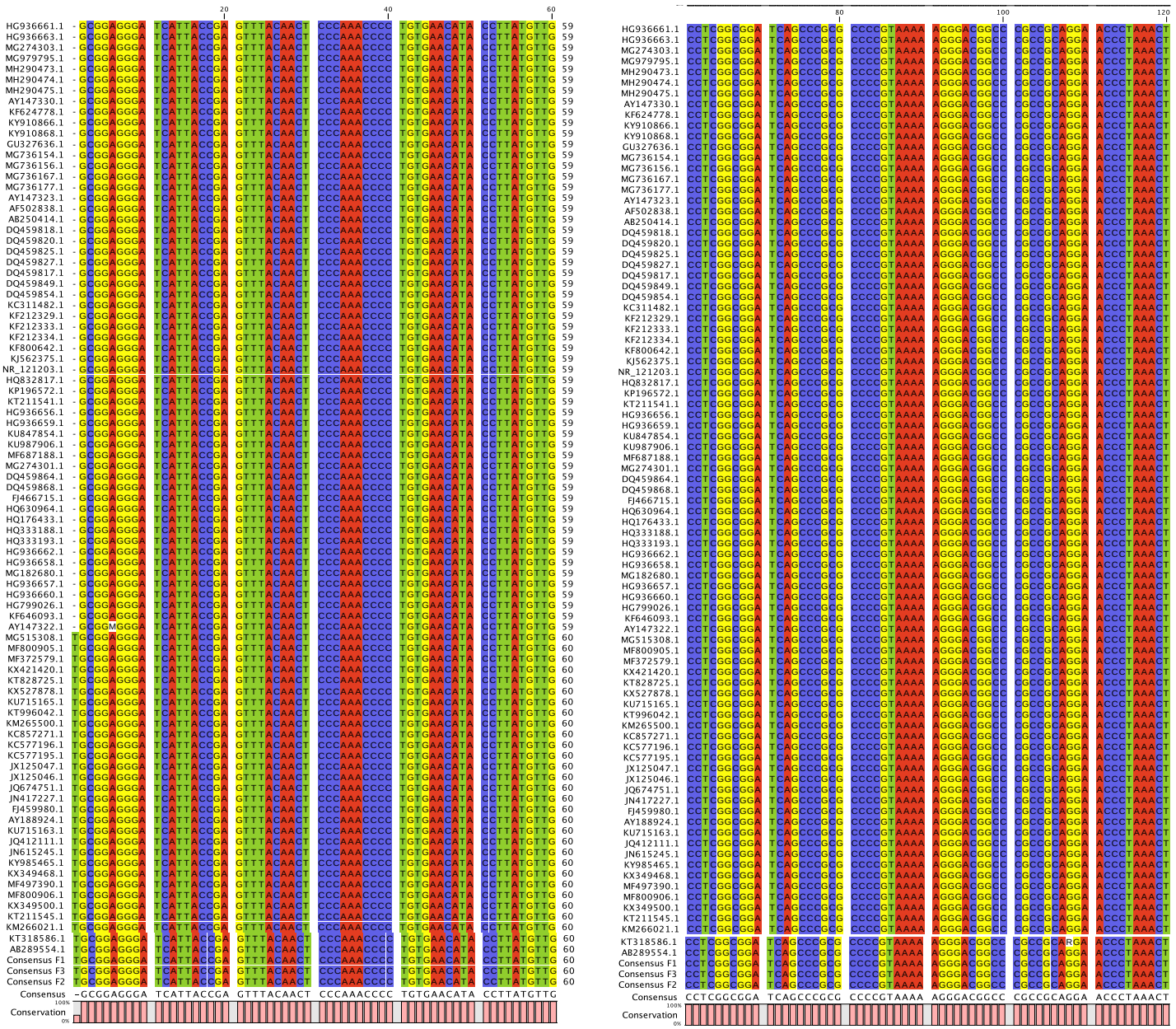
HG936661.1
HG936663.1
MG274303.1
MG979795.1
MH290473.1
MH290474.1
MH290475.1
AY147330.1
KF624778.1
KY910866.1
KY910868.1
GU327636.1
MG736154.1
MG736156.1
MG736167.1
MG736177.1
AY147323.1
AF502838.1
AB250414.1
DQ459818.1
DQ459820.1
DQ459825.1
DQ459827.1
DQ459817.1
DQ459849.1
DQ459854.1
KC311482.1
KF212329.1
KF212333.1
KF212334.1
KF800642.1
KJ562375.1
NR_121203.1
HQ832817.1
KP196572.1
KT211541.1
HG936656.1
HG936659.1
KU847854.1
KU987906.1
MF687188.1
MG274301.1
DQ459864.1
DQ459868.1
FJ466715.1
HQ630964.1
HQ176433.1
HQ333188.1
HQ333193.1
HG936662.1
HG936658.1
MG182680.1
HG936657.1
HG936660.1
HG799026.1
KF646093.1
AY147322.1
MG515308.1
MF800905.1
MF372579.1
KX421420.1
KT828725.1
KX527878.1
KU715165.1
KT996042.1
KM265500.1
KC857271.1
KC577196.1
KC577195.1
JX125047.1
JX125046.1
JQ674751.1
JN417227.1
FJ459980.1
AY188924.1
KU715163.1
JQ412111.1
JN615245.1
KY985465.1
KX349468.1
MF497390.1
MF800906.1
KX349500.1
KT211545.1
KM266021.1
KT318586.1
AB289554.1
Consensus F1
Consensus F3
Consensus F2
Consensus
Conservation
100%
0%


260
280
300
Consensus
Conservation
Consensus F1
Consensus F3
Consensus F2
320
340
360

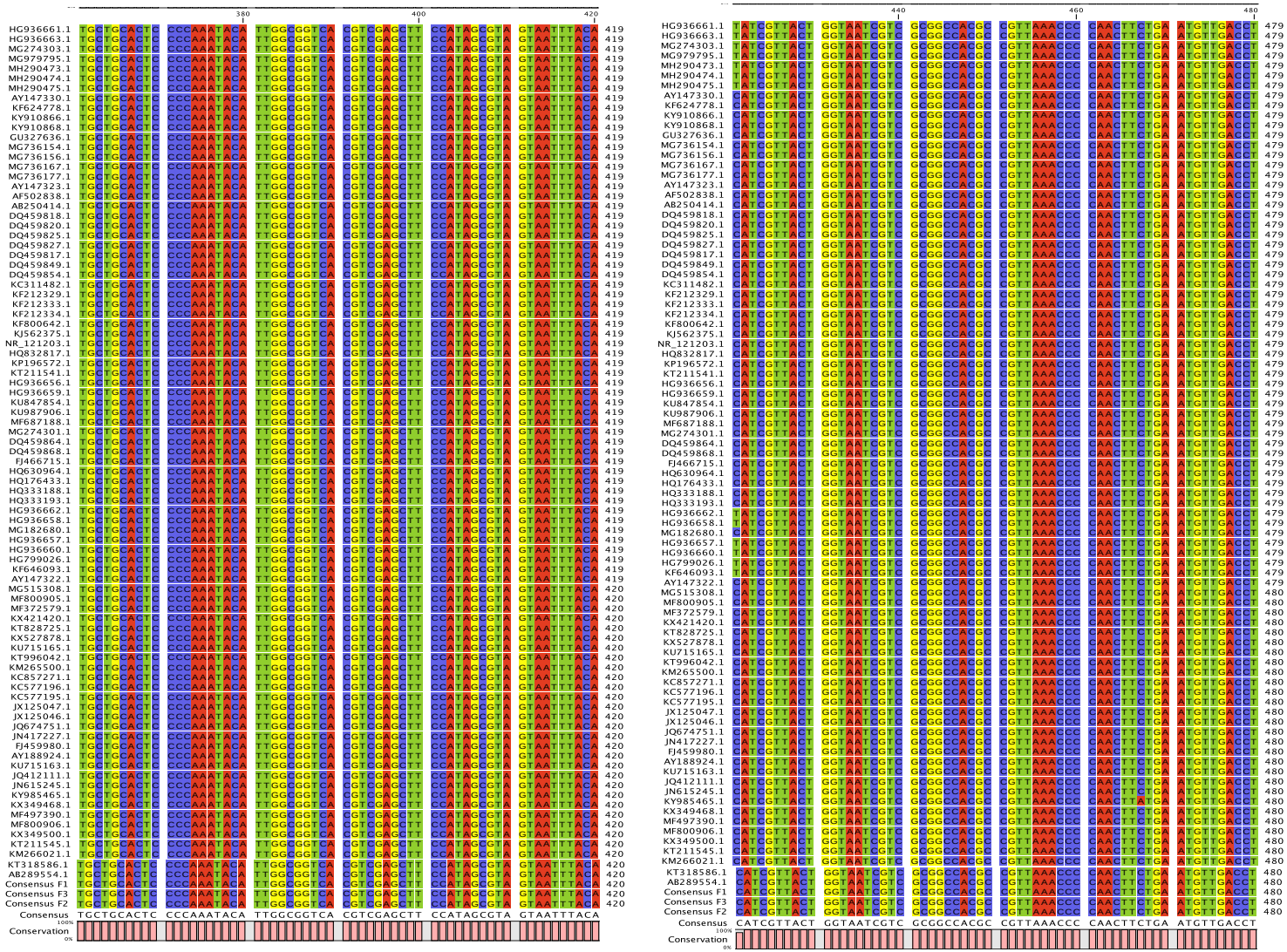
380
400
420
440
460
480
Consensus
Conservation

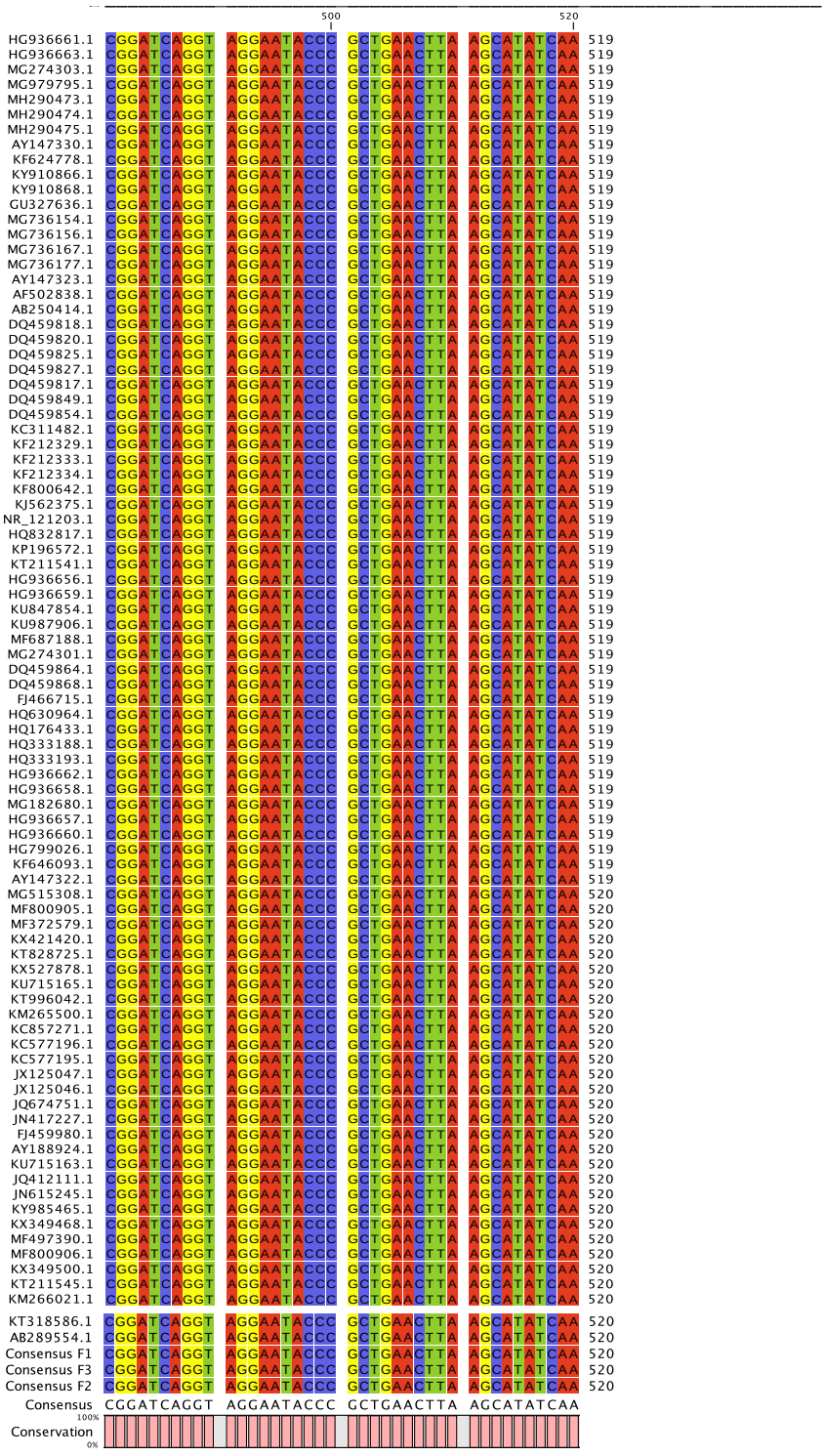

Figure 4.4: ITS region based multiple sequence alignments with comparison to the Fusaria species in GenBank databases. The alignments were created using CLC Bio Genomics Workbench v9.

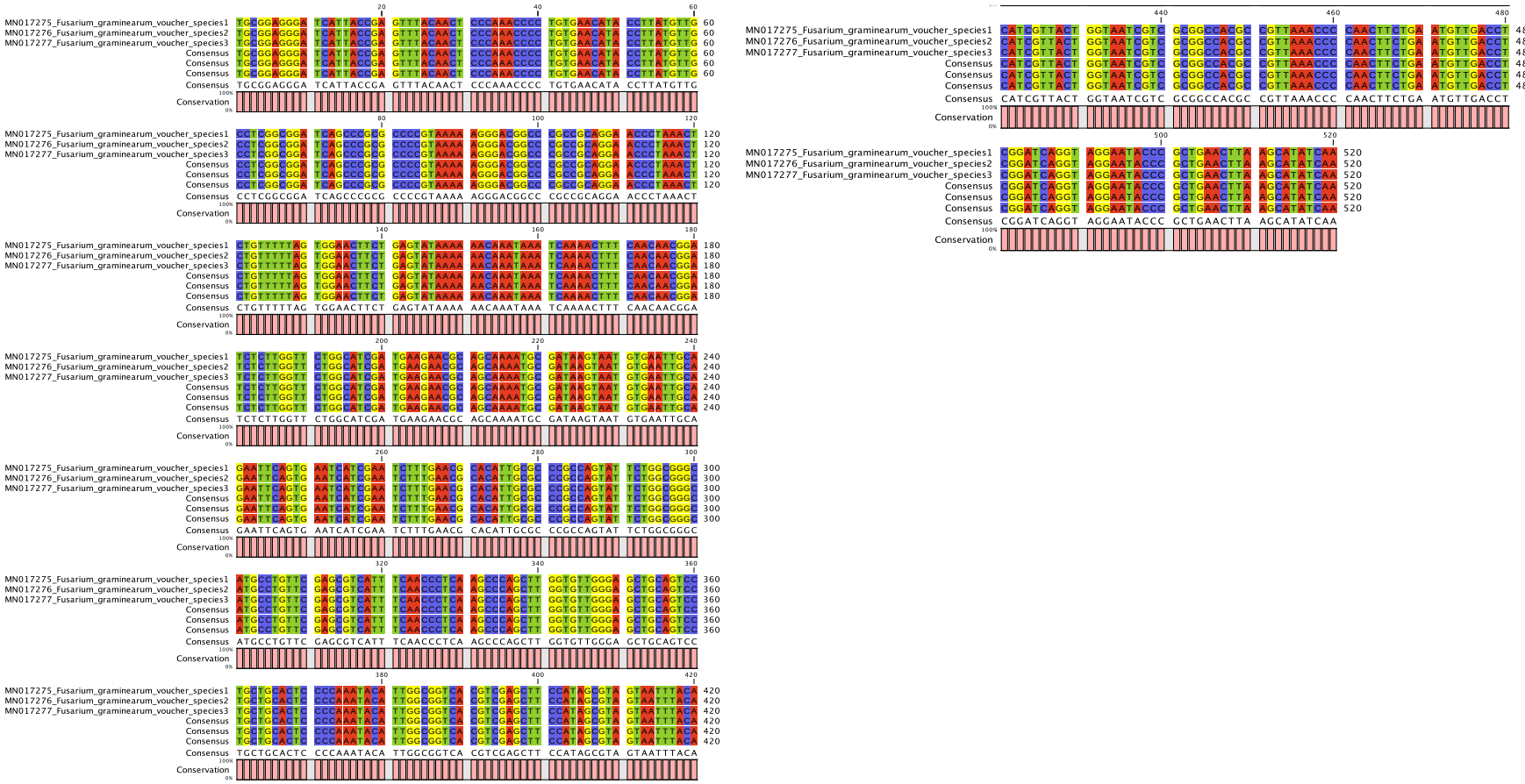
MN017275_Fusarium_graminearum_voucher_species1
MN017276_Fusarium_graminearum_voucher_species2
MN017277_Fusarium_graminearum_voucher_species3
Consensus
Conservation

Figure 4.5: Multiple sequence alignments of ITS region of *Fusarium graminearum* species that aligned with comparison to the GenBank *Fusarium graminearum* voucher species (MN017275- MN017277). The alignments were created using CLC Bio Genomics Workbench v9

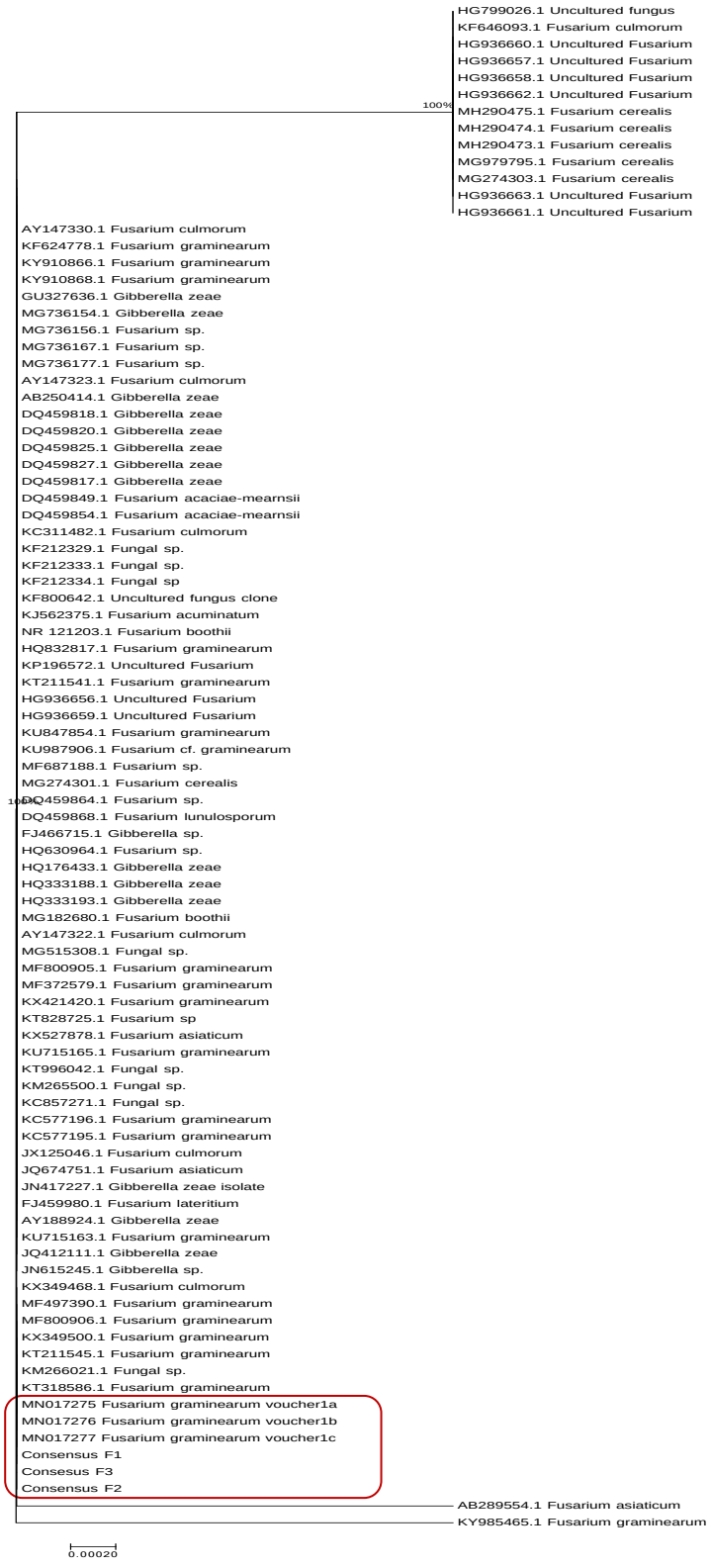
HG799026.1 Uncultured fungus
KF646093.1 Fusarium culmorum
HG936660.1 Uncultured Fusarium
HG936657.1 Uncultured Fusarium
HG936658.1 Uncultured Fusarium
HG936662.1 Uncultured Fusarium
100%
MH290475.1 Fusarium cerealis
MH290474.1 Fusarium cerealis
MH290473.1 Fusarium cerealis
MG979795.1 Fusarium cerealis
MG274303.1 Fusarium cerealis
HG936663.1 Uncultured Fusarium
HG936661.1 Uncultured Fusarium
AY147330.1 Fusarium culmorum
KF624778.1 Fusarium graminearum
KY910866.1 Fusarium graminearum
KY910868.1 Fusarium graminearum
GU327636.1 Gibberella zeae
MG736154.1 Gibberella zeae
MG736156.1 Fusarium sp.
MG736167.1 Fusarium sp.
MG736177.1 Fusarium sp.
AY147323.1 Fusarium culmorum
AB250414.1 Gibberella zeae
DQ459818.1 Gibberella zeae
DQ459820.1 Gibberella zeae
DQ459825.1 Gibberella zeae
DQ459827.1 Gibberella zeae
DQ459817.1 Gibberella zeae
DQ459849.1 Fusarium acaciae-mearnsii
DQ459854.1 Fusarium acaciae-mearnsii
KC311482.1 Fusarium culmorum
KF212329.1 Fungal sp.
KF212333.1 Fungal sp.
KF212334.1 Fungal sp
KF800642.1 Uncultured fungus clone
KJ562375.1 Fusarium acuminatum
NR 121203.1 Fusarium boothii
HQ832817.1 Fusarium graminearum
KP196572.1 Uncultured Fusarium
KT211541.1 Fusarium graminearum
HG936656.1 Uncultured Fusarium
HG936659.1 Uncultured Fusarium
KU847854.1 Fusarium graminearum
KU987906.1 Fusarium cf. graminearum
MF687188.1 Fusarium sp.
MG274301.1 Fusarium cerealis
100%
DQ459864.1 Fusarium sp.
DQ459868.1 Fusarium lunulosporum
FJ466715.1 Gibberella sp.
HQ630964.1 Fusarium sp.
HQ176433.1 Gibberella zeae
HQ333188.1 Gibberella zeae
HQ333193.1 Gibberella zeae
MG182680.1 Fusarium boothii
AY147322.1 Fusarium culmorum
MG515308.1 Fungal sp.
MF800905.1 Fusarium graminearum
MF372579.1 Fusarium graminearum
KX421420.1 Fusarium graminearum
KT828725.1 Fusarium sp
KX527878.1 Fusarium asiaticum
KU715165.1 Fusarium graminearum
KT996042.1 Fungal sp.
KM265500.1 Fungal sp.
KC857271.1 Fungal sp.
KC577196.1 Fusarium graminearum
KC577195.1 Fusarium graminearum
JX125046.1 Fusarium culmorum
JQ674751.1 Fusarium asiaticum
JN417227.1 Gibberella zeae isolate
FJ459980.1 Fusarium lateritium
AY188924.1 Gibberella zeae
KU715163.1 Fusarium graminearum
JQ412111.1 Gibberella zeae
JN615245.1 Gibberella sp.
KX349468.1 Fusarium culmorum
MF497390.1 Fusarium graminearum
MF800906.1 Fusarium graminearum
KX349500.1 Fusarium graminearum
KT211545.1 Fusarium graminearum
KM266021.1 Fungal sp.
KT318586.1 Fusarium graminearum
MN017275 Fusarium graminearum voucher1a
MN017276 Fusarium graminearum voucher1b
MN017277 Fusarium graminearum voucher1c
Consensus F1
Consesus F3
Consensus F2
AB289554.1 Fusarium asiaticum
KY985465.1 Fusarium graminearum
0.00020

Figure 4.6: Maximum likelihood phylogenetic tree of *Fusarium graminearum* species derived from *Fusarium graminearum* and other Fusaria species (unique GenBank accession number (MN017275- MN017277) targeting ITS regions. The ITS amplicons could not distinguish between other Fusaria sp. Bootstrap values were calculated from 10,000 replicates.

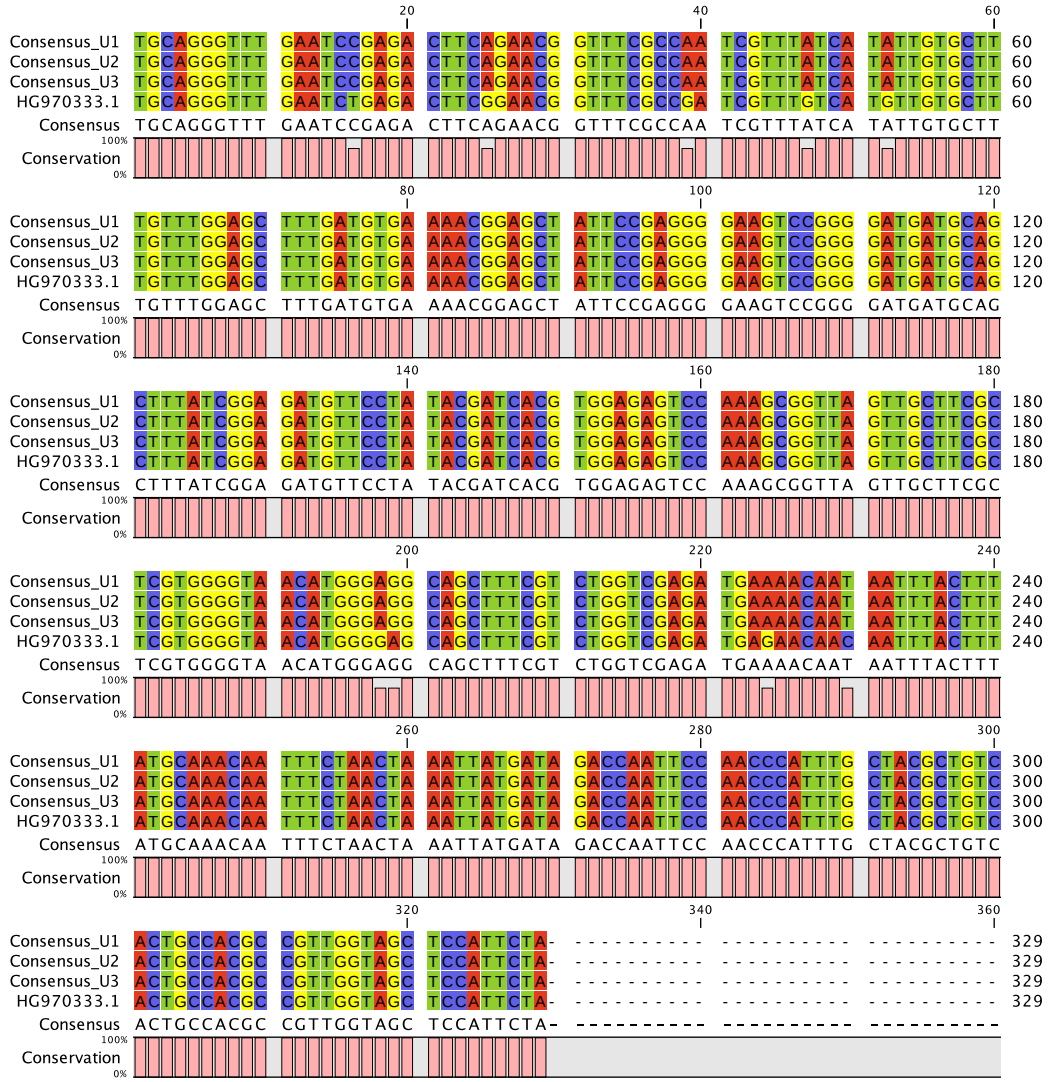

Figure 4.7: UBC region based multiple sequence alignments of *Fusarium graminearum* with comparison to the GenBank databases. The alignments were created using CLC Bio Genomics Workbench v9.

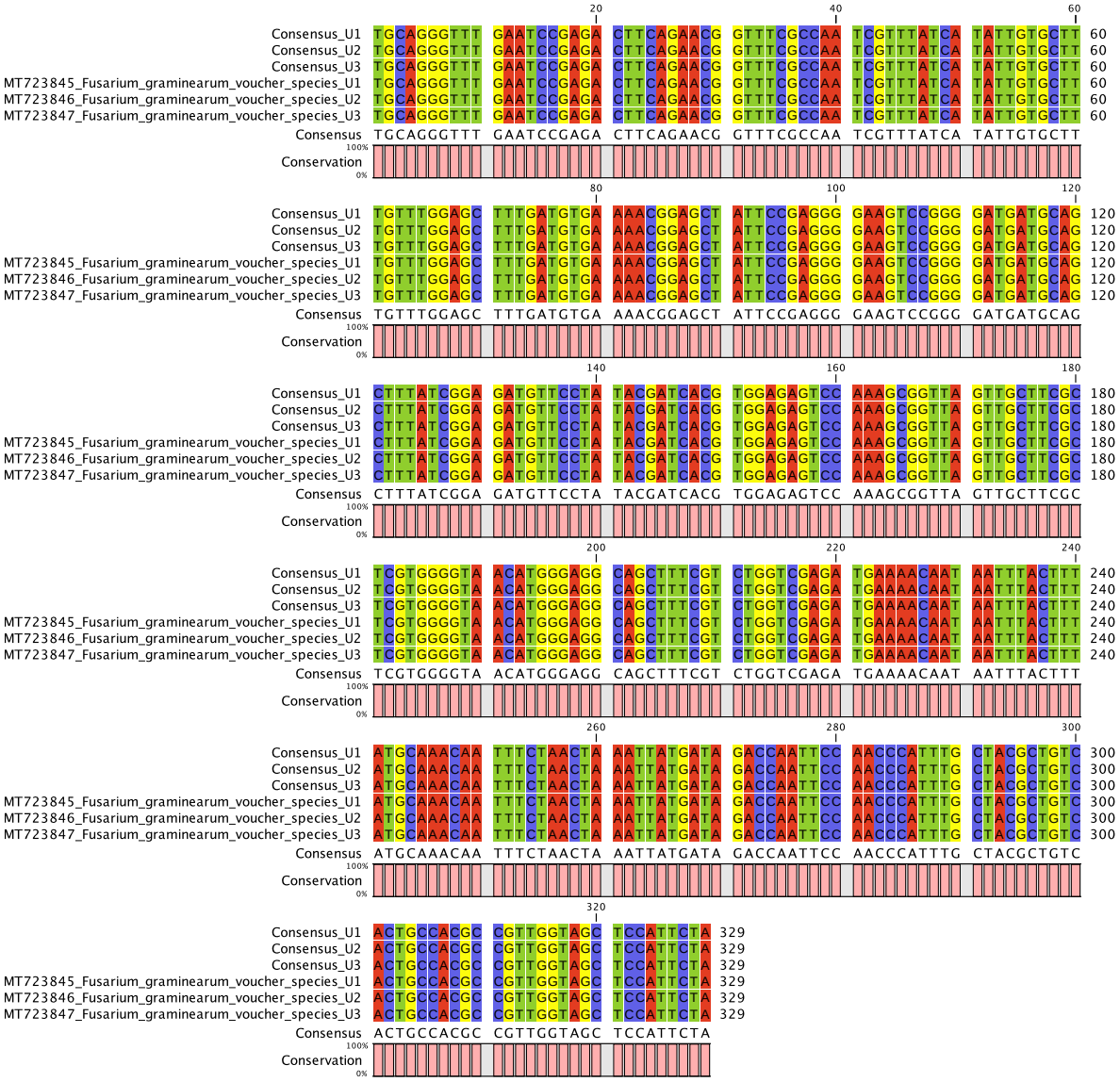

Figure 4.8: UBC region based multiple sequence alignments of *Fusarium graminearum* with comparison to the GenBank *Fusarium graminearum* voucher species. (MT723845-MT723847). The alignments were created using CLC Bio Genomics Workbench v9

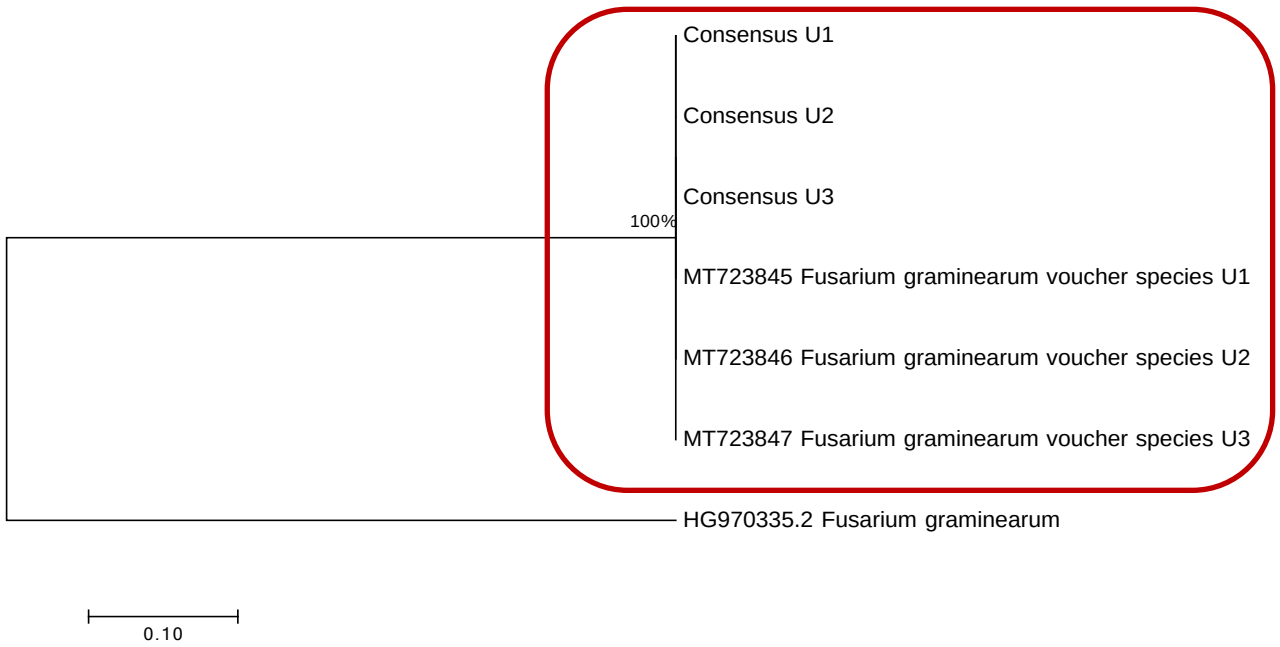

Figure 4.9: Maximum likelihood phylogenetic tree of *Fusarium graminearum* species (circled) clustered with only *Fusarium graminearum*. UBC set of primers specific to *Fusarium graminearum* identification exclusively clustered with *Fusarium graminearum* voucher species unique GenBank accession number (MT723845-MT723847) at 100% sequence identity. Bootstrap values were calculated from 10,000 replicates

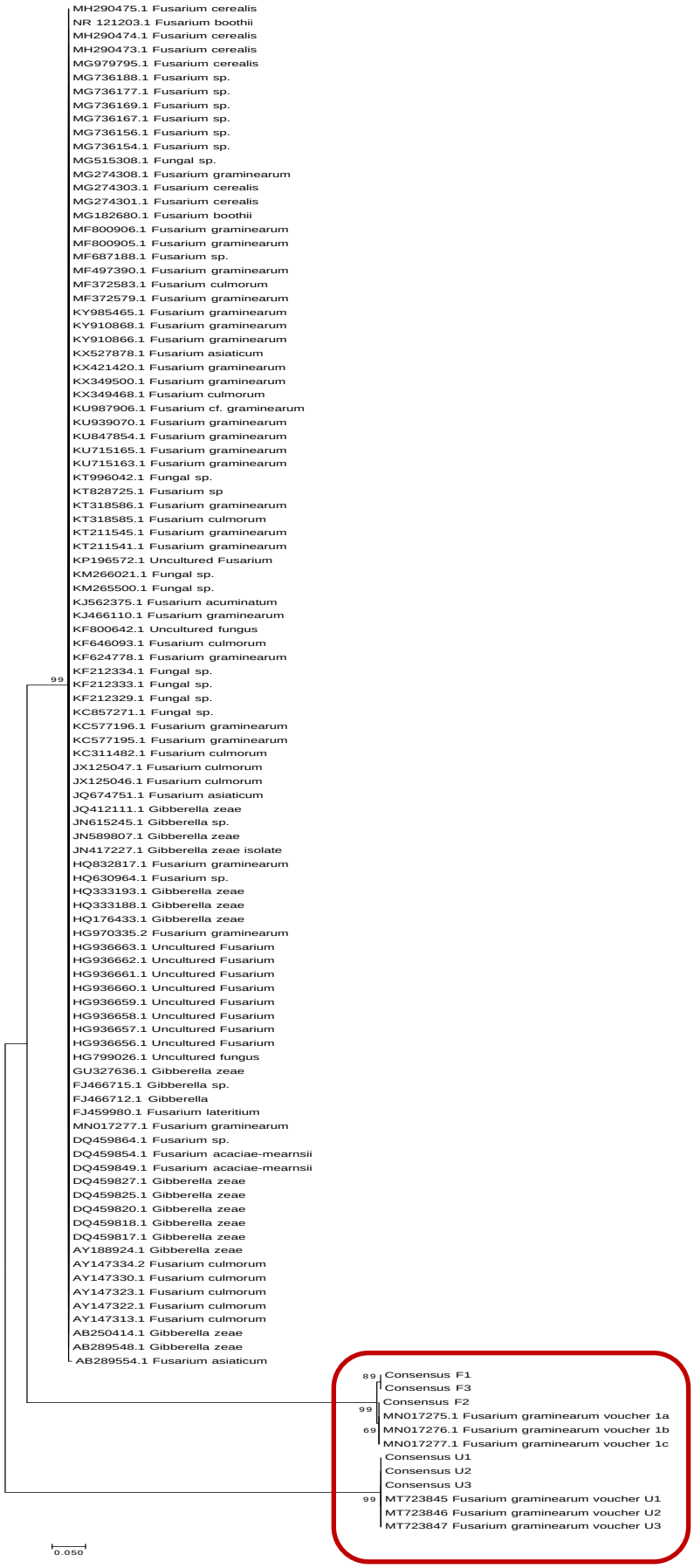
MH290475.1 Fusarium cerealis
NR 121203.1 Fusarium boothii
MH290474.1 Fusarium cerealis
MH290473.1 Fusarium cerealis
MG979795.1 Fusarium cerealis
MG736188.1 Fusarium sp.
MG736177.1 Fusarium sp.
MG736169.1 Fusarium sp.
MG736167.1 Fusarium sp.
MG736156.1 Fusarium sp.
MG736154.1 Fusarium sp.
MG515308.1 Fungal sp.
MG274308.1 Fusarium graminearum
MG274303.1 Fusarium cerealis
MG274301.1 Fusarium cerealis
MG182680.1 Fusarium boothii
MF800906.1 Fusarium graminearum
MF800905.1 Fusarium graminearum
MF687188.1 Fusarium sp.
MF497390.1 Fusarium graminearum
MF372583.1 Fusarium culmorum
MF372579.1 Fusarium graminearum
KY985465.1 Fusarium graminearum
KY910868.1 Fusarium graminearum
KY910866.1 Fusarium graminearum
KX527878.1 Fusarium asiaticum
KX421420.1 Fusarium graminearum
KX349500.1 Fusarium graminearum
KX349468.1 Fusarium culmorum
KU987906.1 Fusarium cf. graminearum
KU939070.1 Fusarium graminearum
KU847854.1 Fusarium graminearum
KU715165.1 Fusarium graminearum
KU715163.1 Fusarium graminearum
KT996042.1 Fungal sp.
KT828725.1 Fusarium sp
KT318586.1 Fusarium graminearum
KT318585.1 Fusarium culmorum
KT211545.1 Fusarium graminearum
KT211541.1 Fusarium graminearum
KP196572.1 Uncultured Fusarium
KM266021.1 Fungal sp.
KM265500.1 Fungal sp.
KJ562375.1 Fusarium acuminatum
KJ466110.1 Fusarium graminearum
KF800642.1 Uncultured fungus
KF646093.1 Fusarium culmorum
KF624778.1 Fusarium graminearum
99
KF212334.1 Fungal sp.
KF212333.1 Fungal sp.
KF212329.1 Fungal sp.
KC857271.1 Fungal sp.
KC577196.1 Fusarium graminearum
KC577195.1 Fusarium graminearum
KC311482.1 Fusarium culmorum
JX125047.1 Fusarium culmorum
JX125046.1 Fusarium culmorum
JQ674751.1 Fusarium asiaticum
JQ412111.1 Gibberella zeae
JN615245.1 Gibberella sp.
JN589807.1 Gibberella zeae
JN417227.1 Gibberella zeae isolate
HQ832817.1 Fusarium graminearum
HQ630964.1 Fusarium sp.
HQ333193.1 Gibberella zeae
HQ333188.1 Gibberella zeae
HQ176433.1 Gibberella zeae
HG970335.2 Fusarium graminearum
HG936663.1 Uncultured Fusarium
HG936662.1 Uncultured Fusarium
HG936661.1 Uncultured Fusarium
HG936660.1 Uncultured Fusarium
HG936659.1 Uncultured Fusarium
HG936658.1 Uncultured Fusarium
HG936657.1 Uncultured Fusarium
HG936656.1 Uncultured Fusarium
HG799026.1 Uncultured fungus
GU327636.1 Gibberella zeae
FJ466715.1 Gibberella sp.
FJ466712.1 Gibberella
FJ459980.1 Fusarium lateritium
MN017277.1 Fusarium graminearum
DQ459864.1 Fusarium sp.
DQ459854.1 Fusarium acaciae-mearnsii
DQ459849.1 Fusarium acaciae-mearnsii
DQ459827.1 Gibberella zeae
DQ459825.1 Gibberella zeae
DQ459820.1 Gibberella zeae
DQ459818.1 Gibberella zeae
DQ459817.1 Gibberella zeae
AY188924.1 Gibberella zeae
AY147334.2 Fusarium culmorum
AY147330.1 Fusarium culmorum
AY147323.1 Fusarium culmorum
AY147322.1 Fusarium culmorum
AY147313.1 Fusarium culmorum
AB250414.1 Gibberella zeae
AB289548.1 Gibberella zeae
AB289554.1 Fusarium asiaticum
89
Consensus F1
Consensus F3
Consensus F2
99
MN017275.1 Fusarium graminearum voucher 1a
69
MN017276.1 Fusarium graminearum voucher 1b
MN017277.1 Fusarium graminearum voucher 1c
Consensus U1
Consensus U2
Consensus U3
99
MT723845 Fusarium graminearum voucher U1
MT723846 Fusarium graminearum voucher U2
MT723847 Fusarium graminearum voucher U3
0.050

Figure 4.10: Maximum likelihood phylogenetic tree of UBC and ITS primer sets NCBI database sequences together with their voucher species. UBC and ITS primer set exclusively clustered with *Fusarium graminearum* voucher species with unique GenBank accession number (MT723845-MT723847; MN017275-MN017277) at 100% sequence identity. While the Fusaria species in the NCBI database were highly variable. Bootstrap values were calculated from 10,000 replicates

4.4 DISCUSSION

The purpose of this chapter was to confirm the identity of the pathogen and check the viability of the pathogen to ensure infection initiation. Previous studies relied on morphological identification which requires considerable expertise in physiology and taxonomy and are time consuming. Furthermore, the identification and classification of *Fusarium* spp. using morphological characteristics is difficult even for specialists because of the large morphological variation of isolates within a single species and also because of the varieties, number, and forms of species (Abedi-Tizaki and Sabbagh, 2012; Leslie et al., 2005).

The amplification of ITS regions (ITS 1 and ITS 4) in this study resulted in the expected ~600 base pairs (bp) products. The ITS sequences of the 3 individual samples clustered with *Fusarium graminearum* (*Gibberella zeae*) voucher sequences which were deposited in the NCBI database. The three individual ITS samples (voucher species) were assigned NCBI unique gene accession numbers (MN017275- MN017277). As much as primers targeted to the internal transcribed sequence (ITS) of the ribosomal DNA (Schilling et al., 1996) were used, the identification and detection of *Fusarium graminearum* sequences in the ITS regions has been reported to be highly variable in fusaria (Frenkel et al., 2012; O'Donnell, 1992). This was illustrated in the current study through the alignment of the isolated species and NCBI GenBank fusaria sequences. However, through multiple sequence alignment, voucher sequences aligned with the isolates used in this study.

The proper identification of *Fusarium* spp. is critical to predict the potential mycotoxigenic risk of the isolates, as there is a need for complementary and accurate tools that permit sensitive, specific, reliable and rapid diagnosis of *Fusarium* spp. (Sampietro et al., 2010). Hence, PCR assays that are species-specific are usually needed for accurate identification. Accordingly, species-specific PCR was conducted to confirm the *Fusarium graminearum* species identity with strain specific primers ($UBC85F_{410}$-$UBC85R_{410}$), which were subsequently confirmed through Sanger sequencing. The UBC primer sets generated sequences of the three individual isolates with a fragment size of ~450 bp. The isolates exclusively showed the percentage similarity with only *Fusarium graminearum*, in contrast with the ITS primer sets which presented isolates that aligned with other *Fusarium* spp.

showing high variability. Furthermore, phylogenetic and multiple alignments analysis have shown that the species-specific isolates used in this study clustered and aligned with voucher *Fusarium graminearum* species at 100% sequence similarity. With regards to the viability of the spores, the percentage was calculated through the automated cell counter. The re-suspended conidial concentration of 1×10^6 to 2×10^4 resulted in live cells being more than the dead cells in terms of cell number and concentration. The automated cell counter measured the live spores (cell concentration) of the pathogen to 2.25 x 10^7 cells/ml, and the spore viability was at 65% which was enough to initiate pathogen infection (Barua et al., 2017).

4.5 CONCLUSION

Molecular analyses pointed to the confirmation of *Fusarium graminearum* using the fungal ITS primers set and strain specific primers ($UBC85F_{410}$-$UBC85R_{410}$). This study also confirms through the alignment and phylogenetic analysis that the species is *Fusarium graminearum* and not any other related *Fusarium* spp. One of the aims of this chapter was also to count the number of live cells/spores present in a given sample solution, to ensure that plant pathogen infection will occur in the subsequent chapter through the automated cell counter. The percentage of the live spores was over 60% which ensured that viability of the *Fusarium graminearum* will allow for the infection of the plant by the pathogen.

CHAPTER 5

Gene expression patterns in susceptible and resistant recombinant inbred line (RILs) in response to *Fusarium graminearum* infection across different time-points

5.1 INTRODUCTION

Sorghum, like any other plant, is subjected to a wide variety of biotic and abiotic constraints. Plants are susceptible to infection by agents of varying complexity including eukaryotic parasites such as fungi. Pathogen infection instigate a dynamic cascade of events which culminates in gene expression patterns that are altered in both interacting organisms (Westermann et al., 2017). These changes give rise to the pathogen adaptation and persistence or to its clearance from the host by the immune response. A global and an unbiased understanding of the transcriptomes of both host and pathogen can provide new insights by identifying pathways in the host cell that respond to pathogen-associated molecular patterns (PAMPs) exposure to specific pathogens.

Fusarium graminearum has been found in this study to be associated with highly diseased RILs. Sorghum has been previously reported as both a host and an important alternative host of the fungal pathogen *Fusarium graminearum* (Goswami and Kistler, 2004). *Fusarium graminearum* has also shown the highest pathogenicity on sorghum grain compared to other fusaria species (Quazi et al., 2010). The *Fusarium graminearum* species is a significant, pathogen in maize and winter cereals, and has been associated with stalk rot and grain mould of sorghum (Nida et al., 2019; Kelly et al., 2017; Menkir et al., 1996; Trimboli and Burgess, 1985). Not only is it a major biotic sorghum production constraint, *Fusarium graminearum* causes Gibberella ear rot of maize, and Fusarium head blight (FHB) of wheat and barley (Harris et al., 2016).

Additionally, *Fusarium graminearum* can be a toxicological risk to animals and humans (Pena et al., 2019; Burgess et al., 2002), since this species has the potential to produce 15-acetyldeoxynivalenol (15-ADON), deoxynivalenol (DON), nivalenol (NIV), 3-acetyldeoxynivalenol (3-ADON) and zearalenone (ZEA) (Yerkovich et al., 2017). The toxicological effect of *Fusarium graminearum* is that, it is responsible for the majority of important mycotoxins in winter cereals as they cause reduced kernel germination, mass and density, reduced nutritional quality, market value, storage quality and unfavourable processing

characteristics (Balota et al., 2012; Navi et al., 2005; Marley and Ajayi, 1999; Menkir et al., 1996).

The total loss of 130 million US dollars in the semi-arid tropical areas of Asia and Africa due to mycotoxins has been reported by the International Crops Research Institute for the Semi-Arid Tropics (ICRISAT) (Gosal and Wani, 2018). Currently, the most prominent way to control mycotoxins is through the use of traditional ways that are laborious. Additionally, they have proved to be inefficient in the mycotoxins on grains. The best way to remove/limit mycotoxins from contaminated food crop is to be able to control *Fusarium graminearum*. Several recent transcriptome studies in *Arabidopsis,* wheat, and maize have been conducted to study the response to *Fusarium graminearum* (Kheiri et al., 2019; Sarowar et al., 2019; Zhou et al., 2019). The mechanisms underlying the host defence response against *Fusarium graminearum* using comparative transcriptome analysis in susceptible and resistant maize and wheat genotypes has been conducted (Brauer et al., 2019; Yuan et al., 2019). To the best of our knowledge there is no reported study of gene expression study using RNA-Seq studies conducted in the response of sorghum upon *Fusarium graminearum* infection. Therefore, the aim of this chapter was to do comparative gene profiling to inspect the difference between the resistant (RIL 103) and the susceptible (RIL 131) recombinant inbred lines (RILs) upon *Fusarium graminearum* infection across time-points 24 hours post infection (hpi), 48 hpi, 7 days post infection (dpi) and 14 dpi using the RNA-Seq technique. And also, to determine if *Fusarium graminearum* induces specific defence-related genes in the resistant RIL.

5.2 MATERIALS AND METHODS

5.2.1 Sorghum cultivation

Sorghum recombinant inbred lines (RILS) were cultivated in vermiculate and perlite medium in pre-sterilized pots. The plants were watered to 60% water holding capacity and the moisture content was maintained by watering to weight every 2–3 days. The experiment was carried out in a controlled-environment glasshouse where the temperature was maintained at 25 ± 2 ^{o}C.

5.2.2 Fungal inoculation on the plant

Sorghum leaves were inoculated at seedling stage in triplicate using point inoculation method (artificial inoculation of the pathogen inoculum applied on the host surface). The wounds were made on the host surface directly on the underside of the leaf and the leaves were inoculated with conidial suspension of fungi. Inoculated leaves were covered with paper bags for 24 hours post infection (hpi).

5.2.3 Sampling

Both susceptible and resistant sorghum RILs leaves were collected, according to the time-points 24 hours and 48 hours post inoculation (hpi) for early pathogenesis, and at 7 days and 14 days post inoculation (dpi) for late pathogenesis. The RILs leaves were collected in biological triplicates as shown in Figure 5.1.

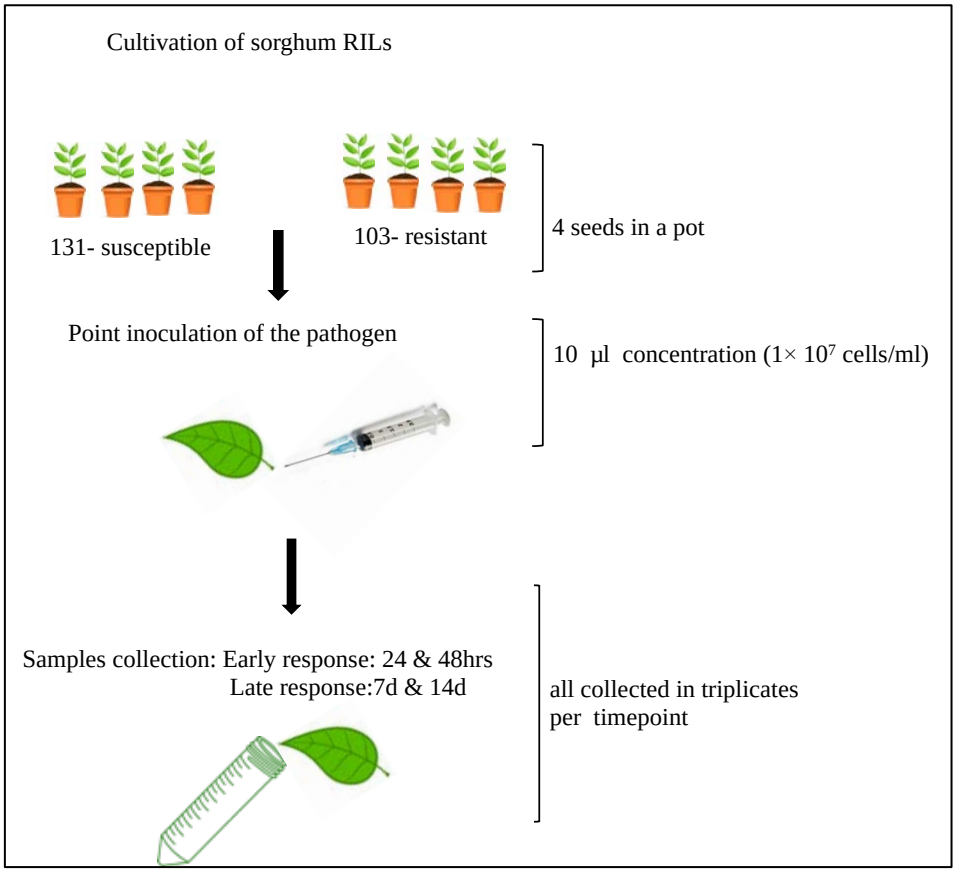

Figure 5.1: Experimental setup and sampling strategy. The resistant and the susceptible RILs were cultivated and point inoculation was used to infect both resistant and susceptible RILs. The leaf samples were collected in biological replicates in timepoints 24 hours post infection (hpi), 48 hpi, 7 days post infection (dpi) and 14 dpi.

5.2.4 Treatment of equipment and glassware for RNA isolation

Pestles and mortars, spatulas and tweezers that were used for RNA preparations and isolations were treated with DEPC in water, then autoclaved at 121 ^{o}C for 15 min to sterilize. After autoclaving, the instruments and glassware were subjected to 80 °C dry heat to dry before being utilized. Equipment such as gel preparation trays, combs, and gel running tank were treated with DEPC water before being used.

5.2.5 RNA extraction and quantification

Leaf tissues (100 mg) from infected resistant and susceptible RILs for time points 24 hpi, 48 hpi, 7 dpi and 14 dpi were ground in liquid nitrogen. For each biological replicate (at each time point), three plants were used. RNA was isolated from leaf material using the Nucleospin RNA plant kit (Macherey-Nagel, Germany), following manufacturer's instructions. RNA was digested with DNase using the RNase-Free DNase kit (Qiagen, Valencia, CA), subsequently eluted in 50 µl RNase-free water, and stored at -80 °C (to ensure that the leaf samples produces a high quality RNA) until further usage. RNA concentration was quantified using a Qubit® fluorometer.

5.2.6 Gel electrophoresis

RNA quality was viewed with agarose gel electrophoresis. Briefly, the cast gels were equilibrated in the running buffer 1xTBE (Tris base: Boric acid: EDTA at 10 V/cm for 30 min. A RiboRuler RNA ladder was used as molecular size marker (RiboRuler, Fermentas). Ethidium bromide stained images were captured on a BioRad Gel/Chemi DOC (BioRad laboratories Inc., CA). After quantifying concentrations using a Qubit® fluorometer, all RNA samples were adjusted to the same concentration.

5.2.7 Library preparation and RNA sequencing

Library preparations were performed from total RNA using the TruSeq Stranded mRNA Sample Preparation Kit (Illumina, San Diego, CA, USA) that captures poly A tails of mRNA molecules. First strand cDNA was synthesized using random hexamers and reverse

transcriptase followed by the synthesis of the second strand. The cDNA fragments were 3′ adenylated followed by ligation of the adapter with RNA adapter indexes. PCR amplification was performed to enrich for adapter ligated fragments. The concentration of the libraries was determined using a Qubit® fluorometer following the manufacturer's instructions, and the libraries were further validated by electrophoresis on a 1% 1xTBE agarose gel. Library dilutions were prepared and loaded on a cBOT system (Illumina, San Diego, CA, USA) for cluster generation and sequenced using an Illumina HiSeq 2500 (ARC-BTP). Each biological replicate (3 per time point) was sequenced separately for each recombinant inbred line (131 and 103) at 24 hpi, 48 hpi, 7 dpi and 14 dpi.

5.2.8 Bioinformatic analysis

The quality of the sequenced data was assessed using the FastQC v0.10.1 tools (Andrews, 2010). Trimmomatic v0.36 (Bolger et al., 2014) was used to remove adapters and low-quality reads from the RNA-Seq data in raw fastq files. The quality-filtered reads were then mapped to the sorghum v3.3.1 reference genome using HISAT2 v2.0.5 (McCormick et al., 2018; Karlovsky et al., 2016; Pertea et al., 2016). For this process, a maximum of two mismatches were allowed, and all other parameters were used with the default settings. The mapped data was assembled into transcripts and quantified using StringTie v1.3.1 (Pertea et al., 2015). Default parameter settings were used for the quantification, based on the sorghum annotation file. StringTie generated a matrix of expression values in fragments per kilobase of exon model per million reads mapped (FPKM). Samtools (Li et al., 2009) was used to convert sequence alignment map (SAM) output files to binary alignment map (BAM) format and transcript assembly was completed using Cufflinks (Trapnell et al., 2010). A combined gene transfers format (GTF) assembly file was created for differential expression analysis, using Cuffmerge, containing the reference GTF genome as well as the Cufflinks output for each sample (Trapnell et al., 2012). Gene expression data from the biological replicates of each genotype was compared to determine the positive correlation of biological replicates within the same time-point using MS Excel measured with Fragments Per Kilobase of transcript per Million mapped reads (FPKM) values (Figures 5.2A and 5.2B). The biological triplicates data was not pooled and each biological replicate was analysed separately per time-point for each genotype before differentially expressed genes analysis.

5.2.9 Differential analyses with Cuffdiff

The files were amalgamated into a single, unified transcript catalog and the transcribed fragments that may be artefacts were filtered out using Cuffmerge. The reference annotation file was included to allow gene names and other details such as, exon number, transcript ID, coding sequence ID and transcription start site ID to be added to the merged transcript catalogue. The merged GTF file was then provided to Cuffdiff along with the original alignment files produced from HISAT2. Cuffdiff was used to determine pairwise differential gene expression between the various time-points, and the cummeRbund R package was used to generate graphical representations of the RNA-Seq data set (Trapnell et al., 2012, 2010). Differentially expressed genes (DEGs) were determined with a log2 fold change ≥ 0 cut-off and an absolute FDR-value of ≤ 0.05.

5.2.10 Gene expression clustering and pathway enrichment

Gene expression values (FPKMs) for all the time points (24 hpi, 48 hpi, 7 dpi and 14 dpi) were analysed for significant expression in the resistant and susceptible RILs. The differentially expressed genes for both the susceptible and resistant RILs generated by cuffdiff as mentioned in section 5.2.5 were used for gene expression clustering analysis. Each transcript expression value (FPKM) of the differentially expressed transcripts was $\log_2$ transformed to normalise the data. DPGP clustering of genes with respect to expression levels was done using Dirichlet Process Gaussian Process mixture model (DPGP) software (McDowell et al., 2018). A maximum number of (1000) of iterations of clustering were performed with default software parameters. The resistant and susceptible RILs were clustered into closely related expression profiles to determine cluster membership across all timepoints in each RIL. KEGG mapping and pathway enrichment for each cluster group were analysed using KEGG Orthology Based Annotation System (KOBAS) (Xie et al., 2011) version 3.0 (http://kobas.cbi.pku.edu.cn/). Gene enrichment was done using default settings against *Arabidopsis*. $P<0.05$ and input number >3 were considered to be the most significant (Wu et al., 2017). The complete list of commands and packages are listed in Appendix C.

5.2.11 Profiling of time-points using keyword Gene Ontology terms and pathway analyses

The Gene Ontology (GO) terms associated with differential expressed genes (DEGs) were described into biological processes, molecular functions and cellular components. The WEGO program was used to plot GO annotations (http://wego.genomics.org.cn) (Ye et al., 2018). Pathway analysis was performed using the Kyoto Encyclopedia of Genes and Genomes (KEGG) annotation service (http://www.genome.jp/kegg/pathway.html) (Moriya et al., 2007; Kanehisa et al., 2004). KEGG Orthology (KO) terms were assigned to DEGs using the *Sorghum bicolor* annotation file (www.phytozome.net). The list of assigned KO terms for each time point and RIL type were then mapped to KEGG pathways for enzyme function. Pathway annotation to reveal the trend of physiological processes affected by enriched pathway enzymes encoded by the DEGs were clustered (Section 5.2.7). A comparison of the overall DEGs between the resistant and susceptible RIL across all timepoints were then mapped to KEGG pathways and significantly enriched terms were further identified in comparison with the *Arabidopsis thaliana* genome background.

5.3 RESULTS

5.3.1 Biological replicate variability and sequenced data information

A detailed account of all sequencing reads generated per time point (an average of 3 replicates) is provided in Table 5.1. RNA-Seq data was acquired for RIL 131 and 103 from *Fusarium graminearum* inoculated leaves at 24 hpi, 48 hpi, 7 dpi and 14 dpi in biological triplicates. The RNA-Seq reads resulted in high quality raw reads represented by (Figure 5.1A). Figure 5.1B represents a trimmed sequence, where low quality reads and reads containing adaptor sequences were trimmed, and their quality was then assessed before and after trimming using FastQC (Andrews, 2010). High quality reads were generated, resulting in the retention of an average of 83% of the sequences after trimming (Table 5.1). Paired end reads only were considered in the mapping to the reference genome. The reads for each biological replicate in each time-point were mapped individually to the reference genome with HISAT2 (Pertea et al., 2015). On average, 87% of the trimmed reads could be mapped to the sorghum reference genome (Table 5.1). The assessed intergroup variation of gene expression of replicates using excel, presented a good correlation between reads from the different biological replicates of each sorghum RIL (in both susceptible and resistant RILs). The correlation coefficient values ranged from R^2 = 0.92 - 0.99 (Figures 5.2A and 5.2B) in 24 hpi, 48 hpi, 7 dpi and 14 dpi timepoints. Results show that transcripts in the sorghum samples were highest in the susceptible RIL based on differentially expressed genes (DEG s) at False Discovery Rate (FDR $\leq$ 0.05).

Table 5.1: Summary of raw and trimmed reads generated per time-point after pooling across the three biological replicates and subsequently mapping to the sorghum reference genome (Sbicolor_454_v3.0.1.fa).

RIL Dataset	Hours/days post-infection	No. of raw reads	Trimmed reads	%Trimmed reads	% Mapped reads
131	24 hpi	80 million reads	66 million reads	83	84
	48 hpi	112 million reads	91 million reads	82	90
	7 dpi	55 million reads	51 million reads	93	78
	14 dpi	44 million reads	38 million reads	88	91
103	24 hpi	20 million reads	15 million reads	75	81
	48 hpi	75 million reads	56 million reads	75	90
	7 dpi	34 million reads	28 million reads	83	91

	14 dpi	188 million reads	152 million reads	81	91

RNA-Seq data acquired for RIL 131 and 103 from *Fusarium graminearum* inoculated leaves at 24 hpi, 48 hpi, 7 dpi, 14 dpi. Paired end reads generated through Trimmomatic (v0.36) (Bolger et al., 2014) only were considered in the mapping to the reference genome (average mapping rate of 87%).

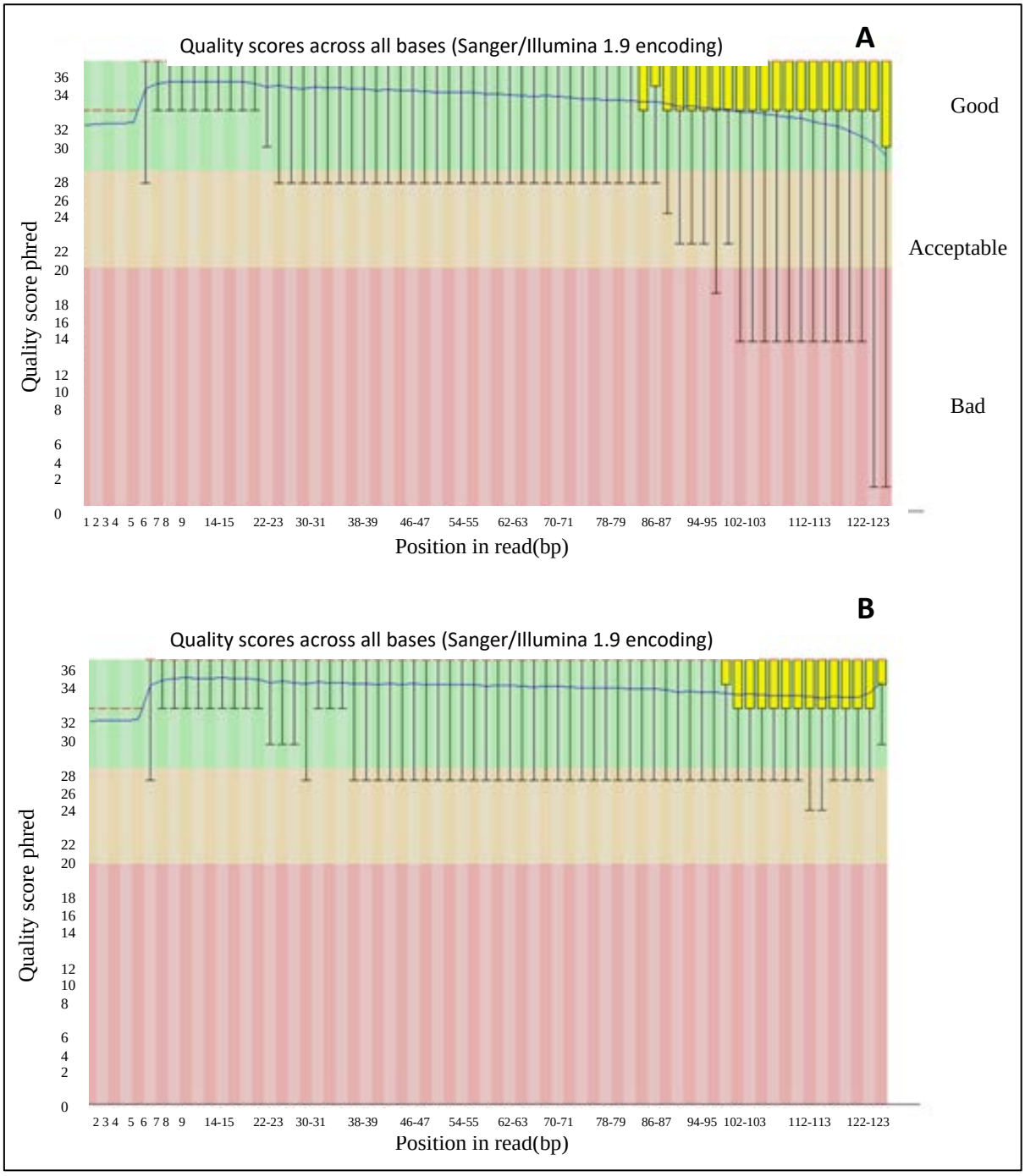

Figure 5.2: Quality analysis of reads before and after adapter clipping and trimming. A=analysis of raw reads, B = analysis of read quality after read processing. Read quality was viewed using FastQC version 0.11.8 (Andrews, 2010). The green area indicates the good reads suitable for further analysis and data representation, orange is acceptable reads, and the pink area is the bad unacceptable reads.

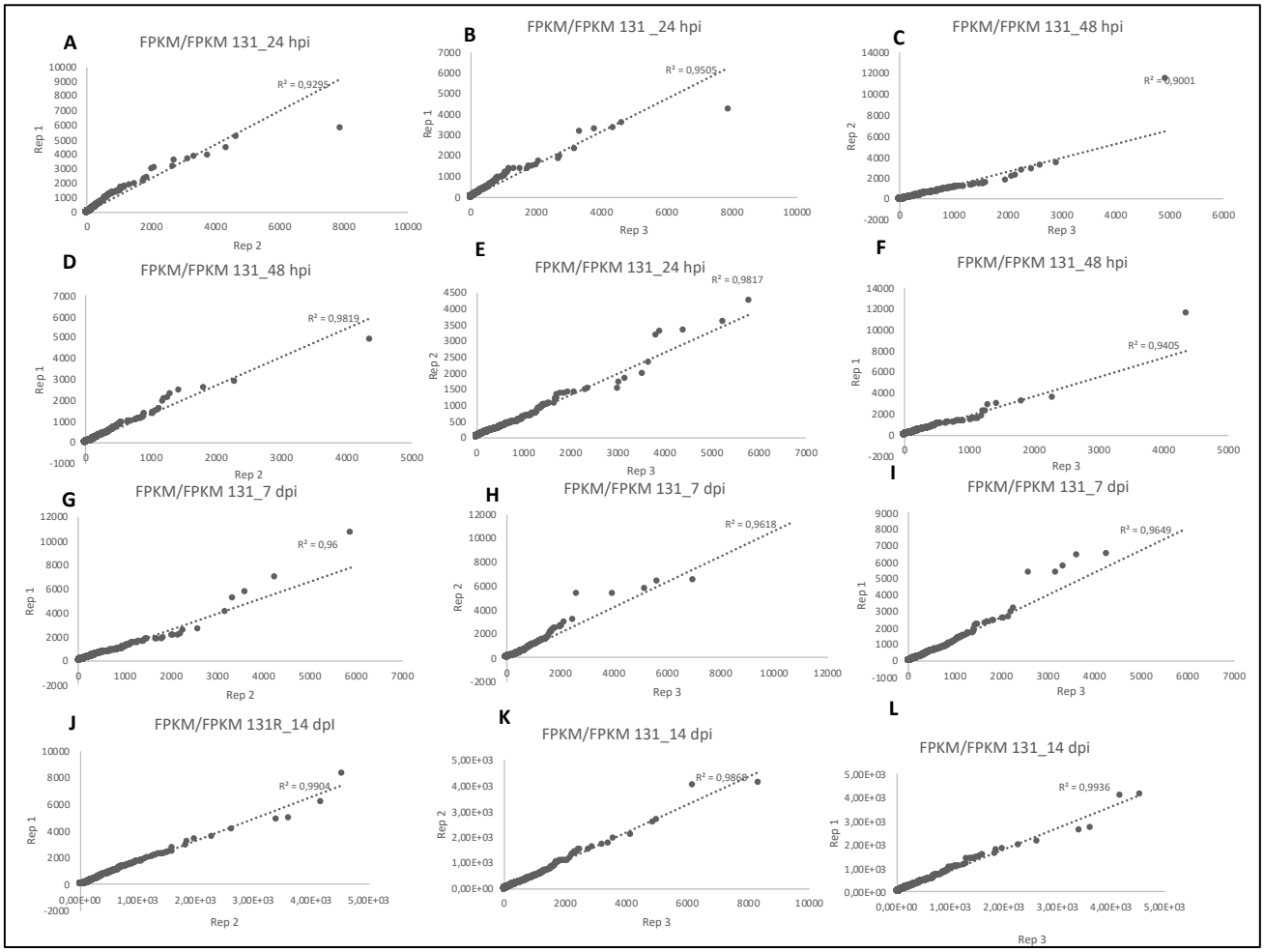

Figure 5.3A: FPKM/FPKM scatter charts of the susceptible RIL leaf samples infected with *Fusarium graminearum* (24 hpi – 14 dpi). Coefficient of determination (r^2) measuring the degree of relationship between two variables within 3 biological replicates. Images A-C show 24 hpi (infected at 24 h), D-F show correlations of 3 biological replicates at 48 hpi (infected at 48 h), G-I show correlations of 3 biological replicates at 7 dpi (infected at 7 days), and J-L show correlations of 3 biological replicates at 14 dpi (infected at 14 dpi).

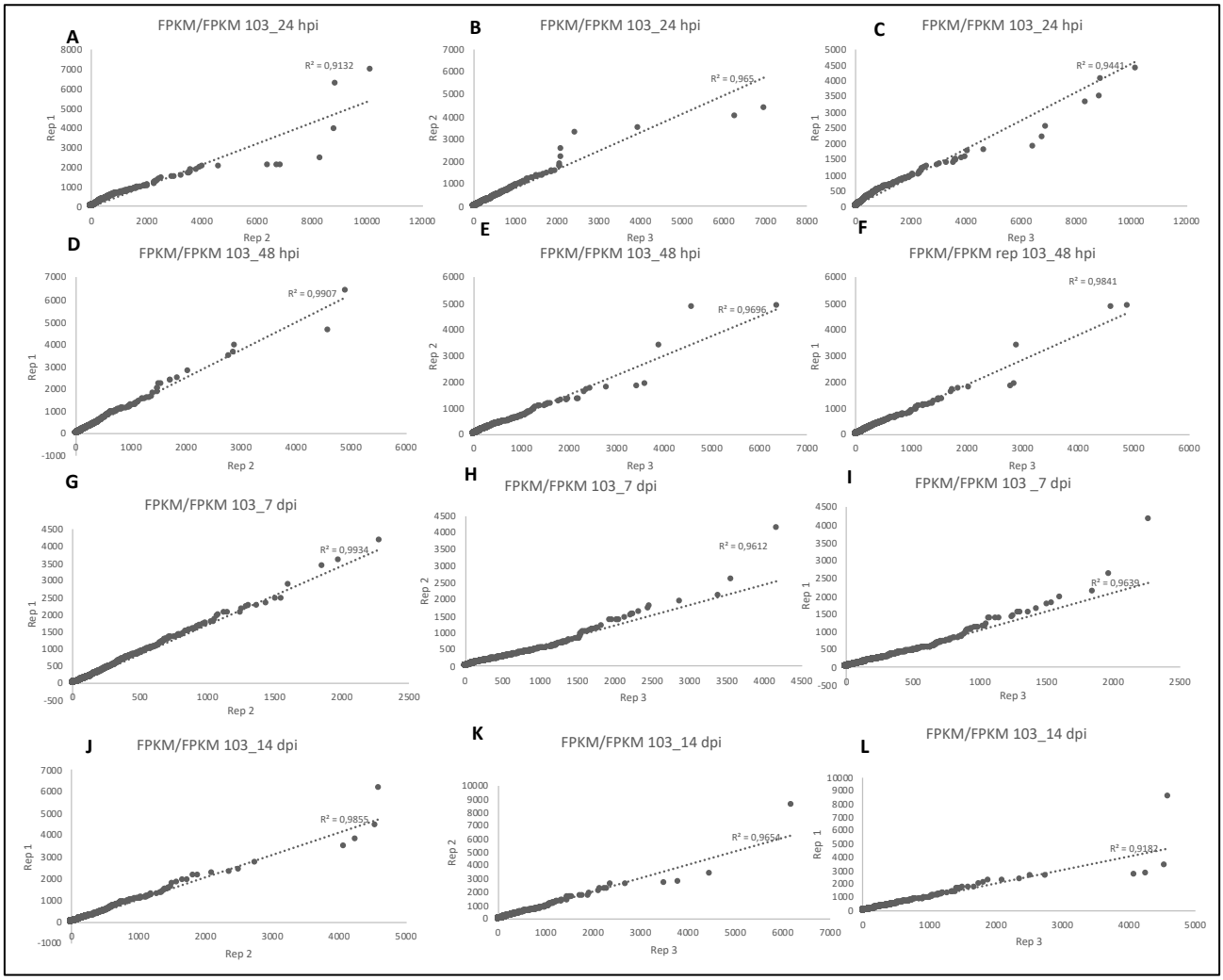

Figure 5.3B: FPKM/FPKM scatter charts of the resistant RIL leaf samples infected with *Fusarium graminearum* (24 hpi – 14 dpi). Coefficient of determination (r^2) measuring the degree of relationship between two variables within 3 biological replicates. Images A-C show 24 hpi (infected at 24 h), D-F show correlations of 3 biological replicates at 48 hpi (infected at 48 h), G-I show correlations of 3 biological replicates at 7 dpi (infected at 7 days), and J-L show correlations of 3 biological replicates at 14 dpi (infected at 14 dpi).

5.3.2 Differential Gene Expression differences within resistant and susceptible over a time period (24 hpi, 48 hpi, 7dpi and 14 dpi)

There were significant differences in the expression levels using the False Discovery Rate (FDR $\leq$ 0.05) and log2 fold change (Appendix: Table 5A.1, Table 5A.2), the significance overall expression matrix displaying the number of differentially expressed genes across all time-points post infection is shown in Figures 5.3A & 5.3B for susceptible and resistant respectively. A total of 235 and 37 differentially expressed genes were observed, between the time points in both susceptible and resistant RILs, respectively. Volcano plots (Goff et al., 2012) Figures 5.4A & 5.4B) also displayed the number of differentially expressed genes (DEGs) identified pairwise between each group. Up- and down-regulated genes were represented with red dots, with more DEGs represented in the susceptible than in the resistant samples. In both susceptible and resistant RILs, RIL infection resulted in a steady increase observed in the number of DEGs with increase in time post-infection 48 hpi vs 7 dpi and 7 dpi vs 14 dpi (Table 5.2). There was also an increase in the number of DEGs between 24 hpi and 48 hpi, and an observed decrease between 7 dpi and 14 dpi.

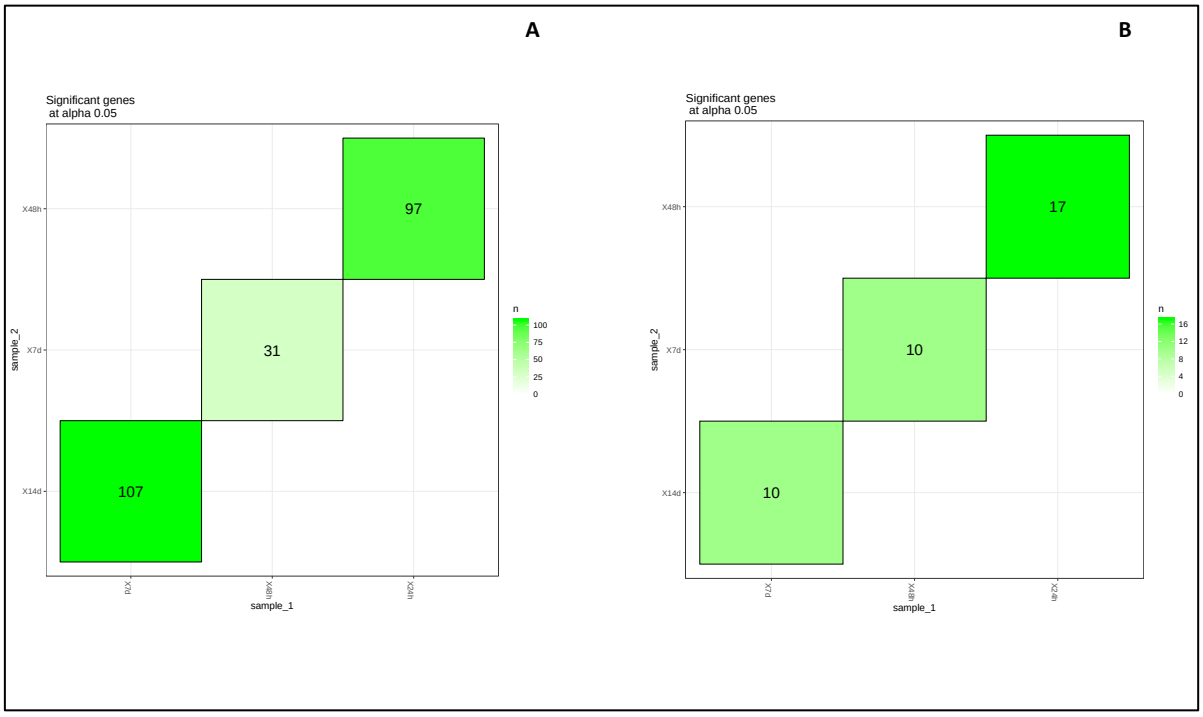

Figure 5.4: The expression matrix displaying the significant number of differentially expressed genes in (A) susceptible, and (B) resistant between each experimental group (24 hpi, 48 hpi, 7 dpi and 14 dpi) at a given alpha (0.05) with 235 DEGs in susceptible and 37

DEGs resistant RIL. Differentially expressed transcripts obtained using Cuffdiff tool (Trapnell et al., 2012) were subjected to CummeRbund R software package (Trapnell et al., 2012).

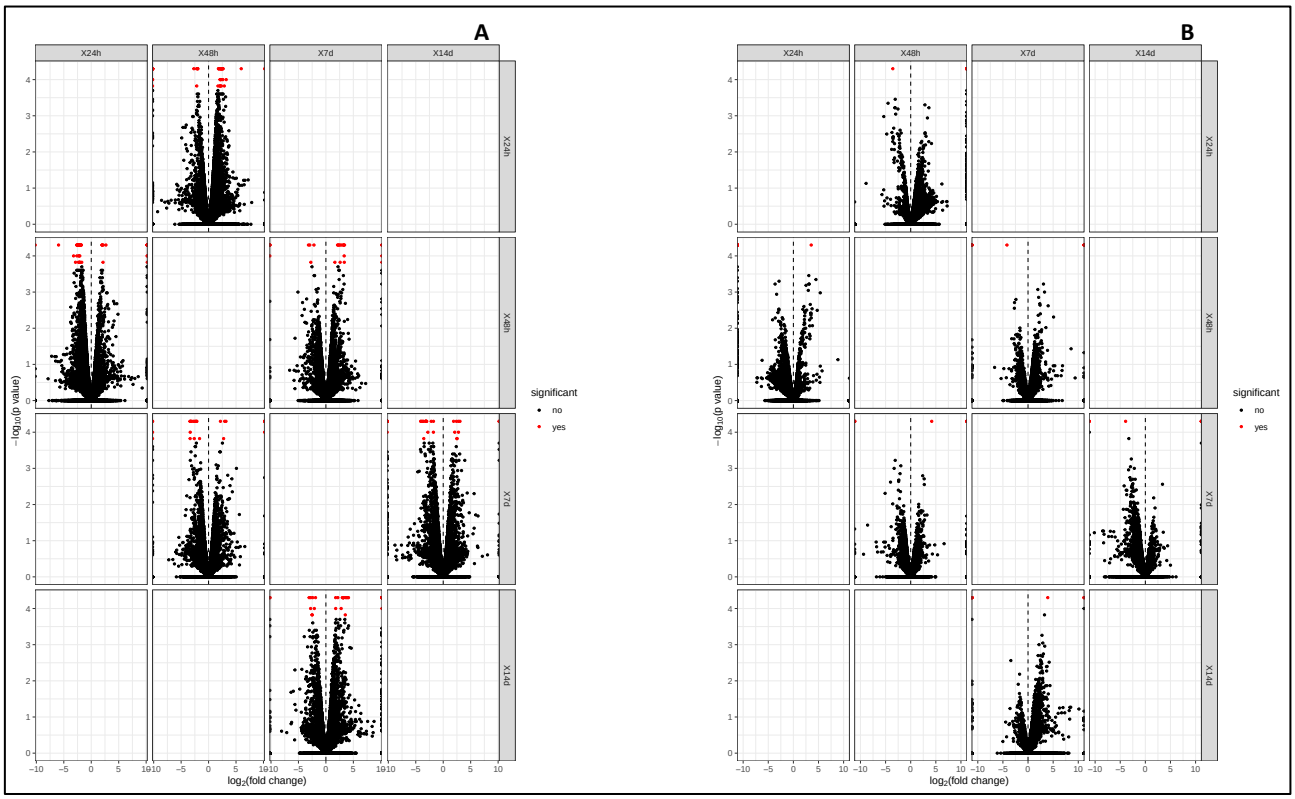

Figure 5.5: Pairwise volcano plots indicating significant DEGs between 24 hpi, 48 hpi, 7 dpi and 14 dpi in A- susceptible, B- resistant RILs respectively. Following the identification of differential expressed genes with Cuffdiff (Trapnell et al., 2012). Significant DEGs were identified with q values (P value adjusted to false discovery rate) of less than 0.05. CummeRbund R software package was used to visualize the significant DEGs. Red spots represent significant DE genes, and black spots are for non-DE genes.

A total of 235 and 37 genes from the susceptible and resistant RILs were differentially expressed (log2 fold change and FDR ≤ 0.05) across all time-points (24 hpi -14 dpi) following *Fusarium graminearum* infection (Table 5.2). In both susceptible and resistant RILs, RIL infection resulted in a steady increase observed in the number of DEGs with increase in time post-infection 48 hpi vs 7 dpi and 7 dpi vs 14 dpi (Table 5.2). There was also an increase in the DEGs number between 24 hpi and 48 hpi, and an observed decrease between 7 dpi and 14 dpi.

Table 5.2: An overview of the number of up- and down-regulated genes (DEGs) identified across 24 hpi, 48 hpi, 7 dpi and 14 dpi in susceptible and resistant RILs response to *Fusarium graminearum* infection.

RIL Dataset	Timepoints	Up-regulated	Down-regulated	Total
131 (Susceptible)	24h vs 48h	68 (70%)	29 (30%)	97
	48h vs 7d	25 (81%)	6 (19%)	31
	7d vs 14 dpi	37 (35%)	70 (65%)	107
	Total	**130 (55%)**	**105 (46%)**	**235**
103 (Resistant)	24h vs 48h	16 (94%)	1 (6%)	17
	48h vs 7d	9 (90%)	1 (11)	10
	7d vs 14d	9 (90%)	1 (9%)	10
	Total	**34 (92%)**	**3 (8%)**	**37**

Displays the significant total number of down-and up regulated DEGs obtained using Cuffdiff (Trapnell et al., 2012) between each experimental group (24 hpi, 48 hpi, 7 dpi and 14 dpi) in susceptible and resistant RIL.

Comparative analysis revealed that most of the DEGs observed were uniquely expressed at specific time-points and that there were less common DEGs across different time-points in both RILs (Figure 5.6) A high proportion of DEGs in the susceptible RIL was shared between 7 dpi and 14 dpi, and 24 hpi and 48 hpi (39% and 36% respectively). Over ten percent (11%) DEGs were uniquely found in the 24 hpi.

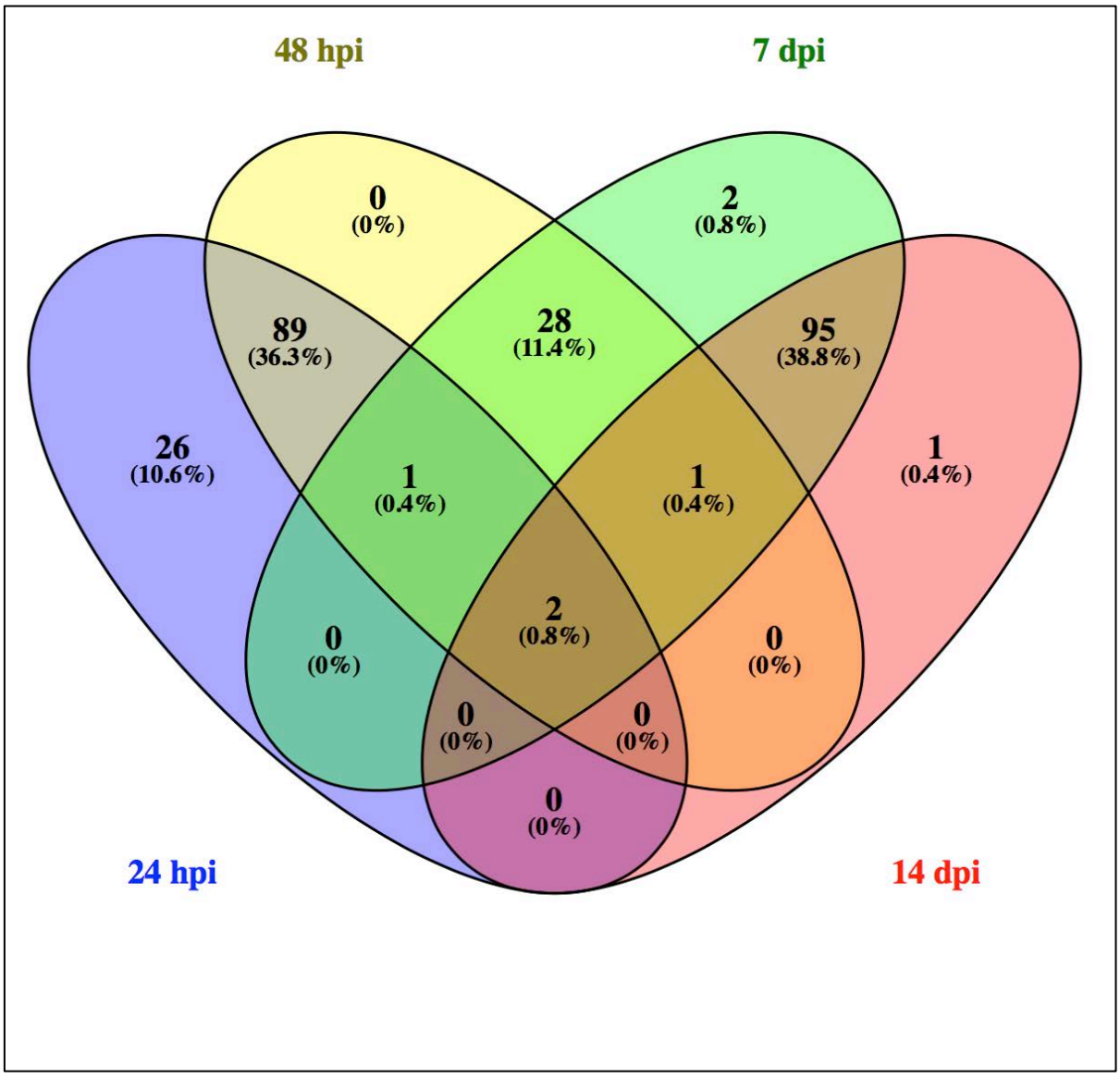

Figure 5.6: Distribution of shared and unique differentially expressed genes (DEGs) among three biological replicates at respective time points (24 hpi, 48 hpi, 7 dpi, 14 dpi) in the susceptible RIL post-infection with *Fusarium graminearum*. Only transcripts with a minimum of FDR ≤ 0.05 were included in the data. Each coloured circle represents a time-point, with shared and unique DEGs among different samples. The number of shared DEGs

showed a rising trend in the susceptible RIL at late infection stage (48 hpi - 14 dpi). The early infection stage indicated a decrease in the number of shared DEGs trend 24 hpi and 48 hpi).

In the resistant RIL, of the DEGs identified, 3% were common across all time-points (Figure 5.7). Similar to the susceptible RIL a high proportion (43%) of DEGs was shared between 24 hpi and 48 hpi. Time-points 7 dpi and 14 dpi had the least proportion of shared DEGs (14%). 48 hpi, 7dpi and 14 dpi shared 27% of DEGs.

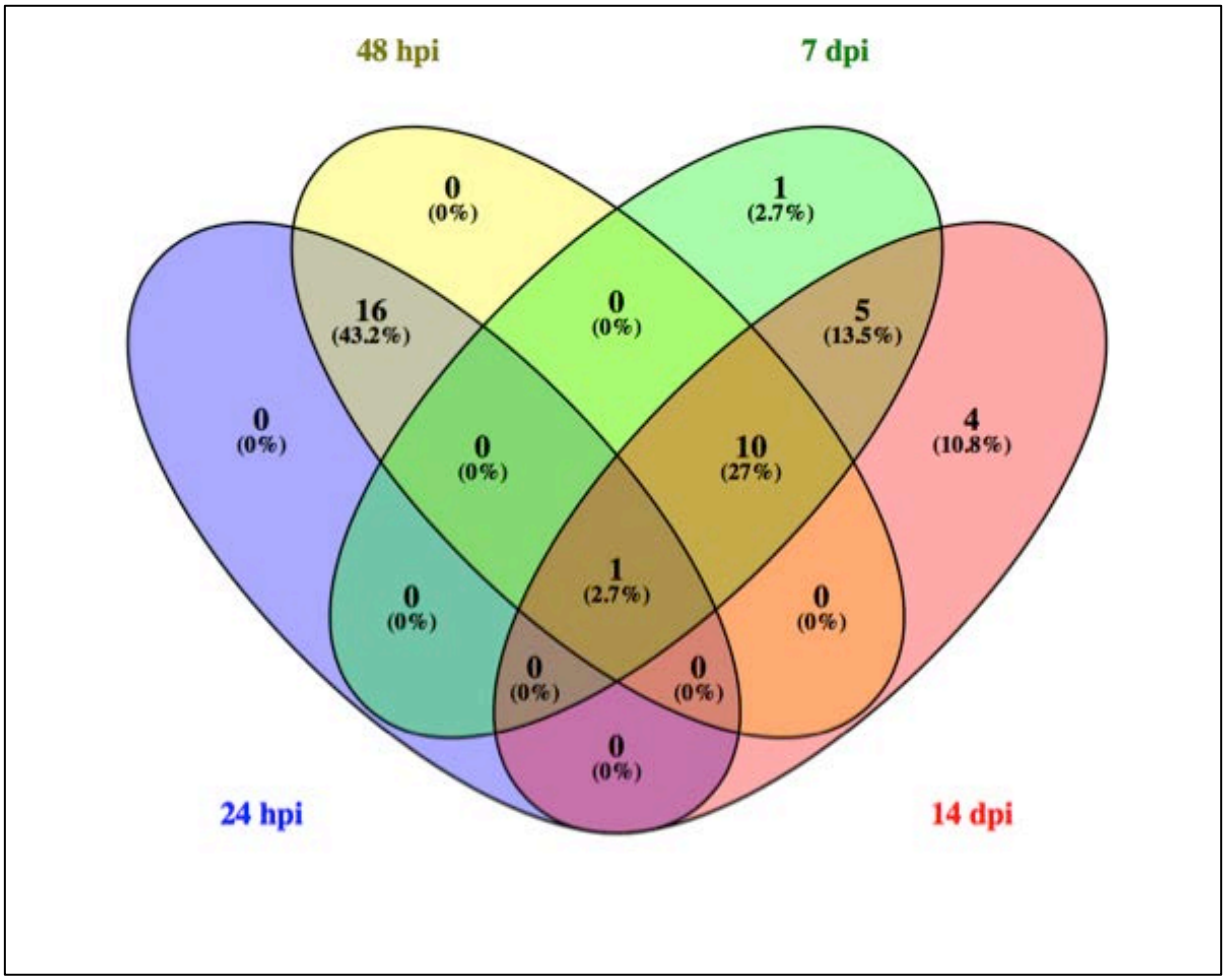

Figure 5.7: Distribution of shared and unique differentially expressed genes (DEGs) among three biological replicates at respective time points (24 hpi, 48 hpi, 7 dpi, 14 dpi) in the resistant RIL post-infection with *Fusarium graminearum*. Only transcripts with a minimum of FDR ≤0.05 were included in the data. Each coloured circle represents a time-point, with shared and unique DEGs among different samples. The number of shared DEGs showed a rising trend in the resistant RIL at early infection stage (24 hpi - 48 hpi). Late infection stage (time-points 7 dpi and 14 dpi) showed a decrease trend in the number of shared DEGs at late infection.

5.3.3 DEGs expression clustering

Clusters in the susceptible RIL were grouped into 6 groups of distinct general expression trends through DPGP software (Figure 5.8; Appendix Table 5A.3). The grouping of gene clusters was done based on genes which had similar expression patterns. Groups 4 and 5 constituted 60% of the total DEGs (Table 5.3). Genes encoding enzymes in the metabolic pathway were highly enriched in group 2 and group 4 (Table 5.3). In group 2 the physiological trend showed an increase at the late infection stage. Genes encoding enzymes in the biosynthesis of secondary metabolites pathway were highly enriched in groups 2 and 4, and an increasing trend progressed with infection time.

Genes encoding plant hormone signal transduction pathways were highly enriched in group 2 and the gene expression pattern increased with infection time, the increase was more pronounced at the late infection stage 14 dpi. Genes encoding MAPK signalling pathways were enriched in group 2, the expression trend also decreased with time. The genes encoding starch sucrose metabolism and cyanoamino acid metabolism pathways were highly enriched in group 4, and presented an increase in the gene expression in the early infection stage and a decrease in the late infection stage. Genes encoding ubiquinone and other terpenoid-quinone biosynthesis (exclusively clustered in group 4) presented a significant decline from early infection stage (24 hpi and 48 dpi) to late infection stage (7 dpi and 14 dpi).

Group 2, clustered into several multigene families within the susceptible RIL which are reportedly involved in pathogenesis and included Sobic.007G059100 (methyltransferase), Sobic.004G182300 - mildew locus (MLO) gene, Sobic.010G078100 (pantothenate kinase (PanK). Group 3 presented an increased pattern in reported pathogen related genes negatively and positively influencing immunity in 48 hpi-14 dpi. Genes associated with the expression trends in group 3 included Sobic.006G248300 - 5-lipoxygenase (LOX5), Sobic.003G139500 (CBL-interacting protein kinase 1) and Sobic.001G482600 (jasmonate-zim-domain protein 1; (JAZ1). The gene expression pattern, in group 2 increased with infection time, the increase was more pronounced at the late infection stage 14 dpi. Group 1, exclusively presented a gene encoding sesquiterpene metabolism pathway and presented a decrease with reported defence

related genes in late infection stage (7-14 dpi); while group 6 presented an increase in the reported defence related pathways at 48 hpi and a significant decline in14 dpi.

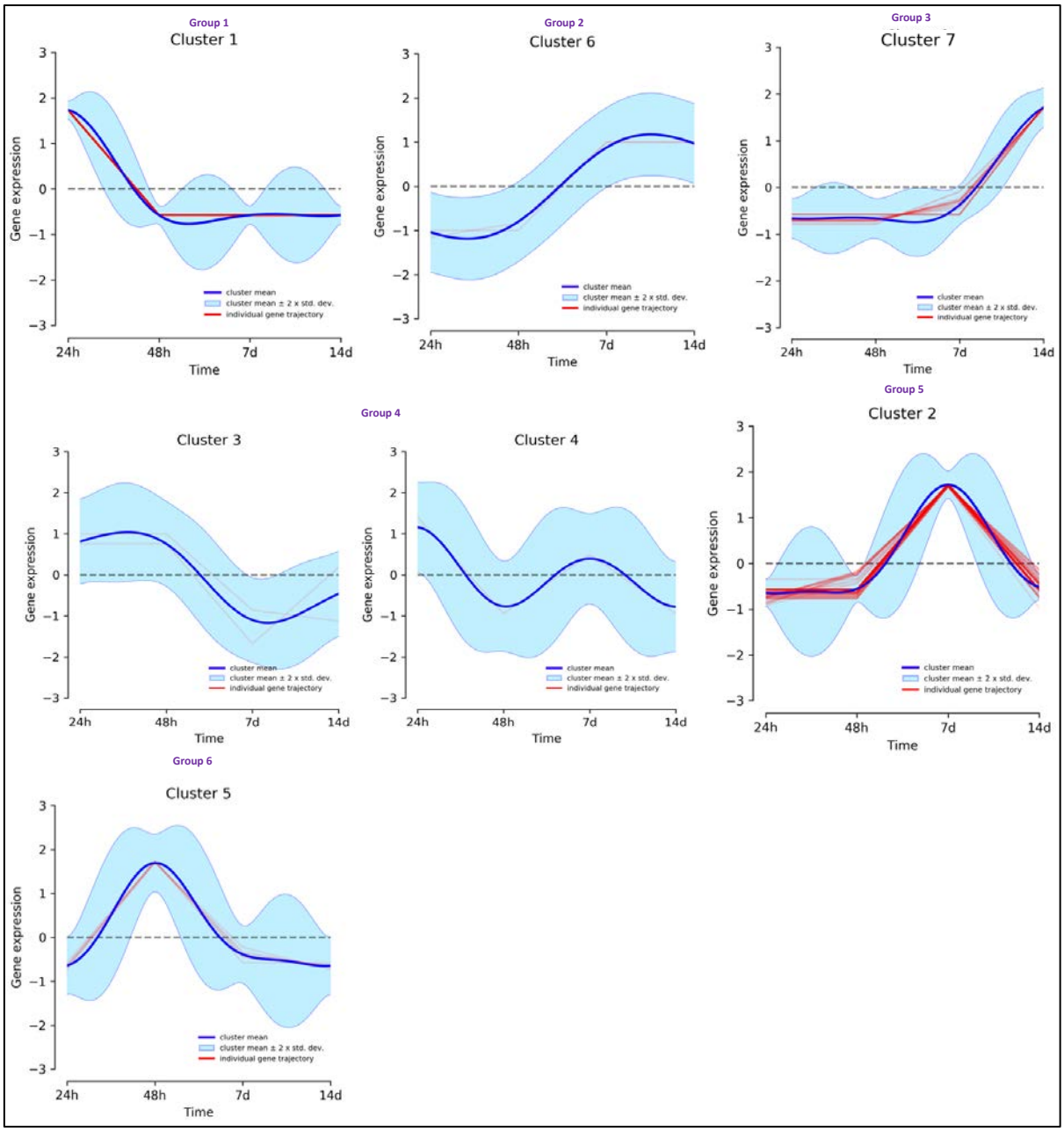

Figure 5.8: Cluster analysis of statistically significantly susceptible RIL genes using k-means. Clustering of genes with respect to expression levels was done using Dirichlet Process Gaussian Process mixture model DPGP. 1000 iterations of clustering were performed with default software parameters. Differentially expressed genes obtained using cuffdiff (Trapnell et al., 2012) were subjected to DPGP clustering to identify susceptible RIL significantly expressed transcripts upon *Fusarium graminearum* infection, which were then separated into closely correlated clusters of expression trends. Six general expression trends were observed.

The general trend groups depicted: group 1, a decrease with reported defence related genes in late infection stage (7-14 dpi); group 2, an increase with reported pathogen related genes that positively and negatively affects susceptibility in the late infection stage; group 3, an increase in reported pathogen related genes negatively influencing immunity in 48 hpi-14 dpi; group 4, an increase in the reported defence related pathways at 24 hpi and a pronounced decline in 7-14 dpi; group 5, an increase in the reported pathogen related genes that negatively influence the plant at 7-14 dpi; group 6, an increase in the reported defence related pathways at 48 hpi and pronounced decline in 14 dpi. The number of genes per cluster is shown in the left upper corner. Group number is written in the left upper corner of each colour-coded group. The horizontal axis is the hours and days post infection and the y-axis is the gene expression values (FPKM) which were log2 transformed to normalize the data. For each cluster, standardized FPKM as well as the posterior cluster mean ±2 standard deviations is shown. The blueline depicts the median expression level of the genes in a cluster.

Table 5.3: Analysis of pathway enrichment of susceptible RIL differentially expressed genes

Group number	Pathway ID	Category Term	PValue	Corrected P-Value	Input number
Group 1 **Cluster 1**	ath00902	Biosynthesis of secondary metabolites	2.81e-3	8.43e-3	1
	ath01110		1.23e-2	1.23e-2	2
	ath00904	Metabolic pathways	3.66e-2	4.39e-2	1
	ath00941	MAPK signalling pathway – plant	6.31e-3	9.47e-3	1
	ath04016	Flavonoid biosynthesis	6.31e-3	9.47e-3	1
	ath01100	Sesquiterpene metabolism pathway			
Group 2 **Cluster 6**	ath01100	Metabolic pathways	4.79e-5	7.18e-4	7
	ath01110	Biosynthesis of secondary metabolites	1.44e-4	1.08e-3	5
	ath00940		1.12e-2	3.36e-2	1
	ath00196	Photosynthesis - antenna proteins	1.12e-2	3.36e-2	1
	ath00770	Flavonoid biosynthesis	1.26e-2	1.26e-2	2
	ath04712	Plant hormone signal transduction	1.41e-2	3.52e-2	1
	ath00561	Pantothenate and CoA biosynthesis	1.80e-2	3.85e-2	1
	ath00460		2.94e-2	5.52e-2	1
	ath00564	Circadian rhythm – plant	3.37e-2	5.62e-2	1
	ath00480	Glycerolipid metabolism	4.69e-2	6.71e-2	1
	ath00270	Cyanoamino acid metabolism	4.92e-2	6.71e-2	1
	ath04016	Glycerophospholipid metabolism	5.81e-2	7.26e-2	2
	ath00500	Glutathione metabolism	6.41e-2	7.39e-2	3
	ath04075	Cysteine and methionine metabolism	7.82e-2	8.38e-2	1
		MAPK signalling pathway - plant	2.47e-3	8.43e-3	1
		Photosynthesis - antenna proteins			
		Starch and sucrose metabolism			

Group 3 **Cluster 7**	ath00480 ath00270 ath04016 ath00500 ath00480	Plant hormone signal transduction Glutathione metabolism Cysteine and methionine metabolism Starch and sucrose metabolism	1.26e-2 4.92e-2 5.81e-2 6.41e-2	1.26e-2 6.71e-2 7.26e-2 7.39e-2	1 1 1 11
Group 4 **Cluster 3 & 4**	ath00460 ath01100 ath00500 ath01110 ath04933 ath00730 ath00941 ath04712 ath00410 ath00860 ath00330 ath00195 ath04145 ath00480 ath04075 ath00130	Cyanoamino acid metabolism Metabolic pathways Starch and sucrose metabolism Biosynthesis of secondary metabolites Thiamine metabolism Flavonoid biosynthesis Circadian rhythm – plant beta-Alanine metabolism Porphyrin and chlorophyll metabolism Arginine and proline metabolism Photosynthesis Phagosome Glutathione metabolism Plant hormone signal transduction Ubiquinone and other terpenoid-quinone biosynthesis	1.46e-3 1.49e-3 7.77e-3 1.09e-2 1.73e-2 1.81e-2 2.90e-2 3.98e-2 4.21e-2 4.28e-2 6.02e-3 6.39e-3 7.87e-3 1.96e-2 2.93e-2	1.19e-2 1.19e-2 3.14e-2 3.49e-2 3.63e-2 3.63e-2 5.16e-2 5.71e-2 5.71e-2 5.71e-2 7.31e-3 7.31e-3 8.40e-3 1.96e-2 7.21e-2	2 7 3 3 4 1 1 1 1 1 1 1 1 1 1
Group 5 and 6 **Cluster 5 and 2**	ath01100 ath00196 ath03010 ath01200 ath01110 ath00500 ath04712 ath00860 ath00710 ath00460 ath00195	Metabolic pathways Photosynthesis - antenna proteins Carbon metabolism Biosynthesis of secondary metabolism Starch and sucrose metabolism Circadian rhythm - plant Porphyrin and chlorophyll metabolism Cyanoamino acid metabolism Photosynthesis	1.17e-5 2.20e-12 1.83e-2 1.23e-2 8.75e-3 8.80e-3 2.02e-2 3.78e-2	7.05e-5 2.64e-11 1.53e-2 1.48e-2 1.17e-2 1.17e-2 7.21e-2 7.21e-3	8 5 2 1 1 1 1 1 1

The enriched pathways per cluster were pooled into groups with similar expression pattern in the susceptible RIL and changes thereof across the six expression patterns. Cluster group = a collection of similar expression trend. The pathway enrichment analysis of genes in the groups was performed using KEGG Orthology Based Annotation System (KOBAS) (Xie et al., 2011) $P<0.05$ and input number >3 were considered to be significant. Pathway ID = KEGG orthology term (accession) of each pathway, Category term = KEGG pathway description of the pathway.

In the resistant RIL within the 5 closely correlated clusters (Figure 5.9, Appendix Table 5A.4), 5 general expression trends were noted. Only cluster (group) 1, 4 and 5 could be assigned gene pathways because of the unassigned KO terms on DEGs in group 2 and 3 (Table 5.4). Group 4 had equal number of genes encoding metabolic and glutathione pathway. The genes encoding autophagy pathway were exclusively clustered in group 5. The genes encoding autophagy pathway presented an increase from 24- 48 hpi and a sharp decrease to 7 dpi, and it further progressed to increase again in a late infection stage (14 dpi). The upregulated pathway is shown in (Figure 5.10). Group 1 was the most enriched with genes in the metabolic pathway (2) and biosynthesis of metabolites (2) in contrast to group 4. In group 1, there was an increase in genes encoding metabolic pathways from 48 hpi and a decrease which was constant throughout the late infection stage (7-14 dpi). A similar trend was observed in genes encoding galactose, phenylpropanoid and glycolysis pathway, which were upregulated at this time point and the pathways are represented by Figures 5.11, 5.12 and 5.13 respectively. Various reported defence related proteins were found in group 1 which included Sobic.001G432500 - glutathione S-transferase (GST29, GSTU1), Sobic.001G432550 (Ankyrin repeat family), Sobic.002G353900 (polyols), Sobic.006G205600 (xyloglucan endotransglucosylase), Sobic.002G109500 - dirigent protein 1 (DIR1) and Sobic.008G182900 (osmotin). Group 4 presented an increase in genes encoding metabolic pathways from 48 hpi-7 dpi and a decrease at the late infection stage (7-14 dpi). Group 2, represented reported defence related genes Sobic.010G020200 - 4-amino-2-trifluoromethyl-phenyl retina (ATPR1), Sobic.002G109500 dirigent proteins (DIR) and Sobic.005G212700 glutathione S-transferase (GST29, GSTU18) which were more pronounced at late infection stage. Group 3 related proteins presented an increase at 24 hpi -7 dpi and a significant decrease at 14 dpi.

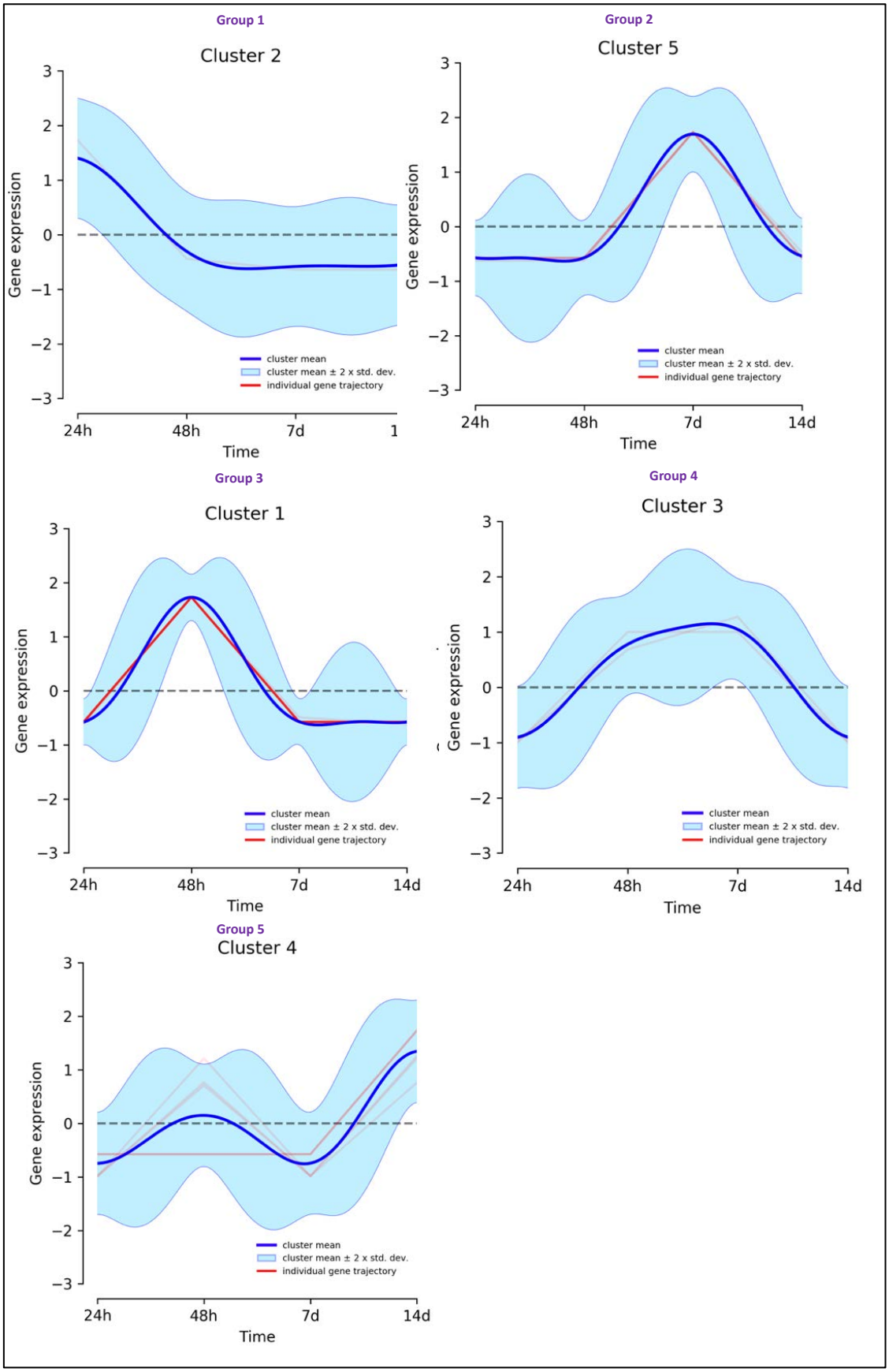
Group 1
Cluster 2
Group 2
Cluster 5
Group 3
Cluster 1
Group 4
Cluster 3
Group 5
Cluster 4
Gene expression
Time
24h
48h
7d
14d
cluster mean
cluster mean ± 2 x std. dev.
individual gene trajectory

Figure 5.9: Cluster analysis of statistically significantly resistant RIL expressed genes using k-means. Clustering of genes with respect to expression levels was done using Dirichlet Process Gaussian Process mixture model DPGP (McDowell et al., 2018). 1000 iterations of clustering were performed with default software parameters. Differentially expressed genes obtained using cuffdiff (Trapnell et al., 2012) were then separated into closely correlated clusters of expression trends. Five general distinct expression trends were observed and the clusters were not re-grouped. The general trend groups depicted: group 1, an increase with reported basal defence related genes at early infection stage and a decrease at late infection stage; group 2, an increase in reported defence related genes at the late infection stage; group 3, an increase at 24 hpi &7 dpi and a significant drop at 14 dpi; group 4, a decrease at the late infection stage (7-14 dpi); group 5 an increase in reported defence related pathways at late infection stage (14 dpi). The number of genes per cluster is shown in the left upper corner. Group number is written in the left upper corner of each colour-coded group. The horizontal axis is the hours and days post infection and the y-axis is the gene expression values (FPKM) which were $\log_2$ transformed to normalize the data. For each cluster, standardized FPKM as well as the posterior cluster mean ±2 standard deviations is shown. The blueline depicts the median expression level of the genes in a cluster.

Table 5.4: Analysis of pathway enrichment of resistant RIL differentially expressed genes

Group number	Pathway ID	Category Term	PValue	Corrected P-Value	Input number
Group 1 **Cluster 1**	ath00380 ath01210 ath01110 ath01100 ath00941 ath00940 ath00010 ath00052	Glycolysis biosynthesis Tryptophan metabolism Oxocarboxylic acid metabolism Biosynthesis of secondary metabolism Metabolic pathways Phenylpropanoid biosynthesis Galactose Metabolism	4.40e-3 1.11e-2 1.37e2 1.87e-2 3.48e-2 3.00e-3 7.86e-3	2.20e-2 2.28e-22 2.28e-2 2.34e-2 3.48e-2 1.26e2 3.14e-2	1 1 1 2 2 3 2
Group 2 **Cluster 6**	-	-	-	-	-
Group 3 Cluster 7	-	-	-	-	-
Group 4 **Cluster 3 & 4**	ath01110 ath04016 ath04626 ath04075 ath00480	MAPK signalling pathway - plant Plant-pathogen interaction Plant hormone signal transduction Metabolic pathways Glutathione metabolism	1.23e-2 1.56e2 2.49e2 1.23e-2 2.80e-2	2.34e-2 2.34e-2 2.49e-2 1.37e-2 5.60e-2	1 1 1 2 2
Group 5 and 6 **Cluster 5 and 2**	ath04136	Autophagy - other	1.25e-3	1.25e-3	1

The enriched pathways per cluster pooled into groups with similar expression pattern in the resistant RIL and changes thereof across the five expression patterns. Cluster group = a collection of similar expression trend. The pathway enrichment analysis of genes in the groups was performed using KEGG Orthology Based Annotation System (KOBAS) (Xie et al., 2011). $P<0.05$ and input number >3 were considered to be the most significant. Pathway ID = KEGG orthology term (accession) of each pathway, Category term = KEGG pathway description of the pathway.

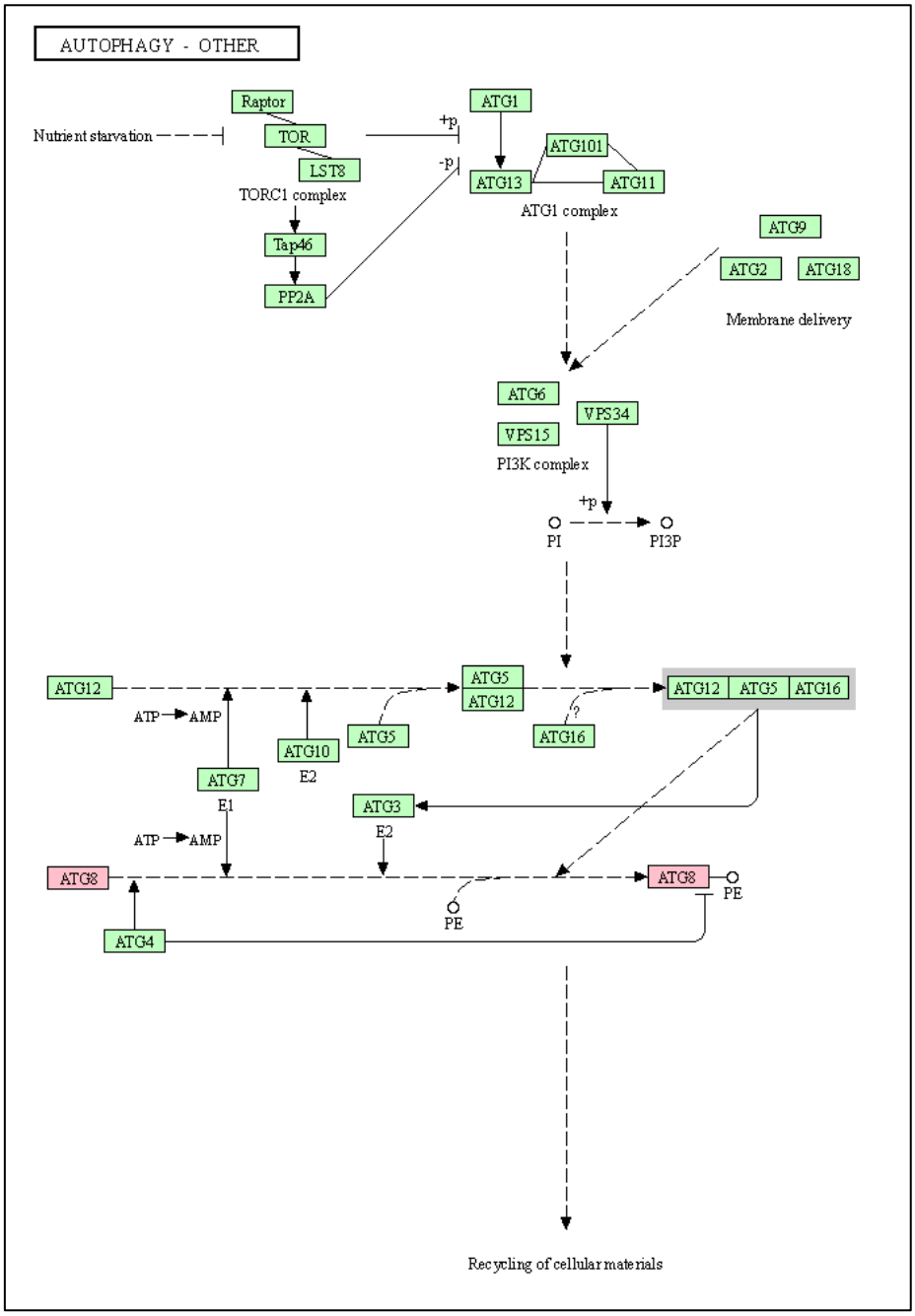

Figure 5.10: Localization of up-regulated autophagy pathway on the leaf tissues of the resistant RIL post-infestation with *Fusarium graminearum*. Boxes highlighted in green represents genes that are present in the *Arabidopsis thaliana* genome (organism used for KEGG maps), while boxes highlighted in pink are the up-regulated DEGs in the leaf tissues post *Fusarium graminearum* infection. Boxes that are not highlighted are the genes that are not present in the *Arabidopsis thaliana* genome. Names of enriched enzymes are written close to the enzyme commission (EC) number.

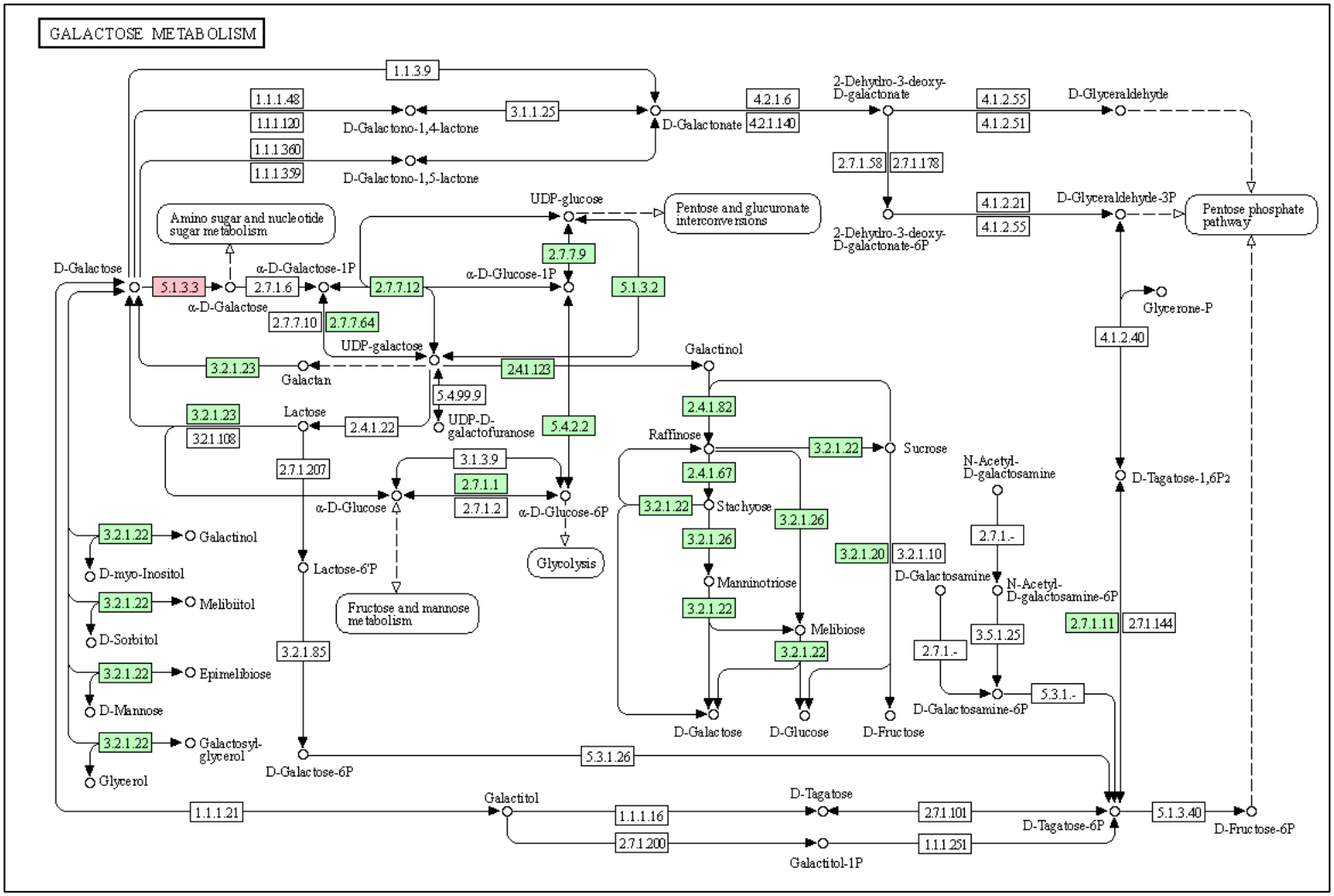
GALACTOSE METABOLISM
1.1.3.9
1.1.1.48
1.1.1.120
1.1.1.360
1.1.1.359
D-Galactono-1,4-lactone
D-Galactono-1,5-lactone
3.1.1.25
D-Galactonate
4.2.1.6
4.2.1.140
2-Dehydro-3-deoxy-D-galactonate
4.1.2.55
4.1.2.51
D-Glyceraldehyde
2.7.1.58
2.7.1.178
2-Dehydro-3-deoxy-D-galactonate-6P
4.1.2.21
4.1.2.55
D-Glyceraldehyde-3P
Pentose phosphate pathway
Pentose and glucuronate interconversions
UDP-glucose
Amino sugar and nucleotide sugar metabolism
D-Galactose
5.1.3.3
α-D-Galactose
2.7.1.6
α-D-Galactose-1P
2.7.7.12
α-D-Glucose-1P
2.7.7.9
5.1.3.2
2.7.7.10
2.7.7.64
UDP-galactose
Glycerone-P
4.1.2.40
3.2.1.23
Galactan
2.4.1.123
Galactinol
5.4.99.9
UDP-D-galactofuranose
5.4.2.2
3.2.1.23
3.2.1.108
Lactose
2.4.1.22
2.4.1.82
Raffinose
3.2.1.22
Sucrose
2.7.1.207
3.1.3.9
2.7.1.1
2.7.1.2
α-D-Glucose
α-D-Glucose-6P
2.4.1.67
3.2.1.22
Stachyose
3.2.1.26
N-Acetyl-D-galactosamine
D-Tagatose-1,6P2
3.2.1.22
Galactinol
D-myo-Inositol
Lactose-6'P
Glycolysis
3.2.1.26
3.2.1.20
3.2.1.10
Manninotriose
D-Galactosamine
2.7.1.-
N-Acetyl-D-galactosamine-6P
3.2.1.22
Melibiitol
D-Sorbitol
Fructose and mannose metabolism
3.2.1.22
Melibiose
2.7.1.11
2.7.1.144
3.5.1.25
3.2.1.85
3.2.1.22
2.7.1.-
Epimelibiose
D-Mannose
5.3.1.-
D-Galactosamine-6P
3.2.1.22
Galactosyl-glycerol
Glycerol
D-Galactose
D-Glucose
D-Fructose
5.3.1.26
D-Galactose-6P
Galactitol
D-Tagatose
1.1.1.21
1.1.1.16
2.7.1.101
5.1.3.40
D-Tagatose-6P
D-Fructose-6P
2.7.1.200
1.1.1.251
Galactitol-1P

Figure 5.11: Localization of up-regulated Galactose metabolism pathway on the leaf tissues of the resistant RIL post-infestation with *Fusarium graminearum*. Boxes highlighted in green represents genes that are present in the *Arabidopsis thaliana* genome (organism used for KEGG maps), while boxes highlighted in pink are the up-regulated DEGs in the leaf tissues post *Fusarium graminearum* infection. Boxes that are not highlighted are the genes that are not present in the *Arabidopsis thaliana* genome. Names of enriched enzymes are written close to the enzyme commission (EC) number.

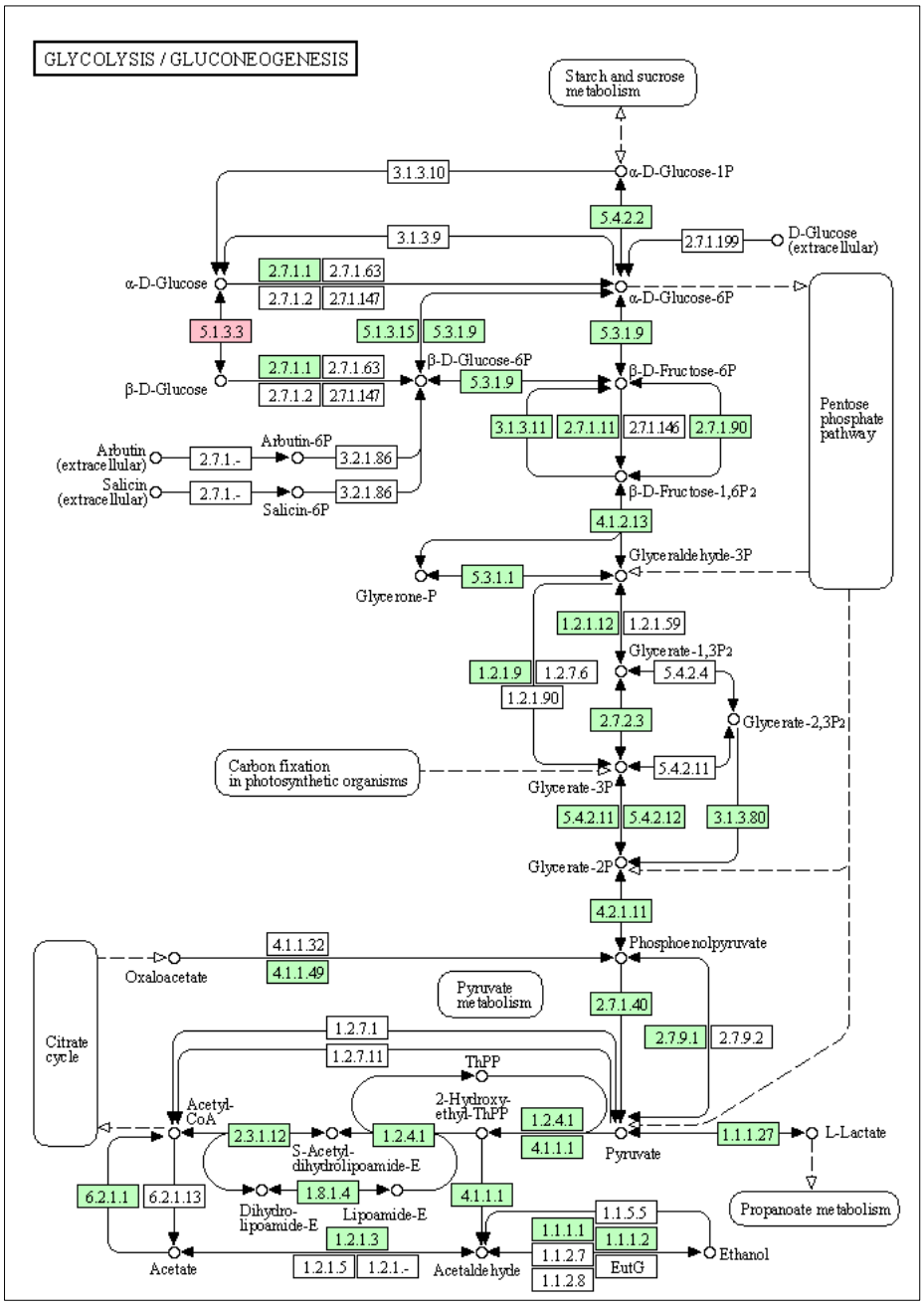

Figure 5.12: Localization of up-regulated glycolysis pathway on the leaf tissues of the resistant RIL post-infestation with *Fusarium graminearum*. Boxes highlighted in green represents genes that are present in the *Arabidopsis thaliana* genome (organism used for KEGG maps), while boxes highlighted in pink are the up-regulated DEGs in the leaf tissues post *Fusarium graminearum* infection. Boxes that are not highlighted are the genes that are not present in the *Arabidopsis thaliana* genome. Names of enriched enzymes are written close to the enzyme commission (EC) number.

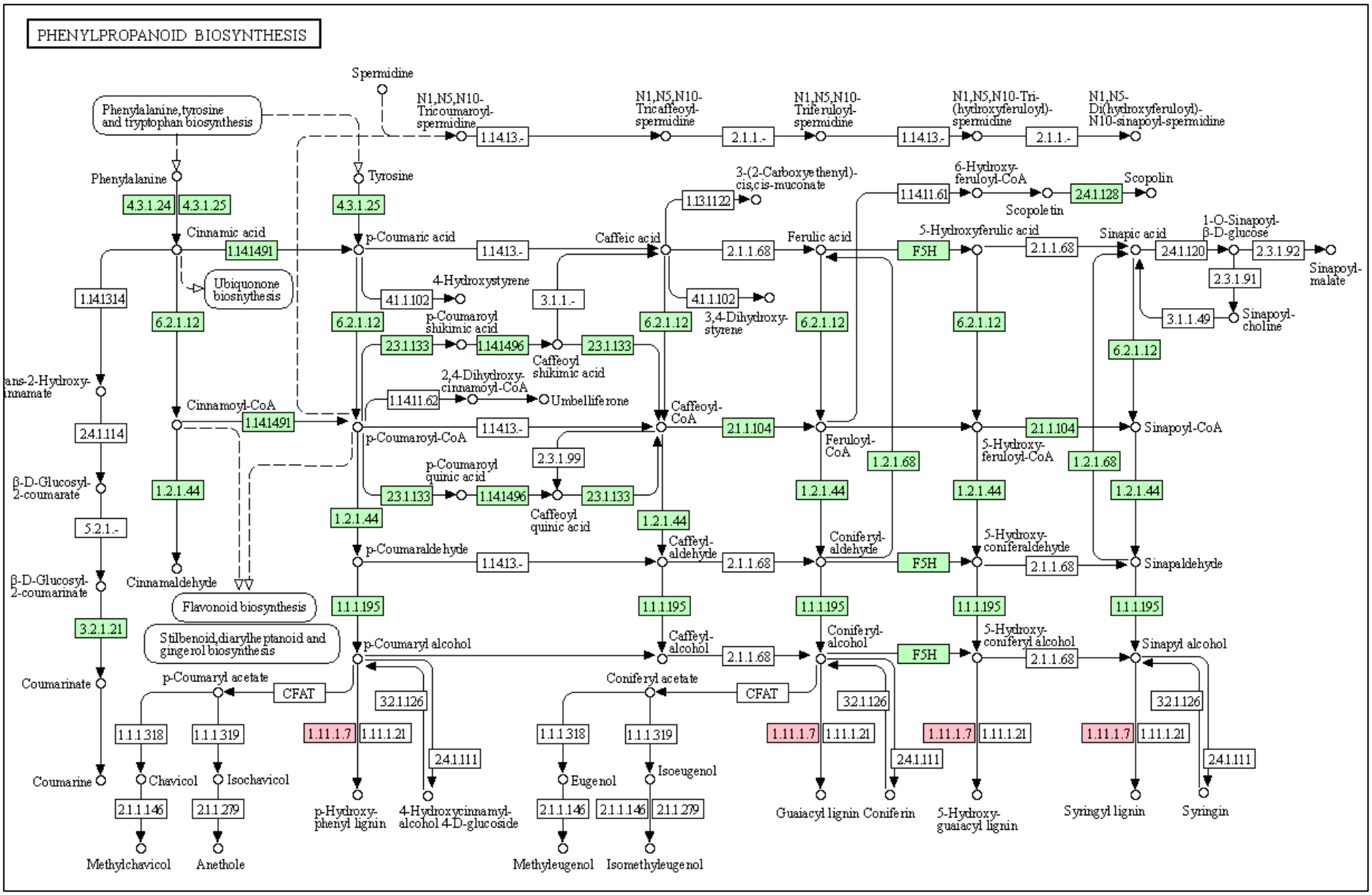
PHENYLPROPANOID BIOSYNTHESIS
Spermidine
Phenylalanine,tyrosine and tryptophan biosynthesis
N1,N5,N10-Tricoumaroyl-spermidine
N1,N5,N10-Tricaffeoyl-spermidine
N1,N5,N10-Triferuloyl-spermidine
N1,N5,N10-Tri-(hydroxyferuloyl)-spermidine
N1,N5-Di(hydroxyferuloyl)-N10-sinapoyl-spermidine
1.14.13.-
2.1.1.-
Phenylalanine
Tyrosine
4.3.1.24
4.3.1.25
3-(2-Carboxyethenyl)-cis,cis-muconate
1.13.11.22
6-Hydroxy-feruloyl-CoA
1.14.11.61
Scopoletin
2.4.1.128
Scopolin
Cinnamic acid
1.14.14.91
p-Coumaric acid
Caffeic acid
Ferulic acid
5-Hydroxyferulic acid
F5H
Sinapic acid
1-O-Sinapoyl-β-D-glucose
2.4.1.120
2.3.1.92
Sinapoyl-malate
2.3.1.91
Sinapoyl-choline
3.1.1.49
Ubiquonone biosinthesis
1.14.13.11
4-Hydroxystyrene
4.1.1.102
3.1.1.-
3,4-Dihydroxy-styrene
6.2.1.12
p-Coumaroyl shikimic acid
23.1.133
1.14.14.96
Caffeoyl shikimic acid
trans-2-Hydroxy-cinnamate
2,4-Dihydroxy-cinnamoyl-CoA
1.14.11.62
Umbelliferone
Cinnamoyl-CoA
Caffeoyl-CoA
2.1.1.104
Sinapoyl-CoA
p-Coumaroyl-CoA
Feruloyl-CoA
5-Hydroxy-feruloyl-CoA
1.2.1.68
2.4.1.114
2.3.1.99
p-Coumaroyl quinic acid
β-D-Glucosyl-2-coumarate
1.2.1.44
5.2.1.-
Caffeoyl quinic acid
p-Coumaraldehyde
Caffeyl-aldehyde
Coniferyl-aldehyde
5-Hydroxy-coniferaldehyde
Sinapaldehyde
β-D-Glucosyl-2-coumarinate
Cinnamaldehyde
1.1.1.195
3.2.1.21
Flavonoid biosynthesis
Stilbenoid,diarylheptanoid and gingerol biosynthesis
p-Coumaryl alcohol
Caffeyl-alcohol
Coniferyl-alcohol
5-Hydroxy-coniferyl alcohol
Sinapyl alcohol
Coumarinate
p-Coumaryl acetate
CFAT
Coniferyl acetate
32.1.126
1.1.1.318
1.1.1.319
1.11.1.7
1.11.1.21
24.1.111
Coumarine
Chavicol
Isochavicol
Eugenol
Isoeugenol
2.1.1.146
2.1.1.279
p-Hydroxy-phenyl lignin
4-Hydroxycinnamyl-alcohol 4-D-glucoside
Guaiacyl lignin
Coniferin
5-Hydroxy-guaiacyl lignin
Syringyl lignin
Syringin
Methylchavicol
Anethole
Methyleugenol
Isomethyleugenol

Figure 5.13: Localization of up-regulated phenylpropanoid pathway on the leaf tissues of the resistant RIL post-infestation with *Fusarium graminearum*. Boxes highlighted in green represents genes that are present in the *Arabidopsis thaliana* genome (organism used for KEGG maps), while boxes highlighted in pink are the up-regulated DEGs in the leaf tissues post *Fusarium graminearum* infection. Boxes that are not highlighted are the genes that are not present in the *Arabidopsis thaliana* genome. Names of enriched enzymes are written close to the enzyme commission (EC) number.

5.3.4 Profiling of sorghum RILs using keyword gene ontology (GO) terms

Profiling of sorghum using keyword gene ontology, annotated 77 genes under the GO functional categorization. DEGs were highly represented in the biological processes, cellular processes and molecular function respectively. The gene ontology result of the resistant RIL was distinctly different from that of the susceptible RIL. In the resistant RIL, the cellular component encoding genes were more pronounced, in which the most prominent number of DEGs classified as cell (GO:0005623), cell part (GO:0044464), organelle (GO:0043226), extracellular region (GO:0005576) and extracellular region part (GO:0044421) in contrast to the susceptible RIL. There were three common GO terms between susceptible and resistant RILs, which includes response to stimuli (GO:0051716) metabolic process (GO:0008152) and binding (GO:0005488), among which, the GO term denoting binding and response to stimuli were more highly represented (Figure 5.14).

5.3.5 Profiling of sorghum RILs using keyword KEGG Orthology (KO) terms

A pathway analysis was performed for the additional characterization of how *Fusarium graminearum* affects genes involved in the plant-pathogen response. The metabolic pathway analysis, using the KEGG database, revealed that 73 out of 244 unique DEGs (30%) identified from susceptible mapped to KEGG pathways (Table 5.2; Appendix Table 5A.1 and 5A.2). There were more up-regulated than down-regulated genes in almost all of the KEGG pathways mapped in both susceptible and resistant RILs (Figures 5.14A and 5.14B) although a high percentage of genes could not be mapped due to a lack of KO terms. Both up- and down-regulated genes mapped to the metabolic pathway in susceptible (Figures 5.15A; 5.15B) with

more up-regulated genes pronounced in the resistant compared to the susceptible RIL. Enriched up-regulated DEGs in the susceptible RIL at $P<0.05$ and input number >3 encoded pathways, glutathione biosynthesis, biosynthesis of secondary metabolites, plant hormone signal transduction, linoleic acid, plant circadian rhythm and photosynthesis. The most down-regulated DEGs per pathway encoded metabolic pathways, biosynthesis of secondary metabolites, starch and sucrose metabolism, cyano-amino acid metabolism and flavonoid biosynthesis.

In the resistant RIL the pathways with the most up-regulated DEGs were found to be metabolic, biosynthesis of secondary metabolites, phenylpropanoid biosynthesis and glutathione metabolism. Glycolysis and galactose metabolism pathways had the same DEGs number and were also amongst the most up-regulated. DEGs encoding autophagy were among the pathways that were up-regulated and exclusively found in the resistant RIL. Similarly, the pathways 2-Oxocarboxylic acid metabolism, MAPK signalling pathway and plant hormone signal transduction had similar number of significantly enriched DEGs. The down-regulated DEGs pathways were not as pronounced in the resistant plant as the up-regulated genes. (Figure 5.15B).

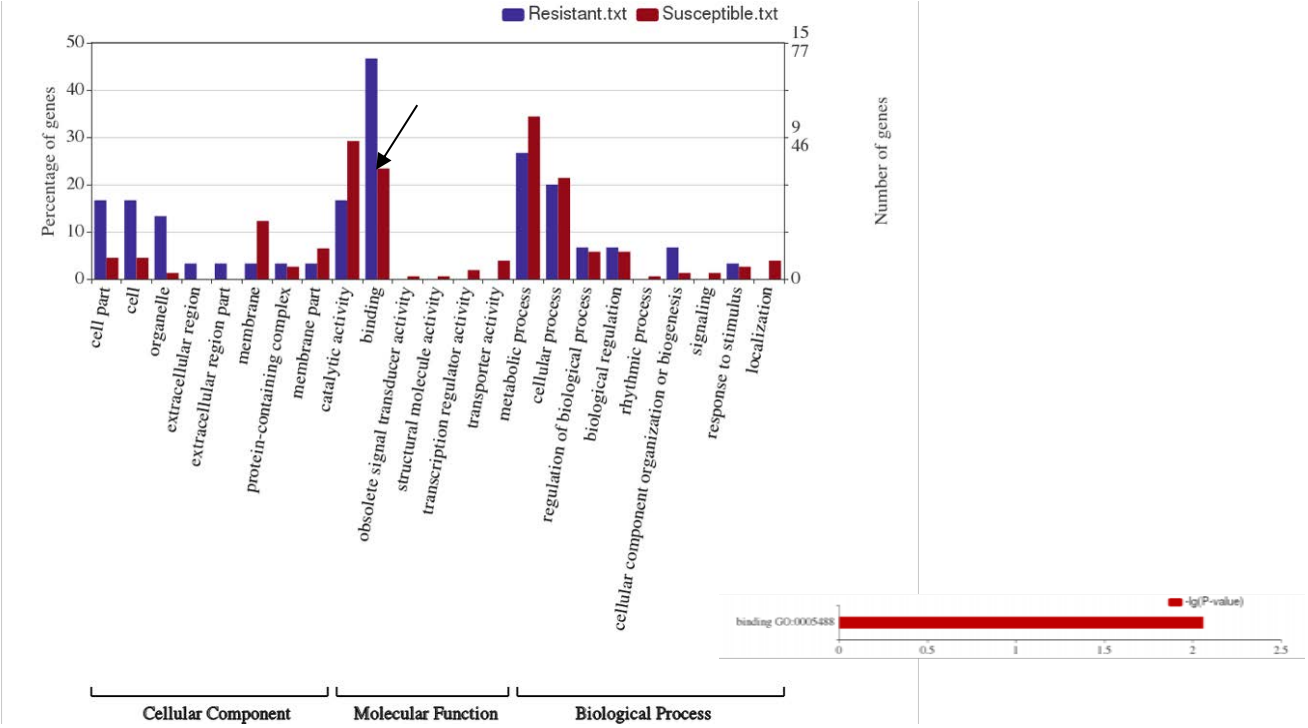

Figure 5.14: The top GO functional annotations of differentially expressed proteins of sorghum RILs response upon *Fusarium graminearum* infection in susceptible (red) and resistant (blue) sorghum RILs. Differences observed between the two RILs are pointed with arrows.

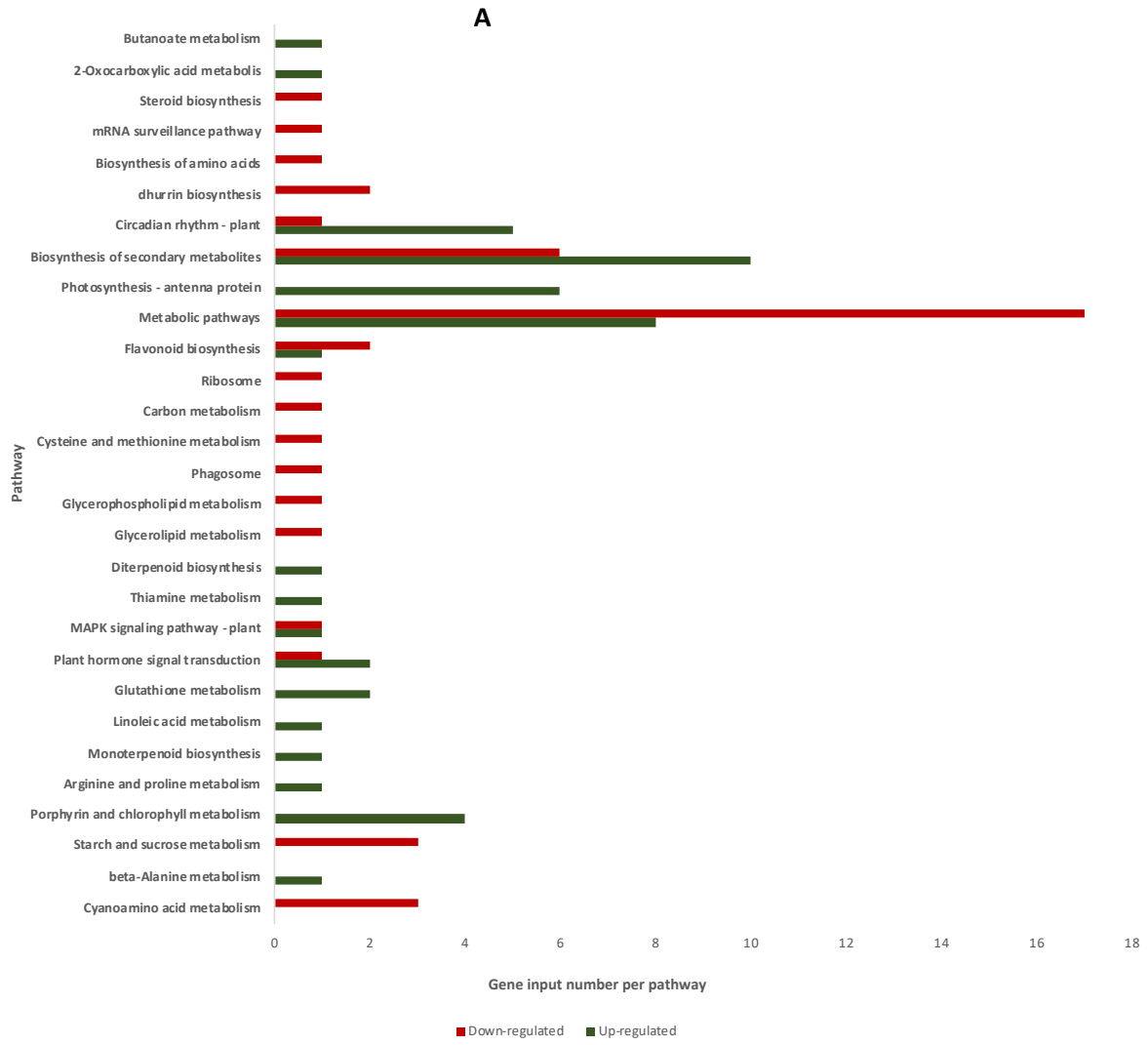
A
Butanoate metabolism
2-Oxocarboxylic acid metabolis
Steroid biosynthesis
mRNA surveillance pathway
Biosynthesis of amino acids
dhurrin biosynthesis
Circadian rhythm - plant
Biosynthesis of secondary metabolites
Photosynthesis - antenna protein
Metabolic pathways
Flavonoid biosynthesis
Ribosome
Carbon metabolism
Cysteine and methionine metabolism
Phagosome
Glycerophospholipid metabolism
Glycerolipid metabolism
Diterpenoid biosynthesis
Thiamine metabolism
MAPK signaling pathway - plant
Plant hormone signal transduction
Glutathione metabolism
Linoleic acid metabolism
Monoterpenoid biosynthesis
Arginine and proline metabolism
Porphyrin and chlorophyll metabolism
Starch and sucrose metabolism
beta-Alanine metabolism
Cyanoamino acid metabolism
Pathway
0
2
4
6
8
10
12
14
16
18
Gene input number per pathway
Down-regulated
Up-regulated

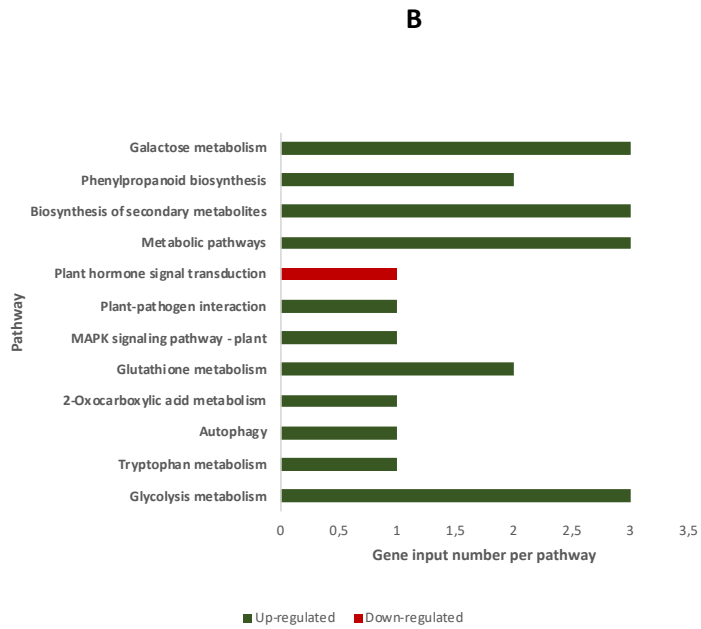
B
Galactose metabolism
Phenylpropanoid biosynthesis
Biosynthesis of secondary metabolites
Metabolic pathways
Plant hormone signal transduction
Plant-pathogen interaction
MAPK signaling pathway - plant
Glutathione metabolism
2-Oxocarboxylic acid metabolism
Autophagy
Tryptophan metabolism
Glycolysis metabolism
Pathway
0
0,5
1
1,5
2
2,5
3
3,5
Gene input number per pathway
Up-regulated
Down-regulated

Figure 5.15: The KEGG pathway distribution of DEGs in A- susceptible, B- resistant in response to *Fusarium graminearum* infection using *Arabidopsis thaliana* as the reference. The graph represents the enriched pathways (in terms of the number of DEGs allocated in each pathway). The pathway enrichment analysis of genes in the groups was performed using KEGG Orthology Based Annotation System (KOBAS) (Xie, et al., 2011) $P<0.05$ and input number >3 were considered to be the most significant.

5.4 DISCUSSION

Exploring the plant host-pathogen interface is important to revealing the molecular mechanisms that regulate progression of disease. RNA-Seq was used to evaluate the expression patterns of sorghum host in response to *Fusarium graminearum* infection at four time-points (24 hpi, 48 hpi, 7 dpi, 14 dpi), in order to identify changes in gene expression patterns that could be linked to key aspects of the infection process.

5.4.1 Susceptible RIL and its associated pathways and genes in 6 groups

The number of differentially expressed genes in the susceptible RIL was greater than in the resistant RIL in response to *Fusarium graminearum* infection. A similar observation was observed by Zhang et al. (2017), where the number of genes differentially expressed in the susceptible Lemont cassava leaves was higher than that in the tolerant TeQing cassava leaves throughout *Rhizoctonia solani* infection, which can suggest that different sorghum RILs activate distinct mechanisms upon infection.

Group 1 presented an induction of genes that have been reported to have negative and positive influence in defence response at the early infection stage, and the significant decline at the late infection stage in the susceptible RIL. The genes encoding the sesquiterpene metabolism pathway, which is one of the major physiological changes occurring in response to fungal infection, were exclusively found in group 1 (Bönnighausen et al., 2019). This pathway has been previously reported to provide the building blocks for trichothecene, which are mycotoxins associated with Fusarium head blight (FHB) of cereals (Bönnighausen et al., 2019; Foroud et al., 2019). The reported defence genes included WRKY DNA-binding protein, copine, RING domain ligase, Nodulin MtN21, *jmjC* domain containing protein and glyoxalase enzymes also presented a decline at the late infection stage. Nodulin-like proteins are positively influencing the pathogens as they enhance their fitness during host colonization (Denancé et al., 2014). An increase in this protein at 24 hpi could suggests enhancing pathogen fitness during colonization. Not only reported defence response genes were associated with group 1, betagalactosidase and cytochrome 50 which are proteins associated with *Fusarium graminearum* and negatively influence the plant, were associated with group 1.

Genes encoding metabolic pathways were more enriched in group 2 and the physiological trend showed induced pattern at the late infection stage. In a similar transcriptomics study, a detailed primary metabolic profile was induced at a late infection stage in alfalfa leaves response to *Phoma medicaginis* infection and this might induce senescence in leaves leading to plant death (Fan et al., 2018). Group 2 also presented enriched genes encoding proteins that function in the catalysis of metabolic pathways to the biosynthesis of metabolites, which has been reported to threaten global food security by enabling pathogenic fungi to cause disease, particularly on important agricultural crops (Kimura et al., 2001).

Group 3 presented a pattern increase of the LOX 5 gene expressed from 48 hpi-14 dpi timepoints. The loss and silencing of LOX5 function has resulted in improved disease resistance in the *Arabidopsis* and wheat response to *Fusarium graminearum* (Nalam et al., 2015). Results presented in this study could suggests that LOX5 could have a function as a susceptibility factor in disease caused by *Fusarium graminearum* in sorghum RILs. CIPK6 gene was also associated with this group. CBL-interacting protein kinase 6 negatively regulates immune response to *Pseudomonas syringae* in *Arabidopsis* as plants overexpressing CIPK6 were more susceptible to *Pseudomonas syringae* (Sardar et al., 2017).

The genes encoding the starch and sucrose metabolism pathway physiological pattern presented by group 4 had a sharp decline from 48 hpi - 14 dpi (at a later stage of infection). Upon infection of pathogen, a reduction in the content of starch has also been observed in the infected region, suggesting that the starch degradation provides more substrates to sucrose synthesis (Tauzin and Giardina, 2014). Similarly, group 4 had an increase in genes encoding cyanoaminoacid metabolism pathway at the early infection stage and a significant decline from 48 hpi which remained constant to a late stage (14 dpi). Cyanoamino acid metabolism, is involved in chemical defence against pathogens (Zambrano et al., 2017). Similar to this study, the concentration of most plant derived amino acids and total nitrogen content of the leaf apoplast increased during the initial contact during the hemi-biotrophic compatible interaction between *Cladosporium fulvum* and tomato (Solomon and Oliver, 2001). One possibility mentioned for amino acid increase during infection could be an increase in apoplastic protease activity, probably a serine protease, induced in tomato upon infection (Planas-Marques et al., 2018; Solomon and Oliver, 2001). The fungus could therefore manipulate plant metabolism to

maintain or increase the apoplastic concentration of nitrogen compounds (Solomon and Oliver, 2001). This is particularly the case for biotrophs and hemibiotrophs fungal pathogens that derive nutrients from living plant cells (Dulermo et al., 2009). This metabolic imbalance of amino acids leads to host plant necrosis and even chlorosis, and possibly facilitates pathogen growth, because of the nutrient release (Arrebola et al., 2011). Additionally DEGs encoding ubiquinone and other terpenoid-quinone biosynthesis pathways were exclusively enriched in group 4, and these pathways has been involved in defence response to biotic stress (Fan et al., 2019; Tholl, 2015). This could suggests that, as the time progresses in the susceptible RIL the pathways which are important in plant defence declines/deteriorates at a late infection stage allowing the infection.

5.4.2 Transcriptional response on the resistant RIL revealed reported plant defence genes

Transcriptional response of a resistant RIL to infection with *Fusarium graminearum* presented an increase in genes encoding proteins that function in the catalysis of metabolic pathways to the biosynthesis of metabolites in group 1 and group 4 at early infection stage and a sharp decline in the late infection stage. It has been proposed that during plant–pathogen interactions, the function of primary metabolism is to support the cellular energy needs for plant defence responses to create an energy balance favourable for defence (Andolfo and Ercolano, 2015; Kangasjärvi et al., 2012). An increase in the genes encoding these pathways in earlier infection stage could suggest the establishment of a favourable energy balance for defence (Zhang et al., 2017). Galactose metabolism pathway encoded by Galactose mutarotase-like superfamily protein was exclusively expressed in the resistant RIL. The galactose metabolism pathway transcriptional response has also been observed in tolerant soybean to aphids (Prochaska et al., 2015). In most fungal pathogen–plant systems, plant resistance is enhanced by plant tissues high level of sugars (Morkunas and Ratajczak, 2014). Sugars represent the primary substrate providing energy and structural material for defence responses in plants, and it also act as signalling molecules interacting with the hormonal signalling network regulating the plant immune system (Khan et al., 2019). Fungal infection initiates the degradation of galactose via the enzymes of the Leloir pathway. Galactose, a disaccharide of glucose and galactose (from the milk sugar lactose), enters glycolysis by its conversion to glucose-1-phosphate (G1P) (Sasaoka et al., 2018). Galactose can occur in two different forms; α-D and β-D-galactose. The

enzyme galactose mutarotase also known as aldose 1-epimerase (encoded by the GALM gene) is required in order to convert the β-form of galactose to the α-form (Kulcsár et al., 2017). Galactose metabolism through the glycolytic pathway needs a constant supply of UDP-glucose generated from glucose-1-phosphate via the action of UDP-glucose pyrophosphorylase 2 (encoded by the UGP2 gene). It has also been reported that sugar can play a role that is significant in fungal pathogens resistance through phenylpropanoid metabolism stimulation (La Camera et al., 2019; Morkunas and Ratajczak, 2014; Giberti et al., 2012).

Additionally, phenylpropanoid pathway (PAL) encoded by peroxidase enzyme was amongst the pathways increased at early stages of infection in group 1. Similar to our study, PAL genes were up-regulated at the early stage of the fungal *Ganoderma boninense* infection on palm seedlings (Govender et al., 2017). This suggests that, expression of genes encoding defence pathways at the early stage, could play a role in plant defence. The pathogen elimination is determined by the efficiency and speed of early defence responses initiated by the plant and activates a series of events (Morkunas and Ratajczak, 2014).

Previous reports has also showed, that the phenylpropanoid pathway could play a part in resistance of wheat to *Fusarium graminearum* and deoxynivalenol (the most important mycotoxin produced by *Fusarium graminearum*) (Sorahinobar et al., 2017; Ding et al., 2011). PAL have been previously shown to be expressed more quickly or at higher levels during pathogen attack and has been linked with production of phytoalexins and increased lignin deposition (Little and Magill, 2003)

Additionally, the phenylpropanoid pathway allows for production of various secondary metabolites by plants in defence response (Bajaj et al., 2018; Morkunas and Ratajczak, 2014). These include flavonoids (isoflavonoids specifically), which can play a part in plant phytoalexins (Morkunas and Ratajczak, 2014). Isoflavonoids can be toxic to pathogens caused by fungi, i.e., reducing the fungal development by inhibiting the spore germination, mycelial growth, while they also limit fungal pathogenicity. The peroxidase protein within the phenylpropanoid pathway has been associated with wound repair, injury and disease resistance (Mhlongo et al., 2016; Singh et al., 2010). Peroxidases are involved in the

polymerization of suberin, lignin and oxidation of phenolic compounds in cell walls (Pandey et al., 2017). They catalyze the oxidation of phenol substrates and its derivates by hydrogen peroxide and are responsible for dehydrogenation of coniferyl and sinapyl alcohol during lignin synthesis (Harman-Ware et al., 2017).

Various reported defence related proteins were associated with group 1. Ankyrin repeat family protein has been observed at a number of different cellular levels, which includes transcriptional expression of defence genes in the nucleus and has contributed in the plant defence response (Vo et al., 2015). Polyols also found in this group can play a role in translocation of antioxidants and carbon skeletons which may be involved in some plants to be resistant to biotic and abiotic constraints (Tian et al., 2017). In a transcriptional response of citrus to candida xyloglucan endotransglucosylation (XET) activity level was found to peak at the penetrating stage of *Cuscuta reflexa* on its host *Pelargonium zonale* (Olsen and Krause, 2017). In addition to the reported defence related genes mentioned above, osmotin was amongst the reported defence DEGs in group 1. Transgenic plants overexpressing osmotin displayed increased resistance to pathogenic fungi (Anil Kumar et al., 2015) clearly pointing to a role as a defence system against these pathogens (González et al., 2017). An increase in the physiological trend of defence DEGs in earlier infection stage further suggests the establishment of a favourable energy balance for defence.

Group 2 presented an increase in reported defence related genes at the late infection stage. This group cluster was represented by DIR1, which has been previously found to be involved in the resistance to different *Fusarium* pathogens (Gottwald et al., 2012). The 4-amino-2-trifluoromethyl-phenyl retinate (AtPR-5) encoding specific components involved in salicylic acid (SA) regulation, synthesis, and signalling, also showed an increased trend in group 2. SA signalling contributes to wheat defence against *F. graminearum* (Hao et al., 2019; Sarowar et al., 2019).

GST genes activities induction were frequently noted in plants treated with microbes that are beneficial and stimulate a systemic resistance response (ISR) to subsequent pathogen infections. Silencing or overexpression of specific GSTs can noticeably modify pathogen multiplication rates and disease symptoms. However, not much is known about the exact

metabolic functions of disease-induced GST isoenzymes (Gullner et al., 2018). The GST genes in this study has been expressed in both the susceptible and resistant groups.

Group 4 and 5 also encompassed reported plant defence related genes. The physiological trend in group 4 presented an increase at the early infection stage and a sharp decline in the late infection stage. This group encompassed proteins defective in induced resistance 1 (DIR1), which has also been identified in *Arabidopsis.* Multiple compounds including DIR1 were identified as putative systemic acquired resistance (SAR) signals or important factors for influencing SAR signalling element movement in tobacco and *Arabidopsis*. Systemic acquired resistance (SAR) is a defence mechanism that stimulates protection against a broad range of pathogens (Ádám et al., 2018). Not only DIR protein was found in this group, pathogenesis-related genes1 (PR1) was also found. The expression of PR1 gene was previously observed in the mulberry induced by pathogens and phytohormones (Fang et al., 2019). The heterogeneous expression of Mulberry PR1 in *Arabidopsis* enhanced transgenic plant resistance to bacterial strain *Pseudomonas syringae* (Fang et al., 2019). Over-expression of *Arabidopsis* PR1 enhanced FHB resistance in wheat, together with faster and stronger SAR activation (Ding et al., 2011). An increase in the pathways in earlier infection state could suggest the establishment of a favourable energy balance for defence (Zhang et al., 2017).

Interestingly an autophagy-related protein, ATG8C was exclusively expressed in group 5 and in the resistant RIL and the physiological pattern presented an increase in the 14 dpi (late infection stage), plant autophagy plays an important role in various stress responses and pathogen defence (Di Berardino et al., 2018). This pathway has been reported to play a critical role in plant resistance to biotic stress in model crops (tobacco and *Arabidopsis*) and agriculturally important crops (wheat, rice, banana, cassava, tomato, rice and barley) (Bárány et al., 2018; Zhou et al., 2018; Yue et al., 2018; Wei et al., 2017; Avila-Ospina et al., 2016; Cui et al., 2016; Zhou et al., 2015; Miozzi et al., 2014; Nakahara et al., 2012; Xia et al., 2011; Zientara-Rytter et al., 2011). The gene ATG8 was associated with autophagy pathway and it presented an increased trend at late infection stage.

Autophagy is triggered by starvation and stress and leads to rearrangement of cellular membranes (autophagosomes) to sequester cargo delivery to the lysosome, where sequestrated

materials are then recycled and degraded. This pathway is required for vegetative growth, asexual/sexual sporulation, DON production and pathogenesis in *Fusarium graminearum*. There are 38 autophagy related genes (ATG). Josefsen et al. (2012) suggested that autophagy provides nutrients for non-assimilating fungal structure and is necessary for plant colonization but not infection in *Fusarium graminearum.* The results found in the resistant RIL could suggest that no infection was initiated as this gene was over expressed at 14 dpi at late infection stage.

5.4.3 Gene enrichment using Gene Ontology terms of DEGs profiles between susceptible and resistant RILs

The genes encoding the main biological processes enriched in the resistant RILs were biogenesis and response to stimulus. Guerra-Guimarães et al. (2016) indicated that 18% to 29% of the total apoplastic proteins are implicated in cell wall organization and biogenesis. Many microbes attack plant cells initially in the apoplast, an extracellular space in plant tissues that serves as the first battlefield between microbial invaders and their plant hosts (Doehlemann and Hemetsberger, 2013). The functional analysis also revealed that major changes were occurring in the cell wall component as most genes within the component were enriched in the resistant RIL. The reported resistant gene (Auxin-responsive protein IAA26 - Sobic.009G203700) encoded intracellular proteins carrying a nucleotide binding site (NBS). A similar response in both barley and wheat was observed where genes encoding cell wall degradation were expressed in both crops (Hofstad et al., 2016; Zhang et al., 2012; Güldener et al., 2006). Thickened cell wall has been reported to cause reduced spread of infection (Hofstad et al., 2016).

Resistance mechanisms of sorghum to *Fusarium graminearum* are divided into two, the constitutive and the inducible systems. Constitutive resistance includes structural features, which prevent penetration into the host tissues and cells. The thickness of the cuticle and cell wall may limit penetration into the cells, thus hindering the progress of the fungi within the cells themselves. Constitutive defence prevents infection in the first place, while induced defence typically shortens the infectious period (Boots and Best, 2018). The observed initial defence processes upon pathogen infection could suggests that it is type I – resistance

(constitutive resistance) to *Fusarium graminearum* initial infection (Khaledi et al., 2018). The DEGs related to stress response, response to stimulus, cellular protein modification, and transcription factor activity in the resistant lines might explain its efficiency in restraining infection at earlier stages, which probably leads to its higher disease resistance. Furthermore, plant mutants that show leaf wax composition alterations can be less susceptible to fungal invasion (Li et al., 2018; Weidenbach et al., 2014; Vardhan et al., 2013; Uppalapati et al., 2012).

5.4.4 Transcriptional changes using KEGG Orthology reveals overrepresentation of defence related pathways in the resistant RIL

Phenylpropanoid (PAL), galactose and glycolysis pathway were amongst the pathways whose genes were upregulated and exclusively enriched in the resistant RIL. Galactose metabolism pathway encoded by Galactose mutarotase-like superfamily protein was exclusively expressed in the resistant RIL. The transcriptional response has also been observed in tolerant soybean to aphids (Prochaska et al., 2015). In most fungal pathogen–plant systems, a high level of sugars in plant tissues enhances plant resistance (Morkunas and Ratajczak, 2014). Sugars represent the primary substrate providing energy and structural material for defence responses in plants. The phenylpropanoid pathway offers precursors for the formation of coumarins, benzoic acids, monolignols/lignin and flavonoids/isoflavonoids, as well as stilbenes, a small family of secondary metabolites that have antifungal activity (Dixon et al., 2002). PAL have been previously shown to be expressed more quickly or at higher levels during pathogen attack and has been associated with increased lignin deposition and production of phytoalexins (Little and Magill 2003). The DEGs encoding proteins that function in the catalysis of metabolic pathways to the biosynthesis of metabolites pathway was more pronounced and up-regulated in the resistant RIL. The plant defence against pathogens requires the synthesis of a plethora of secondary metabolites (Nussbaumer et al., 2015; Walter et al., 2010). Additionally, DEG encoding the autophagy pathway was exclusively associated with the resistant RIL, this pathway has been reported to play a critical role in plant resistance to biotic stress in model and agriculturally important crops. Genes associated with autophagy were reportedly linked with anthracnose resistance to sorghum (Upadhyaya et al., 2013).

5.5. CONCLUSION

In summary, the transcriptomes of the resistant and susceptible RILs at 24 hpi, 48 hpi, 7 dpi and 14 dpi were investigated. The transcriptional response upon *Fusarium graminearum* infection presented differences in the closely related clustered expression profiles across all timepoints through the use of the Dirichlet Process Gaussian Process mixture model software between groups in both susceptible and resistant RILs. In the susceptible RIL, group 2 exclusively clustered the genes encoding the sesquiterpene metabolism pathway, which is one of the major physiological changes occurring in response to fungal infection and has been previously reported to provide the mycotoxins associated with Fusarium head blight (FHB) of cereals. This pathway presented a pattern increase from the early infection stage to the late infection stage. In group 4, the genes encoding the two pathways i.e. starch, sucrose metabolism and cyanoamino acid presented a pattern that had a sharp decline from 48 hpi -14 dpi (at a later stage of infection). This could suggest that as the time progresses in the susceptible RIL the pathways which are important in plant defence decline at a late infection stage. The transcriptional response of the resistant RIL 103 to infection with *Fusarium graminearum* presented an increase in DEGs encoding proteins that function in the catalysis of metabolic pathways to the biosynthesis of metabolites in group 1 and group 4 at early infection stage and a sharp decline in the late infection stage. An increase in DEGs encoding these pathways in earlier infection stages could suggest the establishment of a favourable energy balance for defence. Additionally, DEGs encoding phenylpropanoid (PAL), galactose and glycolysis pathway were amongst the genes increased at early stages of infection in group 1. Sugar can play an important role in resistance to fungal pathogens through phenylpropanoid metabolism stimulation, and previous reports indicated that the phenylpropanoid pathway could play a part in resistance of wheat to *Fusarium graminearum* and deoxynivalenol. Overall, this study represents a first step in understanding the molecular mechanisms involved in resistance to *Fusarium graminearum* in sorghum. The transcriptome data generated will help guide further research to develop novel strategies for disease management in sorghum RILs.

CHAPTER 6

General discussion

6.1 Introduction

This concluding chapter consolidates the most significant outcomes and highlights the contribution of the thesis to sorghum metagenomics (metabarcoding) and transcriptomics. Sorghum is one of the most important field crops and is consumed as a major dietary source worldwide. Despite the important role that the crop plays in the livelihood of human and animal populations, sorghum production and yield are limited by biotic and abiotic stresses. Plant pathogens represent a constant and major food production constraint, with global crop losses estimated to be 20% – 30% principally in areas that have food shortages (Savary et al., 2019). To mitigate the constraints, measures such as pesticide use, resistance gene breeding, and genetic manipulation of plant immune systems have been previously used (Mushtaq et al., 2019; Niks et al., 2019; Vannier et al., 2019). However, host range expansion together with accelerated evolution of pathogen resistance, contribute to severe disease outbreaks, particularly in the context of current agricultural practices. Global trade in agricultural products has allowed the rapid movement of crop pathogens around the world, and has led to the transmission of highly damaging pathogens (McDonald and Stukenbrock, 2016). The spread and introduction of wheat blast pathogen *Pyricularia graminis-tritici* into Asia has been previously noted (Callaway, 2016).

Metagenomic amplicon sequencing was used in this study to extensively characterize bacterial and fungal populations on/or within leaves naturally infected with various diseases and identify the pathogenic taxa that are associated with susceptible plants. *Fusarium graminearum* has been found in this study to be associated with highly susceptible sorghum recombinant inbred lines. Interestingly, this pathogen has been previously isolated in sorghum (Choi et al., 2013; Quazi et al., 2010; Tarekegn et al., 2006; Menkir et al., 1996). *Fusarium graminearum* is a significant pathogen that has been associated with stalk rot and grain mould in sorghum, winter cereals and maize (Kelly et al., 2017; Das et al., 2012; Trimboli and Burgess, 1985). However it has been indicated that sorghum only acts as a *F. graminearum* host, that does not exhibit any disease symptoms although this condition can pose a toxicological risk (Pena et al., 2019; Burgess et al., 2002), since this species has the ability to produce 3-acetyldeoxynivalenol (3-ADON), deoxynivalenol (DON), nivalenol (NIV), 15-acetyldeoxynivalenol (15-ADON) and zearalenone (ZEA) (Yerkovich et al., 2017). Studies testing the pathogenicity of several fusaria

spp. including, *Fusarium subglutinans, Fusarium solani, Fusarium verticillioides* and *Fusarium graminearum* have been previously conducted (Van Rooyen, 2019; Bodoči et al., 2013). *Fusarium graminearum* had the highest pathogenicity on sorghum grain, followed by *Fusarium solani, Fusarium verticillioides* and lastly *Fusarium subglutinans.* In addition to that, the grain sorghum susceptibility to *Fusarium graminearum* colonization was assessed by isolation studies involving plants grown in the glasshouse. *Fusarium graminearum* infection studies on sorghum seedlings indicated that this pathogen can infect the host at initial growth stages and slowly colonize adjacent tissues as an endophyte. The findings also showed that stem tissues as well as roots are susceptible to infection. Indeed, the above studies suggests that the fungus could infect and colonize the proximal parts of roots, leaf sheaths and stem tissues (Quazi et al., 2010).

To the best of our knowledge there is no reported study of gene expression study using RNA-Seq studies conducted in the response of sorghum upon *Fusarium graminearum* infection despite it being highly pathogenic to sorghum. Substantial gene expression studies upon *Fusarium graminearum* infection have been conducted on other crops, including wheat, maize and barley. Recent studies investigating the mechanisms underlying the host defence response against *Fusarium graminearum* using comparative transcriptome analysis in susceptible and resistant maize and wheat genotypes have been conducted (Brauer et al., 2019; Yuan et al., 2019).

This metagenomics and transcriptomics analysis will help in identifying the beneficial microbes and resistant genes. Thus, positively facilitates in the development of *Fusarium graminearum* resistant genotypes in future through the integration/incorporation of beneficial microorganisms (bacteria and fungi) and resistant genes in breeding strategies.

6.2 Characterization of bacterial and fungal community through metabarcoding

DNA metabarcoding, regularly used in exploratory microbial ecology studies, is a promising tool for the concurrent in planta detection of multiple pathogens and beneficial microbes associated with diseased plants (Morales-Cruz et al., 2018). Amplicon barcoding was used in this study to profile the fungal and bacterial taxa associated with different disease groups in

sorghum. It was shown that metabarcoding of ribosomal ITS, amplified with commonly-adopted universal primers, allowed the characterization of the abundance of sorghum pathogenic taxa. Fungal families *Nectriaceae* and *Didymellaceae* classified as *Gibberella* and *Epicoccum* genera respectively, were significantly linked to the HS and (HS and S) disease groups, respectively. The *Gibberella* and *Epicoccum* genera were assigned fungal species potentially classified as *Gibberella zeae* and *Epicoccum sorghinum*, respectively, which were highly linked to the HS and S disease groups, respectively. These species are potential pathogenic taxa and have been previously reported to be a major causative species in sorghum grain mould disease (de Oliveira et al., 2018; Kelly et al., 2017). The taxonomic assignments for the fungal and bacterial species were classified as either potential or possible species because accurate annotation of lower taxonomic ranks due to a relatively short sequences generated from amplicon studies is still a challenge (Meola et al., 2019). The members of the genera *Ascochyta* (potential classified as *Ascochyta paspali*) and *Ustilago* (potentially classified as *Ustilago kamerunensis*) causing sorghum leaf stripe disease and leaf smut, respectively, were also associated with the HS and S disease groups (Xu et al., 2019; Jayashree and Wesely, 2018; Kruse et al., 2018; Omayio et al., 2018; Tivoli and Banniza, 2007). In contrast to fungi few potential pathogenic bacterial taxa could be identified. There is reports that sorghum hosts more fungal diseases in comparison to bacterial diseases (Das, 2019; Klein et al., 2001). *Pantoea*, a sorghum bacterial pathogen causing leaf spot, was exclusively associated with the HS disease group. Members of the *Serratia* genus, causing cucurbit yellow vine disease on cucurbits, sunflower, alfalfa were associated with the S disease group (Besler and Little 2017). Interestingly, a newly identified potential pathogenic *Mixta gaviniae* taxa of the *Erwiniaceae* family was highly associated with the HS disease group (Palmer et al., 2018).

Not only reported pathogenic fungi were detected, but bacterial and fungal taxa previously reported to have plant growth promoting capabilities were found in this study. The genera *Methylorubrum*, *Enterobacter* and *Sphingomonas* were more abundant and highly enriched in the R and MR group, with members of the latter genus significantly enriched in the R group. *Enterobacter* and *Sphingomonas* have been previously reported to exhibit plant growth-promotion traits (Schlemper et al., 2018; Knief et al., 2010). Little is known regarding the phylogenetic taxa and functional attributes of the recently classified *Methylorubrum* genus

(Grossi et al., 2020; Green and Ardley, 2018). However, members of this genus are abundant in the phyllosphere and have shown to be associated with plants which displayed resistance to disease (Schisler et al., 2019; Wallace et al., 2018; Zhang et al., 2018b; Rakotoarisoa et al., 2015; Trivedi et al., 2010). The resistant fungal group had a majority of OTUs showing similarity to well-known plant growth-promoting fungal genus including *Papiliotrema* (*Tremellaceae* family), which are known biocontrol agents (Schisler et al., 2019). The yeast *Hannaella* was highly linked with the resistant plants. Some *Hannaella* species are known to produce indole acetic acid (IAA) (Kaewwichian et al., 2015; Sun et al., 2014). The IAA producing microorganisms are reported to be efficient bio-fertilizer inoculants used for promoting plant growth (Mehmood et al., 2018). The RILs in the R group also had more diverse fungi and bacteria than other disease groups. The results suggest that natural pathogen infection results in distinct foliar microbial communities in sorghum RILs.

6.3 Molecular analysis and cell viability of *Fusarium graminearum*

The control of economically important pathogens involves the identification of the causative species (Srivastava et al., 2018). Identification of pathogenic species is done by traditional morphological and molecular methods (Aslam et al., 2017). Traditional diagnostic tools for *Fusarium graminearum* identification in culture or in infected grains are based on morphological features. This process is laborious and it can often be difficult to make a distinction between species that are similar. This study utilized molecular methods for the identification of *Fusarium graminearum.* Molecular methods are more sensitive, faster and are also employed for species level identification of *Fusarium*. PCR with primers targeted to the internal transcribed sequence (ITS) between the ribosomal DNA genes (Schilling et al., 1996) for the detection and identification of *Fusarium graminearum* has been used extensively. However, sequences in the ITS regions have shown to be highly variable in Fusaria (O'Donnell, 1992). In this study, molecular methods were used to confirm *Fusarium graminearum* with both ITS and UBC (Ubiquitin C) primers specific to the *Fusarium graminearum*. An approach for the identification of *Fusarium graminearum* using both species specific and ITS primer regions successfully confirmed the *Fusarium graminearum* species. In addition to molecular identification of *Fusarium graminearum*, the cell/spore viability of the identified species using

culture dependent techniques was checked through the automated cell counter. The spores were found to be highly viable with a live cell percentage of 64%, confirming that the pathogen can initiate plant infection.

6.4 Gene profiling for identification of defence related genes in response to *Fusarium graminearum*

To determine if *Fusarium graminearum* induced specific defence-related genes, RNA-Seq analyses was used to assess the expression patterns of sorghum (resistant and susceptible RILs) in response to *Fusarium graminearum* at four time-points (24 hpi, 48 hpi, 7 dpi, 14 dpi), in order to identify changes in gene expression that could be linked to key aspects of the defence process. RNA-Seq data was acquired for RIL 131 and 103 from *Fusarium graminearum* inoculated leaves at 24 hpi, 48 hpi, 7 dpi and 14 dpi. An average of 76 million reads raw reads across all the samples was recovered. Paired end reads only were considered in the mapping to the reference genome and an average of 87% reads could be mapped across all the samples to the sorghum genome.

The transcripts identified in this study will also contribute significantly to the sorghum database, and can be used to improve the annotation of the sorghum genome. Sorghum is known for its high genetic variability, however the genes that play roles in pathways controlling stress tolerance are not known. For example, approximately 50% of the 47,121 existing protein coding genes lack experimentally validated information and 14% of the sorghum transcriptome (sorghum annotation) represent unknown protein function (McCormick et al., 2018; Paterson et al., 2009). Compared to the rice genome which was annotated 7 times to date and the *Arabidopsis* genome that has been annotated 5 times (Sakai et al., 2013; Lamesch et al., 2012). Additionally, the sorghum genome has undergone 4 versions of annotation updates. To our knowledge relatively few studies have reported on sorghum functional annotation using RNA-Seq technology sequencing (Woldesemayat et al., 2017)

There was also good correlation between reads from the different biological replicates of each sorghum RIL, with correlation coefficient values ranging from R^2 = 0.92 - 0.99 in 24 hpi, 48

hpi, 7 dpi and 14 dpi timepoints within both RILs. There were significant differences in the expression levels at the queried time points between groups in both susceptible and resistant samples. A total of 235 and 37 genes from susceptible and resistant lines respectively were differentially expressed (log2 fold change and FDR ≤ 0.05) across all time points (24 hpi-14 dpi) following *Fusarium graminearum* infection. The higher number of the expressed genes in susceptible RIL, could suggest that different sorghum RILs activate different mechanisms upon infection.

The resistant and susceptible RILs have differentially expressed genes (DEGs) that were clustered into closely related expression profiles to determine cluster membership across all timepoints through the Dirichlet Process Gaussian Process mixture model software and grouped according to the same expression trends. In the susceptible RIL, group 1 presented the induction of genes with reported negative influence to defence response at the early infection stage, and the significant decline at the late infection stage. This group was represented by genes encoding proteins that function in the catalysis of metabolic pathways to the biosynthesis of metabolites associated with *Fusarium graminearum* but negatively influences the plant. Nodulin-like proteins found in this group has reported positive influence to the pathogens as they enhance their fitness during host colonization (Denancé et al., 2014). The DEGs encoding the sesquiterpene metabolism pathway, which is one of the major physiological changes occurring in response to fungal infection, was exclusively found in group 1 (Bönnighausen et al., 2019). It has been previously reported to provide the building blocks for trichothecene which are mycotoxins associated with Fusarium head blight (FHB) of cereals (Bönnighausen et al., 2019; Foroud et al., 2019).

DEGs encoding metabolic pathways were more enriched in group 2 and the expression trend showed increased pattern at a later stage of infection. In a similar study, a detailed primary metabolic profile of the response of alfalfa leaves to *Phoma medicaginis* infection at a later stage of infection was also observed and this might induce senescence in leaves leading to plant death (Fan et al., 2018). An enriched metabolic pathways in group 2 was observed, which has been reported to threaten global food security by enabling pathogenic fungi to cause disease, particularly on important agricultural crops (Kimura et al., 2001). Secondary metabolites and small secreted proteins are known to play significant roles in the fungal plant pathogens

lifestyle and virulence. Group 3 presented a pattern increase of the LOX 5 gene expressed at 48 hpi-14 dpi timepoints. LOX 5 gene has previously been reported to have a role as a susceptibility factor in diseases caused by *Fusarium graminearum* in *Arabidopsis* and wheat (Nalam et al., 2015).

The genes encoding the starch and sucrose pathway pattern presented by group 4 had a sharp decline from 48 hpi -14 dpi (at a later stage of infection). Upon infection of pathogen, a reduction in the content of starch has also been observed in the infected region, suggesting that the starch degradation provides more substrates to sucrose synthesis (Tauzin and Giardina, 2014). Similarly, group 4 had an increase in DEGs encoding cyanoaminoacid metabolism pathway at the early infection stage and a significant decline from 48 hpi which remained constant to a late stage (14 dpi). Cyanoamino acid metabolism, is involved in chemical defence against pathogens (Zambrano et al., 2017). Similar to this study, the concentration of most plant derived amino acids of the leaf apoplast increased during the hemi-biotrophic compatible initial interaction between *Cladosporium fulvum* and tomato (Solomon and Oliver, 2001). Additionally, DEGs encoding ubiquinone and other terpenoid-quinone biosynthesis pathways were exclusively enriched in group 4, and have been reported to be defence compounds (e.g., volatile compounds) in response to biotic stress (Fan et al., 2019; Tholl, 2015). This could suggests that, as the time progresses in the susceptible RIL, the pathways which are important in plant defence decline at a late infection stage.

The transcriptional response of a resistant RIL, number 103, to infection with *Fusarium graminearum* presented an increase in DEGs encoding metabolic pathways and biosynthesis of metabolites in group 1 and group 4 at the initial infection stage and a sharp decline in the late infection stage. An increase in the pathways at the earlier stage of infection could suggest the establishment of a favourable energy balance for defence (Zhang et al., 2017). Ankyrin and polyols, reported defence related proteins were clustered in group 1. An ankyrin repeat family protein (Sobic.001G432500) has contributed to the plant defence response (Vo et al., 2015). Polyols can act as an energy means between source and sink organs, for the translocation of carbon skeletons as well as being osmoprotective antioxidants and solutes that could be involved in the resistance of some plants to biotic and abiotic stresses (Tian et al., 2017). In addition to the reported defence related genes mentioned above, osmotin was amongst the

reported defence DEGs clustered. Transgenic plants overexpressing osmotin displayed increased resistance to pathogenic fungi (Anil Kumar et al., 2015) clearly pointing to a role as a defence system against these pathogens (González et al., 2017).

Additionally, DEGs encoding enzymes for the phenylpropanoid (PAL), galactose and glycolysis pathway were amongst the genes increased at early stages of infection in group 1. The galactose metabolism pathway encoded by galactose mutarotase-like superfamily protein was exclusively expressed in the resistant RIL. The transcriptional response has also been observed in tolerant soybean to aphids (Prochaska et al., 2015). In most fungal pathogen–plant systems, plant resistance is enhanced by a high level of sugars in plant tissues (Morkunas and Ratajczak, 2014). Sugars represents the primary substrate providing energy and structural material for defence responses in plants, and they also act as signal molecules interacting with the hormonal signalling network regulating the plant immune system.

It has also been reported that sugar can play an fundamental role in resistance to fungal pathogens through phenylpropanoid metabolism stimulation (La Camera et al., 2019; Morkunas and Ratajczak, 2014; Giberti et al., 2012). DEGs encoding phenylpropanoid (PAL) pathway were amongst the genes increased at early stages of infection in group 1. Similar to the current study, PAL genes were up-regulated at the initial phase of the fungal *Ganoderma boninense* infection on palm seedlings (Govender et al., 2017). The expression of PAL genes at the early stages of pathogen infection, could play a role in plant defence. This is because the pathogen elimination is determined by the efficiency and speed of early defence responses initiated by the plant (Morkunas and Ratajczak, 2014). Previous reports presented that the phenylpropanoid pathway could play a part in resistance of wheat to *Fusarium graminearum* and deoxynivalenol (as the most important mycotoxin produced by *Fusarium graminearum*) (Sorahinobar et al., 2017; Ding et al., 2011).

Group 4 and 5 also observed the expression of PR1 protein. Mulberry PR1 in *Arabidopsis* enhanced transgenic plant resistance to bacterial strain *Pseudomonas syringae* (Fang et al., 2019). Interestingly an autophagy-related protein, ATG8C was exclusively expressed in group 5 and in the resistant RIL, plant autophagy plays an important role in various stress responses,

including pathogen defence (Di Berardino et al., 2018). This pathway has been reported to play a critical role in plant resistance to biotic stress in model crops (tobacco and *Arabidopsis*) and agriculturally important crops such as wheat, rice, banana, cassava, tomato, rice and barley (Bárány et al., 2018; Zhou et al., 2018; Yue et al., 2018; Wei et al., 2017; Avila-Ospina et al., 2016; Zhou et al., 2015; Cui et al., 2016; Miozzi et al., 2014; Nakahara et al., 2012; Xia et al., 2011; Zientara-Rytter et al., 2011). Genes linked to autophagy were reported to be associated with anthracnose resistance to sorghum (Upadhyaya et al., 2013).

In conclusion, this thesis highlighted the most significant outcomes contributing to sorghum metagenomics and transcriptomics.

- Through metabarcoding and phenotype characteristics (according to the foliar disease scale used in this study) it was identified that RIL 103 was associated with highly resistant group as there was no pathogenic foliar symptoms and RIL 131 was associated with the highly susceptible disease group.
- The current analyses revealed that the potential fungal pathogens of sorghum, *Fusarium graminearum* and *Epicoccum sorghinum*, were associated with highly susceptible disease group. In addition to previously reported sorghum pathogens, other potential pathogenic fungal taxa including *Ascochyta paspali* and *Ustilago kamerunensis* were found.
- The bacterial genera *Methylorubrum*, *Enterobacter* and *Sphingomonas* with reported plant growth promotion traits were more abundant and highly enriched in the R and MR group, with members of the latter genus significantly enriched in the R group.
- The resistant fungal group had a majority of OTUs showing similarity to well-known plant growth-promoting fungal genus including *Papiliotrema* (*Tremellaceae* family), which are known biocontrol agents.
- These data further suggests natural pathogen infection results in distinct foliar microbial communities in sorghum RILs.
- The results of bacterial and fungal community composition, community co-occurrences further suggest the importance of keystone taxa which may disproportionately shape the structure of foliar microbiomes.
- The current data provides a baseline for testing hypothesis related to the importance of keystone taxa in foliar microbiota. Cultivation studies may shed light on the nature of the putative symbiotic relationships between bacteria and fungi.

The transcriptional response upon *Fusarium graminearum* infection presented differences of the closely related clustered expression profiles across all timepoints through the use of Dirichlet Process Gaussian Process mixture model software between groups in both susceptible and resistant RILs

- Transcriptional response of the susceptible RIL number, 131 to infection with *Fusarium graminearum* in group 1, presented an induction of genes that have reported negative influences to defence response at the early infection stage, and the significant decline at the late infection stage. This group was represented by genes associated with *Fusarium graminearum* and negatively influencing the plant. Nodulin-like proteins are reported to positively influence the pathogens as they enhance their fitness during host colonization.
- Genes encoding metabolic pathways were mostly enriched in group 2, and the physiological trend showed induced pattern at a later stage of infection. This enrichment observed has been reported to induce senescence in leaves leading to plant death.
- In addition to the pathways enriched in this group, the genes encoding the sesquiterpene metabolism pathway, which is one of the major physiological change occurring in response to fungal infection and has been previously reported to provide the mycotoxins associated with Fusarium head blight (FHB) of cereals, presented an increase from the early infection stage to the late infection stage.
- Group 3 presented a pattern increase of the LOX 5 gene expressed at 48 hpi-14 dpi timepoints. Results presented, suggests that LOX5 could have a function as a susceptibility factor in disease caused by *Fusarium graminearum* in *Arabidopsis* and wheat as reported in previous studies.
- The genes encoding starch, sucrose metabolism and cyanoamino acid pathways in group 4 presented an expression pattern that had a sharp decline from 48 hpi -14 dpi (at a later stage of infection). This could suggests that, as the time progresses in the susceptible RIL the pathways which are important in plant defence declines at a late infection stage. After pathogen infection, a decrease in the starch content, decrease in the concentration of most plant derived amino acids and total nitrogen content has also been observed in the infected region in other studies.

- Transcriptional response of a resistant RIL no 103 to infection with *Fusarium graminearum* presented an increase in metabolic pathways and biosynthesis of metabolites pathways in group 1 and group 4 at early infection stage and a sharp decline in the late infection stage. An increase in the pathways trends in earlier infection state could suggest the establishment of a beneficial energy balance for defence.
- Additionally, the genes encoding phenylpropanoid (PAL), galactose and glycolysis pathways were amongst the genes increased at early stages of infection in group 1. Galactose mutarotase-like superfamily encoding galactose metabolism pathway was exclusively expressed in the resistant RIL. In most fungal pathogen–plant systems, a high level of sugars in plant tissues enhances plant resistance.
- It has also been reported that sugar can play a significant role in resistance to fungal pathogens through phenylpropanoid metabolism stimulation, DEGs encoding phenylpropanoid (PAL) were amongst the genes increased at early stages of infection in group 1. The expression of PAL genes at the early stages of pathogen infection, could play a role in plant defence. This is because the pathogen elimination is determined by the efficiency and speed of early defence responses initiated by the plant and activates a sequence of events. Earlier studies showed that the phenylpropanoid pathway could play a role in resistance of wheat to *Fusarium graminearum* and deoxynivalenol.
- Group 4 and 5 also observed the expression of PR1 protein. Mulberry PR1 in *Arabidopsis* enhanced transgenic plant resistance to bacterial strain *Pseudomonas syringae*. Various reported defence related proteins were found in group 1 and includes Ankyrin repeat family protein and Polyols.
- Interestingly an autophagy-related protein, ATG8C was exclusively expressed in group 5 and in the resistant RIL, plant autophagy has been reported to play a critical role in plant resistance to biotic stress in model crops and agriculturally important crops (wheat, rice, banana, cassava, tomato, rice and barley).

Overall, this study represents a first step in understanding the molecular mechanisms involved in resistance to *Fusarium graminearum*. The transcriptome and metagenomic data generated will help guide further research to develop novel strategies for disease management in sorghum RILs. The cultivation of varieties that are resistant is the most cost-effective and sustainable

ways to control contamination with mycotoxins and yield losses. The results of bacterial and fungal community composition, community co-occurrences further suggest the importance of keystone taxa which may disproportionately shape the structure of foliar microbiomes. This analysis has also identified the reported beneficial microbes and reported defence related genes and pathways. Cultivation studies may shed light on the nature of the putative symbiotic relationships between bacteria and fungi. Together, the current findings suggest that different 'resident' consortia found in naturally infected and uninfected sorghum plants may be viable biocontrol and plant-growth promoting targets. These results have consequences for crop breeding, and the analysis of microbial diversity and community composition can be useful biomarkers for assessing disease status in plants. This provides the baseline information and will positively impact in the development of *Fusarium graminearum* resistant genotypes in future through the integration/incorporation of beneficial microorganisms (bacteria and fungi) and resistant genes in breeding strategies

REFERENCE LIST

Abdelfattah, A., Malacrinò, A., Wisniewski, M., Cacciola, S.O., Schena, L., 2018. Metabarcoding: A powerful tool to investigate microbial communities and shape future plant protection strategies. Biol. Control 120, 1–10.

Abdullah, A.S., Moffat, C.S., Lopez-Ruiz, F.J., Gibberd, M.R., Hamblin, J., Zerihun, A., 2017. Host–multi-pathogen warfare: pathogen interactions in co-infected plants. Front. Plant Sci. 8, 1806.

Abedi-Tizaki, M., Sabbagh, S.K., 2012. Morphological and molecular identification of'Fusarium'head blight isolates from wheat in north of Iran. Aust. J. Crop Sci. 6, 1356.

Ádám, A., Nagy, Z., Kátay, G., Mergenthaler, E., Viczián, O., 2018. Signals of systemic immunity in plants: Progress and open questions. Int. J. Mol. Sci. 19, 1146.

Adriaens, M.E., Jaillard, M., Waagmeester, A., Coort, S.L.M., Pico, A.R., Evelo, C.T.A., 2008. The public road to high-quality curated biological pathways. Drug Discov. Today 13, 856–862.

Akinrinlola, R.J., Yuen, G.Y., Drijber, R.A., Adesemoye, A.O., 2018. Evaluation of bacillus strains for plant growth promotion and predictability of efficacy by in vitro physiological traits. Int. J. Microbiol. 2018.

Al Rwahnih, M., Daubert, S., Golino, D., Rowhani, A., 2009. Deep sequencing analysis of RNAs from a grapevine showing Syrah decline symptoms reveals a multiple virus infection that includes a novel virus. Virology 387, 395–401.

Aleklett, K., Hart, M., Shade, A., 2014. The microbial ecology of flowers: an emerging frontier in phyllosphere research. Botany 92, 253–266.

Allali, I., Arnold, J.W., Roach, J., Cadenas, M.B., Butz, N., Hassan, H.M., Koci, M., Ballou, A., Mendoza, M., Ali, R., 2017. A comparison of sequencing platforms and bioinformatics pipelines for compositional analysis of the gut microbiome. BMC Microbiol. 17, 194.

Almario, J., Jeena, G., Wunder, J., Langen, G., Zuccaro, A., Coupland, G., Bucher, M., 2017. Root-associated fungal microbiota of nonmycorrhizal *Arabis alpina* and its contribution to plant phosphorus nutrition. Proc. Natl. Acad. Sci. U. S. A. 114, 9403–9412.

Almodares, A., Hadi, M.R., 2009. Production of bioethanol from sweet sorghum: A review. African J. Agric. Res. 4, 772–780.

Amend, A.S., Seifert, K.A., Bruns, T.D., 2010. Quantifying microbial communities with 454 pyrosequencing: does read abundance count? Mol. Ecol. 19, 5555–5565.

Amir, A., McDonald, D., Navas-Molina, J.A., Kopylova, E., Morton, J.T., Zech Xu, Z., Kightley, E.P., Thompson, L.R., Hyde, E.R., Gonzalez, A., Knight, R., 2017. Deblur Rapidly Resolves Single-Nucleotide Community Sequence Patterns. mSystems 2, 10.

Amor, D.R., Montañez, R., Duran-Nebreda, S., Solé, R., 2017. Spatial dynamics of synthetic microbial mutualists and their parasites. PLoS Comput. Biol. 13, e1005689.

Andersen, E.J., Ali, S., Byamukama, E., Yen, Y., Nepal, M.P., 2018. Disease resistance mechanisms in plants. Genes (Basel). 9, 339.

Andolfo, G., Ercolano, M.R., 2015. Plant innate immunity multicomponent model. Front. Plant Sci. 6, 987.

Andrews, J.H., Harris, R.F., 2000. The ecology and biogeography of microorganisms on plant surfaces. Annu. Rev. Phytopathol. 38, 145–180.

Andrews, S., 2010. No Title. FastQC a Qual. Control tool high throughput Seq. data. Babraham Bioinformatics, Babraham Institute. 1.

Anil Kumar, S., Hima Kumari, P., Shravan Kumar, G., Mohanalatha, C., Kavi Kishor, P.B., 2015. Osmotin: a plant sentinel and a possible agonist of mammalian adiponectin. Front. Plant Sci. 6, 163.

Aoki, T., O'Donnell, K., 1999. Morphological and molecular characterization of *Fusarium pseudograminearum* sp. nov., formerly recognized as the Group 1 population of F. graminearum. Mycologia 91, 597–609.

Aquino, J.P.A. de, Macedo Junior, F.B. de, Antunes, J.E.L., Figueiredo, M. do V.B., Alcântara Neto, F. de, Araujo, A.S.F. de, 2019. Plant growth-promoting endophytic bacteria on maize and sorghum1. Pesqui. Agropecuária Trop. 49.

Arenz, B.E., Schlatter, D.C., Bradeen, J.M., Kinkel, L.L., 2015. Blocking primers reduce co-amplification of plant DNA when studying bacterial endophyte communities. J. Microbiol. Methods 117, 1–3.

Arnold, A.E., Maynard, Z., Gilbert, G.S., Coley, P.D., Kursar, T.A., 2000. Are tropical fungal endophytes hyperdiverse? Ecol. Lett. 3, 267–274.

Arrebola, E., Cazorla, F.M., Perez-García, A., Vicente, A. de, 2011. Chemical and metabolic aspects of antimetabolite toxins produced by *Pseudomonas syringae* pathovars. Toxins

(Basel). 3, 1089–1110.

Aslam, S., Tahir, A., Aslam, M.F., Alam, M.W., Shedayi, A.A., Sadia, S., 2017. Recent advances in molecular techniques for the identification of phytopathogenic fungi–a mini review. J. Plant Interact. 12, 493–504.

Assefa, A.T., De Paepe, K., Everaert, C., Mestdagh, P., Thas, O., Vandesompele, J., 2018. Differential gene expression analysis tools exhibit substandard performance for long non-coding RNA-sequencing data. Genome Biol. 19, 96.

Astoreca, A.L., Emateguy, L.G., Alconada, T.M., 2019. Fungal contamination and mycotoxins associated with sorghum crop: its relevance today. Eur. J. Plant Pathol. 1–12.

Audilakshmi, S., Das, I.K., Ghorade, R.B., Mane, P.N., Kamatar, M.Y., Narayana, Y.D., Seetharama, N., 2011. Genetic improvement of sorghum for grain mould resistance: I. Performance of sorghum recombinant inbred lines for grain mould reactions across environments. Crop Prot. 30, 753–758.

Avila-Ospina, L., Marmagne, A., Soulay, F., Masclaux-Daubresse, C., 2016. Identification of barley (*Hordeum vulgare* L.) autophagy genes and their expression levels during leaf senescence, chronic nitrogen limitation and in response to dark exposure. Agronomy 6, 15.

Ayana, A., Bryngelsson, T., Bekele, E., 2000. Genetic variation of Ethiopian and Eritrean sorghum (*Sorghum bicolor* (L.) Moench) germplasm assessed by random amplified polymorphic DNA (RAPD). Genet. Resour. Crop Evol. 47, 471–482.

Bai, L., Sun, H., Zhang, X., Cai, B., 2018. Next-generation sequencing of root fungal communities in continuous cropping soybean. Chil. J. Agric. Res. 78, 528–538.

Bajaj, R., Huang, Y., Gebrechristos, S., Mikolajczyk, B., Brown, H., Prasad, R., Varma, A., Bushley, K.E., 2018. Transcriptional responses of soybean roots to colonization with the root endophytic fungus *Piriformospora indica* reveals altered phenylpropanoid and secondary metabolism. Sci. Rep. 8, 1–18.

Bálint, M., Schmidt, P., Sharma, R., Thines, M., Schmitt, I., 2014. An Illumina metabarcoding pipeline for fungi. Ecol. Evol. 4, 2642–2653.

Balota, M., Herbert, D.A., Rutto, L., 2012. Performance of Sorghum Hybrids in Virginia, 2012.

Bandara, Y., Weerasooriya, D.K., Liu, S., Little, C.R., 2018. The necrotrophic fungus *Macrophomina phaseolina* promotes charcoal rot susceptibility in grain sorghum through

induced host cell-wall-degrading enzymes. Phytopathology 108, 948–956.

Bandara, Y., Weerasooriya, D.K., Tesso, T.T., Prasad, P.V. V, Little, C.R., 2017. Stalk rot fungi affect grain sorghum yield components in an inoculation stage-specific manner. Crop Prot. 94, 97–105.

Bárány, I., Berenguer, E., Solís, M.-T., Pérez-Pérez, Y., Santamaría, M.E., Crespo, J.L., Risueño, M.C., Díaz, I., Testillano, P.S., 2018. Autophagy is activated and involved in cell death with participation of cathepsins during stress-induced microspore embryogenesis in barley. J. Exp. Bot. 69, 1387–1402.

Bari, R., Jones, J.D.G., 2009. Role of plant hormones in plant defence responses. Plant Mol. Biol. 69, 473–488.

Barua, P., You, M.P., Bayliss, K., Lanoiselet, V., Barbetti, M.J., 2017. A rapid and miniaturized system using Alamar blue to assess fungal spore viability: implications for biosecurity. Eur. J. Plant Pathol. 148, 139–150.

Beckers, G.J.M., Spoel, S.H., 2006. Fine-tuning plant defence signalling: salicylate versus jasmonate. Plant Biol. 8, 1–10.

Bennett, A., Ponder, M.M., Garcia-Diaz, J., 2018. Phoma infections: classification, potential food sources, and their clinical impact. Microorganisms 6, 58.

Berendsen, R.L., Vismans, G., Yu, K., Song, Y., de Jonge, R., Burgman, W.P., Burmølle, M., Herschend, J., Bakker, P.A.H.M., Pieterse, C.M.J., 2018. Disease-induced assemblage of a plant-beneficial bacterial consortium. ISME J. 12, 1496.

Berg, G., Köberl, M., Rybakova, D., Müller, H., Grosch, R., Smalla, K., 2017. Plant microbial diversity is suggested as the key to future biocontrol and health trends. FEMS Microbiol. Ecol. 93.

Berg, G., Smalla, K., 2009. Plant species and soil type cooperatively shape the structure and function of microbial communities in the rhizosphere. FEMS Microbiol. Ecol. 68, 1–13.

Berg, G., Zachow, C., Müller, H., Philipps, J., Tilcher, R., 2013. Next-generation bio-products Sow. seeds success Sustain. Agric.1.

Bertuzzi, M., Hayes, G.E., Bignell, E.M., 2019. Microbial uptake by the respiratory epithelium: outcomes for host and pathogen. FEMS Microbiol. Rev. 43, 145–161.

Besler, K.R., Little, E.L., 2017. Diversity of *Serratia marcescens* strains associated with cucurbit yellow vine disease in Georgia. Plant Dis. 101, 129–136.

Besset-Manzoni, Y., Rieusset, L., Joly, P., Comte, G., Prigent-Combaret, C., 2018. Exploiting rhizosphere microbial cooperation for developing sustainable agriculture strategies. Environ. Sci. Pollut. Res. 25, 29953–29970.

Beukes, I., Rose, L.J., Shephard, G.S., Flett, B.C., Viljoen, A., 2017. Mycotoxigenic *Fusarium* species associated with grain crops in South Africa-A review. S. Afr. J. Sci. 113, 1–12.

Bingpeng, X., Heshan, L., Zhilan, Z., Chunguang, W., Yanguo, W., Jianjun, W., 2018. DNA barcoding for identification of fish species in the Taiwan Strait. PLoS One 13.

Bodoči, K.S., Bagi, F.F., Berenji, J.J., Stojšin, V.B., Budakov, D.B., Nađ, L.T., 2013. Level of seed infection of cultivated sorghum with fungi from genus *Fusarium*. Zb. Matice Srp. za Prir. Nauk. 85–90.

Bolger, A.M., Lohse, M., Usadel, B., 2014. Trimmomatic: a flexible trimmer for Illumina sequence data. Bioinformatics 30, 2114–2120.

Bolton, M.D., Thomma, B.P.H.J., Nelson, B.D., 2006. Sclerotinia sclerotiorum (Lib.) de Bary: biology and molecular traits of a cosmopolitan pathogen. Mol. Plant Pathol. 7, 1–16.

Bönnighausen, J., Schauer, N., Schäfer, W., Bormann, J., 2019. Metabolic profiling of wheat rachis node infection by *Fusarium graminearum*–decoding deoxynivalenol-dependent susceptibility. New Phytol. 221, 459–469.

Boon, E., Meehan, C.J., Whidden, C., Wong, D.H.-J., Langille, M.G.I., Beiko, R.G., 2014. Interactions in the microbiome: communities of organisms and communities of genes. FEMS Microbiol. Rev. 38, 90–118.

Boots, M., Best, A., 2018. The evolution of constitutive and induced defences to infectious disease. Proc. R. Soc. B Biol. Sci. 285, 20180658.

Bowers, J.E., Abbey, C., Anderson, S., Chang, C., Draye, X., Lattu, A.H., Jessup, R., Lemke, C., Lennington, J., Li, Z., 2003. A high-density genetic recombination map of sequence-tagged sites for Sorghum for comparative structural and evolutionary genomics of tropical grains and grasses. Int. Sorghum Millets Newsl. 44, 74–75.

Brauer, E.K., Rocheleau, H., Balcerzak, M., Pan, Y., Fauteux, F., Liu, Z., Wang, L., Zheng, W., Ouellet, T., 2019. Transcriptional and hormonal profiling of *Fusarium graminearum*-infected wheat reveals an association between auxin and susceptibility. Physiol. Mol. Plant Pathol. 107, 33–39.

Broman, K.W., 2005. The genomes of recombinant inbred lines. Genetics 169, 1133–1146.

Bruez, E., Vallance, J., Gerbore, J., Lecomte, P., Da Costa, J.-P., Guerin-Dubrana, L., Rey, P., 2014. Analyses of the temporal dynamics of fungal communities colonizing the healthy wood tissues of esca leaf-symptomatic and asymptomatic vines. PLoS One 9.

Buée, M., De Boer, W., Martin, F., Van Overbeek, L., Jurkevitch, E., 2009. The rhizosphere zoo: an overview of plant-associated communities of microorganisms, including phages, bacteria, archaea, and fungi, and of some of their structuring factors. Plant Soil 321, 189–212.

Bukin, Y.S., Galachyants, Y.P., Morozov, I. V, Bukin, S. V, Zakharenko, A.S., Zemskaya, T.I., 2019. The effect of 16S rRNA region choice on bacterial community metabarcoding results. Sci. data 6, 190007.

Bulgarelli, D., Rott, M., Schlaeppi, K., van Themaat, E.V.L., Ahmadinejad, N., Assenza, F., Rauf, P., Huettel, B., Reinhardt, R., Schmelzer, E., 2012. Revealing structure and assembly cues for *Arabidopsis* root-inhabiting bacterial microbiota. Nature 488, 91–95.

Bulgarelli, D., Schlaeppi, K., Spaepen, S., van Themaat, E.V.L., Schulze-Lefert, P., 2013. Structure and functions of the bacterial microbiota of plants. Annu. Rev. Plant Biol. 64, 807–838.

Bulgari, D., Casati, P., Crepaldi, P., Daffonchio, D., Quaglino, F., Brusetti, L., Bianco, P.A., 2011. Restructuring of endophytic bacterial communities in grapevine yellows-diseased and recovered *Vitis vinifera* L. plants. Appl. Environ. Microbiol. 77, 5018–5022.

Bullard, J.H., Purdom, E., Hansen, K.D., Dudoit, S., 2010. Evaluation of statistical methods for normalization and differential expression in mRNA-Seq experiments. BMC Bioinformatics 11, 94.

Burgess, L.W., Summerell, B.A., Giblett, G., Backhouse, D., Blake, M.L., Smith-White, J., Colville, M., 2002. Role of sorghum in overseasoning of Gibberella zeae. Sorghum Millets Dis. 301–303.

Busby, P.E., Soman, C., Wagner, M.R., Friesen, M.L., Kremer, J., Bennett, A., Morsy, M., Eisen, J.A., Leach, J.E., Dangl, J.L., 2017. Research priorities for harnessing plant microbiomes in sustainable agriculture. PLoS Biol. 15.

Callaway, E., 2016. Devastating wheat fungus appears in Asia for first time. Nat. News 532, 421.

Caporaso, J.G., Lauber, C.L., Walters, W. a, Berg-Lyons, D., Huntley, J., Fierer, N., Owens,

S.M., Betley, J., Fraser, L., Bauer, M., Gormley, N., Gilbert, J. A, Smith, G., Knight, R., 2012. Ultra-high-throughput microbial community analysis on the Illumina HiSeq and MiSeq platforms. ISME J. 6, 1621–4.

Caporaso, J.G., Lauber, C.L., Walters, W.A., Berg-Lyons, D., Lozupone, C.A., Turnbaugh, P.J., Fierer, N., Knight, R., 2011. Global patterns of 16S rRNA diversity at a depth of millions of sequences per sample. Proc. Natl. Acad. Sci. U. S. A. 108, 4516–4522.

Caporaso, J.G., Kuczynski, J., Stombaugh, J., Bittinger, K., Bushman, F.D., Costello, E.K., Fierer, N., Pena, A.G., Goodrich, J.K., Gordon, J.I., 2010. QIIME allows analysis of high-throughput community sequencing data. Nat. Methods 7, 335–336.

Cardenas, E., Tiedje, J.M., 2008. New tools for discovering and characterizing microbial diversity. Curr. Opin. Biotechnol. 19, 544–9.

Cernava, T., Chen, X., Krug, L., Li, H., Yang, M., Berg, G., 2019. The tea leaf microbiome shows specific responses to chemical pesticides and biocontrol applications. Sci. Total Environ. 667, 33–40.

Chakraborty, S., Luck, J., Hollaway, G., Freeman, A., Norton, R., Garrett, K.A., Percy, K., Hopkins, A., Davis, C., Karnosky, D.F., 2010. Impacts of global change on diseases of agricultural crops and forest trees. CAB Rev. Perspect. Agric. Vet. Sci. Nutr. Nat. Resour. 3.

Chakravorty, S., Helb, D., Burday, M., Connell, N., Alland, D., 2007. A detailed analysis of 16S ribosomal RNA gene segments for the diagnosis of pathogenic bacteria. J. Microbiol. Methods 69, 330–339.

Chala, A., Degefu, T., Brurberg, M.B., 2019. Phylogenetically Diverse *Fusarium* Species Associated with Sorghum (*Sorghum Bicolor* L. Moench) and Finger Millet (*Eleusine Coracana* L. Garten) Grains from Ethiopia. Diversity 11, 93.

Chang, P., Gerhardt, K.E., Huang, X.-D., Yu, X.-M., Glick, B.R., Gerwing, P.D., Greenberg, B.M., 2014. Plant growth-promoting bacteria facilitate the growth of barley and oats in salt-impacted soil: implications for phytoremediation of saline soils. Int. J. Phytoremediation 16, 1133–1147.

Chebotar, V.K., Malfanova, N. V, Shcherbakov, A. V, Ahtemova, G.A., Borisov, A.Y., Lugtenberg, B., Tikhonovich, I.A., 2015. Endophytic bacteria in microbial preparations that improve plant development. Appl. Biochem. Microbiol. 51, 271–277.

Chisi, M., 2010. Sorghum Breeding Programme. Zambia Agricultural Research Institute.1.

Chittenden, L.M., Schertz, K.F., Lin, Y.R., Wing, R.A., Paterson, A.H., 1994. A detailed RFLP map of *Sorghum bicolor* x *S. propinquum*, suitable for high-density mapping, suggests ancestral duplication of Sorghum chromosomes or chromosomal segments. Theor. Appl. Genet. 87, 925–933.

Choi, H., Hong, S., Lee, Y., Kim, W., 2013. Diversity and pathogenicity of *Fusarium* species associated with grain mold of sorghum. Korean J. Mycol. 41, 142–148.

Choueiri, E., Jreijiri, F., Chlela, P., Mayet, V., Comont, G., Liminana, J.-M., Mostert, L., Fischer, M., Lecomte, P., 2014. Fungal community associated with grapevine wood lesions in Lebanon. OENO One 48, 293–302.

Clayton, W.D., 1961. (79) Proposal to Conserve the Generic Name Sorghum Moench (Gramineae) versus *Sorgum Adans*.(Gramineae). Taxon 10, 242–243.

Coissac, E., Hollingsworth, P.M., Lavergne, S., Taberlet, P., 2016. From barcodes to genomes: extending the concept of DNA barcoding. Mol. Ecol. 25, 1423–1428.

Čolović, R., Puvača, N., Cheli, F., Avantaggiato, G., Greco, D., Đuragić, O., Kos, J., Pinotti, L., 2019. Decontamination of Mycotoxin-Contaminated Feedstuffs and Compound Feed. Toxins (Basel). 11, 617.

Compant, S., Mitter, B., Colli-Mull, J.G., Gangl, H., Sessitsch, A., 2011. Endophytes of grapevine flowers, berries, and seeds: identification of cultivable bacteria, comparison with other plant parts, and visualization of niches of colonization. Microb. Ecol. 62, 188–97.

Conesa, A., Madrigal, P., Tarazona, S., Gomez-Cabrero, D., Cervera, A., McPherson, A., Szcześniak, M.W., Gaffney, D.J., Elo, L.L., Zhang, X., 2016. A survey of best practices for RNA-seq data analysis. Genome Biol. 17, 13.

Copeland, J.K., Yuan, L., Layeghifard, M., Wang, P.W., Guttman, D.S., 2015. Seasonal community succession of the phyllosphere microbiome. Mol. Plant-Microbe Interact. 28, 274–285.

Corrêa, B.O., Schafer, J.T., Moura, A.B., 2014. Spectrum of biocontrol bacteria to control leaf, root and vascular diseases of dry bean. Biol. Control 72, 71–75.

Cota, L. V, Costa, R. V, Silva, D.D., Parreira, D.F., Lana, U.G.P., Casela, C.R., 2010. First report of pathogenicity of P*antoea ananatis* in sorghum (Sorghum bicolor) in Brazil.

Australas. Plant Dis. Notes 5, 120–122.

Cuadros-Orellana, S., Leite, L.R., Smith, A., Medeiros, J.D., Badotti, F., Fonseca, P.L.C., Vaz, A.B.M., Oliveira, G., Góes-Neto, A., 2013. Assessment of fungal diversity in the environment using metagenomics: a decade in review. Fungal Genomics Biol. 3, 1.

Cuevas, H.E., Fermin-Pérez, R.A., Prom, L.K., Cooper, E.A., Bean, S., Rooney, W.L., 2019. Genome-Wide Association Mapping of Grain Mold Resistance in the US Sorghum Association Panel. Plant Genome 12.

Cui, J., Chen, B., Wang, H., Han, Y., Chen, X., Zhang, W., 2016. Glucosidase II β-subunit, a novel substrate for caspase-3-like activity in rice, plays as a molecular switch between autophagy and programmed cell death. Sci. Rep. 6, 31764.

[DAFF] Department of Agriculture, Forestry and Fisheries. 2018. Trends in Agricultural Sector 2017. DAFF report. 16. [cited 2018 February 13]. Available from: https://www.daff.gov.za/Daffweb3/Portals/0/Statistics and Economic Analysis/Statistical Information/Trends in the Agricultural Sector 2017.pdf

D'Argenio, V., Casaburi, G., Precone, V., Salvatore, F., 2014. Comparative metagenomic analysis of human gut microbiome composition using two different bioinformatic pipelines. Biomed Res. Int. 2014, 325340.

Dahlberg, J.A., Zhang, X., Hart, G.E., Mullet, J.E., 2002. Comparative assessment of variation among sorghum germplasm accessions using seed morphology and RAPD measurements. Crop Sci. 42, 291–296.

Dar, Z.A., Rifat, B., Bhat, J.I.A., Bhatti, A.A., Haq, S., Amin, A., Dar, S.A., 2019. Potential Role of Endophytes for Sustainable Environment, in: Climate Change and Its Impact on Ecosystem Services and Biodiversity in Arid and Semi-Arid Zones. IGI Global, pp. 78–95.

Das, I.K., 2019. Advances in Sorghum Disease Resistance, in: Breeding Sorghum for Diverse End Uses. Elsevier, pp. 313–324.

Das, I.K., Padmaja, P.G., 2016. Biotic stress resistance in millets. Academic Press, 1.

Das, S., Deb, B., 2015. DNA barcoding of fungi using Ribosomal ITS Marker for genetic diversity analysis: a review. Int.J.Pure Appl.Biosci 3, 160–167.

Das, I.K., Audilakshmi, S., Patil, J. V, 2012. Fusarium grain mold: the major component of grain mold disease complex in sorghum (*Sorghum bicolor* L. Moench). Eur.J.Plant

Sci.Biotech 6, 45–55.

Dash, N., Dangar, T.K., 2017. Perspectives of Phosphate Solubilizing Microbes for Plant Growth Promotion, Especially Rice-A Review. Int. J. Biochem. Res. Rev. 1–16.

De Beeck, M.O., Lievens, B., Busschaert, P., Declerck, S., Vangronsveld, J., Colpaert, J. V, 2014. Comparison and validation of some ITS primer pairs useful for fungal metabarcoding studies. PLoS One 9, 97629.

de la Cuesta-Zuluaga, J., Escobar, J.S., 2016. Considerations for optimizing microbiome analysis using a marker gene. Front. Nutr. 3, 26.

del Carmen Orozco-Mosqueda, M., Glick, B.R., Santoyo, G., 2020. ACC deaminase in plant growth-promoting bacteria (PGPB): an efficient mechanism to counter salt stress in crops. Microbiol. Res. 126439.

de Oliveira, R.C., Carnielli-Queiroz, L., Correa, B., 2018. *Epicoccum sorghinum* in food: occurrence, genetic aspects and tenuazonic acid production. Curr. Opin. Food Sci. 23, 44–48.

Dees, M.W., Lysoe, E., Nordskog, B., Brurberg, M.B., 2015. Bacterial communities associated with surfaces of leafy greens: shift in composition and decrease in richness over time. Appl. Environ. Microbiol. 81, 1530–1539.

Del Frari, G., Cabral, A., Nascimento, T., Boavida Ferreira, R., Oliveira, H., 2019. *Epicoccum layuense* a potential biological control agent of esca-associated fungi in grapevine. PLoS One 14.

DeLeon-Rodriguez, N., Lathem, T.L., Rodriguez-R, L.M., Barazesh, J.M., Anderson, B.E., Beyersdorf, A.J., Ziemba, L.D., Bergin, M., Nenes, A., Konstantinidis, K.T., 2013. Microbiome of the upper troposphere: species composition and prevalence, effects of tropical storms, and atmospheric implications. Proc. Natl. Acad. Sci. U. S. A. 110, 2575–2580.

Denancé, N., Szurek, B., Noël, L.D., 2014. Emerging functions of nodulin-like proteins in non-nodulating plant species. Plant Cell Physiol. 55, 469–474.

DeSantis, T.Z., Brodie, E.L., Moberg, J.P., Zubieta, I.X., Piceno, Y.M., Andersen, G.L., 2007. High-density universal 16S rRNA microarray analysis reveals broader diversity than typical clone library when sampling the environment. Microb. Ecol. 53, 371–383.

Deveau, A., Bonito, G., Uehling, J., Paoletti, M., Becker, M., Bindschedler, S., Hacquard, S.,

Hervé, V., Labbé, J., Lastovetsky, O.A., 2018. Bacterial–fungal interactions: ecology, mechanisms and challenges. FEMS Microbiol. Rev. 42, 335–352.

Deyett, E., Pouzoulet, J., Yang, J., Ashworth, V.E., Castro, C., Roper, M.C., Rolshausen, P.E., 2019. Assessment of Pierce's disease susceptibility in Vitis vinifera cultivars with different pedigrees. Plant Pathol. 68, 1079–1087.

Deyett, E., Rolshausen, P.E., 2019. Temporal dynamics of the sap microbiome of grapevine under high Pierce's disease pressure. Front. Plant Sci. 10.

Di Berardino, J., Marmagne, A., Berger, A., Yoshimoto, K., Cueff, G., Chardon, F., Masclaux-Daubresse, C., Reisdorf-Cren, M., 2018. Autophagy controls resource allocation and protein storage accumulation in *Arabidopsis* seeds. J. Exp. Bot. 69, 1403–1414.

Ding, L., Xu, H., Yi, H., Yang, L., Kong, Z., Zhang, L., Xue, S., Jia, H., Ma, Z., 2011. Resistance to hemi-biotrophic *F. graminearum* infection is associated with coordinated and ordered expression of diverse defense signaling pathways. PLoS One 6.

Ditta, Y.A., Mahad, S., Bacha, U., 2018. Aflatoxins: Their Toxic Effect on Poultry and Recent Advances in Their Treatment, in: Mycotoxins-Impact and Management Strategies. IntechOpen.

Dixon, R.A., Achnine, L., Kota, P., Liu, C., Reddy, M.S.S., Wang, L., 2002. The phenylpropanoid pathway and plant defence—a genomics perspective. Mol. Plant Pathol. 3, 371–390.

Djè, Y., Forcioli, D., Ater, M., Lefèbvre, C., Vekemans, X., 1999. Assessing population genetic structure of sorghum landraces from North-western Morocco using allozyme and microsatellite markers. Theor. Appl. Genet. 99, 157–163.

Dobrovol'skaya, T.G., Golovchenko, A. V, Yakushev, A. V, Yurchenko, E.N., Manucharov, N.A., Chernov, I.Y., 2017. Bacterial complexes of a high moor related to different elements of microrelief. Eurasian Soil Sci. 50, 470–475.

do Nascimento, M.A., do Nascimento, C.V., Antunes, J.E., do Vale Figueiredo, M., Tabosa, J.N., Martínez, C.R., 2014. Selection of plant growth-promoting bacteria in sweet sorghum (*Sorghum bicolor* (L.) Moench) under the effects of salinity, in: BMC Proceedings. BioMed Central, 1.

Doehlemann, G., Hemetsberger, C., 2013. Apoplastic immunity and its suppression by filamentous plant pathogens. New Phytol. 198, 1001–1016.

dos Santos, C.L.R., Alves, G.C., de Matos Macedo, A.V., Giori, F.G., Pereira, W., Urquiaga, S., Reis, V.M., 2017. Contribution of a mixed inoculant containing strains of *Burkholderia* spp. and *Herbaspirillum* ssp. to the growth of three sorghum genotypes under increased nitrogen fertilization levels. Appl. soil Ecol. 113, 96–106.

Dulermo, T., Bligny, R., Gout, E., Cotton, P., 2009. Amino acid changes during sunflower infection by the necrotrophic fungus *B. cinerea*. Plant Signal. Behav. 4, 859–861.

Edwards, A., Debbonaire, A.R., Nicholls, S.M., Rassner, S.M.E., Sattler, B., Cook, J.M., Davy, T., Soares, A., Mur, L.A.J., Hodson, A.J., 2019. In-field metagenome and 16S rRNA gene amplicon nanopore sequencing robustly characterize glacier microbiota. BioRxiv 73965.

Edwards, J., Johnson, C., Santos-Medellin, C., Lurie, E., Podishetty, N.K., Bhatnagar, S., Eisen, J.A., Sundaresan, V., 2015. Structure, variation, and assembly of the root-associated microbiomes of rice. Proc. Natl. Acad. Sci. U. S. A. 112, 911-20.

Eisen, M.B., Spellman, P.T., Brown, P.O., Botstein, D., 1998. Cluster analysis and display of genome-wide expression patterns. Proc. Natl. Acad. Sci. U. S. A. 95, 14863–14868.

El-Tarabily, K.A., Al Khajeh, A.S., Ayyash, M.M., Alnuaimi, L.H., Sham, A., ElBaghdady, K.S., Tariq, S., AbuQamar, S.F., 2019. Growth promotion of *Salicornia bigelovii* by *Micromonospora chalcea* UAE1, an endophytic 1-aminocyclopropane-1-carboxylic acid deaminase-producing actinobacterial isolate. Front. Microbiol. 10, 1694.

[FAO] Food and Agriculture Organization of the United Nations. 1998. The State of the World's Plant Genetic Resources for Food and Agriculture - Part 2. [cited 2017 April 15. Environmental monitoring and assessment(Vol. 7). http://www.fao.org/3/i1500e/i1500e00.pdf.

[FAOSTAT] FAO Statistical Database. 2018. FAOSTAT database (online). Food and Agriculture Organization of the United Nations. Rome. [cited 2018 Mar 24]. http://www.fao.org/faostat/en/#data/QC.

Esitken, A., Yildiz, H.E., Ercisli, S., Donmez, M.F., Turan, M., Gunes, A., 2010. Effects of plant growth promoting bacteria (PGPB) on yield, growth and nutrient contents of organically grown strawberry. Sci. Hortic. (Amsterdam). 124, 62–66.

Fabregat, A., Jupe, S., Matthews, L., Sidiropoulos, K., Gillespie, M., Garapati, P., Haw, R., Jassal, B., Korninger, F., May, B., 2018. The reactome pathway knowledgebase. Nucleic Acids Res. 46, 649–655.

Fajarningsih, N.D., 2016. Internal Transcribed Spacer (ITS) as DNA barcoding to identify fungal species: a review. Squalen Bull. Mar. Fish. Postharvest Biotechnol. 11, 37–44.

Fall, L.A., Salazar, M.M., Drnevich, J., Holmes, J.R., Tseng, M.-C., Kolb, F.L., Mideros, S.X., 2019. Field pathogenomics of Fusarium head blight reveals pathogen transcriptome differences due to host resistance. Mycologia 111, 563–573.

Fan, H., Li, K., Yao, F., Sun, L., Liu, Y., 2019. Comparative transcriptome analyses on terpenoids metabolism in field-and mountain-cultivated ginseng roots. BMC Plant Biol. 19, 82.

Fan, Q., Creamer, R., Li, Y., 2018. Time-course metabolic profiling in alfalfa leaves under *Phoma medicaginis* infection. PLoS One 13.

Fang, L.-J., Qin, R.-L., Liu, Z., Liu, C.-R., Gai, Y.-P., Ji, X.-L., 2019. Expression and functional analysis of a PR-1 Gene, MuPR1, involved in disease resistance response in mulberry (Morus multicaulis). J. Plant Interact. 14, 376–385.

Farrar, K., Bryant, D., Cope-Selby, N., 2014. Understanding and engineering beneficial plant–microbe interactions: plant growth promotion in energy crops. Plant Biotechnol. J. 12, 1193–1206.

Fatima, U., Senthil-Kumar, M., 2015. Plant and pathogen nutrient acquisition strategies. Front. Plant Sci. 6, 750.

Feau, N., Vialle, A., Allaire, M., Tanguay, P., Joly, D.L., Frey, P., Callan, B.E., Hamelin, R.C., 2009. Fungal pathogen (mis-) identifications: a case study with DNA barcodes on Melampsora rusts of aspen and white poplar. Mycol. Res. 113, 713–724.

Feltus, F.A., 2006. Genetic map alignment and QTL correspondence between inter-and intra-specific sorghum populations. Theor.Appl.Genet. 112, 1295–1305.

Fernández-González, A.J., Villadas, P.J., Cabanás, C.G.-L., Valverde-Corredor, A., Belaj, A., Mercado-Blanco, J., Fernández-López, M., 2019. Defining the root endosphere and rhizosphere microbiomes from the World Olive Germplasm Collection. bioRxiv 636530.

Finkel, O.M., Salas-González, I., Castrillo, G., Spaepen, S., Law, T.F., Teixeira, P.J.P.L., Jones, C.D., Dangl, J.L., 2019. The effects of soil phosphorus content on plant microbiota are driven by the plant phosphate starvation response. PLoS Biol. 17.

Finotello, F., Di Camillo, B., 2015. Measuring differential gene expression with RNA-seq: challenges and strategies for data analysis. Brief. Funct. Genomics 14, 130–142.

Fitt, B.D.L., Brun, H., Barbetti, M.J., Rimmer, S.R., 2006. World-wide importance of phoma stem canker (*Leptosphaeria maculans* and *L. biglobosa*) on oilseed rape (*Brassica napus*), in: Sustainable Strategies for Managing Brassica Napus (Oilseed Rape) Resistance to *Leptosphaeria Maculans* (*Phoma* Stem Canker). Springer, pp. 3–15.

Fitzpatrick, C.R., Lu-Irving, P., Copeland, J., Guttman, D.S., Wang, P.W., Baltrus, D.A., Dlugosch, K.M., Johnson, M.T.J., 2018. Chloroplast sequence variation and the efficacy of peptide nucleic acids for blocking host amplification in plant microbiome studies. Microbiome 6, 144.

Foroud, N.A., Baines, D., Gagkaeva, T.Y., Thakor, N., Badea, A., Steiner, B., Bürstmayr, M., Bürstmayr, H., 2019. Trichothecenes in Cereal Grains–An Update. Toxins (Basel). 11, 634.

Francis, R.G., Burgess, L.W., 1977. Characteristics of two populations of *Fusarium roseum* "Graminearum"in eastern Australia. Trans. Br. Mycol. Soc. 68, 421–427.

Frank, A.C., Saldierna Guzmán, J.P., Shay, J.E., 2017. Transmission of bacterial endophytes. Microorganisms 5, 70.

Franke-Whittle, I.H., Manici, L.M., Insam, H., Stres, B., 2015. Rhizosphere bacteria and fungi associated with plant growth in soils of three replanted apple orchards. Plant Soil 1–17.

Frederiksen, R.A., Odvody, G.N., 2000. Compendium of sorghum diseases. American Phytopathological Society (APS Press) 1.

Frenkel, O., Portillo, I., Brewer, M.T., Péros, J.P., Cadle-Davidson, L., Milgroom, M.G., 2012. Development of microsatellite markers from the transcriptome of *Erysiphe necator* for analysing population structure in North America and Europe. Plant Pathol. 61, 106–119.

Funnell-Harris, D.L., Scully, E.D., Sattler, S.E., French, R.C., O'Neill, P.M., Pedersen, J.F., 2017. Differences in *Fusarium* species in brown midrib sorghum and in air populations in production fields. Phytopathology 107, 1353–1363.

Funnell-Harris, D.L., Prom, L.K., Sattler, S.E., Pedersen, J.F., 2013. Response of near-isogenic sorghum lines, differing at the P locus for plant colour, to grain mould and head smut fungi. Ann. Appl. Biol. 163, 91–101.

Gao, Y., Xu, G., 2014. Development of an effective nonchemical method against *Plasmodiophora brassicae* on Chinese cabbage. Int. J. Agron. 2014.

Gardes, M., Bruns, T.D., 1993. ITS primers with enhanced specificity for basidiomycetes-

application to the identification of mycorrhizae and rusts. Mol. Ecol. 2, 113–118.

Geng, X., Jin, L., Shimada, M., Kim, M.G., Mackey, D., 2014. The phytotoxin coronatine is a multifunctional component of the virulence armament of *Pseudomonas syringae*. Planta 240, 1149–1165.

Gentleman, R.C., Carey, V.J., Bates, D.M., Bolstad, B., Dettling, M., Dudoit, S., Ellis, B., Gautier, L., Ge, Y., Gentry, J., 2004. Bioconductor: open software development for computational biology and bioinformatics. Genome Biol. 5, 80.

Gerhardson, B., 2002. Biological substitutes for pesticides. Trends Biotechnol. 20, 338–343.

Gerland, P., Raftery, A.E., Sevcikova, H., Li, N., Gu, D., Spoorenberg, T., Alkema, L., Fosdick, B.K., Chunn, J., Lalic, N., Bay, G., Buettner, T., Heilig, G.K., Wilmoth, J., 2014. World population stabilization unlikely this century. Science 346, 234–237.

Giberti, S., Bertea, C.M., Narayana, R., Maffei, M.E., Forlani, G., 2012. Two phenylalanine ammonia lyase isoforms are involved in the elicitor-induced response of rice to the fungal pathogen Magnaporthe oryzae. J. Plant Physiol. 169, 249–254.

Gilbert, J., Fernando, W.G.D., 2004. Epidemiology and biological control of *Gibberella zeae*/*Fusarium graminearum.* Can. J. Plant Pathol. 26, 464–472.

Gkarmiri, K., Finlay, R.D., Alström, S., Thomas, E., Cubeta, M.A., Högberg, N., 2015. Transcriptomic changes in the plant pathogenic fungus *Rhizoctonia solani* AG-3 in response to the antagonistic bacteria *Serratia proteamaculans* and *Serratia plymuthica*. BMC Genomics 16, 630.

Gleadow, R.M., Ottman, M.J., Kimball, B.A., Wall, G.W., Pinter, P.J., LaMorte, R.L., Leavitt, S.W., 2016. Drought-induced changes in nitrogen partitioning between cyanide and nitrate in leaves and stems of sorghum grown at elevated CO 2 are age dependent. F. Crop. Res. 185, 97–102.

Glick, B.R., 2005. Modulation of plant ethylene levels by the bacterial enzyme ACC deaminase. FEMS Microbiol. Lett. 251, 1–7.

Glick, B.R., 2014. Bacteria with ACC deaminase can promote plant growth and help to feed the world. Microbiol. Res. 169, 30–39.

Glushakova, A.M., Chernov, I.Y., 2004. Seasonal dynamics in a yeast population on leaves of the common wood sorrel *Oxalis acetosella* L. Microbiology 73, 184–188.

Goff, L.A., Trapnell, C., Kelley, D., 2012. CummeRbund: visualization and exploration of

Cufflinks high-throughput sequencing data. R Packag. version 2.

Golonka, R., Yeoh, B.S., Vijay-Kumar, M., 2019. The Iron Tug-of-War between Bacterial Siderophores and Innate Immunity. J. Innate Immun. 11, 249–262.

Gómez-Lama Cabanás, C., Legarda, G., Ruano-Rosa, D., Pizarro-Tobías, P., Valverde-Corredor, A., Niqui, J.L., Triviño, J.C., Roca, A., Mercado-Blanco, J., 2018. Indigenous *Pseudomonas* spp. strains from the olive (Olea europaea L.) rhizosphere as effective biocontrol agents against Verticillium dahliae: from the host roots to the bacterial genomes. Front. Microbiol. 9, 277.

González, M., Brito, N., González, C., 2017. The *Botrytis cinerea* elicitor protein BcIEB1 interacts with the tobacco PR5-family protein osmotin and protects the fungus against its antifungal activity. New Phytol. 215, 397–410.

Gopalakrishnan, S., Sathya, A., Vijayabharathi, R., Varshney, R.K., Gowda, C.L.L., Krishnamurthy, L., 2015. Plant growth promoting rhizobia: challenges and opportunities. 3 Biotech 5, 355–377.

Gordon, M.S., Olson, E.C., 2013. Invasions of the land: the transitions of organisms from aquatic to terrestrial life. Columbia University Press, 1.

Gosal, S.S., Wani, S.H., 2018. Biotechnologies of Crop Improvement, Volume 3.

Goswami, R.S., Kistler, H.C., 2004. Heading for disaster: *Fusarium graminearum* on cereal crops. Mol. Plant Pathol. 5, 515–525.

Gottwald, S., Samans, B., Lück, S., Friedt, W., 2012. Jasmonate and ethylene dependent defence gene expression and suppression of fungal virulence factors: two essential mechanisms of Fusarium head blight resistance in wheat? BMC Genomics 13, 369.

Govender, N.T., Mahmood, M., Seman, I.A., Wong, M.-Y., 2017. The phenylpropanoid pathway and lignin in defense against *Ganoderma boninense* colonized root tissues in oil palm (*Elaeis guineensis* Jacq.). Front. Plant Sci. 8, 1395.

Grain SA (2017), Gibberella on maize, sorghum and wheat [cited 2017 February 13]., https://www.grainsa.co.za/gibberella-on-maize,-sorghum-and-wheat.pdf

Grant, M., Lamb, C., 2006. Systemic immunity. Curr. Opin. Plant Biol. 9, 414–420.

Green, P.N., Ardley, J.K., 2018. Review of the genus *Methylobacterium* and closely related organisms: a proposal that some *Methylobacterium* species be reclassified into a new genus, *Methylorubrum* gen. nov. Int. J. Syst. Evol. Microbiol. 68, 2727–2748.

Grossi, C.E.M., Fantino, E., Serral, F., Zawoznik, M.S., Fernandez Do Porto, D.A., Ulloa, R.M., 2020. *Methylobacterium* sp. 2A is a plant growth-promoting rhizobacteria that has the potential to improve potato crop yield under adverse conditions. Front. Plant Sci. 11, 71.

Group, N.I.H.H.M.P.W., Peterson, J., Garges, S., Giovanni, M., McInnes, P., Wang, L., Schloss, J.A., Bonazzi, V., McEwen, J.E., Wetterstrand, K.A., Deal, C., Baker, C.C., Di Francesco, V., Howcroft, T.K., Karp, R.W., Lunsford, R.D., Wellington, C.R., Belachew, T., Wright, M., Giblin, C., David, H., Mills, M., Salomon, R., Mullins, C., Akolkar, B., Begg, L., Davis, C., Grandison, L., Humble, M., Khalsa, J., Little, A.R., Peavy, H., Pontzer, C., Portnoy, M., Sayre, M.H., Starke-Reed, P., Zakhari, S., Read, J., Watson, B., Guyer, M., 2009. The NIH Human Microbiome Project. Genome Res. 19, 2317–2323.

Gu, L., Bai, Z., Jin, B., Hu, Q., Wang, H., Zhuang, G., Zhang, H., 2010a. Assessing the impact of fungicide enostroburin application on bacterial community in wheat phyllosphere. J. Environ. Sci. 22, 134–141.

Gu, L., Bai, Z., Jin, B., Hu, Q., Wang, H., Zhuang, G., Zhang, H., 2010b. je sc sc 22, 134–141.

Guazzaroni, M.-E., Platero, R.A., Silva-Rocha, R., 2018. Genomic and Postgenomic

Gubb, E., Matthiesen, R., 2010. Introduction to omics, in: Bioinformatics Methods in Clinical Research. Springer, pp. 1–23.

Guerra-Guimarães, L., Pinheiro, C., Chaves, I., Barros, D., Ricardo, C., 2016. Protein dynamics in the plant extracellular space. Proteomes 4, 22.

Guetskyl, R., Shtienberg, D., Dinoor, A., Elad, Y., 2002. Establishment, survival and activity of the biocontrol agents *Pichia guilermondii* and *Bacillus mycoides* applied as a mixture on strawberry plants. Biocontrol Sci. Technol. 12, 705–714.

Güldener, U., Seong, K.-Y., Boddu, J., Cho, S., Trail, F., Xu, J.-R., Adam, G., Mewes, H.-W., Muehlbauer, G.J., Kistler, H.C., 2006. Development of a *Fusarium graminearum* Affymetrix GeneChip for profiling fungal gene expression in vitro and in planta. Fungal Genet. Biol. 43, 316–325.

Gullner, G., Komives, T., Király, L., Schröder, P., 2018. Glutathione S-transferase enzymes in plant-pathogen interactions. Front. Plant Sci. 9.

Guo, J., 2016. Rhizosphere metagenomics of three biofuel crops. Michigan State University.

Guo, J., 2016. Rhizosphere metagenomics of three biofuel crops. Michigan State University.

Hadebe, S.T., Modi, A.T., Mabhaudhi, T., 2017. Drought tolerance and water use of cereal crops: A focus on sorghum as a food security crop in sub-Saharan Africa. J. Agron. Crop Sci. 203, 177–191.

Hall, N., 2007. Advanced sequencing technologies and their wider impact in microbiology. J. Exp. Biol. 210, 1518–1525.

Halleen, F., Crous, R.W., Petrin, O., 2003. Fungi associated with healthy grapevine cuttings in nurseries, with special reference to pathogens involved in the decline of young vines. Australas. Plant Pathol. 32, 47–52.

Hamady, M., Walker, J.J., Harris, J.K., Gold, N.J., Knight, R., 2008. Error-correcting barcoded primers for pyrosequencing hundreds of samples in multiplex. Nat. Methods 5, 235–237.

Hamonts, K., Trivedi, P., Garg, A., Janitz, C., Grinyer, J., Holford, P., Botha, F.C., Anderson, I.C., Singh, B.K., 2018. Field study reveals core plant microbiota and relative importance of their drivers. Environ. Microbiol. 20, 124–140.

Handelsman, J., Rondon, M.R., Brady, S.F., Clardy, J., Goodman, R.M., 1998. Molecular biological access to the chemistry of unknown soil microbes: a new frontier for natural products. Chem. Biol. 5, 245–249.

Hanudin, H., Budiarto, K., Marwoto, B., 2017. Application of PGPR and antagonist fungi-based biofungicide for white rust disease control and its economyc analysis in chrysanthemum production. AGRIVITA, J. Agric. Sci. 39, 266–278.

Hao, G., Naumann, T.A., Vaughan, M.M., McCormick, S., Usgaard, T., Kelly, A., Ward, T.J., 2019. Characterization of a *Fusarium graminearum* salicylate hydroxylase. Front. Microbiol. 9, 3219.

Hara, S., Morikawa, T., Wasai, S., Kasahara, Y., Koshiba, T., Yamazaki, K., Fujiwara, T., Tokunaga, T., Minamisawa, K., 2019. Identification of nitrogen-fixing Bradyrhizobium associated with roots of field-grown sorghum by metagenome and proteome analyses. Front. Microbiol. 10, 407.

Harlan, J.R., 1975. Our vanishing genetic resources. Science 80, 1.

Harman-Ware, A.E., Happs, R.M., Davison, B.H., Davis, M.F., 2017. The effect of coumaryl alcohol incorporation on the structure and composition of lignin dehydrogenation polymers. Biotechnol. Biofuels 10, 281.

Harris, L.J., Balcerzak, M., Johnston, A., Schneiderman, D., Ouellet, T., 2016. Host-

preferential *Fusarium graminearum* gene expression during infection of wheat, barley, and maize. Fungal Biol. 120, 111–123.

Hassani, M.A., Durán, P., Hacquard, S., 2018. Microbial interactions within the plant holobiont. Microbiome 6, 58.

Haussmann, B.I.G., Hess, D.E., Welz, H.-G., Geiger, H.H., 2000. Improved methodologies for breeding Striga-resistant sorghums. F. Crop. Res. 66, 195–211.

Hayat, W., Aman, H., Irshad, U., Azeem, M., Iqbal, A., Nazir, R., 2017. Analysis of ecological attributes of bacterial phosphorus solubilizers, native to pine forests of Lower Himalaya. Appl. Soil Ecol. 112, 51–59.

Hebert, P.D.N., Cywinska, A., Ball, S.L., Dewaard, J.R., 2003. Biological identifications through DNA barcodes. Proc. R. Soc. London.Series B Biol. Sci. 270, 313–321.

Herlemann, D.P.R., Labrenz, M., Jürgens, K., Bertilsson, S., Waniek, J.J., Andersson, A.F., 2011. Transitions in bacterial communities along the 2000 km salinity gradient of the Baltic Sea. ISME J. 5, 1571.

Heruth, D.P., Xiong, M., Jiang, X., 2016. Microbiome-seq data analysis. Big Data Anal. Bioinforma. Biomed. Discov. 97.

Hofstad, A.N., Nussbaumer, T., Akhunov, E., Shin, S., Kugler, K.G., Kistler, H.C., Mayer, K.F.X., Muehlbauer, G.J., 2016. Examining the transcriptional response in wheat Fhb1 near-isogenic lines to *Fusarium graminearum* infection and deoxynivalenol treatment. Plant Genome 9.

Hofstetter, V., Buyck, B., Croll, D., Viret, O., Couloux, A., Gindro, K., 2012. What if esca disease of grapevine were not a fungal disease? Fungal Divers. 54, 51–67.

Hong, C., Si, Y., Xing, Y., Li, Y., 2015. Illumina MiSeq sequencing investigation on the contrasting soil bacterial community structures in different iron mining areas. Environ. Sci. Pollut. Res. 22, 10788–10799.

Howe, E.A., Sinha, R., Schlauch, D., Quackenbush, J., 2011. RNA-Seq analysis in MeV. Bioinformatics 27, 3209–3210.

Hrdlickova, R., Toloue, M., Tian, B., 2017. RNA-Seq methods for transcriptome analysis. Wiley Interdiscip. Rev. RNA 8, 1364.

Hu, J., Guo, C., Wang, B., Ye, J., Liu, M., Wu, Z., Xiao, Y., Zhang, Q., Li, H., King, G.J., 2018. Genetic properties of a nested association mapping population constructed with

semi-winter and spring oilseed rapes. Front. Plant Sci. 9, 1740.

Hugerth, L.W., Andersson, A.F., 2017. Analysing microbial community composition through amplicon sequencing: from sampling to hypothesis testing. Front. Microbiol. 8, 1561.

Hundekar, R., Kamatar, M.Y., Brunda, S.M., Pattar, V., 2016. Heterosis for yield and grain mold resistance in rainy season Sorghum [*Sorghum bicolor* (L.) Moench]. Environ. Ecol. 34, 1570–1576.

Hwang, E.E., Wang, M.B., Bravo, J.E., Banta, L.M., 2015. Unmasking host and microbial strategies in the *Agrobacterium*-plant defense tango. Front. Plant Sci. 6, 200.

Inácio, J., Pereira, P., Carvalho, de M., Fonseca, A., Amaral-Collaco, M.T., Spencer-Martins, I., 2002. Estimation and diversity of phylloplane mycobiota on selected plants in a Mediterranean-type ecosystem in Portugal. Microb. Ecol. 44, 344–353.

Ismail, A., Gonçalves, B.L., de Neeff, D. V, Ponzilacqua, B., Coppa, C.F.S.C., Hintzsche, H., Sajid, M., Cruz, A.G., Corassin, C.H., Oliveira, C.A.F., 2018. Aflatoxin in foodstuffs: Occurrence and recent advances in decontamination. Food Res. Int. 113, 74–85.

Jayashree, M., Wesely, E.G., 2018. Studies on fungi associated with stored grains of sorghum.

Jones, P., Garcia, B.J., Furches, A., Tuskan, G.A., Jacobson, D., 2019. Plant host-associated mechanisms for microbial selection. Front. Plant Sci. 10.

Josefsen, L., Droce, A., Sondergaard, T.E., Sørensen, J.L., Bormann, J., Schäfer, W., Giese, H., Olsson, S., 2012. Autophagy provides nutrients for nonassimilating fungal structures and is necessary for plant colonization but not for infection in the necrotrophic plant pathogen *Fusarium graminearum.* Autophagy 8, 326–337.

Jumpponen, A.R.I., Jones, K.L., David Mattox, J., Yaege, C., 2010. Massively parallel 454-sequencing of fungal communities in *Quercus* spp. ectomycorrhizas indicates seasonal dynamics in urban and rural sites. Mol. Ecol. 19, 41–53.

Kaewwichian, R., Jindamorakot, S., Am-In, S., Sipiczki, M., Limtong, S., 2015. Hannaella siamensis sp. nov. and *Hannaella phetchabunensi*s sp. nov., two new anamorphic basidiomycetous yeast species isolated from plants. Int. J. Syst. Evol. Microbiol. 65, 1297–1303.

Kanehisa, M., Goto, S., Kawashima, S., Okuno, Y., Hattori, M., 2004. The KEGG resource for deciphering the genome. Nucleic Acids Res. 32, 277–280.

Kang, J.B., Siranosian, B.A., Moss, E.L., Banaei, N., Andermann, T.M., Bhatt, A.S., 2019.

Intestinal microbiota domination under extreme selective pressures characterized by metagenomic read cloud sequencing and assembly. BMC Bioinformatics 20, 585.

Kangasjärvi, S., Neukermans, J., Li, S., Aro, E.-M., Noctor, G., 2012. Photosynthesis, photorespiration, and light signalling in defence responses. J. Exp. Bot. 63, 1619–1636.

Kange, A.M., Cheruiyot, E.K., Ogendo, J.O., Arama, P.F., 2015. Effect of sorghum (*Sorghum bicolor* L. Moench) grain conditions on occurrence of mycotoxin-producing fungi. Agric. Food Secur. 4, 15.

Kaplin, V.G., Matvienko, E.V., Kovalenko, M.V., 2017. The defeat of sorghum with bacterial leaf stripe (*Pseudomonas andropogonis*) in the forest-steppe of the average volga region. Bull. Samara State Agric. Acad. 2, 27–31.

Karlovsky, P., Suman, M., Berthiller, F., De Meester, J., Eisenbrand, G., Perrin, I., Oswald, I.P., Speijers, G., Chiodini, A., Recker, T., 2016. Impact of food processing and detoxification treatments on mycotoxin contamination. Mycotoxin Res. 32, 179–205.

Katile, S.O., Perumal, R., Rooney, W.L., Prom, L.K., Magill, C.W., 2010. Expression of pathogenesis-related protein PR-10 in sorghum floral tissues in response to inoculation with *Fusarium thapsinum* and *Curvularia lunata*. Mol. Plant Pathol. 11, 93–103.

Kazan, K., Gardiner, D.M., 2018. Transcriptomics of cereal–*Fusarium graminearum* interactions: what we have learned so far. Mol. Plant Pathol. 19, 764–778.

Kelly, L.A., Tan, Y.P., Ryley, M.J., Aitken, E.A.B., 2017. *Fusarium* species associated with stalk rot and head blight of grain sorghum in Queensland and New South Wales, Australia. Plant Pathol. 66, 1413–1423.

Kembel, S.W., O'Connor, T.K., Arnold, H.K., Hubbell, S.P., Wright, S.J., Green, J.L., 2014. Relationships between phyllosphere bacterial communities and plant functional traits in a neotropical forest. Proc. Natl. Acad. Sci. U. S. A. 111, 13715–13720.

Kembel, S.W., Wu, M., Eisen, J.A., Green, J.L., 2012. Incorporating 16S gene copy number information improves estimates of microbial diversity and abundance. PLoS Comput Biol 8, 1002743.

Khaledi, N., Taheri, P., Falahati-Rastegar, M., 2018. Evaluation of resistance and the role of some defense responses in wheat cultivars to Fusarium head blight. J. Plant Prot. Res. 1.

Khan, M.I.R., Reddy, P.S., Ferrante, A., Khan, N.A., 2019. Plant Signaling Molecules: Role and Regulation Under Stressful Environments. Woodhead Publishing, 1.

Kheiri, A., Jorf, S.A.M., Malihipour, A., 2019. Infection process and wheat response to Fusarium head blight caused by *Fusarium graminearum*. Eur. J. Plant Pathol. 153, 489–502.

Kim, M., Singh, D., Lai-Hoe, A., Go, R., Rahim, R.A., Ainuddin, A.N., Chun, J., Adams, J.M., 2012. Distinctive phyllosphere bacterial communities in tropical trees. Microb. Ecol. 63, 674–681.

Kimura, M., Anzai, H., Yamaguchi, I., 2001. Microbial toxins in plant-pathogen interactions: Biosynthesis, resistance mechanisms, and significance. J. Gen. Appl. Microbiol. 47, 149–160.

Kinge, T.R., Cason, E.D., Valverde Portal, Á., Nyaga, M., Gryzenhout, M., 2019. Endophytic seed mycobiome of six sorghum (*Sorghum bicolor*) cultivars from commercial seedlots using an Illumina sequencing approach.

Klein, R.R., Rodriguez-Herrera, R., Schlueter, J.A., Klein, P.E., Yu, Z.H., Rooney, W.L., 2001. Identification of genomic regions that affect grain-mould incidence and other traits of agronomic importance in sorghum. Theor. Appl. Genet. 102, 307–319.

Klindworth, A., Pruesse, E., Schweer, T., Peplies, J., Quast, C., Horn, M., Glockner, F.O., 2013. Evaluation of general 16S ribosomal RNA gene PCR primers for classical and next-generation sequencing-based diversity studies. Nucleic Acids Res. 41.

Knief, C., 2014. Analysis of plant microbe interactions in the era of next generation sequencing technologies. Front. Plant Sci. 5.

Knief, C., Delmotte, N., Chaffron, S., Stark, M., Innerebner, G., Wassmann, R., von Mering, C., Vorholt, J.A., 2012. Metaproteogenomic analysis of microbial communities in the phyllosphere and rhizosphere of rice. ISME J. 6, 1378–1390.

Knief, C., Ramette, A., Frances, L., Alonso-Blanco, C., Vorholt, J.A., 2010. Site and plant species are important determinants of the *Methylobacterium* community composition in the plant phyllosphere. ISME J. 4, 719–728.

Köberl, M., Roßmann, B., Lukesch, B., Staver, C., Ramadan, E.M., Berg, G., Grube, M., Fürnkranz, M., 2011. Using ecological knowledge and molecular tools to develop effective and safe biocontrol strategies. Intech Open Access Publisher.

Koskimaki, J.J., Pirttila, A.M., Ihantola, E.L., Halonen, O., Frank, A.C., 2015. The intracellular Scots pine shoot symbiont *Methylobacterium extorquens* DSM13060 aggregates around

the host nucleus and encodes eukaryote-like proteins. MBio 6, 10.

Kong, W., Jin, H., Franks, C.D., Kim, C., Bandopadhyay, R., Rana, M.K., Auckland, S.A., Goff, V.H., Rainville, L.K., Burow, G.B., Woodfin, C., Burke, J.J., Paterson, A.H., 2013. Genetic analysis of recombinant inbred lines for *Sorghum bicolor* x *Sorghum propinquum*. G3 (Bethesda). 3, 101–108.

Kover, P.X., Schaal, B.A., 2002. Genetic variation for disease resistance and tolerance among *Arabidopsis thaliana* accessions. Proc. Natl. Acad. Sci. U. S. A. 99, 11270–11274.

Kress, W.J., Erickson, D.L., 2008. DNA barcodes: genes, genomics, and bioinformatics. Proc. Natl. Acad. Sci. U. S. A. 105, 2761–2762.

Kruse, J., Dietrich, W., Zimmermann, H., Klenke, F., Richter, U., Richter, H., Thines, M., 2018. *Ustilago* species causing leaf-stripe smut revisited. IMA Fungus 9, 49–73.

Kukurba, K.R., Montgomery, S.B., 2015. RNA Sequencing and Analysis. Cold Spring Harb. Protoc. 2015, 951–969.

Kulcsár, L., Flipphi, M., Jónás, Á., Sándor, E., Fekete, E., Karaffa, L., 2017. Identification of a mutarotase gene involved in D-galactose utilization in *Aspergillus nidulans*. FEMS Microbiol. Lett. 364.

Kumar, A., Verma, J.P., 2019. The role of microbes to improve crop productivity and soil health, in: Ecological Wisdom Inspired Restoration Engineering. Springer, pp. 249–265.

Kuntzmann, P., Villaume, S., Larignon, P., Bertsch, C., 2010. Esca, BDA and Eutypiosis: foliar symptoms, trunk lesions and fungi observed in diseased vinestocks in two vineyards in Alsace. Vitis 49, 71–76.

Kuramae, E.E., Derksen, S., Schlemper, T.R., Dimitrov, M.R., Costa, O.Y.A., da Silveira, A.P.D., 2020. Sorghum Growth Promotion by *Paraburkholderia tropica* and *Herbaspirillum frisingense*: Putative Mechanisms Revealed by Genomics and Metagenomics. Microorganisms 8, 725.

Kurepin, L. V, Park, J.M., Lazarovits, G., Bernards, M.A., 2015. *Burkholderia phytofirmans*-induced shoot and root growth promotion is associated with endogenous changes in plant growth hormone levels. Plant Growth Regul. 75, 199–207.

Kurtz, Z.D., Muller, C.L., Miraldi, E.R., Littman, D.R., Blaser, M.J., Bonneau, R.A., 2015. Sparse and compositionally robust inference of microbial ecological networks. PLoS Comput. Biol. 11, e1004226.

Kushwaha, U.K.S., Mangal, V., Bairwa, A.K., Adhikari, S., Ahmed, T., Bhat, P., Yadav, A., Dhaka, N., Prajapati, D.R., Gaur, A., 2017. Association mapping, principles and techniques. J.Biol.Environ.Eng 2, 1–9.

Kwak, M.-J., Jeong, H., Madhaiyan, M., Lee, Y., Sa, T.-M., Oh, T.K., Kim, J.F., 2014. Genome information of *Methylobacterium oryzae*, a plant-probiotic methylotroph in the phyllosphere.

La Camera, S., Goddard, M.-L., Laloue, H., Mestre, P., Chong, J., 2019. Overexpression of the VvSWEET4 transporter in grapevine hairy roots increases sugar transport and contents and enhances resistance to *Pythium irregulare*, a soilborne pathogen. Front. Plant Sci. 10, 884.

Lambais, M.R., Lucheta, A.R., Crowley, D.E., 2014. Bacterial Community Assemblages Associated with the Phyllosphere, Dermosphere, and Rhizosphere of Tree Species of the Atlantic Forest are Host Taxon Dependent. Microb. Ecol. 68, 567–574.

Lamesch, P., Berardini, T.Z., Li, D., Swarbreck, D., Wilks, C., Sasidharan, R., Muller, R., Dreher, K., Alexander, D.L., Garcia-Hernandez, M., 2012. The *Arabidopsis* Information Resource (TAIR): improved gene annotation and new tools. Nucleic Acids Res. 40, 1202–1210.

Lamichhane, J.R., Venturi, V., 2015. Synergisms between microbial pathogens in plant disease complexes: a growing trend. Front. Plant Sci. 6, 385.

Lana, U.G.D.P., Gomes, E.A., Silva, D.D., Costa, R.V., Cota, L.V., Parreira, D.F., Souza, I.R.P., Guimarães, C.T., 2012. Detection and molecular diversity of *Pantoea ananatis* associated with white spot disease in maize, sorghum and crabgrass in Brazil. J. Phytopathol. 160, 441–448.

Lateef, A., Adelere, I.A., Gueguim-Kana, E.B., Asafa, T.B., Beukes, L.S., 2015. Green synthesis of silver nanoparticles using keratinase obtained from a strain of *Bacillus safensi*s LAU 13. Int. Nano Lett. 5, 29–35.

Layeghifard, M., Hwang, D.M., Guttman, D.S., 2017. Disentangling interactions in the microbiome: a network perspective. Trends Microbiol. 25, 217–228.

Lebreton, L., Guillerm-Erckelboudt, A.-Y., Gazengel, K., Linglin, J., Ourry, M., Glory, P., Sarniguet, A., Daval, S., Manzanares-Dauleux, M.J., Mougel, C., 2019. Temporal dynamics of bacterial and fungal communities during the infection of *Brassica rapa* roots

by the protist *Plasmodiophora brassicae*. PLoS One 14, e0204195.

Lenaerts, B., Collard, B.C.Y., Demont, M., 2019. Improving global food security through accelerated plant breeding. Plant Sci. 110207.

Leslie, J.F., Zeller, K.A., Lamprecht, S.C., Rheeder, J.P., Marasas, W.F.O., 2005. Toxicity, pathogenicity, and genetic differentiation of five species of *Fusarium* from sorghum and millet. Phytopathology 95, 275–283.

Leveau, J.H.J., Tech, J.J., 2010. Grapevine microbiomics: bacterial diversity on grape leaves and berries revealed by high-throughput sequence analysis of 16S rRNA amplicons, in: International Symposium on Biological Control of Postharvest Diseases: Challenges and Opportunities 905. pp. 31–42.

Li, C., Haslam, T.M., Krüger, A., Schneider, L.M., Mishina, K., Samuels, L., Yang, H., Kunst, L., Schaffrath, U., Nawrath, C., 2018. The β-Ketoacyl-CoA Synthase Hv KCS1, Encoded by Cer-zh, Plays a Key Role in Synthesis of Barley Leaf Wax and Germination of Barley Powdery Mildew. Plant Cell Physiol. 59, 811–827.

Li, H., Handsaker, B., Wysoker, A., Fennell, T., Ruan, J., Homer, N., Marth, G., Abecasis, G., Durbin, R., 2009. The sequence alignment/map format and SAMtools. Bioinformatics 25, 2078–2079.

Li, T., Kim, J.-H., Jung, B., Ji, S., Seo, M.W., Han, Y.K., Lee, S.W., Bae, Y.S., Choi, H.-G., Lee, S.-H., 2018. Transcriptome analyses of the ginseng root rot pathogens Cylindrocarpon destructans and *Fusarium solani* to identify radicicol resistance mechanisms. J. Ginseng Res, 1.

Lindow, S.E., Brandl, M.T., 2003. Microbiology of the phyllosphere. Appl. Environ. Microbiol. 69, 1875–1883.

Little, C.R., Magill, C.W., 2003. Elicitation of defense response genes in sorghum floral tissues infected by *Fusarium thapsinum* and *Curvularia lunata* at anthesis. Physiol. Mol. Plant Pathol. 63, 271–279.

Little, C.R., Perumal, R., Tesso, T.T., Prom, L.K., Odvody, G.N., Magill, C.W., 2012. Sorghum pathology and biotechnology-A fungal disease perspective: part I. Grain mold, head smut, and ergot. Eur. J. Plant Sci. Biotechnol. 6, 10–30.

Liu, G.E., 2009. Applications and case studies of the next-generation sequencing technologies in food, nutrition and agriculture. Recent Pat. Food. Nutr. Agric. 1, 75–79.

Liu, J.L., Xie, B.M., Shi, X.H., Ma, J.M., Guo, C.H., 2015. Effects of two plant growth-promoting rhizobacteria containing 1-aminocyclopropane-1-carboxylate deaminase on oat growth in petroleum-contaminated soil. Int. J. Environ. Sci. Technol. 12, 3887–3894.

Loman, N.J., Misra, R. V, Dallman, T.J., Constantinidou, C., Gharbia, S.E., Wain, J., Pallen, M.J., 2012. Performance comparison of benchtop high-throughput sequencing platforms. Nat. Biotechnol. 30, 434–439.

Love, M.I., Huber, W., Anders, S., 2014. Moderated estimation of fold change and dispersion for RNA-seq data with DESeq2. Genome Biol. 15, 550.

Ludwig-Müller, J., 2015. Bacteria and fungi controlling plant growth by manipulating auxin: balance between development and defense. J. Plant Physiol. 172, 4–12.

Luján, A.M., Gómez, P., Buckling, A., 2015. Siderophore cooperation of the bacterium *Pseudomonas fluorescens* in soil. Biol. Lett. 11, 20140934.

Lundberg, D.S., Lebeis, S.L., Paredes, S.H., Yourstone, S., Gehring, J., Malfatti, S., Tremblay, J., Engelbrektson, A., Kunin, V., Del Rio, T.G., 2012. Defining the core *Arabidopsis thaliana* root microbiome. Nature 488, 86–90.

Luo, H., Zhao, W., Wang, Y., Xia, Y., Wu, X., Zhang, L., Tang, B., Zhu, J., Fang, L., Du, Z., 2016. SorGSD: a sorghum genome SNP database. Biotechnol. Biofuels 9, 1.

Luo, S., Xu, T., Chen, L., Chen, J., Rao, C., Xiao, X., Wan, Y., Zeng, G., Long, F., Liu, C., 2012. Endophyte-assisted promotion of biomass production and metal-uptake of energy crop sweet sorghum by plant-growth-promoting endophyte *Bacillus* sp. SLS18. Appl. Microbiol. Biotechnol. 93, 1745–1753.

Ma, J.-Q., Wei, L.-J., Lin, A., Zhang, C., Sun, W., Yang, B., Lu, K., Li, J.-N., 2019. The Alternative Splicing Landscape of *Brassica napus* Infected with *Leptosphaeria maculans*. Genes (Basel). 10, 296.

Mace, E.S., Tai, S., Gilding, E.K., Li, Y., Prentis, P.J., Bian, L., Campbell, B.C., Hu, W., Innes, D.J., Han, X., 2013. Whole-genome sequencing reveals untapped genetic potential in Africa's indigenous cereal crop sorghum. Nat. Commun. 4.

Mandal, S., Van Treuren, W., White, R.A., Eggesbø, M., Knight, R., Peddada, S.D., 2015. Analysis of composition of microbiomes: a novel method for studying microbial composition. Microb. Ecol. Health Dis. 26, 27663.

Marley, P.S., Ajayi, O., 1999. Sorghum grain mold and the influence of head bug *Eurystylus oldi* in West and Central Africa. J. Sustain. Agric. 13, 35–44.

Maropola, M.K.A., Ramond, J.-B., Trindade, M., 2015. Impact of metagenomic DNA extraction procedures on the identifiable endophytic bacterial diversity in Sorghum bicolor (l. Moench). J. Microbiol. Methods 112, 104–117.

Marra, L.M., Soares, C.R.F.S., de Oliveira, S.M., Ferreira, P.A.A., Soares, B.L., de Fráguas Carvalho, R., de Lima, J.M., de Souza Moreira, F.M., 2012. Biological nitrogen fixation and phosphate solubilization by bacteria isolated from tropical soils. Plant Soil 357, 289–307.

Mavhunga, M., 2013. No Title. *Fusarium graminearum* mycotoxins Assoc. with grain Mould maize sorghum South Africa, 1.

McCormick, R.F., Truong, S.K., Sreedasyam, A., Jenkins, J., Shu, S., Sims, D., Kennedy, M., Amirebrahimi, M., Weers, B.D., McKinley, B., 2018. The *Sorghum bicolor* reference genome: improved assembly, gene annotations, a transcriptome atlas, and signatures of genome organization. Plant J. 93, 338–354.

McDonald, B.A., Stukenbrock, E.H., 2016. Rapid emergence of pathogens in agro-ecosystems: global threats to agricultural sustainability and food security. Philos. Trans. R. Soc. B Biol. Sci. 371, 20160026.

McDowell, I.C., Manandhar, D., Vockley, C.M., Schmid, A.K., Reddy, T.E., Engelhardt, B.E., 2018. Clustering gene expression time series data using an infinite Gaussian process mixture model. PLoS Comput. Biol. 14, e1005896.

McMurdie, P.J., Holmes, S., 2013. phyloseq: an R package for reproducible interactive analysis and graphics of microbiome census data. PLoS One 8, e61217.

McMurdie, P.J., Holmes, S., 2014. Waste not, want not: why rarefying microbiome data is inadmissible. PLoS Comput Biol 10, 1003531.

Medraoui, L., Ater, M., Benlhabib, O., Msikine, D., Filali-Maltouf, A., 2007. Evaluation of genetic variability of sorghum (*Sorghum bicolor* L. Moench) in northwestern Morocco by ISSR and RAPD markers. C. R. Biol. 330, 789–797.

Meena, K.K., Kumar, M., Kalyuzhnaya, M.G., Yandigeri, M.S., Singh, D.P., Saxena, A.K., Arora, D.K., 2012. Epiphytic pink-pigmented methylotrophic bacteria enhance germination and seedling growth of wheat (Triticum aestivum) by producing

phytohormone. Antonie Van Leeuwenhoek 101, 777–786.

Mehmood, A., Khan, N., Irshad, M., Hamayun, M., 2018. IAA Producing Endopytic Fungus *Fusariun oxysporum* wlw Colonize Maize Roots and Promoted Maize Growth Under Hydroponic Condition. Eur Exp Biol 8, 24.

Mekbib, F., 2007. Infra-specific folk taxonomy in sorghum (*Sorghum bicolor* (L.) Moench) in Ethiopia: folk nomenclature, classification, and criteria. J. Ethnobiol. Ethnomed. 3, 1.

Mendes, L.W., Kuramae, E.E., Navarrete, A.A., van Veen, J.A., Tsai, S.M., 2014. Taxonomical and functional microbial community selection in soybean rhizosphere. ISME J. 8, 1577–1587.

Mendes, R., Garbeva, P., Raaijmakers, J.M., 2013. The rhizosphere microbiome: significance of plant beneficial, plant pathogenic, and human pathogenic microorganisms. FEMS Microbiol. Rev. 37, 634–663.

Mengesha, M.H., Rao, K.E.P., 1982. Current situation and future of sorghum germplasm. Sorghum eighties.Patancheru, India Int. Crop. Res. Inst. Semi-Arid Trop. 323–345.

Mengistu, M.G., Steyn, J.M., Kunz, R.P., Doidge, I., Hlophe, H.B., Everson, C.S., Jewitt, G.P.W., Clulow, A.D., 2016. A preliminary investigation of the water use efficiency of sweet sorghum for biofuel in South Africa. Water SA 42, 152–160.

Menkir, A., Ejeta, G., Butler, L.G., Melakeberhan, A., Warren, H.L., 1996. Fungal invasion of kernels and grain mold damage assessment in diverse sorghum germ plasm. Plant Dis.

Menz, M.A., Klein, R.R., Unruh, N.C., Rooney, W.L., Klein, P.E., Mullet, J.E., 2004. Genetic diversity of public inbreds of sorghum determined by mapped AFLP and SSR markers. Crop Sci. 44, 1236–1244.

Meola, M., Rifa, E., Shani, N., Delbès, C., Berthoud, H., Chassard, C., 2019. DAIRYdb: a manually curated reference database for improved taxonomy annotation of 16S rRNA gene sequences from dairy products. BMC Genomics 20, 560.

Meyer, F., Overbeek, R., Rodriguez, A., 2009. FIGfams: yet another set of protein families. Nucleic Acids Res. 37, 6643–6654.

Mhlongo, M.I., Piater, L.A., Madala, N.E., Steenkamp, P.A., Dubery, I.A., 2016. Phenylpropanoid Defences in *Nicotiana tabacum* Cells: Overlapping Metabolomes Indicate Common Aspects to Priming Responses Induced by Lipopolysaccharides, Chitosan and Flagellin-22. PLoS One 11, e0151350.

Mia, M.A.B., Shamsuddin, Z.H., Mahmood, M., 2014. Effects of rhizobia and plant growth promoting bacteria inoculation on germination and seedling vigor of lowland rice. African J. Biotechnol. 11, 3758–3765.

Mihajlovski, A., Seyer, D., Benamara, H., Bousta, F., Di Martino, P., 2015. An overview of techniques for the characterization and quantification of microbial colonization on stone monuments. Ann. Microbiol. 65, 1243–1255.

Miozzi, L., Napoli, C., Sardo, L., Accotto, G.P., 2014. Transcriptomics of the interaction between the monopartite phloem-limited geminivirus tomato yellow leaf curl Sardinia virus and *Solanum lycopersicum* highlights a role for plant hormones, autophagy and plant immune system fine tuning during infection. PLoS One. 9.

Mishra, J., Singh, R., Arora, N.K., 2017. Plant growth-promoting microbes: diverse roles in agriculture and environmental sustainability, in: Probiotics and Plant Health. Springer, pp. 71–111.

Moral, J., Lichtemberg, P.S.F., Papagelis, A., Sherman, J., Michailides, T.J., 2018. *Didymella glomerata* causing leaf blight on pistachio. Eur. J. Plant Pathol. 151, 1095–1099.

Morales-Cruz, A., Figueroa-Balderas, R., Garcia, J.F., Tran, E., Rolshausen, P.E., Baumgartner, K., Cantu, D., 2018. Profiling grapevine trunk pathogens in planta: a case for community-targeted DNA metabarcoding. BMC Microbiol. 18, 214.

Moreira, D., López-García, P., 2002. The molecular ecology of microbial eukaryotes unveils a hidden world. Trends Microbiol. 10, 31–38.

Morgan, J.A., Bending, G.D., White, P.J., 2005. Biological costs and benefits to plant-microbe interactions in the rhizosphere. J. Exp. Bot. 56, 1729–1739.

Moriya, Y., Itoh, M., Okuda, S., Yoshizawa, A.C., Kanehisa, M., 2007. KAAS: an automatic genome annotation and pathway reconstruction server. Nucleic Acids Res. 35, W182–W185.

Morkunas, I., Ratajczak, L., 2014. The role of sugar signaling in plant defense responses against fungal pathogens. Acta Physiol. Plant. 36, 1607–1619.

Morris, C.E., Kinkel, L.L., Lindow, S.E., Hecht-Poinar, E.I., Elliott, V.J., 2002. Fifty years of phyllosphere microbiology: significant contributions to research in related fields. Phyllosph. Microbiol. 365–375.

Morris, G.P., Ramu, P., Deshpande, S.P., Hash, C.T., Shah, T., Upadhyaya, H.D., Riera-

Lizarazu, O., Brown, P.J., Acharya, C.B., Mitchell, S.E., Harriman, J., Glaubitz, J.C., Buckler, E.S., Kresovich, S., 2013. Population genomic and genome-wide association studies of agroclimatic traits in sorghum. Proc. Natl. Acad. Sci. U. S. A. 110, 453–458.

Morrissey, J., Guerinot, M. Lou, 2009. Iron uptake and transport in plants: the good, the bad, and the ionome. Chem. Rev. 109, 4553–4567.

Motlhaodi, T.M., 2016. Genetic diversity and nutritional content of sorghum [*Sorghum bicolor* (L.) Moench] accessions from Southern Africa.

Mpofu, L.T., McLaren, N.W., 2014. Ergosterol concentration and variability in genotype-by-pathogen interaction for grain mold resistance in sorghum. Planta 240, 239–250.

Mukhtar, I., Khokhar, I., Mushtaq, S., Ali, A., 2010. Diversity of epiphytic and endophytic microorganisms in some dominant weeds. Pakistan J. Weed Sci. Res. 16.

Müller, D.B., Vogel, C., Bai, Y., Vorholt, J.A., 2016. The plant microbiota: systems-level insights and perspectives. Annu. Rev. Genet. 50, 211–234.

Mundia, C.W., Secchi, S., Akamani, K., Wang, G., 2019. A Regional Comparison of Factors Affecting Global Sorghum Production: The Case of North America, Asia and Africa's Sahel. Sustainability 11, 2135.

Mushtaq, M., Sakina, A., Wani, S.H., Shikari, A.B., Tripathi, P., Zaid, A., Galla, A., Abdelrahman, M., Sharma, M., Singh, A.K., 2019. Harnessing genome editing techniques to engineer disease resistance in plants. Front. Plant Sci. 10.

Mutegi, E., Sagnard, F., Semagn, K., Deu, M., Muraya, M., Kanyenji, B., De Villiers, S., Kiambi, D., Herselman, L., Labuschagne, M., 2011. Genetic structure and relationships within and between cultivated and wild sorghum (*Sorghum bicolor* (L.) Moench) in Kenya as revealed by microsatellite markers. Theor. Appl. Genet. 122, 989–1004.

Nakahara, K.S., Masuta, C., Yamada, S., Shimura, H., Kashihara, Y., Wada, T.S., Meguro, A., Goto, K., Tadamura, K., Sueda, K., Sekiguchi, T., Shao, J., Itchoda, N., Matsumura, T., Igarashi, M., Ito, K., Carthew, R.W., Uyeda, I., 2012. Tobacco calmodulin-like protein provides secondary defense by binding to and directing degradation of virus RNA silencing suppressors. Proc. Natl. Acad. Sci. U. S. A. 109, 10113–10118.

Nalam, V.J., Alam, S., Keereetaweep, J., Venables, B., Burdan, D., Lee, H., Trick, H.N., Sarowar, S., Makandar, R., Shah, J., 2015. Facilitation of *Fusarium graminearum* infection by 9-lipoxygenases in *Arabidopsis* and wheat. Mol. Plant-Microbe Interact. 28,

1142–1152.

Nasanit, R., Krataithong, K., Tantirungkij, M., Limtong, S., 2015. Assessment of epiphytic yeast diversity in rice (O*ryza sativa*) phyllosphere in Thailand by a culture-independent approach. Antonie Van Leeuwenhoek 107, 1475–1490.

Navi, S.S., 2006. Fungi associated with sorghum grains in rural Indian storages. J. New Seeds 7, 51–68.

Navi, S.S., Bandyopadhyay, R., Reddy, R.K., Thakur, R.P., Yang, X.-B., 2005. Effects of wetness duration and grain development stages on sorghum grain mold infection. Plant Dis. 89, 872–878.

Nemergut, D.R., Schmidt, S.K., Fukami, T., O'Neill, S.P., Bilinski, T.M., Stanish, L.F., Knelman, J.E., Darcy, J.L., Lynch, R.C., Wickey, P., Ferrenberg, S., 2013. Patterns and processes of microbial community assembly. Microbiol. Mol. Biol. Rev. 77, 342–356.

Ngah, N., Thomas, R., Shaw, M., Fellowes, M., 2018. Asymptomatic host plant infection by the widespread pathogen *Botrytis cinerea* alters the life histories, behaviors, and interactions of an aphid and its natural enemies. Insects 9, 80.

Nguyen, T.-M., Shafi, A., Nguyen, T., Draghici, S., 2019. Identifying significantly impacted pathways: a comprehensive review and assessment. Genome Biol. 20, 1–15.

Nida, H., Girma, G., Mekonen, M., Lee, S., Seyoum, A., Dessalegn, K., Tadesse, T., Ayana, G., Senbetay, T., Tesso, T., 2019. Identification of sorghum grain mold resistance loci through genome wide association mapping. J. Cereal Sci. 85, 295–304.

Nihorimbere, V., Ongena, M., Smargiassi, M., Thonart, P., 2011. Beneficial effect of the rhizosphere microbial community for plant growth and health. Biotechnol. Agron. Société Environ. 15, 327–337.

Niks, R.E., Parlevliet, J.E., Lindhout, P., Bai, Y., 2019. Breeding crops with resistance to diseases and pests. Wageningen Academic Publishers.

Nilsson, R.H., Anslan, S., Bahram, M., Wurzbacher, C., Baldrian, P., Tedersoo, L., 2019. Mycobiome diversity: high-throughput sequencing and identification of fungi. Nat. Rev. Microbiol. 17, 95–109.

Nürnberger, T., Kemmerling, B., 2018. Pathogen-Associated Molecular Patterns (PAMP) and PAMP-Triggered Immunity. Annu. Plant Rev. online 16–47.

Nussbaumer, T., Warth, B., Sharma, S., Ametz, C., Bueschl, C., Parich, A., Pfeifer, M.,

Siegwart, G., Steiner, B., Lemmens, M., Schuhmacher, R., Buerstmayr, H., Mayer, K.F., Kugler, K.G., Schweiger, W., 2015. Joint Transcriptomic and Metabolomic Analyses Reveal Changes in the Primary Metabolism and Imbalances in the Subgenome Orchestration in the Bread Wheat Molecular Response to *Fusarium graminearum*. G3 (Bethesda). 5, 2579–2592.

Nutaratat, P., Srisuk, N., Arunrattiyakorn, P., Limtong, S., 2014. Plant growth-promoting traits of epiphytic and endophytic yeasts isolated from rice and sugar cane leaves in Thailand. Fungal Biol. 118, 683–694.

O'Donnell, K., 1992. Ribosomal DNA internal transcribed spacers are highly divergent in the phytopathogenic ascomycete *Fusarium sambucinum* (*Gibberella pulicaris*). Curr. Genet. 22, 213–220.

Oksanen, J., Kindt, R., Legendre, P., O'Hara, B., Stevens, M.H.H., Oksanen, M.J., Suggests, M., 2007. The vegan package. Community Ecol. Packag. 10, 719.

Oliveira, R.C., Davenport, K.W., Hovde, B., Silva, D., Chain, P.S., Correa, B., Rodrigues, D.F., 2017a. Draft Genome Sequence of Sorghum Grain Mold Fungus *Epicoccum sorghinum*, a Producer of Tenuazonic Acid. Genome Announc. 5.

Oliveira, R.C., Goncalves, S.S., Oliveira, M.S., Dilkin, P., Mallmann, C.A., Freitas, R.S., Bianchi, P., Correa, B., 2017b. Natural occurrence of tenuazonic acid and *Phoma sorghina* in Brazilian sorghum grains at different maturity stages. Food Chem. 230, 491–496.

Olsen, S., Krause, K., 2017. Activity of xyloglucan endotransglucosylases/hydrolases suggests a role during host invasion by the parasitic plant *Cuscuta reflexa*. PLoS One 12, e0176754.

Olson, A., Klein, R.R., Dugas, D. V, Lu, Z., Regulski, M., Klein, P.E., Ware, D., 2014. Expanding and vetting *Sorghum bicolor* gene annotations through transcriptome and methylome sequencing. Plant Genome 7.

Omayio, D.O., Musyimi, D.M., Muyekho, F.N., Ajanga, S.I., Midega, C.A.O., Wekesa, C.S., Okoth, P., Kariuki, I.W., 2018. Molecular Diversity of a Seemingly Altitude Restricted *Ustilago kamerunensis* Isolates in Kenya: A Pathogen of Napier Grass.

Oulas, A., Pavloudi, C., Polymenakou, P., Pavlopoulos, G.A., Papanikolaou, N., Kotoulas, G., Arvanitidis, C., Iliopoulos, loannis, 2015. Metagenomics: tools and insights for analyzing

next-generation sequencing data derived from biodiversity studies. Bioinform. Biol. Insights 9, BBI. S12462.

Palmer, M., Steenkamp, E.T., Coetzee, M.P.A., Avontuur, J.R., Chan, W.Y., Van Zyl, E., Blom, J., Venter, S.N., 2018. *Mixta* gen. nov., a new genus in the *Erwiniaceae*.

Pancher, M., Ceol, M., Corneo, P.E., Longa, C.M., Yousaf, S., Pertot, I., Campisano, A., 2012. Fungal endophytic communities in grapevines (*Vitis vinifera* L.) respond to crop management. Appl. Environ. Microbiol. 78, 4308–4317.

Pandey, V.P., Awasthi, M., Singh, S., Tiwari, S., Dwivedi, U.N., 2017. A comprehensive review on function and application of plant peroxidases. Biochem. Anal. Biochem. 6, 1–16.

Panpatte, D.G., Jhala, Y.K., Shelat, H.N., Vyas, R. V, 2016. *Pseudomonas fluorescens*: a promising biocontrol agent and PGPR for sustainable agriculture, in: Microbial Inoculants in Sustainable Agricultural Productivity. Springer, pp. 257–270.

Pascale, A., Proietti, S., Pantelides, I.S., Stringlis, I.A., 2020. Modulation of the root microbiome by plant molecules: the basis for targeted disease suppression and plant growth promotion. Front. Plant Sci. 10, 1741.

Paterson, A.H., Bowers, J.E., Bruggmann, R., Dubchak, I., Grimwood, J., Gundlach, H., Haberer, G., Hellsten, U., Mitros, T., Poliakov, A., 2009. The *Sorghum bicolor* genome and the diversification of grasses. Nature 457, 551–556.

Pena, G.A., Cavaglieri, L.R., Chulze, S.N., 2019. *Fusarium* species and *moniliformin* occurrence in sorghum grains used as ingredient for animal feed in Argentina. J. Sci. Food Agric. 99, 47–54.

Peñuelas, J., Terradas, J., 2014. The foliar microbiome. Trends Plant Sci. 19, 278–280.

Perez-Carrillo, E., Serna-Saldivar, S.O., Chuck-Hernandez, C., Cortes-Callejas, M.L., 2012. Addition of protease during starch liquefaction affects free amino nitrogen, fusel alcohols and ethanol production of fermented maize and whole and decorticated sorghum mashes. Biochem. Eng. J. 67, 1–9.

Pertea, M., Kim, D., Pertea, G.M., Leek, J.T., Salzberg, S.L., 2016. Transcript-level expression analysis of RNA-seq experiments with HISAT, StringTie and Ballgown. Nat. Protoc. 11, 1650.

Pertea, M., Pertea, G.M., Antonescu, C.M., Chang, T.-C., Mendell, J.T., Salzberg, S.L., 2015.

StringTie enables improved reconstruction of a transcriptome from RNA-seq reads. Nat. Biotechnol. 33, 290.

Philippot, L., Raaijmakers, J.M., Lemanceau, P., van der Putten, W.H., 2013. Going back to the roots: the microbial ecology of the rhizosphere. Nat. Rev. Microbiol. 11, 789–799.

Pinotti, L., Ottoboni, M., Giromini, C., Dell'Orto, V., Cheli, F., 2016. Mycotoxin contamination in the EU feed supply chain: A focus on cereal byproducts. Toxins (Basel). 8, 45.

Planas-Marques, M., Bernardo-Faura, M., Paulus, J., Kaschani, F., Kaiser, M., Valls, M., van der Hoorn, R.A.L., Coll, N.S., 2018. Protease Activities Triggered by *Ralstonia solanacearum* Infection in Susceptible and Tolerant Tomato Lines. Mol. Cell. Proteomics 17, 1112–1125.

Plummer, E., Twin, J., Bulach, D.M., Garland, S.M., Tabrizi, S.N., 2015. A Comparison of Three Bioinformatics Pipelines for the Analysis of Preterm Gut Microbiota using 16S rRNA Gene Sequencing Data. J. Proteomics Bioinform. 2015.

Porter, T.M., Brian Golding, G., 2011. Are similarity-or phylogeny-based methods more appropriate for classifying internal transcribed spacer (ITS) metagenomic amplicons? New Phytol. 192, 775–782.

Postma, J., Montanari, M., van den Boogert, P.H.J.F., 2003. Microbial enrichment to enhance the disease suppressive activity of compost. Eur. J. Soil Biol. 39, 157–163.

Poudel, R., Jumpponen, A., Schlatter, D.C., Paulitz, T.C., Gardener, B.B.M., Kinkel, L.L., Garrett, K.A., 2016. Microbiome networks: a systems framework for identifying candidate microbial assemblages for disease management. Phytopathology 106, 1083–1096.

Praveen Kumar, G., Desai, S., Leo Daniel Amalraj, E., Mir Hassan Ahmed, S.K., Reddy, G., 2012. Plant growth promoting *Pseudomonas* spp. from diverse agro-ecosystems of India for Sorghum bicolor L. J Biofert Biopest S 7, 2.

Price, M.N., Dehal, P.S., Arkin, A.P., 2010. FastTree 2–approximately maximum-likelihood trees for large alignments. PLoS One 5, e9490.

Prochaska, T.J., Donze-Reiner, T., Marchi-Werle, L., Palmer, N.A., Hunt, T.E., Sarath, G., Heng-Moss, T., 2015. Transcriptional responses of tolerant and susceptible soybeans to soybean aphid (*Aphis glycines Matsumura*) herbivory. Arthropod. Plant. Interact. 9, 347–

359.

Prom, L.K., Radwan, G., Perumal, R., Cuevas, H., Katile, S.O., Isakeit, T., Magill, C., 2017. Grain biodeterioration of sorghum converted lines inoculated with a mixture of *Fusarium thapsinum* and *Curvularia lunata*. Plant Pathol. J. 16, 19–24.

Prospero, S., Cleary, M., 2017. Effects of host variability on the spread of invasive forest diseases. Forests 8, 80.

Puri, A., Padda, K.P., Chanway, C.P., 2018. Nitrogen-fixation by endophytic bacteria in agricultural crops: recent advances. Nitrogen Agric. London, GBR 73–94.

Quaedvlieg, W., Verkley, G.J.M., Shin, H.-D., Barreto, R.W., Alfenas, A.C., Swart, W.J., Groenewald, J.Z., Crous, P.W., 2013. Sizing up septoria. Stud. Mycol. 75, 307–390.

Quazi, S.A.J., Burgess, L.W., Smith-White, J., 2010. Colonization type of *Gibberella zeae* in *Sorghum bicolor*. J. Plant Pathol. 261–265.

Raemaekers, R.H., 2001. Crop production in tropical Africa. DGIC, 1.

Raghuwanshi, R., Prasad, J.K., 2018. Perspectives of Rhizobacteria with ACC Deaminase Activity in Plant Growth Under Abiotic Stress, in: Root Biology. Springer, 303–321.

Rakotoarisoa, T.F., Waeber, P.O., Richter, T., Mantilla-Contreras, J., 2015. Water hyacinth (*Eichhornia crassipes*), any opportunities for the Alaotra wetlands and livelihoods? Madagascar Conserv. Dev. 10, 128–136.

Ramírez, M.B., Ferrari, M.D., Lareo, C., 2016. Fuel ethanol production from commercial grain sorghum cultivars with different tannin content. J. Cereal Sci. 69, 125–131.

Ramoni, M.F., Sebastiani, P., Kohane, I.S., 2002. Cluster analysis of gene expression dynamics. Proc. Natl. Acad. Sci. U. S. A. 99, 9121–9126.

Rana, K.L., Kour, D., Sheikh, I., Dhiman, A., Yadav, N., Yadav, A.N., Rastegari, A.A., Singh, K., Saxena, A.K., 2019. Endophytic fungi: biodiversity, ecological significance, and potential industrial applications, in: Recent Advancement in White Biotechnology through Fungi. Springer, pp. 1–62.

Rastogi, G., Coaker, G.L., Leveau, J.H.J., 2013. New insights into the structure and function of phyllosphere microbiota through high-throughput molecular approaches. FEMS Microbiol. Lett. 348, 1–10.

Rastogi, G., Sani, R.K., 2011. Microbes and Microbial Technology 29–58.

Rathinasabapathi, B., Liu, X., Cao, Y., Ma, L.Q., 2018. Phosphate-solubilizing *Pseudomonads*

for improving crop plant nutrition and agricultural productivity, in: Crop Improvement Through Microbial Biotechnology. Elsevier, pp. 363–372.

Rausch, P., Rühlemann, M., Hermes, B., Doms, S., Dagan, T., Dierking, K., Domin, H., Fraune, S., Frieling, J. von, Humeida, U.H., 2019. Comparative analysis of amplicon and metagenomic sequencing methods reveals key features in the evolution of animal metaorganisms.

Ravanbakhsh, M., Sasidharan, R., Voesenek, L.A.C.J., Kowalchuk, G.A., Jousset, A., 2018. Microbial modulation of plant ethylene signaling: ecological and evolutionary consequences. Microbiome 6, 52.

Ravisankar, D., Nithya, C., 2018. Significance and Applications of Plant Growth Promoting Rhizobacteria (PGPR) In Agriculture: A Review. Res. Rev. J. Agric. Sci. Technol. 1, 9–22.

Reddy, T.A., Maor, I., Panjapornpon, C., 2007. Calibrating detailed building energy simulation programs with measured data—Part I: General methodology (RP-1051). Hvac&R Res. 13, 221–241.

Redford, A.J., Bowers, R.M., Knight, R., Linhart, Y., Fierer, N., 2010. The ecology of the phyllosphere: geographic and phylogenetic variability in the distribution of bacteria on tree leaves. Environ. Microbiol. 12, 2885–2893.

Rico, L., Ogaya, R., Terradas, J., Penuelas, J., 2014. Community structures of N2-fixing bacteria associated with the phyllosphere of a Holm oak forest and their response to drought. Plant Biol. 16, 586–593.

Riesenfeld, C.S., Schloss, P.D., Handelsman, J., 2004. Metagenomics: genomic analysis of microbial communities. Annu.Rev.Genet. 38, 525–552.

Ritpitakphong, U., Falquet, L., Vimoltust, A., Berger, A., Métraux, J., L'Haridon, F., 2016. The microbiome of the leaf surface of *Arabidopsis* protects against a fungal pathogen. New Phytol. 210, 1033–1043.

Ritter, K.B., McIntyre, C.L., Godwin, I.D., Jordan, D.R., Chapman, S.C., 2007. An assessment of the genetic relationship between sweet and grain sorghums, within *Sorghum bicolor* ssp. bicolor (L.) Moench, using AFLP markers. Euphytica 157, 161–176.

Roberts, R.J., Carneiro, M.O., Schatz, M.C., 2013. The advantages of SMRT sequencing. Genome Biol. 14, 1.

Rodriguez-Moreno, L., Ebert, M.K., Bolton, M.D., Thomma, B.P.H.J., 2018. Tools of the crook-infection strategies of fungal plant pathogens. Plant J. 93, 664–674.

Rosenzweig, N., Tiedje, J.M., Quensen III, J.F., Meng, Q., Hao, J.J., 2012. Microbial communities associated with potato common scab-suppressive soil determined by pyrosequencing analyses. Plant Dis. 96, 718–725.

Rosselli, R., Squartini, A., 2015. Metagenomics of Plant–Microbe Interactions, in: Advances in the Understanding of Biological Sciences Using Next Generation Sequencing (NGS) Approaches. Springer, pp. 135–153.

Rossmann, M., Sarango-Flores, S.W., Chiaramonte, J.B., Kmit, M.C.P., Mendes, R., 2017. Plant microbiome: composition and functions in plant compartments, in: The Brazilian Microbiome. Springer, pp. 7–20.

Roy, N.C., Altermann, E., Park, Z.A., McNabb, W.C., 2011. A comparison of analog and next-generation transcriptomic tools for mammalian studies. Brief. Funct. Genomics 10, 135–150.

Ruppert, K.M., Kline, R.J., Rahman, M.S., 2019. Past, present, and future perspectives of environmental DNA (eDNA) metabarcoding: A systematic review in methods, monitoring, and applications of global eDNA. Glob. Ecol. Conserv. e00547.

Ryan, R.P., Germaine, K., Franks, A., Ryan, D.J., Dowling, D.N., 2008. Bacterial endophytes: recent developments and applications. FEMS Microbiol. Lett. 278, 1–9.

Ryu, C., Murphy, J.F., Reddy, M.S., Kloepper, J.W., 2007. A two-strain mixture of rhizobacteria elicits induction of systemic resistance against *Pseudomonas syringae* and Cucumber mosaic virus coupled to promotion of plant growth on *Arabidopsis thaliana*. J. Microbiol. Biotechnol. 17, 280.

[SAGL] Southern African Grain Laboratory. 2019. South African maize crop quality report 2017/2018 [document on the Internet]. [cited 2019 Mar 24]. Available from: https://sagl.co.za/wp-content/uploads/Reports/Sorghum/Page-37-46.pdf

Saad, M.M., Eida, A.A., Hirt, H., 2020. Tailoring plant-associated microbial inoculants in agriculture: a roadmap for successful application. J. Exp. Bot.

Sagaram, U.S., DeAngelis, K.M., Trivedi, P., Andersen, G.L., Lu, S.E., Wang, N., 2009. Bacterial diversity analysis of Huanglongbing pathogen-infected citrus, using PhyloChip arrays and 16S rRNA gene clone library sequencing. Appl. Environ. Microbiol. 75, 1566–

1574.

Sakai, H., Lee, S.S., Tanaka, T., Numa, H., Kim, J., Kawahara, Y., Wakimoto, H., Yang, C., Iwamoto, M., Abe, T., 2013. Rice Annotation Project Database (RAP-DB): an integrative and interactive database for rice genomics. Plant Cell Physiol. 54, 6.

Saldajeno, M.G.B., Ito, M., Hyakumachi, M., 2012. Interaction between the plant growth-promoting fungus *Phoma* sp. GS8-2 and the arbuscular mycorrhizal fungus *Glomus mosseae*: impact on biocontrol of soil-borne diseases, microbial population, and plant growth. Australas. Plant Pathol. 41, 271–281.

Saleem, M., Ali, M.S., Hussain, S., Jabbar, A., Ashraf, M., Lee, Y.S., 2007. Marine natural products of fungal origin. Nat. Prod. Rep. 24, 1142–1152.

Sallam, A., Alqudah, A.M., Dawood, M.F.A., Baenziger, P.S., Börner, A., 2019. Drought Stress Tolerance in Wheat and Barley: Advances in Physiology, Breeding and Genetics Research. Int. J. Mol. Sci. 20, 3137.

Sampietro, D.A., Marín, P., Iglesias, J., Presello, D.A., Vattuone, M.A., Catalán, C.A.N., Jaen, M.T.G., 2010. A molecular based strategy for rapid diagnosis of toxigenic *Fusarium* species associated to cereal grains from Argentina. Fungal Biol. 114, 74–81.

Samson, R.A., Houbraken, J., Thrane, U., Frisvad, J.C., Andersen, B., 2019. Food and indoor fungi. Westerdijk Fungal Biodiversity Institute, 1.

Sanmartín, P., DeAraujo, A., Vasanthakumar, A., 2018. Melding the old with the new: trends in methods used to identify, monitor, and control microorganisms on cultural heritage materials. Microb. Ecol. 76, 64–80.

Sanschagrin, S., Yergeau, E., 2014. Next-generation sequencing of 16S ribosomal RNA gene amplicons. JoVE (Journal Vis. Exp. 51709.

Sardar, A., Nandi, A.K., Chattopadhyay, D., 2017. CBL-interacting protein kinase 6 negatively regulates immune response to *Pseudomonas syringae* in *Arabidopsis*. J. Exp. Bot. 68, 3573–3584.

Sarowar, S., Alam, S.T., Makandar, R., Lee, H., Trick, H.N., Dong, Y., Shah, J., 2019. Targeting the pattern-triggered immunity pathway to enhance resistance to *Fusarium graminearum.* Mol. Plant Pathol. 20, 626–640.

Sasaoka, N., Imamura, H., Kakizuka, A., 2018. A Trace Amount of Galactose, a Major Component of Milk Sugar, Allows Maturation of Glycoproteins during Sugar Starvation.

iScience 10, 211–221.

Savary, S., Willocquet, L., Pethybridge, S.J., Esker, P., McRoberts, N., Nelson, A., 2019. The global burden of pathogens and pests on major food crops. Nat. Ecol. Evol. 3, 430.

Savoia, D., 2012. Plant-derived antimicrobial compounds: alternatives to antibiotics. Future Microbiol. 7, 979–990.

Schaefer, C.F., Anthony, K., Krupa, S., Buchoff, J., Day, M., Hannay, T., Buetow, K.H., 2009. PID: the pathway interaction database. Nucleic Acids Res. 37, 674–679.

Schenk, P.M., Carvalhais, L.C., Kazan, K., 2012. Unraveling plant–microbe interactions: can multi-species transcriptomics help? Trends Biotechnol. 30, 177–184.

Schilling, A.G., Moller, E.M., Geiger, H.H., 1996. Polymerase chain reaction-based assays for species-specific detection of *Fusarium culmorum*, *F. graminearum*, and *F. avenaceum*. Phytopathology 86, 515–522.

Schirawski, J., Perlin, M., 2018. No Title. Plant–Microbe Interact. 2017—The good, bad Divers, 1.

Schisler, D.A., Yoshioka, M., Vaughan, M.M., Dunlap, C.A., Rooney, A.P., 2019. Nonviable biomass of biocontrol agent *Papiliotrema flavescen*s OH 182.9 3C enhances growth of *Fusarium graminearum* and counteracts viable biomass reduction of Fusarium head blight. Biol. Control 128, 48–55.

Schlemper, T.R., Dimitrov, M.R., Gutierrez, F.A.O.S., van Veen, J.A., Silveira, A.P.D., Kuramae, E.E., 2018. Effect of *Burkholderia tropica* and *Herbaspirillum frisingense* strains on sorghum growth is plant genotype dependent. PeerJ 6, 5346.

Schloss, P.D., Handelsman, J., 2005. Introducing DOTUR, a computer program for defining operational taxonomic units and estimating species richness. Appl. Environ. Microbiol. 71, 1501–1506.

Schloss, P.D., Handelsman, J., 2006. Toward a census of bacteria in soil. PLoS Comput. Biol. 2, 92.

Schloss, P.D., Westcott, S.L., Ryabin, T., Hall, J.R., Hartmann, M., Hollister, E.B., Lesniewski, R.A., Oakley, B.B., Parks, D.H., Robinson, C.J., Sahl, J.W., Stres, B., Thallinger, G.G., Van Horn, D.J., Weber, C.F., 2009. Introducing mothur: open-source, platform-independent, community-supported software for describing and comparing microbial communities. Appl. Environ. Microbiol. 75, 7537–7541.

Schoch, C.L., Seifert, K.A., Huhndorf, S., Robert, V., Spouge, J.L., Levesque, C.A., Chen, W., Consortium, F.B., List, F.B.C.A., 2012. Nuclear ribosomal internal transcribed spacer (ITS) region as a universal DNA barcode marker for Fungi. Proc. Natl. Acad. Sci. U. S. A. 109, 6241–6246.

Schreiner, K., Hagn, A., Kyselkova, M., Moenne-Loccoz, Y., Welzl, G., Munch, J.C., Schloter, M., 2010. Comparison of barley succession and take-all disease as environmental factors shaping the rhizobacterial community during take-all decline. Appl. Environ. Microbiol. 76, 4703–4712.

Serba, D.D., Perumal, R., Tesso, T.T., Min, D., 2017. Status of global pearl millet breeding programs and the way forward. Crop Sci. 57, 2891–2905.

Shade, A., 2017. Diversity is the question, not the answer. ISME J. 11, 1.

Shah, S., Ramanan, V.V., Singh, A., Singh, A.K., 2018. Potential and prospect of plant growth promoting rhizobacteria in lentil. Sci. lentil Prod.Satish Ser. Publ. House, Delhi, India, 1.

Sharma, R., Thakur, R.P., Senthilvel, S., Nayak, S., Reddy, S.V., Rao, V.P., Varshney, R.K., 2011. Identification and characterization of toxigenic Fusaria associated with sorghum grain mold complex in India. Mycopathologia 171, 223–230.

Shearin, Z.R.C., Filipek, M., Desai, R., Bickford, W.A., Kowalski, K.P., Clay, K., 2018. Fungal endophytes from seeds of invasive, non-native *Phragmites australis* and their potential role in germination and seedling growth. Plant Soil 422, 183–194.

Shendure, J., 2008. The beginning of the end for microarrays? Nat. Methods 5, 585.

Shi, Y., Yang, H., Zhang, T., Sun, J., Lou, K., 2014. Illumina-based analysis of endophytic bacterial diversity and space-time dynamics in sugar beet on the north slope of Tianshan mountain. Appl. Microbiol. Biotechnol. 98, 6375–6385.

Shiri, M., Rahjoo, V., Ebrahimi, L., 2017. Reaction of Some Sorghum Varieties Against Grain Mold and Fumonisin Accumulation. J. Plant Physiol. Breed. 7, 91–97.

Shiringani, A.L., Frisch, M., Friedt, W., 2010. Genetic mapping of QTLs for sugar-related traits in a RIL population of *Sorghum bicolor* L. Moench. Theor. Appl. Genet. 121, 323–336.

Short, F.L., Murdoch, S.L., Ryan, R.P., 2014. Polybacterial human disease: the ills of social networking. Trends Microbiol. 22, 508–516.

Singh, J., Behal, A., Singla, N., Joshi, A., Birbian, N., Singh, S., Bali, V., Batra, N., 2009.

Metagenomics: Concept, methodology, ecological inference and recent advances. Biotechnol. J. Healthc. Nutr. Technol. 4, 480–494.

Singh, M., Upadhyaya, H.D., 2015. Genetic and Genomic Resources for Grain Cereals Improvement. Academic Press. 1.

Singh, R., Rastogi, S., Dwivedi, U.N., 2010. Phenylpropanoid metabolism in ripening fruits. Compr. Rev. Food Sci. Food Saf. 9, 398–416.

Sivakumar, S., Dhasarathan, M., Karthikeyan, A., Bharathi, P., Ganesamurthy, K., Senthil, N., 2019. Population structure and association mapping studies for yield-related traits in Maize (Zea mays L.). Curr. Plant Biol. 100103.

Snelders, N.C., Kettles, G.J., Rudd, J.J., Thomma, B.P.H.J., 2018. Plant pathogen effector proteins as manipulators of host microbiomes? Mol. Plant Pathol. 19, 257–259.

Snyder, L.A.S., Loman, N., Pallen, M.J., Penn, C.W., 2009. Next-generation sequencing—the promise and perils of charting the great microbial unknown. Microb. Ecol. 57, 1–3.

Solomon, P.S., Oliver, R.P., 2001. The nitrogen content of the tomato leaf apoplast increases during infection by *Cladosporium fulvum*. Planta 213, 241–249.

Sorahinobar, M., Soltanloo, H., Niknam, V., Ebrahimzadeh, H., Moradi, B., Safaie, N., Behmanesh, M., Bahram, M., 2017. Physiological and molecular responses of resistant and susceptible wheat cultivars to *Fusarium graminearum* mycotoxin extract. Can. J. plant Pathol. 39, 444–453.

Srivastava, S., Kadooka, C., Uchida, J.Y., 2018. *Fusarium* species as pathogen on orchids. Microbiol. Res. 207, 188–195.

Stach, E.M., Bull, A.T., 2005. Estimating and comparing the diversity of marine actinobacteria. Antonie Van Leeuwenhoek 87, 3–9.

Stone, B.W.G., Weingarten, E.A., Jackson, C.R., 2018. The role of the phyllosphere microbiome in plant health and function. Annu. Plant Rev. 1, 1–24.

Summerell, B.A., Salleh, B., Leslie, J.F., 2003. A utilitarian approach to *Fusarium* identification. Plant Dis. 87, 117–128.

Sun, P.-F., Fang, W.-T., Shin, L.-Y., Wei, J.-Y., Fu, S.-F., Chou, J.-Y., 2014. Indole-3-acetic acid-producing yeasts in the phyllosphere of the carnivorous plant *Drosera indica* L. PLoS One 9, 114196.

Sun, Y., Xiao, J., Jia, X., Ke, P., He, L., Cao, A., Wang, H., Wu, Y., Gao, X., Wang, X., 2016.

The role of wheat jasmonic acid and ethylene pathways in response to *Fusarium graminearum* infection. Plant Growth Regul. 80, 69–77.

Tagliaferri, R., Formenti, E., Wit, E., 2014. Computational intelligence methods for bioinformatics and biostatistics. Springer, 1.

Tamayo, P., Slonim, D., Mesirov, J., Zhu, Q., Kitareewan, S., Dmitrovsky, E., Lander, E.S., Golub, T.R., 1999. Interpreting patterns of gene expression with self-organizing maps: methods and application to hematopoietic differentiation. Proc. Natl. Acad. Sci. 96, 2907–2912.

Tamura, K., Peterson, D., Peterson, N., Stecher, G., Nei, M., Kumar, S., 2011. MEGA5: molecular evolutionary genetics analysis using maximum likelihood, evolutionary distance, and maximum parsimony methods. Mol. Biol. Evol. 28, 2731–2739.

Tao, Y., Manners, J.M., Ludlow, M.M., Henzell, R.G., 1993. DNA polymorphisms in grain sorghum (*Sorghum bicolor* (L.) Moench). Theor. Appl. Genet. 86, 679–688.

Tarekegn, G., McLaren, N.W., Swart, W.J., 2006. Effects of weather variables on grain mould of sorghum in South Africa. Plant Pathol. 55, 238–245.

Tauzin, A.S., Giardina, T., 2014. Sucrose and invertases, a part of the plant defense response to the biotic stresses. Front. Plant Sci. 5, 293.

Tavazoie, S., Hughes, J.D., Campbell, M.J., Cho, R.J., Church, G.M., 1999. Systematic determination of genetic network architecture. Nat. Genet. 22, 281–285.

TeBeest, D., Kirkpatrick, T., Cartwright, R., 2004. Common and Important Diseases of Grain Sorghum. Grain sorghum Prod. Handb. 37–46.

Tedersoo, L., Sánchez-Ramírez, S., Koljalg, U., Bahram, M., Döring, M., Schigel, D., May, T., Ryberg, M., Abarenkov, K., 2018. High-level classification of the Fungi and a tool for evolutionary ecological analyses. Fungal Divers. 90, 135–159.

Tett, A.J., Turner, T.R., Poole, P.S., 2012. Genomics and the Rhizosphere. eLS, 1.

Thakur, R.P., Reddy, B.V.S., Indira, S., Rao, V.P., Navi, S.S., Yang, X.B., Ramesh, S., 2006. Sorghum Grain Mold Information Bulletin No. 72.

Tholl, D., 2015. Biosynthesis and biological functions of terpenoids in plants, in: Biotechnology of Isoprenoids. Springer, 63–106.

Thomas, P.D., Campbell, M.J., Kejariwal, A., Mi, H., Karlak, B., Daverman, R., Diemer, K., Muruganujan, A., Narechania, A., 2003. PANTHER: a library of protein families and

subfamilies indexed by function. Genome Res. 13, 2129–2141.

Thornsberry, J.M., Goodman, M.M., Doebley, J., Kresovich, S., Nielsen, D., Buckler, E.S., 2001. Dwarf8 polymorphisms associate with variation in flowering time. Nat. Genet. 28, 286–289.

Tian, L., Liu, L., Yin, Y., Huang, M., Chen, Y., Xu, X., Wu, P., Li, M., Wu, G., Jiang, H., 2017. Heterogeneity in the expression and subcellular localization of Polyol/monosaccharide transporter genes in Lotus japonicus. PLoS One. 12.

Tivoli, B., Banniza, S., 2007. Comparison of the epidemiology of *ascochyta* blights on grain legumes, in: Ascochyta Blights of Grain Legumes. Springer, pp. 59–76.

Toju, H., Yamamoto, S., Tanabe, A.S., Hayakawa, T., Ishii, H.S., 2016. Network modules and hubs in plant-root fungal biomes. J. R. Soc. Interface 13, 20151097.

Trapnell, C., Roberts, A., Goff, L., Pertea, G., Kim, D., Kelley, D.R., Pimentel, H., Salzberg, S.L., Rinn, J.L., Pachter, L., 2012. Differential gene and transcript expression analysis of RNA-seq experiments with TopHat and Cufflinks. Nat. Protoc. 7, 562.

Trapnell, C., Williams, B.A., Pertea, G., Mortazavi, A., Kwan, G., Van Baren, M.J., Salzberg, S.L., Wold, B.J., Pachter, L., 2010. Transcript assembly and quantification by RNA-Seq reveals unannotated transcripts and isoform switching during cell differentiation. Nat. Biotechnol. 28, 511–515.

Trimboli, D.S., Burgess, L.W., 1985. Fungi associated with basal stalk rot and root rot of dryland grain sorghum in New South Wales. Plant Prot. Q. 1, 3–9.

Tripathi, M., Singh, D.N., Vikram, S., Singh, V.S., Kumar, S., 2018. Metagenomic approach towards bioprospection of novel biomolecule (s) and environmental bioremediation. Annu. Res. Rev. Biol. 1–12.

Trivedi, P., Duan, Y., Wang, N., 2010. Huanglongbing, a systemic disease, restructures the bacterial community associated with citrus roots. Appl. Environ. Microbiol. 76, 3427–3436.

Tsolakidou, M.-D., Stringlis, I.A., Fanega-Sleziak, N., Papageorgiou, S., Tsalakou, A., Pantelides, I.S., 2019. Rhizosphere-enriched microbes as a pool to design synthetic communities for reproducible beneficial outputs. FEMS Microbiol. Ecol. 95, 138.

Tsurumaru, H., Okubo, T., Okazaki, K., Hashimoto, M., Kakizaki, K., Hanzawa, E., Takahashi, H., Asanome, N., Tanaka, F., Sekiyama, Y., Ikeda, S., Minamisawa, K., 2015.

Metagenomic analysis of the bacterial community associated with the taproot of sugar beet. Microbes Environ. 30, 63–69.

Turbat, A., Rakk, D., Vigneshwari, A., Kocsubé, S., Thu, H., Szepesi, Á., Bakacsy, L., D Škrbić, B., Jigjiddorj, E.-A., Vágvölgyi, C., 2020. Characterization of the Plant Growth-Promoting Activities of Endophytic Fungi Isolated from *Sophora flavescens*. Microorganisms 8, 683.

Turner, T.R., James, E.K., Poole, P.S., 2013. The plant microbiome. Genome Biol. 14, 1–10.

Upadhyaya, H.D., Sharma, S., Dwivedi, S.L., Singh, S.K., 2014. Sorghum Genetic Resources: Conservation and Diversity Assessment for Enhanced Utilization in Sorghum Improvement. Genet. Genomics Breed. Sorghum 28.

Upadhyaya, H.D., Wang, Y.-H., Sharma, R., Sharma, S., 2013. Identification of genetic markers linked to anthracnose resistance in sorghum using association analysis. Theor. Appl. Genet. 126, 1649–1657.

Uppalapati, S.R., Ishiga, Y., Doraiswamy, V., Bedair, M., Mittal, S., Chen, J., Nakashima, J., Tang, Y., Tadege, M., Ratet, P., Chen, R., Schultheiss, H., Mysore, K.S., 2012. Loss of abaxial leaf epicuticular wax in *Medicago truncatula* irg1/palm1 mutants results in reduced spore differentiation of anthracnose and nonhost rust pathogens. Plant Cell 24, 353–370.

Uppalapati, S.R., Ishiga, Y., Wangdi, T., Kunkel, B.N., Anand, A., Mysore, K.S., Bender, C.L., 2007. The phytotoxin coronatine contributes to pathogen fitness and is required for suppression of salicylic acid accumulation in tomato inoculated with *Pseudomonas syringae* pv. tomato DC3000. Mol. Plant-Microbe Interact. 20, 955–965.

Úrbez-Torres, J.R., Gubler, W.D., 2011. Susceptibility of grapevine pruning wounds to infection by *Lasiodiplodia theobromae* and *Neofusicoccum parvum*. Plant Pathol. 60, 261–270.

[USDA] United States Department of Agriculture., 2019. USDA assessments of commodity and trade issues.[cited 2019 February 12]. washington, dc. 2p. https://apps.fas.usda.gov/newgainapi/api/report pdf

van Dijk, E.L., Auger, H., Jaszczyszyn, Y., Thermes, C., 2014. Ten years of next-generation sequencing technology. Trends Genet. 30, 418–426.

van Elsas, J.D., Chiurazzi, M., Mallon, C.A., Elhottova, D., Kristufek, V., Salles, J.F., 2012.

Microbial diversity determines the invasion of soil by a bacterial pathogen. Proc. Natl. Acad. Sci. U. S. A. 109, 1159–1164.

Van Rooyen, D., 2019. Relationship between sorghum plant and grain characteristics, colonisation by mycotoxigenic *Fusarium spp*. and mycotoxin levels. University of the Free State.1.

Vanamala, J.K.P., Massey, A.R., Pinnamaneni, S.R., Reddivari, L., Reardon, K.F., 2018. Grain and sweet sorghum (Sorghum bicolor L. Moench) serves as a novel source of bioactive compounds for human health. Crit. Rev. Food Sci. Nutr. 58, 2867–2881.

Vannier, N., Agler, M., Hacquard, S., 2019. Microbiota-mediated disease resistance in plants. PLoS Pathog. 15.

Vardhan, S., Yadav, A.K., Pandey, A.K., Arora, D.K., 2013. Diversity analysis of biocontrol *Bacillus* isolated from rhizospheric soil of rice-wheat (*Oryza sativa-Triticum aestivum* L.) at India. J. Antibiot. (Tokyo). 66, 485.

Vernikos, G., Medini, D., Riley, D.R., Tettelin, H., 2015. Ten years of pan-genome analyses. Curr. Opin. Microbiol. 23, 148–154.

Visarada, K., Aruna, C., 2019. Sorghum: A bundle of opportunities in the 21st century, in: Breeding Sorghum for Diverse End Uses. Elsevier, pp. 1–14.

Vo, K.T.X., Kim, C.-Y., Chandran, A.K.N., Jung, K.-H., An, G., Jeon, J.-S., 2015. Molecular insights into the function of ankyrin proteins in plants. J. plant Biol. 58, 271–284.

Vo, T.-T., Lee, C., Han, S.-I., Kim, J.Y., Kim, S., Choi, Y.-E., 2016. Effect of the ethylene precursor, 1-aminocyclopropane-1-carboxylic acid on different growth stages of *Haematococcus pluvialis*. Bioresour. Technol. 220, 85–93.

Von Mark, V.C., Dierig, D.A., 2014. Industrial Crops: Breeding for BioEnergy and Bioproducts. Springer. 9.

Vorholt, J.A., 2012. Microbial life in the phyllosphere. Nat. Rev. Microbiol. 10, 828–840.

Waliyar, F., Ravinder Reddy, C., Alur, A.S., Reddy, S. V, Reddy, B.V.S., Reddy, A.R., Rai, K.N., Gowda, C.L.L., 2008. Management of grain mold and mycotoxins in sorghum, 1.

Wallace, J.G., Kremling, K.A., Kovar, L.L., Buckler, E.S., 2018. Quantitative genetics of the maize leaf microbiome. Phytobiomes J. 2, 208–224.

Walter, S., Nicholson, P., Doohan, F.M., 2010. Action and reaction of host and pathogen during Fusarium head blight disease. New Phytol. 185, 54–66.

Wang, Y.-H., Upadhyaya, H.D., Dweikat, I., 2016. Sorghum, in: Genetic and Genomic Resources for Grain Cereals Improvement. Elsevier, pp. 227–251.

Wei, J., Ma, W., Liu, X., Xu, J., Zhang, N., Shao, W., Chen, R., Xu, J., Yu, G., 2020. First Report of Leaf Spot on Sorghum bicolor Caused by *Alternaria tenuissima* in China. Plant Dis. 1.

Wei, Y., Liu, W., Hu, W., Liu, G., Wu, C., Liu, W., Zeng, H., He, C., Shi, H., 2017. Genome-wide analysis of autophagy-related genes in banana highlights MaATG8s in cell death and autophagy in immune response to *Fusarium* wilt. Plant Cell Rep. 36, 1237–1250.

Wei, Z., Jousset, A., 2017. Plant breeding goes microbial. Trends Plant Sci. 22, 555–558.

Weidenbach, D., Jansen, M., Franke, R.B., Hensel, G., Weissgerber, W., Ulferts, S., Jansen, I., Schreiber, L., Korzun, V., Pontzen, R., Kumlehn, J., Pillen, K., Schaffrath, U., 2014. Evolutionary conserved function of barley and *Arabidopsis* 3-ketoacyl-CoA synthases in providing wax signals for germination of powdery mildew fungi. Plant Physiol. 166, 1621–1633.

Welbaum, G.E., Sturz, A. V, Dong, Z., Nowak, J., 2004. Managing soil microorganisms to improve productivity of agro-ecosystems. CRC. Crit. Rev. Plant Sci. 23, 175–193.

Westermann, A.J., Barquist, L., Vogel, J., 2017. Resolving host–pathogen interactions by dual RNA-seq. PLoS Pathog. 13.

Whipps, J.M., Hand, P., Pink, D., Bending, G.D., 2008b. Phyllosphere microbiology with special reference to diversity and plant genotype. J. Appl. Microbiol. 105, 1744–55.

Whipps, J.M., Hand, P., Pink, D.A.C., Bending, G.D., 2008a. Human pathogens and the phyllosphere. Adv. Appl. Microbiol. 64, 183–221.

White, T.J., Bruns, T., Lee, S., Taylor, J., 1990. Amplification and direct sequencing of fungal ribosomal RNA genes for phylogenetics. PCR Protoc. a Guid. to methods Appl. 18, 315–322.

Wille, L., Messmer, M.M., Studer, B., Hohmann, P., 2019. Insights to plant–microbe interactions provide opportunities to improve resistance breeding against root diseases in grain legumes. Plant. Cell Environ. 42, 20–40.

Williams, T.R., Moyne, A.-L., Harris, L.J., Marco, M.L., 2013. Season, irrigation, leaf age, and Escherichia coli inoculation influence the bacterial diversity in the lettuce phyllosphere. PLoS One 8, 1–14.

Woldesemayat, A.A., Van Heusden, P., Ndimba, B.K., Christoffels, A., 2017. An integrated and comparative approach towards identification, characterization and functional annotation of candidate genes for drought tolerance in sorghum (*Sorghum bicolor* (L.) Moench). BMC Genet. 18, 119.

Wu, S., Wu, F., Jiang, Z., 2017. Identification of hub genes, key miRNAs and potential molecular mechanisms of colorectal cancer. Oncol. Rep. 38, 2043–2050.

Wust, P.K., Nacke, H., Kaiser, K., Marhan, S., Sikorski, J., Kandeler, E., Daniel, R., Overmann, J., 2016. Estimates of Soil Bacterial Ribosome Content and Diversity Are Significantly Affected by the Nucleic Acid Extraction Method Employed. Appl. Environ. Microbiol. 82, 2595–2607.

Xie, Q., Tang, S., Wang, Z., n.d. The prospect of sweet sorghum as the source for high biomass crop. J Agric Sci Bot 2018; 2 5-11.6 J Agric Sci Bot 2018 Vol. 2 Issue 3, 3.

Xia, K., Liu, T.A.O., Ouyang, J.I.E., Wang, R.E.N., Fan, T., Zhang, M., 2011. Genome-wide identification, classification, and expression analysis of autophagy-associated gene homologues in rice (*Oryza sativa* L.). DNA Res. 18, 363–377.

Xie, C., Mao, X., Huang, J., Ding, Y., Wu, J., Dong, S., Kong, L., Gao, G., Li, C.-Y., Wei, L., 2011. KOBAS 2.0: a web server for annotation and identification of enriched pathways and diseases. Nucleic Acids Res. 39, 316–322.

Xu, J., Jiang, Y., Hu, L., Liu, K.-J., Xu, X.-D., Qin, P.-W., Kong, F.-X., Xin, Z.-X., 2019. First Report of Rough Leaf Spot of Sorghum Caused by *Ascochyta sorghi* in China. Plant Dis. 103, 149.

Xu, L., Naylor, D., Dong, Z., Simmons, T., Pierroz, G., Hixson, K.K., Kim, Y.M., Zink, E.M., Engbrecht, K.M., Wang, Y., Gao, C., DeGraaf, S., Madera, M.A., Sievert, J.A., Hollingsworth, J., Birdseye, D., Scheller, H. V, Hutmacher, R., Dahlberg, J., Jansson, C., Taylor, J.W., Lemaux, P.G., Coleman-Derr, D., 2018. Drought delays development of the sorghum root microbiome and enriches for monoderm bacteria. Proc. Natl. Acad. Sci. U. S. A. 115, 4284–4293.

Xu, L., Naylor, D., Dong, Z., Simmons, T., Pierroz, G., Hixson, K.K., Kim, Y.M., Zink, E.M., Engbrecht, K.M., Wang, Y., Gao, C., DeGraaf, S., Madera, M.A., Sievert, J.A., Hollingsworth, J., Birdseye, D., Scheller, H. V, Hutmacher, R., Dahlberg, J., Jansson, C., Taylor, J.W., Lemaux, P.G., Coleman-Derr, D., 2018. Drought delays development of the

sorghum root microbiome and enriches for monoderm bacteria. Proc. Natl. Acad. Sci. U. S. A. 115, 4284–4293.

Yadav, A.N., 2017. Beneficial role of extremophilic microbes for plant health and soil fertility. J Agric Sci 1, 30.

Yaish, M.W., Antony, I., Glick, B.R., 2015. Isolation and characterization of endophytic plant growth-promoting bacteria from date palm tree (*Phoenix dactylifera* L.) and their potential role in salinity tolerance. Antonie Van Leeuwenhoek 107, 1519–1532.

Yalamanchili, H.K., Wan, Y., Liu, Z., 2017. Data Analysis Pipeline for RNA-seq Experiments: From Differential Expression to Cryptic Splicing. Curr. Protoc. Bioinforma. 59, 11.15. 1-11.15. 21.

Yang, H., Li, J., Xiao, Y., Gu, Y., Liu, H., Liang, Y., Liu, X., Hu, J., Meng, D., Yin, H., 2017. An integrated insight into the relationship between soil microbial community and tobacco bacterial wilt disease. Front. Microbiol. 8, 2179.

Yang, W., de Oliveira, A.C., Godwin, I., Schertz, K., Bennetzen, J.L., 1996. Comparison of DNA marker technologies in characterizing plant genome diversity: variability in Chinese sorghums. Crop Sci. 36, 1669–1676.

Ye, J., Zhang, Y., Cui, H., Liu, J., Wu, Y., Cheng, Y., Xu, H., Huang, X., Li, S., Zhou, A., 2018. WEGO 2.0: a web tool for analyzing and plotting GO annotations, 2018 update. Nucleic Acids Res. 46, 71–75.

Yerkovich, N., Palazzini, J.M., Sulyok, M., Chulze, S.N., 2017. Trichothecene genotypes, chemotypes and zearalenone production by *Fusarium graminearum* species complex strains causing Fusarium head blight in Argentina during an epidemic and non-epidemic season. Trop. Plant Pathol. 42, 190–196.

Yilmaz, P., Parfrey, L.W., Yarza, P., Gerken, J., Pruesse, E., Quast, C., Schweer, T., Peplies, J., Ludwig, W., Glöckner, F.O., 2014. The SILVA and “all-species living tree project (LTP)” taxonomic frameworks. Nucleic Acids Res. 42, 643–648.

Yu, J., Holland, J.B., McMullen, M.D., Buckler, E.S., 2008. Genetic design and statistical power of nested association mapping in maize. Genetics 178, 539–551.

Yuan, G., He, X., Li, H., Xiang, K., Liu, L., Zou, C., Lin, H., Wu, J., Zhang, Z., Pan, G., 2019. Transcriptomic responses in resistant and susceptible maize infected with *Fusarium graminearum*. Crop J, 1.

Yuan, Y., Gao, M., 2015. Genomic analysis of a ginger pathogen *Bacillus pumilus* providing the understanding to the pathogenesis and the novel control strategy. Sci. Rep. 5, 10259.
Yuan, Y., Gao, M., 2015. Genomic analysis of a ginger pathogen *Bacillus pumilus* providing the understanding to the pathogenesis and the novel control strategy. Sci. Rep. 5, 10259.
Yue, W., Nie, X., Cui, L., Zhi, Y., Zhang, T., Du, X., Song, W., 2018. Genome-wide sequence and expressional analysis of autophagy Gene family in bread wheat (*Triticum aestivum* L.). J. Plant Physiol. 229, 7–21.

Zambrano, L.S., Usai, G., Vangelisti, A., Mascagni, F., Giordani, T., Bernardi, R., Cavallini, A., Gucci, R., Caruso, G., D'Onofrio, C., 2017. Cultivar-specific transcriptome prediction and annotation in *Ficus carica* L. Genomics data 13, 64–66.

Zarraonaindia, I., Owens, S.M., Weisenhorn, P., West, K., Hampton-Marcell, J., Lax, S., Bokulich, N.A., Mills, D.A., Martin, G., Taghavi, S., van der Lelie, D., Gilbert, J.A., 2015. The soil microbiome influences grapevine-associated microbiota. MBio. 6.

Zegeye, E.K., Brislawn, C.J., Farris, Y., Fansler, S.J., Hofmockel, K.S., Jansson, J.K., Wright, A.T., Graham, E.B., Naylor, D., McClure, R.S., 2019. Selection, succession, and stabilization of soil microbial consortia. Msystems 4.

Zhang, J., Chen, L., Fu, C., Wang, L., Liu, H., Cheng, Y., Li, S., Deng, Q., Wang, S., Zhu, J., 2017. Comparative transcriptome analyses of gene expression changes triggered by *Rhizoctonia solani* AG1 IA infection in resistant and susceptible rice varieties. Front. Plant Sci. 8, 1422.

Zhang, X.-W., Jia, L.-J., Zhang, Y., Jiang, G., Li, X., Zhang, D., Tang, W.-H., 2012. In planta stage-specific fungal gene profiling elucidates the molecular strategies of *Fusarium graminearum* growing inside wheat coleoptiles. Plant Cell 24, 5159–5176.

Zhang, Y., Chen, F.-S., Wu, X.-Q., Luan, F.-G., Zhang, L.-P., Fang, X.-M., Wan, S.-Z., Hu, X.-F., Ye, J.-R., 2018a. Isolation and characterization of two phosphate-solubilizing fungi from rhizosphere soil of moso bamboo and their functional capacities when exposed to different phosphorus sources and pH environments. PLoS One 13.

Zhang, Z., Luo, L., Tan, X., Kong, X., Yang, J., Wang, D., Zhang, D., Jin, D., Liu, Y., 2018b. Pumpkin powdery mildew disease severity influences the fungal diversity of the phyllosphere. PeerJ 6, 4559.

Zheng, L., Abhyankar, W., Ouwerling, N., Dekker, H.L., van Veen, H., van der Wel, N.N.,

Roseboom, W., de Koning, L.J., Brul, S., de Koster, C.G., 2016. *Bacillus subtilis* spore inner membrane proteome. J. Proteome Res. 15, 585–594.

Zhou, D., Jing, T., Chen, Y., Wang, F., Qi, D., Feng, R., Xie, J., Li, H., 2019. Deciphering microbial diversity associated with *Fusarium* wilt-diseased and disease-free banana rhizosphere soil. BMC Microbiol. 19, 161.

Zhou, S., Gan, M., Zhu, J., Liu, X., Qiu, G., 2018. Assessment of Bioleaching Microbial Community Structure and Function Based on Next-Generation Sequencing Technologies. Minerals 8, 596.

Zhou, S., Hong, Q., Li, Y., Li, Q., Wang, M., 2018. Autophagy contributes to regulate the ROS levels and PCD progress in TMV-infected tomatoes. Plant Sci. 269, 12–19.

Zhou, S., Zhang, Y.K., Kremling, K.A., Ding, Y., Bennett, J.S., Bae, J.S., Kim, D.K., Ackerman, H.H., Kolomiets, M. V, Schmelz, E.A., 2019. Ethylene signaling regulates natural variation in the abundance of antifungal acetylated diferuloylsucroses and *Fusarium graminearum* resistance in maize seedling roots. New Phytol. 221, 2096–2111.

Zhou, X., Zhao, P., Wang, W., Zou, J., Cheng, T., Peng, X., Sun, M., 2015. A comprehensive, genome-wide analysis of autophagy-related genes identified in tobacco suggests a central role of autophagy in plant response to various environmental cues. DNA Res. 22, 245–257.

Zientara-Rytter, K., Łukomska, J., Moniuszko, G., Gwozdecki, R., Surowiecki, P., Lewandowska, M., Liszewska, F., Wawrzyńska, A., Sirko, A., 2011. Identification and functional analysis of Joka2, a tobacco member of the family of selective autophagy cargo receptors. Autophagy 7, 1145–1158.

APPENDIX A:

CHAPTER 3

Appendix Table 3A.1: Sorghum RILs disease ratings for resistance and severity in response to natural infection

RIL no	Disease Reaction class	Symptoms & lesions	Severity scale
19	R	1-10%	1-3
29	R	1-10%	1-3
102	R	1-10%	1-3
103	R	1-10%	1-3
112	R	1-10%	1-3
142	R	1-10%	1-3
148	R	1-10%	1-3
159	R	1-10%	1-3
161	R	1-10%	1-3
99	R	1-10%	1-3
212	R	1-10%	1-3
24	MR	11-30%	4-5
98	MR	11-30%	4-5
120	MR	11-30%	4-5
160	MR	11-30%	4-5
106	MR	11-30%	4-5
176	MR	11-30%	4-5
177	MR	11-30%	4-5
187	MR	11-30%	4-5
222	MR	11-30%	4-5
231	MR	11-30%	4-5
53	S	31-50%	6-7
78	S	31-50%	6-7
68	S	31-50%	6-7
134	S	31-50%	6-7
137	S	31-50%	6-7
140	S	31-50%	6-7
162	S	31-50%	6-7
167	S	31-50%	6-7
168	S	31-50%	6-7
171	S	31-50%	6-7
214	S	31-50%	6-7
244	S	31-50%	6-7
27	HS	51-75%	8-9
48	HS	51-75%	8-9
56	HS	51-75%	8-9
66	HS	51-75%	8-9
105	HS	51-75%	8-9
118	HS	51-75%	8-9
125	HS	51-75%	8-9
131	HS	51-75%	8-9

132	HS	51-75%	8-9
136	HS	51-75%	8-9
180	HS	51-75%	8-9
221	HS	51-75%	8-9

Key: The mapping population was originally derived by selfing a single F1 plant from *S. bicolor* grain (M71) and sweet sorghum (SS79) and advanced to the F9 generation by single seed descent (Shiringani et al., 2010)to produce a mapping population of 187 F9 recombinant inbred lines (RILs). The leaf samples were collected at the maturity stage of the sorghum RILs. Forty-five leaf samples were retrieved, and the foliar symptoms were scored according to the method described by (TeBeest et al. (2004). The susceptibility of the RILs was based on the ability to be successfully infected with the pathogen naturally. The scale presented visual foliar symptoms of four models that denoted, resistant, moderately resistant, susceptible and highly susceptible groups under natural infection. The RILs used in this study were chosen based on the even distribution of phenotype (foliar symptoms) across all disease groups.

Appendix Table 3A.2: Fungal taxa counts of sorghum RILs

OTUID	TAXONOMY						
	Domain	Phylum	Class	Order	Family	Genus	Species
909e1fce8a3b094f809bbaafe5dfbc49fd3761bb	Fungi	Basidiomycota	Ustilaginomycetes	Ustilaginales	Ustilaginaceae	Ustilago	Ustilago_kamerunensis
6196b3c562486b86ab10d3cacfc0ade4b5c1ee25	Fungi	Basidiomycota	Tremellomycetes	Filobasidiales	Filobasidiaceae	Filobasidium	NA
0e2584573f96744327e5120456fd6d50a7bfae0f	Fungi	Basidiomycota	Tremellomycetes	Tremellales	Tremellaceae	Cryptococcus	unidentified
2441987855ec0a378b3e27a2e27d8fea273552ae	Fungi	Basidiomycota	Tremellomycetes	Filobasidiales	Filobasidiaceae	Filobasidium	Filobasidium_magnum
41abcad3732332ae4419971eb3d6e6245d8639d	Fungi	Ascomycota	Sordariomycetes	Hypocreales	Nectriaceae	Gibberella	Gibberella_zeae
67d736568200974f12d34ee1c0ff532b8c28b4fc	Fungi	Basidiomycota	Tremellomycetes	Filobasidiales	Filobasidiaceae	Naganishia	Naganishia_albida
60853d18f1b9f685fb8d4424aa5e0496e7e256e2	Fungi	Basidiomycota	Tremellomycetes	Filobasidiales	Filobasidiaceae	Filobasidium	NA
402ea184ed0d45788fbc086878cf884f2001297f	Fungi	Basidiomycota	Tremellomycetes	Filobasidiales	Filobasidiaceae	Filobasidium	NA
887fd12c16aa966ff2fbc81bd57c18907957e853	Fungi	Basidiomycota	Tremellomycetes	Filobasidiales	Filobasidiaceae	Filobasidium	Filobasidium_magnum
03d6c92a025d100fd166f4af07cb07104a9d9ddf	Fungi	Basidiomycota	Tremellomycetes	Filobasidiales	Filobasidiaceae	Filobasidium	Filobasidium_magnum
1e922c5f874d6b65e983e4c85e9487f001e55f51	Fungi	Basidiomycota	Tremellomycetes	Filobasidiales	Filobasidiaceae	Filobasidium	Filobasidium_magnum
6b5b42d973350e6b1fc3ea6cd666ad89e68bfaf4	Fungi	Basidiomycota	Tremellomycetes	Filobasidiales	Filobasidiaceae	Filobasidium	Filobasidium_magnum
f29e8890cdb085dae496b78d61313f16987d56d6	Fungi	Basidiomycota	Tremellomycetes	Filobasidiales	Filobasidiaceae	Filobasidium	Filobasidium_magnum
0247a643761fbeca5976dcab29c44728a7753034	Fungi	Basidiomycota	Tremellomycetes	Filobasidiales	Filobasidiaceae	Filobasidium	Filobasidium_magnum
441ac3822e6230213ee06376cf604222723a6749	Fungi	Basidiomycota	Tremellomycetes	Filobasidiales	Filobasidiaceae	Filobasidium	Filobasidium_magnum
27b8a18ed4ace6f9de26ea2b5f3c255325259f4b	Fungi	Basidiomycota	Tremellomycetes	Filobasidiales	Filobasidiaceae	Filobasidium	Filobasidium_magnum
25722e9c56f80fed8d0ba3fcbc00b3f32b57642e	Fungi	Basidiomycota	Tremellomycetes	Filobasidiales	Filobasidiaceae	Filobasidium	Filobasidium_magnum
131aa858b7063c0127390ade32f34556c1970374	Fungi	Basidiomycota	Tremellomycetes	Filobasidiales	Filobasidiaceae	Filobasidium	Filobasidium_magnum
597ab9cfaf328cc008f9abf9217be5f667022969	Fungi	Basidiomycota	Tremellomycetes	Filobasidiales	Filobasidiaceae	Filobasidium	Filobasidium_magnum
0974b9cab6f1be58c8bbf58da6a7460b15b025ec	Fungi	Basidiomycota	Tremellomycetes	Filobasidiales	Filobasidiaceae	Filobasidium	Filobasidium_magnum
6e7b69c2c7b64c36369bed5930c84d6dee6d5874	Fungi	Basidiomycota	Tremellomycetes	Filobasidiales	Filobasidiaceae	Filobasidium	Filobasidium_magnum
0e923b9147e5125d62d9850afbd0c8ddac068f7c	Fungi	Basidiomycota	Tremellomycetes	Filobasidiales	Filobasidiaceae	Filobasidium	NA
603b5582c40f1c5703ce09095698b758d8debd36	Fungi	Basidiomycota	Tremellomycetes	Filobasidiales	Filobasidiaceae	Filobasidium	Filobasidium_magnum

58a677a563b6a5924b4c1cc878aeb25bd3c28820	Fungi	Basidiomycota	Tremellomycetes	Filobasidiales	Filobasidiaceae	Filobasidium	Filobasidium_magnum
21082f7e21f79916694f0c45b39c6c5f57bec23b	Fungi	Basidiomycota	Tremellomycetes	Filobasidiales	Filobasidiaceae	Filobasidium	NA
08b9fa1e97370cb2e1e370cd881515fedf14d882	Fungi	Basidiomycota	Tremellomycetes	Filobasidiales	Filobasidiaceae	Filobasidium	NA
06371af19a2080241ffb8717cb5b6d8dfd0ec3de	Fungi	Basidiomycota	Tremellomycetes	Filobasidiales	Filobasidiaceae	Naganishia	Naganishia_albida
7db822af5f5a8b87e07b16834a21d1efffe0f2b3	Fungi	Basidiomycota	Tremellomycetes	Filobasidiales	Filobasidiaceae	Naganishia	Naganishia_friedmannii
1f361a35f1ec89498558a770d59f632da4af4903	Fungi	Basidiomycota	Tremellomycetes	Filobasidiales	Filobasidiaceae	Naganishia	Naganishia_friedmannii
356ce33bd21c7efa3584ad33e00e22f7d8bab280	Fungi	Basidiomycota	Tremellomycetes	Filobasidiales	Filobasidiaceae	Filobasidium	unidentified
4924032a9a10707d16fec10873a0e2ef1e49bd87	Fungi	Basidiomycota	Microbotryomycetes	Sporidiobolales	Sporidiobolaceae	Rhodosporidiobolus	Rhodosporidiobolus_fluvialis
ca16465263472b09c7f665774794c98fddd96ca8	Fungi	Basidiomycota	Microbotryomycetes	Sporidiobolales	Sporidiobolaceae	Sporobolomyces	Sporobolomyces_oryzicola
4502834465b415b0ec2536b38478d6407e10b1d9	Fungi	Basidiomycota	Microbotryomycetes	Sporidiobolales	Sporidiobolaceae	Rhodosporidiobolus	Rhodosporidiobolus_fluvialis
bf8fd2d5d4e1b77f2319109e7510b8f1b694fe3b	Fungi	Basidiomycota	Tremellomycetes	Filobasidiales	Filobasidiaceae	Filobasidium	Filobasidium_magnum
03495e1a5276e523d626530b7d8eeb8d80718474	Fungi	unidentified	unidentified	unidentified	unidentified	unidentified	unidentified
2d44d5197feb9650833e79b8d0ac97161b748848	Fungi	unidentified	unidentified	unidentified	unidentified	unidentified	unidentified
3c192e51ebc4e5245b3fa30dc761f19b2e591209	Fungi	unidentified	unidentified	unidentified	unidentified	unidentified	unidentified
03d5c33c3db7c8f5735f4aac18e54a07f206e37a	Fungi	unidentified	unidentified	unidentified	unidentified	unidentified	unidentified
7987c6d25ee69b522cd912bc163120353e37a1e4	Fungi	unidentified	unidentified	unidentified	unidentified	unidentified	unidentified
536902b7a1ef7a7fa3a26bcc06ad301109d23f08	Fungi	unidentified	unidentified	unidentified	unidentified	unidentified	unidentified
5a10926a04aea74745b3961d22883320f49c1d32	Fungi	unidentified	unidentified	unidentified	unidentified	unidentified	unidentified
5beb85c0bd7706988a749a28a1e771ab38c6baaf	Fungi	unidentified	unidentified	unidentified	unidentified	unidentified	unidentified
65c4bd45fc85c328b22b6f07d94fd823d065cd94	Fungi	unidentified	unidentified	unidentified	unidentified	unidentified	unidentified
484214e394bc4affabd2a3d50ecb9d5bb52631cd	Fungi	unidentified	unidentified	unidentified	unidentified	unidentified	unidentified
29dd5564faba0a890d771b1bc8f29966cd0f037b	Fungi	unidentified	unidentified	unidentified	unidentified	unidentified	unidentified
62936f51b7eacdf3f402e87712e17836e3723f62	Fungi	unidentified	unidentified	unidentified	unidentified	unidentified	unidentified
3b9b26439706d054c45d9292202198d141ef2e9a	Fungi	unidentified	unidentified	unidentified	unidentified	unidentified	unidentified
095470191d3a331ef22995fe119f208077dd1544	Fungi	unidentified	unidentified	unidentified	unidentified	unidentified	unidentified
0dcdc221d98cf318a4503018a31e8922e85e104b	Fungi	unidentified	unidentified	unidentified	unidentified	unidentified	unidentified
6025e1d48511050d3972e55a9ada5d820206c744	Fungi	unidentified	unidentified	unidentified	unidentified	unidentified	unidentified
24c517a88ef64bfa665d0a86ce40be886d2f4d7c	Fungi	unidentified	unidentified	unidentified	unidentified	unidentified	unidentified

626868b9f8599903af588cc43d460a4f6dd967be	Fungi	unidentified	unidentified	unidentified	unidentified	unidentified	unidentified
309217233dbf06baffc57edd104d68da04552798	Fungi	unidentified	unidentified	unidentified	unidentified	unidentified	unidentified
152351381f7f8eb30163a63af5c79c8c9b4cac03	Fungi	unidentified	unidentified	unidentified	unidentified	unidentified	unidentified
36e0f5e6071d1e84ce662effa3ab55211640b7df	Fungi	unidentified	unidentified	unidentified	unidentified	unidentified	unidentified
9e6f9c0fc9e8274bfce61aeca6cc75ead11bee87	Fungi	unidentified	unidentified	unidentified	unidentified	unidentified	unidentified
71779ea7d4cc2c1919fe1e88bba405e5fefb3c13	Fungi	unidentified	unidentified	unidentified	unidentified	unidentified	unidentified
a1d78d27788db1845854df5ef0e2d72ec69975b1	Fungi	unidentified	unidentified	unidentified	unidentified	unidentified	unidentified
24d50cd31e38b7386b635100c1890904ccebe2f8	Fungi	unidentified	unidentified	unidentified	unidentified	unidentified	unidentified
SH630454.07FU_KX515887_reps_singleton	Fungi	unidentified	unidentified	unidentified	unidentified	unidentified	unidentified
5fad4304434d51c17a44b9befb36b3e25be5b7a6	Fungi	unidentified	unidentified	unidentified	unidentified	unidentified	unidentified
e55f91dba0da477ac9dfa1a2f1286033aac2c1ee	Fungi	unidentified	unidentified	unidentified	unidentified	unidentified	unidentified
6a3d91a05965720ecab309022d702325b16b80f2	Fungi	unidentified	unidentified	unidentified	unidentified	unidentified	unidentified
bea45c8971f6663429a52a142ed125384acea646	Fungi	unidentified	unidentified	unidentified	unidentified	unidentified	unidentified
2b78f3ea8e290a46c7d71413de4a6fbb0488ef6e	Fungi	unidentified	unidentified	unidentified	unidentified	unidentified	unidentified
c6ff0d67ce5e7ab0c31b56e7e941a01a2b48ecea	Fungi	unidentified	unidentified	unidentified	unidentified	unidentified	unidentified
888325ec776c85951deab95837e5e063f1aa66e0	Fungi	unidentified	unidentified	unidentified	unidentified	unidentified	unidentified
3838a5f37925bac2ee2222229cdcb2575e0aa6e2	Fungi	unidentified	unidentified	unidentified	unidentified	unidentified	unidentified
92d82defa084f898e3705cb7b05d5a85993febcc	Fungi	Basidiomycota	Tremellomycetes	Tremellales	Bulleribasidiaceae	Hannaella	Hannaella_luteola
1a5dcd92f3f7225faf77083c1d5f34aedc07c9d7	Fungi	Basidiomycota	Tremellomycetes	Tremellales	Bulleribasidiaceae	Vishniacozyma	Vishniacozyma_globispora
32773af38a03a5d50ea1f200087af1388e59b5b0	Fungi	Basidiomycota	Tremellomycetes	Tremellales	Bulleribasidiaceae	Vishniacozyma	Vishniacozyma_globispora
ddbe74a209358db98fcbca9204b14d9bca51fac1	Fungi	Basidiomycota	Tremellomycetes	Tremellales	Bulleribasidiaceae	Vishniacozyma	Vishniacozyma_globispora
66b7ec2a1faf82907ccb25dc5318735d78eac2aa	Fungi	Basidiomycota	Tremellomycetes	Tremellales	Trimorphomycetaceae	Saitozyma	Saitozyma_paraflava
2eab34a6eeb64c260008d9957558b0b6c8bc1dfb	Fungi	Basidiomycota	Tremellomycetes	Tremellales	Trimorphomycetaceae	Saitozyma	Saitozyma_flava
6bdcc81a15cdb9c3ff479c3d06a1e1289084c743	Fungi	Ascomycota	Dothideomycetes	Pleosporales	Pleosporaceae	Alternaria	Alternaria_eichhorniae
118af9181b5ddfb1e1b21aef4b2c7c74a83f5623	Fungi	Basidiomycota	Tremellomycetes	Tremellales	Bulleribasidiaceae	Hannaella	Hannaella_oryzae
ffcff92e1941e75fcce2750411dc1478bd06fbdd	Fungi	Basidiomycota	Tremellomycetes	Tremellales	Bulleribasidiaceae	Hannaella	Hannaella_oryzae
7c5eaf724c3854f045697d3ae90f376de677e4cd	Fungi	Basidiomycota	Tremellomycetes	Tremellales	Bulleribasidiaceae	Dioszegia	Dioszegia_takashimae
194005d01c9280d0910d0ff6246d5d96e6dd3f60	Fungi	Basidiomycota	Tremellomycetes	Tremellales	Bulleribasidiaceae	Dioszegia	Dioszegia_takashimae

7b475cbabccabc609ab327a4f1aaac2df467e9e0	Fungi	Basidiomycota	Tremellomycetes	Tremellales	Bulleribasidiaceae	Hannaella	Hannaella_sinensis
225b26608ca5d332eba7c90ef13761c0715ad5aa	Fungi	Basidiomycota	Tremellomycetes	Tremellales	Bulleribasidiaceae	Hannaella	NA
053c1efcde072ba05ce0fcb4fdf0fb54932930a9	Fungi	Basidiomycota	Tremellomycetes	Tremellales	Bulleribasidiaceae	Hannaella	Hannaella_siamensis
1b76dc3e969dd3c37554a3f17deebce8ef6b79e8	Fungi	Basidiomycota	Tremellomycetes	Tremellales	Bulleribasidiaceae	Hannaella	NA
94868471f8780949bc3c498306ddbd618fb74f96	Fungi	Basidiomycota	Tremellomycetes	Tremellales	Bulleribasidiaceae	Hannaella	Hannaella_siamensis
0ecd723741f6740aaedf9102b7db440c05b6fc31	Fungi	Basidiomycota	Tremellomycetes	Tremellales	Bulleribasidiaceae	Hannaella	NA
cc2f4e953a792215890622879fc2271fb0dd059f	Fungi	Basidiomycota	Tremellomycetes	Tremellales	Bulleribasidiaceae	Hannaella	Hannaella_siamensis
a6ea50f5b5e362db0e2d0e023b83e35540eec390	Fungi	Basidiomycota	Tremellomycetes	Tremellales	Bulleribasidiaceae	Hannaella	Hannaella_siamensis
96dddf40f951254109d82e332970e8606141ecb2	Fungi	Basidiomycota	Tremellomycetes	Tremellales	Bulleribasidiaceae	Hannaella	Hannaella_siamensis
077b682cd764fa8a6be9877bd755ec08561ff2c5	Fungi	Basidiomycota	Tremellomycetes	Tremellales	Bulleribasidiaceae	Hannaella	Hannaella_siamensis
481c9cab5f3fa967e68470aac70ea3f05a6a1987	Fungi	Basidiomycota	Tremellomycetes	Tremellales	Bulleribasidiaceae	Hannaella	Hannaella_luteola
4d7d4da5fcb9cc861a8f2622a6f82a846270380b	Fungi	Basidiomycota	Tremellomycetes	Tremellales	Bulleribasidiaceae	Hannaella	NA
27739868049300247627fb5837c524e6cc3e61ee	Fungi	Basidiomycota	Tremellomycetes	Tremellales	Bulleribasidiaceae	Hannaella	Hannaella_luteola
abcc13b412dac96f7989260a017eea48ebe9d37b	Fungi	Basidiomycota	Tremellomycetes	Tremellales	Bulleribasidiaceae	Hannaella	Hannaella_luteola
00dec8f288db2e0db2d60831f0a32572446ad226	Fungi	Basidiomycota	Tremellomycetes	Tremellales	Bulleribasidiaceae	Hannaella	Hannaella_luteola
1c9eb326549bc3b876fc84758e7f2e081646847d	Fungi	Basidiomycota	Tremellomycetes	Tremellales	Bulleribasidiaceae	Hannaella	Hannaella_luteola
24d01e97d0ef1c6498fb1cdb7fb5e0c5def9cc7e	Fungi	Basidiomycota	Tremellomycetes	Tremellales	Bulleribasidiaceae	Hannaella	Hannaella_luteola
16164be9003c372221402d7c3e61fb4d9e4caae8	Fungi	Basidiomycota	Tremellomycetes	Tremellales	Bulleribasidiaceae	Hannaella	Hannaella_sinensis
221a32b281a023a33457be5fa67256bf396e4994	Fungi	Basidiomycota	Tremellomycetes	Tremellales	Bulleribasidiaceae	Hannaella	Hannaella_luteola
c234b0d25469890b443602ed0f387248686719b7	Fungi	Basidiomycota	Tremellomycetes	Tremellales	Bulleribasidiaceae	Hannaella	Hannaella_sinensis
01a9803e303a5c3464ed469aa357a6c566301523	Fungi	Basidiomycota	Tremellomycetes	Tremellales	Bulleribasidiaceae	Hannaella	Hannaella_sinensis
67cf81113fe3083581fe8b28af5d900913b89791	Fungi	Basidiomycota	Tremellomycetes	Tremellales	Bulleribasidiaceae	Hannaella	Hannaella_sinensis
5927001eb688c4157759f35637f7ed537e8dcab3	Fungi	Basidiomycota	Tremellomycetes	Tremellales	Bulleribasidiaceae	Hannaella	Hannaella_sinensis
b9595357f056c6ccee739de34075c605465e5fab	Fungi	Basidiomycota	Tremellomycetes	Tremellales	Bulleribasidiaceae	Hannaella	Hannaella_sinensis

e96688e5ebf13b8bd40d7aa39eded5bb253347a0	Fungi	Basidiomycota	Tremellomycetes	Tremellales	Bulleribasidiaceae	Hannaella	Hannaella_sinensis
91cd791ac74d2088ff30c114e106ea9ad39f9cf5	Fungi	Basidiomycota	Tremellomycetes	Tremellales	Bulleribasidiaceae	Hannaella	Hannaella_sinensis
9aabefcf88634a5caeaf875a52343e04f01a82fe	Fungi	Basidiomycota	Tremellomycetes	Tremellales	Bulleribasidiaceae	Hannaella	Hannaella_sinensis
a5c43e81ad471b7f86229455c93eae93c685ce76	Fungi	Basidiomycota	Tremellomycetes	Tremellales	Bulleribasidiaceae	Hannaella	Hannaella_luteola
516194bea8e13f5a1cfe46278d91d420c61f7f32	Fungi	Ascomycota	Sordariomycetes	Hypocreales	Nectriaceae	Gibberella	Gibberella_zeae
a001aec982a5ddb0be4200e38fafb39431a45d56	Fungi	Ascomycota	Sordariomycetes	Hypocreales	Nectriaceae	Gibberella	Gibberella_zeae
51f1579e4f3ac7aa4f3179b0eda1f8fec3c2df47	Fungi	Basidiomycota	Tremellomycetes	Tremellales	Bulleribasidiaceae	Hannaella	NA
c37c0bf13aef7458e382ac4e832727bbe995142d	Fungi	Basidiomycota	Tremellomycetes	Tremellales	Bulleribasidiaceae	Hannaella	NA
6aca73137a5926d421b5ba51abc05f7f3db3ae9f	Fungi	Basidiomycota	Tremellomycetes	Filobasidiales	Filobasidiaceae	Naganishia	Naganishia_friedmannii
1480dc92416b5a8eeccd9b0753ac46050bf8dd9b	Fungi	Basidiomycota	Tremellomycetes	Tremellales	Bulleribasidiaceae	Hannaella	Hannaella_luteola
54922780f5c6861d40b20bf512840326d889ff3b	Fungi	Basidiomycota	Tremellomycetes	Tremellales	Rhynchogastremataceae	Papiliotrema	Papiliotrema_flavescens
11b088756734c941e21b25c8368347b8c6efdce3	Fungi	Basidiomycota	Tremellomycetes	Tremellales	Bulleribasidiaceae	Hannaella	Hannaella_sinensis
15e3519c096e1ba7093518b9a7fe162cf3c253cb	Fungi	Basidiomycota	Tremellomycetes	Tremellales	Bulleribasidiaceae	Hannaella	Hannaella_sinensis
3e4dc35c78d902080c81163ac8114c4ca297672d	Fungi	Basidiomycota	Tremellomycetes	Tremellales	Rhynchogastremataceae	Papiliotrema	Papiliotrema_flavescens
91301fac771e2b7ae380d675b6771686fc378cc4	Fungi	Basidiomycota	Tremellomycetes	Tremellales	Rhynchogastremataceae	Papiliotrema	Papiliotrema_flavescens
efef46e8c388257878160c6f38d19eebaa74ff40	Fungi	Basidiomycota	Tremellomycetes	Tremellales	Rhynchogastremataceae	Papiliotrema	Papiliotrema_flavescens
f56822cd57fe1b0af1ebf5186bcbbe646068fd6b	Fungi	Basidiomycota	Tremellomycetes	Tremellales	Rhynchogastremataceae	Papiliotrema	Papiliotrema_flavescens
03c0929ec2ee45cf91f740ac6c665c60e4c750d4	Fungi	Basidiomycota	Tremellomycetes	Tremellales	Rhynchogastremataceae	Papiliotrema	Papiliotrema_flavescens
13eba34c0a8d2ed9f4132e4c7d5aab025c004154	Fungi	Basidiomycota	Tremellomycetes	Tremellales	Bulleribasidiaceae	Hannaella	Hannaella_luteola
bb8b4dd5ce5915418ee12c9f360a1c78fce01181	Fungi	Basidiomycota	Tremellomycetes	Tremellales	Bulleribasidiaceae	Hannaella	NA
1a3f8a61556cfbe3e687df28690207be2cb55957	Fungi	Basidiomycota	Tremellomycetes	Tremellales	Bulleribasidiaceae	Hannaella	Hannaella_sinensis
01199f9325f109c6bb66ce16d2606bd1184a5cb5	Fungi	Basidiomycota	Tremellomycetes	Tremellales	Rhynchogastremataceae	Papiliotrema	Papiliotrema_laurentii
152e585881b9a46116e4532fc2b2d7e745de8b38	Fungi	Basidiomycota	Tremellomycetes	Tremellales	Rhynchogastremataceae	Papiliotrema	Papiliotrema_laurentii
fd006321f8394c9750739fd8ab66d9c55c70025c	Fungi	Basidiomycota	Tremellomycetes	Tremellales	Tremellaceae	Cryptococcus	unidentified
590d3b786e9b0fa9137e164f08e724addc5c553b	Fungi	Basidiomycota	Tremellomycetes	Tremellales	Rhynchogastremataceae	Papiliotrema	Papiliotrema_laurentii
91089d9f2bcff73f338debf59e48adc0f3ad1603	Fungi	Basidiomycota	Tremellomycetes	Tremellales	Rhynchogastremataceae	Papiliotrema	Papiliotrema_laurentii
ea479687db5c5172c1456a75a36c7fb030be29e5	Fungi	Basidiomycota	Tremellomycetes	Tremellales	Rhynchogastremataceae	Papiliotrema	Papiliotrema_laurentii
a6675edf90b6e41a555da027d66f233c54a34d44	Fungi	Basidiomycota	Tremellomycetes	Tremellales	Rhynchogastremataceae	Papiliotrema	Papiliotrema_laurentii

2f2b8662ce42e020b90f548cc737210a0f65cdcd	Fungi	Basidiomycota	Tremellomycetes	Tremellales	Tremellaceae	Cryptococcus	unidentified
164591ad6dfddf0b9be3a5efbb6b12e893bc27b7	Fungi	Basidiomycota	Tremellomycetes	Tremellales	Rhynchogastremataceae	Papiliotrema	Papiliotrema_laurentii
15e34dee2fd4036b8931386ff7d09c573339e57a	Fungi	Basidiomycota	Tremellomycetes	Tremellales	Rhynchogastremataceae	Papiliotrema	Papiliotrema_flavescens
803d968745b8e480ca6f6be678862c1e79583c28	Fungi	Basidiomycota	Tremellomycetes	Tremellales	Rhynchogastremataceae	Papiliotrema	Papiliotrema_flavescens
8d0836a26d659c1cc0a480ba667cee1ec30cc6a3	Fungi	Basidiomycota	Tremellomycetes	Tremellales	Rhynchogastremataceae	Papiliotrema	Papiliotrema_flavescens
8c371568752325fea3b570d0c59e0296543e7420	Fungi	Basidiomycota	Tremellomycetes	Tremellales	Rhynchogastremataceae	Papiliotrema	Papiliotrema_flavescens
2b3a30ebbdc60c0956db36d2ad34cca2e38a280b	Fungi	Basidiomycota	Tremellomycetes	Tremellales	Rhynchogastremataceae	Papiliotrema	Papiliotrema_flavescens
2b03b5a02d686deed84268d1dd845d6a895d2b82	Fungi	Basidiomycota	Tremellomycetes	Tremellales	Rhynchogastremataceae	Papiliotrema	Papiliotrema_flavescens
a447f524b7ec066fcd03a7bc0f888940c518a2b8	Fungi	Basidiomycota	Tremellomycetes	Tremellales	Rhynchogastremataceae	Papiliotrema	Papiliotrema_flavescens
098130524a2948fe396a3f3d1cd333544f6d10bb	Fungi	Basidiomycota	Tremellomycetes	Tremellales	Rhynchogastremataceae	Papiliotrema	Papiliotrema_flavescens
8e2f41a159a7f05d5246218f13f95ed56f271184	Fungi	Basidiomycota	Tremellomycetes	Tremellales	Rhynchogastremataceae	Papiliotrema	Papiliotrema_flavescens
f97b73eec4c5baa7013c760f04e904b3c84ecfd4	Fungi	Basidiomycota	Tremellomycetes	Tremellales	Rhynchogastremataceae	Papiliotrema	Papiliotrema_terrestris
024e93bd9cfd5a7676110fdb25e04aa6c138910d	Fungi	Basidiomycota	Tremellomycetes	Tremellales	Rhynchogastremataceae	Papiliotrema	Papiliotrema_flavescens
1d4ce57b112bea12662d57b7a9aed21fc1d60f5c	Fungi	Basidiomycota	Tremellomycetes	Tremellales	Rhynchogastremataceae	Papiliotrema	Papiliotrema_flavescens
0325bd5ef714b0bfeaaa8f288cd80b27d45b2d95	Fungi	Basidiomycota	Tremellomycetes	Tremellales	Rhynchogastremataceae	Papiliotrema	Papiliotrema_flavescens
9484978c6a9a3d83ec75da04e08bbe7ec446e3ab	Fungi	Basidiomycota	Tremellomycetes	Tremellales	Rhynchogastremataceae	Papiliotrema	Papiliotrema_flavescens
b78914d6e47b2a11f3968c33349a58032cb950ad	Fungi	Basidiomycota	Tremellomycetes	Tremellales	Rhynchogastremataceae	Papiliotrema	Papiliotrema_flavescens
168a5e6a004cfe614f2ab71ffdcac885e770cd09	Fungi	Basidiomycota	Tremellomycetes	Tremellales	Rhynchogastremataceae	Papiliotrema	Papiliotrema_flavescens
51d8a5cd36ec641952e766e5ca3f99ce57e0fe04	Fungi	Basidiomycota	Tremellomycetes	Tremellales	Rhynchogastremataceae	Papiliotrema	Papiliotrema_flavescens
56f0ce6f720b02564b88b3d0dc2ca3aa24f21048	Fungi	Basidiomycota	Tremellomycetes	Tremellales	Rhynchogastremataceae	Papiliotrema	Papiliotrema_flavescens
7e2943f91b4df62cd95191a62b854e0e28c6bdd8	Fungi	Basidiomycota	Tremellomycetes	Tremellales	Rhynchogastremataceae	Papiliotrema	Papiliotrema_flavescens
b078fcb835bb7b6478cde72a2cb3626a76df6e7c	Fungi	Basidiomycota	Tremellomycetes	Tremellales	Rhynchogastremataceae	Papiliotrema	Papiliotrema_flavescens
05fec6e7a5ad0330817d758c5c9755e02d96a15b	Fungi	Basidiomycota	Tremellomycetes	Tremellales	Rhynchogastremataceae	Papiliotrema	Papiliotrema_flavescens
08ad9843fcd696e984f4e5e557e27ab0eb688697	Fungi	Basidiomycota	Tremellomycetes	Tremellales	Rhynchogastremataceae	Papiliotrema	Papiliotrema_flavescens
72adff207f590819254aca87890e7927499fbe7d	Fungi	Basidiomycota	Tremellomycetes	Tremellales	Rhynchogastremataceae	Papiliotrema	Papiliotrema_flavescens
38aae88f9f5126198f2f5687a8a94e54c182dec7	Fungi	Basidiomycota	Tremellomycetes	Tremellales	Rhynchogastremataceae	Papiliotrema	Papiliotrema_flavescens
5375829c95e1531b1196cfd7b27b0c8d47ef710d	Fungi	Basidiomycota	Tremellomycetes	Tremellales	Rhynchogastremataceae	Papiliotrema	Papiliotrema_laurentii
b3605dd5ff0b8327265e27090aacad480d882146	Fungi	Basidiomycota	Tremellomycetes	Tremellales	Rhynchogastremataceae	Papiliotrema	Papiliotrema_laurentii

0e055b31644a0e6c508a4de270638fa8008d71ef	Fungi	Basidiomycota	Tremellomycetes	Tremellales	Rhynchogastremataceae	Papiliotrema	Papiliotrema_laurentii
e5bc3863997ff3e990a6dfc9fb9eee4f8162b5e3	Fungi	Basidiomycota	Tremellomycetes	Tremellales	Rhynchogastremataceae	Papiliotrema	Papiliotrema_pseudoalba
SH033653.07FU_JQ003630_reps	Fungi	Basidiomycota	Tremellomycetes	Tremellales	Rhynchogastremataceae	Papiliotrema	Papiliotrema_laurentii
616597f78600a530dc5ff2e142b525e349195985	Fungi	Basidiomycota	Tremellomycetes	Tremellales	Rhynchogastremataceae	Papiliotrema	Papiliotrema_laurentii
aec19276fafa106bcfe7e404906e3d6a19d1daaf	Fungi	Basidiomycota	Tremellomycetes	Tremellales	Bulleribasidiaceae	Vishniacozyma	Vishniacozyma_heimaeyensis
6a1f91227504847473071c03519cdf12a20b1a4a	Fungi	Basidiomycota	Tremellomycetes	Tremellales	Bulleribasidiaceae	Vishniacozyma	Vishniacozyma_victoriae
83a749f4ab7f27b15b4578c3ed9c8385decfd2e2	Fungi	Basidiomycota	Tremellomycetes	Tremellales	Bulleribasidiaceae	Vishniacozyma	Vishniacozyma_victoriae
1cfb041629cf4c250067e6abee43c7b5020bdd5c	Fungi	Basidiomycota	Tremellomycetes	Tremellales	Bulleribasidiaceae	Vishniacozyma	Vishniacozyma_victoriae
e22810bab8fd35b9107b0027b9702bc4d917f571	Fungi	Basidiomycota	Tremellomycetes	Tremellales	Bulleribasidiaceae	Dioszegia	Dioszegia_takashimae
7fa03f97eb0b5c9c0ce08d72747ebd2d7002bb07	Fungi	Ascomycota	Sordariomycetes	Hypocreales	Nectriaceae	Gibberella	Gibberella_zeae
4e2480a2b37056d6c06ca4a6af4b7ba1254aa9e4	Fungi	Ascomycota	Sordariomycetes	Hypocreales	Nectriaceae	Gibberella	Gibberella_zeae
1bf5a30837134dbe8fa9c1313eb0dbafa98eb429	Fungi	Ascomycota	Sordariomycetes	Hypocreales	Nectriaceae	Gibberella	Gibberella_zeae
b10d45767153d6cdc6aef687e0b557e927708cb0	Fungi	Ascomycota	Sordariomycetes	Hypocreales	Nectriaceae	Gibberella	Gibberella_zeae
12d5c9615000796c1e81f1654b499b1d58471a8f	Fungi	Ascomycota	Sordariomycetes	Hypocreales	Nectriaceae	Gibberella	Gibberella_zeae
9c041adbfee089a0ff43336505f36fc0bd9d8ba8	Fungi	Ascomycota	Dothideomycetes	Pleosporales	Didymellaceae	Didymella	NA
b4ed3ed6515753810749f7f6ba4109e0fa4c6fe7	Fungi	Basidiomycota	Tremellomycetes	Tremellales	unidentified	unidentified	unidentified
1199c91a325dcc8d4176b686a6a215f1bd580e94	Fungi	Basidiomycota	Tremellomycetes	Tremellales	Rhynchogastremataceae	Papiliotrema	Papiliotrema_pseudoalba
63ccfd4e3edda53379f723cca50f6b679de7ac32	Fungi	Ascomycota	Dothideomycetes	Pleosporales	Didymellaceae	Phoma	unidentified
SH496509.07FU_KP843452_reps_singleton	Fungi	Ascomycota	Dothideomycetes	Pleosporales	Didymellaceae	Epicoccum	Epicoccum_sorghinum
aed21b5c8b656775d898c21d62683d645dff1783	Fungi	Ascomycota	Dothideomycetes	Pleosporales	Didymellaceae	Epicoccum	unidentified
0f5fcfae3ac3db16d5b82190c660a5f1bd9663a4	Fungi	Ascomycota	Dothideomycetes	Pleosporales	Didymellaceae	Epicoccum	unidentified
2d0e81d8cb99ed54511954e1b288f0f81fe44a03	Fungi	Ascomycota	Dothideomycetes	Capnodiales	Cladosporiaceae	Cladosporium	NA
01c3312e3ff7995be3161564348daba78b4d23f5	Fungi	Ascomycota	Dothideomycetes	Capnodiales	Cladosporiaceae	Cladosporium	NA
e52b3c64385ca2863054f2f90803cd2744b51b74	Fungi	Ascomycota	Dothideomycetes	Capnodiales	Cladosporiaceae	Cladosporium	NA
d1ced50ec28a004444c7b454ba7947d780525e55	Fungi	Ascomycota	Dothideomycetes	Capnodiales	Cladosporiaceae	Cladosporium	Cladosporium_delicatulum
71f979315ac71a41183d5e78d7e7cd151eef6e82	Fungi	Ascomycota	Dothideomycetes	Capnodiales	Cladosporiaceae	Cladosporium	Cladosporium_delicatulum
f53c9b9e49232dd55960e4536009a1539e70af0d	Fungi	Ascomycota	Sordariomycetes	Hypocreales	Nectriaceae	Gibberella	Gibberella_zeae
23dd12bea48fea467b41e7a1d9cd45d59e91d77c	Fungi	Ascomycota	Sordariomycetes	Hypocreales	Nectriaceae	Gibberella	Gibberella_zeae

1f6d1bb2103f7a5152526d3a96c8fcdacc41c0ed	Fungi	Ascomycota	Sordariomycetes	Hypocreales	Nectriaceae	Gibberella	Gibberella_zeae
384d50292fc7bb26903d5449f4b0d5e68c5aba7d	Fungi	Ascomycota	Sordariomycetes	Hypocreales	Nectriaceae	Gibberella	Gibberella_zeae
4d3e7808f5a77b18685b0ee915603945f25a094b	Fungi	Ascomycota	Sordariomycetes	Hypocreales	Nectriaceae	Gibberella	Gibberella_zeae
08047498dd9177305eb31ed4b029668891a583e0	Fungi	Ascomycota	Sordariomycetes	Hypocreales	Nectriaceae	Gibberella	NA
079dc8443c124c5833e355a57aa4121a3b841b94	Fungi	Ascomycota	Sordariomycetes	Hypocreales	Nectriaceae	Gibberella	Gibberella_zeae
1a24590697e46c8b6a9f7b77d2ae24e15cbb16ea	Fungi	Ascomycota	Dothideomycetes	Capnodiales	Cladosporiaceae	Cladosporium	Cladosporium_delicatulum
789401054070d4bbc6f379957453c2d002f78e65	Fungi	Ascomycota	Dothideomycetes	Capnodiales	Cladosporiaceae	Cladosporium	Cladosporium_delicatulum
040f9e1b91f7824fc61044049491272cc0c97908	Fungi	Ascomycota	Dothideomycetes	Capnodiales	Cladosporiaceae	Cladosporium	Cladosporium_delicatulum
830b823ca38e3122c8fe389654151f27a45746c8	Fungi	Ascomycota	Dothideomycetes	Capnodiales	Cladosporiaceae	Cladosporium	Cladosporium_delicatulum
4951bc3e2e5ccdb0bf56fc008734064697fb2eec	Fungi	Ascomycota	Dothideomycetes	Capnodiales	Cladosporiaceae	Cladosporium	Cladosporium_delicatulum
d1ac6b9839504a5d25ec5586abcca0ace29f2e37	Fungi	Ascomycota	Dothideomycetes	Capnodiales	Cladosporiaceae	Cladosporium	Cladosporium_delicatulum
7e62b9c1ca7cd4464be37be3b861d17c20c5c1f7	Fungi	Ascomycota	Dothideomycetes	Capnodiales	Cladosporiaceae	Cladosporium	Cladosporium_delicatulum
231697768223ac090c9e246aab3bdcf946b8b8cc	Fungi	Ascomycota	Dothideomycetes	Pleosporales	Pleosporaceae	Alternaria	NA
c68ef6d3bad02cae9309bbd52bb65af80226da4d	Fungi	Ascomycota	Dothideomycetes	Dothideales	Aureobasidiaceae	Aureobasidium	Aureobasidium_pullulans
785e1b5a478c2a6abcb4b0cb2272cad7a602dd24	Fungi	Ascomycota	Dothideomycetes	Dothideales	Aureobasidiaceae	Aureobasidium	Aureobasidium_pullulans
5673c12b9e7849510ca14f0989592c9bd7193078	Fungi	Ascomycota	Dothideomycetes	Pleosporales	Didymellaceae	Ascochyta	Ascochyta_manawaorae
19115c1b2bc0b28d1c77c798f691375b1f94c2b5	Fungi	Ascomycota	Dothideomycetes	Pleosporales	Massarinaceae"	Stagonospora	unidentified
935903ad1aab2ef21d35a3f6c7636bba49764b76	Fungi	Ascomycota	Dothideomycetes	Pleosporales	Didymellaceae	Phoma	unidentified
2a1420eec6fb550f254529c4e03ae068a0c71f3e	Fungi	Basidiomycota	Tremellomycetes	Tremellales	Rhynchogastremataceae	Papiliotrema	NA
3f11f1178d1f3f0b9b4c80da18500a1704d055a7	Fungi	Ascomycota	Dothideomycetes	Pleosporales	Didymellaceae	Phoma	unidentified
6abb98bffff246c158e9d18fff4b469521c663e5	Fungi	Ascomycota	Dothideomycetes	Pleosporales	Didymellaceae	Phoma	unidentified
73e46a0738987cdc29d05b491e215f8103b4c74a	Fungi	Ascomycota	Dothideomycetes	Pleosporales	Didymellaceae	Didymella	NA
3ba0f5efa9f0d504ae8507193ec3fd7d0bea8fc3	Fungi	Ascomycota	Dothideomycetes	Pleosporales	Phaeosphaeriaceae	Sclerostagonospora	Sclerostagonospora_phragmiticola
801f7b51e83d303514cd6a148c9462173128cbc1	Fungi	Ascomycota	Dothideomycetes	Pleosporales	Pleosporaceae	Alternaria	Alternaria_eichhorniae
89b500473bba543a02118d9ee1fc491391d22eb0	Fungi	Ascomycota	Dothideomycetes	Pleosporales	Pleosporaceae	Alternaria	Alternaria_eichhorniae
6f20cfd2fb74617967aa7e81c0f1671c80f40c56	Fungi	Ascomycota	Dothideomycetes	Pleosporales	Pleosporaceae	Alternaria	Alternaria_eichhorniae
12a7d4db75d5610c3362af5e87d0df4864e34842	Fungi	Ascomycota	Dothideomycetes	Pleosporales	Pleosporaceae	Alternaria	Alternaria_eichhorniae
87730287c19bce2ea39aebdc2038cdc9bd52653e	Fungi	Ascomycota	Dothideomycetes	Pleosporales	Pleosporaceae	Alternaria	Alternaria_eichhorniae

b1537bfe17b3951dc8f77de94e8f689cac5fa7e2	Fungi	Ascomycota	Dothideomycetes	Pleosporales	Pleosporaceae	Alternaria	Alternaria_eichhorniae
4c2d403e58d5e4bd1d16f598ed0e3ef5f83d535e	Fungi	Ascomycota	Dothideomycetes	Pleosporales	Pleosporaceae	Alternaria	Alternaria_eichhorniae
75781aae97229688e4f55ffd0fe11ba9f119b04c	Fungi	Ascomycota	Dothideomycetes	Pleosporales	Pleosporaceae	Alternaria	Alternaria_eichhorniae
07cd77ac8938cdce1cd8910a0688a346711bc9ef	Fungi	Ascomycota	Dothideomycetes	Pleosporales	Pleosporaceae	Alternaria	Alternaria_eichhorniae
37a92f4ec4d30a4f3cb7fd56439dce8625bf12e5	Fungi	Ascomycota	Dothideomycetes	Pleosporales	Didymellaceae	Didymella	NA
360fc807b13846afad6e7143b992d107b5974293	Fungi	Ascomycota	Dothideomycetes	Pleosporales	Didymellaceae	Didymella	Didymella_glomerata
6c99779749727e5ef432a38273771db2059ffc1b	Fungi	Ascomycota	Dothideomycetes	Pleosporales	Didymellaceae	Didymella	NA
6de037967766de8357866417433dd986f40074a4	Fungi	Ascomycota	Dothideomycetes	Pleosporales	Didymellaceae	Phoma	unidentified
580687dd18bd82a9a99bab36b1aab84a398845fe	Fungi	Ascomycota	Dothideomycetes	Pleosporales	Didymellaceae	Phoma	unidentified
f6fa7f730c924be4a573850707237a8811c1bb61	Fungi	Ascomycota	Dothideomycetes	Pleosporales	Didymellaceae	Phoma	unidentified
1a1f789a02f3c3de12cafdf51e96352b926feb96	Fungi	Ascomycota	Dothideomycetes	Pleosporales	Didymellaceae	Phoma	unidentified
b836e5d83a3b6ada5322a8a43003a952c87c8c64	Fungi	Ascomycota	Dothideomycetes	Pleosporales	Didymellaceae	Phoma	unidentified
0eb123c2e9ae44ff326e8f58b6ad02087a929e81	Fungi	Ascomycota	Dothideomycetes	Pleosporales	Didymellaceae	Phoma	unidentified
0b9ec6c3706916439ab45901609e475cf8cb8ec2	Fungi	Ascomycota	Dothideomycetes	Pleosporales	Didymellaceae	Phoma	unidentified
c0cf94034c321ea9a111e57de4b33976e794cc02	Fungi	Ascomycota	Dothideomycetes	Pleosporales	Didymellaceae	Phoma	unidentified
1a36a0716f11499356ebc8141a12ad723251f442	Fungi	Ascomycota	Dothideomycetes	Pleosporales	Didymellaceae	Phoma	unidentified
1d6d0fbd17111726747bfb85f8af6d754d172198	Fungi	Ascomycota	Dothideomycetes	Pleosporales	Didymellaceae	Phoma	unidentified
0527bd9dd372546c0627b014b51d6c1ce40fe4bc	Fungi	Ascomycota	Dothideomycetes	Pleosporales	Didymellaceae	Phoma	unidentified
19c4c864f1e0feaffd2eb10cca49fc3ea866bde6	Fungi	Ascomycota	Dothideomycetes	Pleosporales	Didymellaceae	Phoma	unidentified
13c58915a2d2e17fe8e004e75e2c071ccfbf6877	Fungi	Ascomycota	Dothideomycetes	Pleosporales	Didymellaceae	Didymella	NA
06b5591f623caa3fd30a457bee83708b0c8ad289	Fungi	Ascomycota	Dothideomycetes	Pleosporales	Didymellaceae	Didymella	NA
7cb45e7bd4edbf739d5f087db136760c1609583c	Fungi	Ascomycota	Dothideomycetes	Pleosporales	Didymellaceae	Didymella	NA
45b0c6e6212162cba84688916a3456ed31de7fd5	Fungi	Ascomycota	Dothideomycetes	Pleosporales	Didymellaceae	Didymella	Didymella_calidophila
e5b41dcf0e6e2f51a64047fc9f1d5bfec312a63b	Fungi	Ascomycota	Dothideomycetes	Pleosporales	Didymellaceae	Didymella	Didymella_calidophila
b43ef721fae216176caa3c434a14fc9a507a3c45	Fungi	Ascomycota	Dothideomycetes	Pleosporales	Didymellaceae	Neoascochyta	Neoascochyta_paspali
a6417a7a0e27bca29b7c2444e3fcb41df47ff16b	Fungi	Ascomycota	Dothideomycetes	Pleosporales	Didymellaceae	Phoma	unidentified
446728c23ac993afee42b34dd185bfde01d5c7f8	Fungi	Ascomycota	Dothideomycetes	Pleosporales	Didymellaceae	Phoma	unidentified
aa3a20cb894920512f1072db588a22ade4b22ca7	Fungi	Ascomycota	Dothideomycetes	Pleosporales	Pleosporaceae	Alternaria	NA

85a29c0c950435653af4c4aaa04d0f94f7985cb3	Fungi	Ascomycota	Sordariomycetes	Hypocreales	Nectriaceae	Gibberella	Gibberella_zeae
a160ecc55d23ed787b152ab2610096714236815a	Fungi	Ascomycota	Sordariomycetes	Hypocreales	Nectriaceae	Gibberella	Gibberella_zeae
35f7fc2b79765f9e64b64856145d02daee375a21	Fungi	Ascomycota	Sordariomycetes	Hypocreales	Nectriaceae	Gibberella	Gibberella_zeae
a3a644d2d3621708f9e58c26c848b9258f647b11	Fungi	Ascomycota	Sordariomycetes	Hypocreales	Nectriaceae	Gibberella	Gibberella_zeae
3a01bf7afba2b940fb7f710a4080ffb2455a8b27	Fungi	Ascomycota	Sordariomycetes	Hypocreales	Nectriaceae	Gibberella	Gibberella_zeae
285d529326ba394969f9bba93b4e642ce3238714	Fungi	Ascomycota	Sordariomycetes	Hypocreales	Nectriaceae	Gibberella	Gibberella_zeae
acacf64d31fcd4564cc2737b72ec2a4d53f24dae	Fungi	Ascomycota	Sordariomycetes	Hypocreales	Nectriaceae	Gibberella	Gibberella_zeae
06c196d3624655a7a28d4b89a5474ae46fa5de7d	Fungi	unidentified	unidentified	unidentified	unidentified	unidentified	unidentified
04bd0ec6a3d8a6b9a846f57b7e66a56ce684623f	Fungi	unidentified	unidentified	unidentified	unidentified	unidentified	unidentified
17767ac5a6b1278eaee9050b8cca0c3d7ee93b65	Fungi	unidentified	unidentified	unidentified	unidentified	unidentified	unidentified
8f6164b252990f5666169faf3150425adab041e0	Fungi	Ascomycota	Dothideomycetes	Pleosporales	Didymellaceae	Phoma	unidentified
2e226e4969cacab39ce017848ed09c1afd94580f	Fungi	Ascomycota	Dothideomycetes	Pleosporales	Pleosporaceae	Alternaria	unidentified
37dcc8f181df6348e6ff49c2cf9f8e52374afe6b	Fungi	Ascomycota	Dothideomycetes	Pleosporales	Pleosporaceae	Alternaria	unidentified
02f0b6577cf8d9f814419b4f48ed322d3de5ca86	Fungi	Ascomycota	Dothideomycetes	Pleosporales	Pleosporaceae	Alternaria	unidentified
16beb1965b116414e643fd920a08f3617dcf1db8	Fungi	Ascomycota	Dothideomycetes	Pleosporales	Pleosporaceae	Alternaria	NA
0c74eaa13c934e25bd3ce818732434303ee33eba	Fungi	Ascomycota	Dothideomycetes	Pleosporales	Pleosporaceae	Alternaria	NA
ae42fd6c74126c6001b022fcd5f5c7937108734a	Fungi	Ascomycota	Dothideomycetes	Pleosporales	Pleosporaceae	Alternaria	NA
7f6ac1a54487b0ad623735994959a3823b6b18dd	Fungi	Ascomycota	Dothideomycetes	Pleosporales	Pleosporaceae	Alternaria	Alternaria_eichhorniae
018ab49be41bff434be6ce054d009bcec91e1028	Fungi	Ascomycota	Dothideomycetes	Pleosporales	Pleosporaceae	Alternaria	Alternaria_eichhorniae
e300f4680afb9e9e9e499cb81129ea099d3a0804	Fungi	Ascomycota	Dothideomycetes	Pleosporales	Pleosporaceae	Alternaria	Alternaria_eichhorniae
bce8441ad7b2c68e7178a7c2d22f586ebfbf0801	Fungi	Ascomycota	Dothideomycetes	Pleosporales	Pleosporaceae	Alternaria	Alternaria_eichhorniae
112f89b8fb26445c6c7ead77c1317c6130dad974	Fungi	Ascomycota	Dothideomycetes	Pleosporales	Pleosporaceae	Alternaria	Alternaria_eichhorniae
7087757ab5a6b73bf15f2b3a90cf6698e38340c5	Fungi	Ascomycota	Dothideomycetes	Pleosporales	Pleosporaceae	Alternaria	Alternaria_eichhorniae
1fd95268d52a48f9fb8d83e950f3448b64949c99	Fungi	Ascomycota	Dothideomycetes	Pleosporales	Pleosporaceae	Alternaria	Alternaria_eichhorniae
c85c1493b09226cad4fa7babd6992379853e2a86	Fungi	Ascomycota	Dothideomycetes	Pleosporales	Pleosporaceae	Alternaria	NA
5a4925f7e847a61a3197639eed733d9155ca64eb	Fungi	Ascomycota	Dothideomycetes	Pleosporales	Pleosporaceae	Alternaria	NA
7a1125af2bee53f1c250fa97e0a2cf6a763e0377	Fungi	Ascomycota	Dothideomycetes	Pleosporales	Pleosporaceae	Alternaria	NA
062218f239034b31f53d963496b5ba8d0a6f6b4f	Fungi	Ascomycota	Dothideomycetes	Pleosporales	Pleosporaceae	Alternaria	NA

2dd9dc5cbc96eaa9215b65aff2fada603b5983c5	Fungi	Ascomycota	Dothideomycetes	Pleosporales	Pleosporaceae	Alternaria	NA
1e1e62d77adc38f06f2a25bf6cbbb0eb256cedcc	Fungi	Ascomycota	Dothideomycetes	Pleosporales	Pleosporaceae	Alternaria	NA
062281e7700d6319021fc4b3d6e1ac838ee97f61	Fungi	Ascomycota	Dothideomycetes	Pleosporales	Pleosporaceae	Alternaria	NA
410031cde3f78ecc543541b0e21abd6572a51e16	Fungi	Ascomycota	Dothideomycetes	Pleosporales	Pleosporaceae	Alternaria	NA
80b21b276ccb95c7d7d32bae3061515f066641b9	Fungi	Ascomycota	Dothideomycetes	Pleosporales	Pleosporaceae	Alternaria	NA
1bd93618c7cc859e2165ddfe837636a972b101c8	Fungi	Ascomycota	Dothideomycetes	Capnodiales	Mycosphaerellaceae	Mycosphaerella	Mycosphaerella_tassiana
da562042497985f48c6191330f6a6e95f9b4ef22	Fungi	Ascomycota	Dothideomycetes	Pleosporales	Pleosporaceae	Alternaria	unidentified
558e89825e995ff09799addf857870ea07cd37aa	Fungi	Ascomycota	Dothideomycetes	Pleosporales	Pleosporaceae	Alternaria	unidentified
3a3e34fd25a66284678461b115a7515bcec845a1	Fungi	Ascomycota	Dothideomycetes	Pleosporales	Pleosporaceae	Alternaria	unidentified
0149958ea7e4cb4b74c70bce34120a82765408fd	Fungi	Ascomycota	Dothideomycetes	Pleosporales	Didymellaceae	Didymella	NA
0a20c916a424f4402ddea5caaf5fe5d4d9838945	Fungi	Ascomycota	Dothideomycetes	Dothideales	Aureobasidiaceae	Aureobasidium	Aureobasidium_pullulans
f426ec41ccf3c32730b241464735f4b53a327a26	Fungi	Ascomycota	Dothideomycetes	Dothideales	Aureobasidiaceae	Aureobasidium	Aureobasidium_pullulans
0aa6721f1f443cbed949ae3189a37935e675e05f	Fungi	Ascomycota	Dothideomycetes	Capnodiales	Cladosporiaceae	Cladosporium	Cladosporium_delicatulum
23c1c8e66476fcc1f774751dccc26fdcbd13fcc2	Fungi	Ascomycota	Sordariomycetes	Hypocreales	Nectriaceae	Gibberella	Gibberella_zeae
a4e1f379ec4d60cd9cf27bc243322b1f003990ac	Fungi	Ascomycota	Sordariomycetes	Hypocreales	Nectriaceae	Gibberella	Gibberella_zeae
62baada5e6f791ad705c630e8d74c4a0e203061c	Fungi	Basidiomycota	Tremellomycetes	Filobasidiales	Filobasidiaceae	Naganishia	Naganishia_albida
c6a2926998568b5da09e79f8ea8985b037ce86ba	Fungi	Ascomycota	Dothideomycetes	Pleosporales	Pleosporaceae	Alternaria	Alternaria_eichhorniae
c260b24c3a0d1b6922080da30db57898e944deaa	Fungi	Ascomycota	Dothideomycetes	Pleosporales	Didymellaceae	Didymella	NA
ca752e517b85379d9edb18cd1be3f79cd4d3367b	Fungi	Ascomycota	Dothideomycetes	Pleosporales	Didymellaceae	Didymella	NA
50bc3eda5d1074e8e255fd7e458f4388d62ba521	Fungi	Ascomycota	Dothideomycetes	Pleosporales	Didymellaceae	Phoma	unidentified
6678434de4dfc36fe8052f8f9427dd8ee299b96e	Fungi	Ascomycota	Dothideomycetes	Pleosporales	Didymellaceae	Didymella	NA
24cb2553805e9a5a019bcc611c131e513556b2d2	Fungi	Ascomycota	Dothideomycetes	Pleosporales	Didymellaceae	Didymella	Didymella_glomerata
8965a22b2e41647a511f95816552a4c4e2515f4f	Fungi	Ascomycota	Dothideomycetes	Pleosporales	Didymellaceae	Didymella	NA
74d7a2145e26eae56d52aaa36fe6ee7231c936f7	Fungi	Ascomycota	Dothideomycetes	Pleosporales	Didymellaceae	Epicoccum	unidentified
18539298c436cedd8a27f7f53f6aacd1f1ec97f3	Fungi	Ascomycota	Dothideomycetes	Pleosporales	Didymellaceae	Epicoccum	unidentified
1c5becee93302ea456eae4874a712c4d2f96c088	Fungi	Ascomycota	Dothideomycetes	Pleosporales	Didymellaceae	Didymella	NA
01d17e8b82124b7a46e954f89665beacfaa0d197	Fungi	Ascomycota	Dothideomycetes	Pleosporales	Didymellaceae	Phoma	unidentified
148a86cdfe70d339c206560ba0e8c5ad6e2080cc	Fungi	Ascomycota	Dothideomycetes	Pleosporales	Didymellaceae	Phoma	unidentified

349d83a5072d958dc809a8ecb11d02c6dd0efdc4	Fungi	Ascomycota	Dothideomycetes	Pleosporales	Didymellaceae	Phoma	unidentified
037871732a33670a4ccec836771a30e7557cb437	Fungi	Ascomycota	Dothideomycetes	Pleosporales	Didymellaceae	Didymella	NA
04b0e69e0468e80a8c43d2c8d0794ee7be2a9da0	Fungi	Ascomycota	Dothideomycetes	Pleosporales	Didymellaceae	Phoma	unidentified
03a36a7bd3b76687b9a83ad270f792297fa260e7	Fungi	Ascomycota	Dothideomycetes	Pleosporales	Didymellaceae	Phoma	unidentified
26d6edc025e8cb98965b6e0ad3918be980794ad4	Fungi	Ascomycota	Dothideomycetes	Pleosporales	Didymellaceae	Phoma	unidentified
a9917f4d2f56ccf3561be3280035275358355714	Fungi	Basidiomycota	Tremellomycetes	Filobasidiales	Filobasidiaceae	Filobasidium	Filobasidium_magnum
1e4bad54e239bc0abf0a48dd7a3c6d8c6cdf3659	Fungi	Basidiomycota	Tremellomycetes	Filobasidiales	Filobasidiaceae	Filobasidium	Filobasidium_magnum
5cf7461d4306b94878162a34618a9999eeb9ec4b	Fungi	Basidiomycota	Tremellomycetes	Filobasidiales	Filobasidiaceae	Naganishia	Naganishia_friedmannii
6be52494c86233d8e4396f76f8eb12f5b9c4c6b5	Fungi	Basidiomycota	Tremellomycetes	Filobasidiales	Filobasidiaceae	Naganishia	Naganishia_uzbekistanensis
34b0c3e7596d0aac8389dff4c5e9b0bfae8a2022	Fungi	Basidiomycota	Tremellomycetes	Filobasidiales	Filobasidiaceae	Filobasidium	Filobasidium_magnum
eb16f0088f280f0a1799a4d990923e43eb7918ba	Fungi	Basidiomycota	Tremellomycetes	Filobasidiales	Filobasidiaceae	Filobasidium	Filobasidium_magnum
250a178b7d392ce150d345411a0a81ba10cd79db	Fungi	Ascomycota	Sordariomycetes	Hypocreales	Nectriaceae	Gibberella	Gibberella_zeae
ae54d23f4d8060b41c8dd0b9ea79ea50935ea721	Fungi	Ascomycota	Sordariomycetes	Hypocreales	Nectriaceae	Gibberella	Gibberella_zeae
3691092522feb3973d7cb5ecf941e63203edeff1	Fungi	Ascomycota	Sordariomycetes	Hypocreales	Nectriaceae	Gibberella	Gibberella_zeae
SH497161.07FU_KT161088_reps_singleton	Fungi	unidentified	unidentified	unidentified	unidentified	unidentified	unidentified
7a4dd568b88e6ae9befece3b06b309cb961b4d3c	Fungi	unidentified	unidentified	unidentified	unidentified	unidentified	unidentified
c21d26b2d7c6f192a1f1ca0a787f1962dd58d0c8	Fungi	Ascomycota	Dothideomycetes	Pleosporales	Didymellaceae	Epicoccum	unidentified
4ede8d86aa512c3b12a38ae961ac0a998a2fbc8d	Fungi	Ascomycota	Dothideomycetes	Pleosporales	Didymellaceae	Epicoccum	unidentified
8a5b8c21adbbd7e3147941fa01a070eab9595938	Fungi	Ascomycota	Dothideomycetes	Pleosporales	Didymellaceae	Epicoccum	unidentified
45ee0e45e6d37dea37c542362a59fc264d4c90b2	Fungi	Ascomycota	Dothideomycetes	Pleosporales	Didymellaceae	Epicoccum	unidentified
e304ba7d6a578e843ba4a99fab63fea4b6137278	Fungi	Ascomycota	Dothideomycetes	Pleosporales	Didymellaceae	Epicoccumun	identified
7f8f48d5623c08aec0e6673866d27d2c08680034	Fungi	Ascomycota	Dothideomycetes	Pleosporales	Didymellaceae	Phoma	unidentified
d8a1afb77f63397b77db968970045e3642becbca	Fungi	Ascomycota	Dothideomycetes	Pleosporales	Didymellaceae	Didymella	Didymella_calidophila
4d87995e987169a300098d30212b9acf18ac7076	Fungi	Ascomycota	Dothideomycetes	Pleosporales	Didymellaceae	Didymella	Didymella_glomerata
5554924747d8f77f07b8d270af6bbc222bc911f0	Fungi	Ascomycota	Dothideomycetes	Pleosporales	Didymellaceae	Didymella	NA
1d41ee3e0a6da1aa42b79dd58db05e2182e806da	Fungi	Ascomycota	Dothideomycetes	Pleosporales	Didymellaceae	Didymella	Didymella_calidophila
01d122c4d84e161cdf5668a24bfe8bd23df948dd	Fungi	Ascomycota	Dothideomycetes	Pleosporales	Didymellaceae	Didymella	NA
5b3f0e096d0d716e82782a7fe285d45e537f9391	Fungi	Ascomycota	Dothideomycetes	Pleosporales	Didymellaceae	Didymella	NA

cca270b60f9365c1f9382ff7396203cbe425bdcc	Fungi	Ascomycota	Dothideomycetes	Pleosporales	Didymellaceae	Phoma	unidentified
2fb88f928f4e217ffddb1fcbe27ab04f6abf8dff	Fungi	Ascomycota	Dothideomycetes	Pleosporales	Didymellaceae	Phoma	unidentified
1db7f37b02876999b97e38c0be30d9cd5c219eae	Fungi	Ascomycota	Dothideomycetes	Pleosporales	Didymellaceae	Phoma	unidentified
8a7b94998347d6b0461a3d02367ed4f60fdcdc81	Fungi	Ascomycota	Dothideomycetes	Pleosporales	Didymellaceae	Didymella	NA
3394c9fa87d5e97504f2f4893efc61cb970777d0	Fungi	Ascomycota	Dothideomycetes	Pleosporales	Didymellaceae	Didymella	NA
2157c6284e9a8e2dbf2d8a7b251a65e8d0fb03e0	Fungi	Ascomycota	Dothideomycetes	Pleosporales	Didymellaceae	Didymella	NA
7d2d82212c0c145955617b0b0c12403a9ed6ecc6	Fungi	Ascomycota	Dothideomycetes	Pleosporales	Didymellaceae	Didymella	NA
2d36f53cc250006edf9fc4fc6a3021f204591e41	Fungi	Ascomycota	Dothideomycetes	Pleosporales	Didymellaceae	Didymella	NA
3aaa84037e390c47eff94411ba4e280c144d09e9	Fungi	Ascomycota	Dothideomycetes	Pleosporales	Didymellaceae	Didymella	NA
1ddbab782dba653be9a41999c8a4f498bb0c9533	Fungi	Ascomycota	Dothideomycetes	Pleosporales	Didymellaceae	Didymella	Didymella_glomerata
41b05c69518fcdfd26fcd836ac16d9b5ff048bb4	Fungi	Ascomycota	Dothideomycetes	Pleosporales	Didymellaceae	Didymella	NA
315d558c33b96b0299f0dd2ecb0a2ce2279820b5	Fungi	Ascomycota	Dothideomycetes	Pleosporales	Didymellaceae	Didymella	Didymella_calidophila
1455da152f2800623ec903d8d87141f5bba2b414	Fungi	Ascomycota	Dothideomycetes	Pleosporales	Didymellaceae	Didymella	NA
38462ce827ad1b9a4aa7f17698ac8931b7aae954	Fungi	Ascomycota	Dothideomycetes	Pleosporales	Didymellaceae	Didymella	NA
1cf019d9331b5eb8590f02b9c0cbc132beec2b28	Fungi	Ascomycota	Dothideomycetes	Pleosporales	Didymellaceae	Didymella	NA
01d204d21461cce4b021f8971832a3ca62249bf2	Fungi	Ascomycota	Dothideomycetes	Pleosporales	Didymellaceae	Didymella	NA
3fd61f8136c3a085564e8465cc2589439ed94d05	Fungi	Ascomycota	Dothideomycetes	Pleosporales	Didymellaceae	Didymella	NA
1a4c0366e6399afbfd601295090555bf1032bf6a	Fungi	Ascomycota	Dothideomycetes	Pleosporales	Didymellaceae	Didymella	NA
64d8f597a04c8aeeae1469f986dd99b9d3c8d1d3	Fungi	unidentified	unidentified	unidentified	unidentified	unidentified	unidentified
2b3a37edb481efeb99222b20fcb06db20e4c26a8	Fungi	unidentified	unidentified	unidentified	unidentified	unidentified	unidentified
fd6f37eec34ecb2be0ef0612cc2334611bab0c61	Fungi	unidentified	unidentified	unidentified	unidentified	unidentified	unidentified
168850e77e1bb555c52c99582f022b76643ff1d6	Fungi	unidentified	unidentified	unidentified	unidentified	unidentified	unidentified
074b1743aaa0b37485c05b472d946cf2f647952a	Fungi	unidentified	unidentified	unidentified	unidentified	unidentified	unidentified
f0c16135fe1a22ecde36d6a496556e10d29f588a	Fungi	unidentified	unidentified	unidentified	unidentified	unidentified	unidentified
32e8053d8904950e3232b31c9878b1f0c42656ac	Fungi	unidentified	unidentified	unidentified	unidentified	unidentified	unidentified
4fe0eb2a7a68529067a8f032a83489e73b9395fc	Fungi	unidentified	unidentified	unidentified	unidentified	unidentified	unidentified
a64d86f63b71372cefae0368e427b934088535bb	Fungi	unidentified	unidentified	unidentified	unidentified	unidentified	unidentified
263b758a460b8db3eb9504d7331310708a99db01	Fungi	unidentified	unidentified	unidentified	unidentified	unidentified	unidentified

a56a069403929a84ceb37e37b78c1891a22a97bd	Fungi	unidentified	unidentified	unidentified	unidentified	unidentified	unidentified
1fe709507f0a86daf7792a86222c09dc8601331a	Fungi	unidentified	unidentified	unidentified	unidentified	unidentified	unidentified
a1a7953f170b0a34860ca76e549037f977f4e4bd	Fungi	unidentified	unidentified	unidentified	unidentified	unidentified	unidentified
75cbf0c8ad28f30fccf7b278674e08e9c5dfc7b0	Fungi	unidentified	unidentified	unidentified	unidentified	unidentified	unidentified
4cb64339e09f165fc473ee564a691a17c3fe67a9	Fungi	unidentified	unidentified	unidentified	unidentified	unidentified	unidentified
23daf2f48093979ea1808b1deefd22e11dac9f68	Fungi	unidentified	unidentified	unidentified	unidentified	unidentified	unidentified
e1772c9eabb5109ca0396e8a9a9364a6e2294434	Fungi	unidentified	unidentified	unidentified	unidentified	unidentified	unidentified
0b3a943c766442b99653506520066ade628f3761	Fungi	unidentified	unidentified	unidentified	unidentified	unidentified	unidentified
0455b80b74e05598765246f837c5fe3dea82494a	Fungi	unidentified	unidentified	unidentified	unidentified	unidentified	unidentified
04a7a21c06409cede80a7999e9b21512177c1a11	Fungi	unidentified	unidentified	unidentified	unidentified	unidentified	unidentified
48ab615373e57fc4c75610b800292f0068382bd7	Fungi	unidentified	unidentified	unidentified	unidentified	unidentified	unidentified
c1543069e98939862421d46bfe9fb18649c12109	Fungi	unidentified	unidentified	unidentified	unidentified	unidentified	unidentified
e42bbbd38c956991f87ac533b919485f6c3de999	Fungi	unidentified	unidentified	unidentified	unidentified	unidentified	unidentified
149819fab265fdb8194f5ee2f39053a2d5a0f686	Fungi	unidentified	unidentified	unidentified	unidentified	unidentified	unidentified
9f72611eee15578cf546573a57fae8572c765ca0	Fungi	Ascomycota	Dothideomycetes	Capnodiales	Cladosporiaceae	Cladosporium	Cladosporium_delicatulum
18519150d27530becd686f72ca57bd357c13f4ad	Fungi	unidentified	unidentified	unidentified	unidentified	unidentified	unidentified
2781a0f3b45be84330b4575f8879ab90a718b79c	Fungi	unidentified	unidentified	unidentified	unidentified	unidentified	unidentified
2a8c598bea11b23013edd44581668c97ae61fca1	Fungi	unidentified	unidentified	unidentified	unidentified	unidentified	unidentified
202137ff9f198a0029a97be3bd03a52b9b54abd5	Fungi	unidentified	unidentified	unidentified	unidentified	unidentified	unidentified
0889d514d2c4c302329607fa27f8972f21205f0b	Fungi	unidentified	unidentified	unidentified	unidentified	unidentified	unidentified
334a944fcdee0e13853290f5ae1ab38cf4e8ba65	Fungi	unidentified	unidentified	unidentified	unidentified	unidentified	unidentified
25b1757319e1e1161bcc7e5147e294b91f10fb98	Fungi	unidentified	unidentified	unidentified	unidentified	unidentified	unidentified
5a7da0b006f59e2881f6f4537f2adfd0d85cd9cb	Fungi	unidentified	unidentified	unidentified	unidentified	unidentified	unidentified
b9e3db2f78c7c946f0cc6c9fa06e19ac7e2b19da	Fungi	unidentified	unidentified	unidentified	unidentified	unidentified	unidentified
40c293fdf31ca7862c514f7b1acbf1d0b3ebee3e	Fungi	unidentified	unidentified	unidentified	unidentified	unidentified	unidentified
212002be03fd1e09a4e7b3e64c2def66d2517e93	Fungi	unidentified	unidentified	unidentified	unidentified	unidentified	unidentified
6b2806cae12f3d52d16804d3d4de53aaa63cad38	Fungi	unidentified	unidentified	unidentified	unidentified	unidentified	unidentified
639687cc3558013d1a40d813fec4e89322a6bdcd	Fungi	unidentified	unidentified	unidentified	unidentified	unidentified	unidentified

705d80d330921fbf1e905e42149fa81d9a94351a	Fungi	unidentified	unidentified	unidentified	unidentified	unidentified	unidentified

Appendix Table 3A.3:Bacterial taxa counts of sorghum RILs

OTUID	TAXONOMY						
	Domain	Phylum	Class	Order	Family	Genus	Species
d244fcdf9c165d2077e6f0f1065a00f5	Bacteria	Proteobacteria	Gammaproteobacteria	Enterobacterales	Erwiniaceae		
4768bf47032e05ed009446d578d074f0	Bacteria	Proteobacteria	Gammaproteobacteria	Enterobacterales	Erwiniaceae		
9ca8b02da6505e4b762030e68608c352	Bacteria	Proteobacteria	Gammaproteobacteria	Enterobacterales	Erwiniaceae		
98578e74c67b47547b7c6b566e1a53f6	Bacteria	Proteobacteria	Gammaproteobacteria	Enterobacterales	Erwiniaceae		
582f3d4e82961f17d865d7ca7c5e767f	Bacteria	Proteobacteria	Gammaproteobacteria	Enterobacterales	Erwiniaceae		
aa4f2793b5b15e929d7f861aa7573e45	Bacteria	Proteobacteria	Gammaproteobacteria	Pseudomonadales	Pseudomonadaceae	Pseudomonas	
0dd4a59680a3485180c85e8a59aef35d	Bacteria	Proteobacteria	Gammaproteobacteria	Enterobacterales	Erwiniaceae		
9e4c3d1e1821f542b5a2d5d9086de0f6	Bacteria	Proteobacteria	Gammaproteobacteria	Pseudomonadales	Pseudomonadaceae	Pseudomonas	
68005cd6e75d35f9ed082cb816e12da7	Bacteria	Proteobacteria	Gammaproteobacteria	Pseudomonadales	Pseudomonadaceae	Pseudomonas	
10a842c1bcbf585a847a4407a547198d	Bacteria	Proteobacteria	Gammaproteobacteria	Pseudomonadales	Pseudomonadaceae	Pseudomonas	
054e2b28c8cbbfd0c8d6513b1a3d65f2	Bacteria	Proteobacteria	Gammaproteobacteria	Pseudomonadales	Pseudomonadaceae	Pseudomonas	
3d465a10e68b477d4a8744aa6b0c9177	Bacteria	Firmicutes	Bacilli	Bacillales	Bacillaceae	Bacillus	
8f87fff663017f23bebd21381ab628de	Bacteria	Proteobacteria	Gammaproteobacteria	Enterobacterales	Erwiniaceae		
08dabc25fb6245ca62fb0a90c6473e61	Bacteria	Firmicutes	Bacilli	Bacillales	Bacillaceae	Bacillus	
1f797ac5545e65821840da6560bd7deb	Bacteria	Proteobacteria	Gammaproteobacteria	Pseudomonadales	Pseudomonadaceae	Pseudomonas	
98c94d54ff8e1f04faa323710b8c65da	Bacteria	Proteobacteria	Gammaproteobacteria	Enterobacterales	Erwiniaceae		
801795849a0cb16f8186ff09fa4ae6e2	Bacteria	Firmicutes	Bacilli	Bacillales	Bacillaceae	Bacillus	
b6734fcb29785e3a46fd0ae2c118ac13	Bacteria	Firmicutes	Bacilli	Bacillales	Bacillaceae	Bacillus	
e98740aaeb2176919e8a1a704f9411c5	Bacteria	Proteobacteria	Gammaproteobacteria	Pseudomonadales	Pseudomonadaceae	Pseudomonas	
f4b89690122026515c06107041bd63a0	Bacteria	Proteobacteria	Gammaproteobacteria	Enterobacterales	Yersiniaceae	Serratia	
cc5698baa986556badf6d5da67b0b1dd	Bacteria	Proteobacteria	Gammaproteobacteria	Enterobacterales	Yersiniaceae	Serratia	
d3f8323680d131469f3c341933239a71	Bacteria	Firmicutes	Bacilli	Bacillales	Bacillaceae	Bacillus	
7e37f2aafa11690450074aee2577522e	Bacteria	Proteobacteria	Gammaproteobacteria	Pseudomonadales	Pseudomonadaceae	Pseudomonas	
2e381ce7051241b12e925c66ecd0e307	Bacteria	Proteobacteria	Gammaproteobacteria	Pseudomonadales	Pseudomonadaceae	Pseudomonas	

b2f1f385cbbfad6706d595f93e6a6d7a	Bacteria	Firmicutes	Bacilli	Bacillales	Bacillaceae	Bacillus	
58b659ff045120adf561122d84d316ab	Bacteria	Proteobacteria	Gammaproteobacteria	Enterobacterales	Yersiniaceae	Serratia	
c401f3386cc1ea1865cf8f2ed14ff32c	Bacteria	Firmicutes	Bacilli	Bacillales	Bacillaceae	Bacillus	
0896ec427b7736da3e045df37a164574	Bacteria	Firmicutes	Bacilli	Bacillales	Bacillaceae	Bacillus	
6c4fc8a73df44add4877493f31d1152e	Bacteria	Firmicutes	Bacilli	Bacillales	Bacillaceae	Bacillus	
5a333103e1bab94cabb642a830a8b693	Bacteria	Firmicutes	Bacilli	Bacillales	Bacillaceae	Bacillus	
f46d90fbc6fa806fde8c059266af9940	Bacteria	Firmicutes	Bacilli	Bacillales	Bacillaceae	Bacillus	
52e5041f6a05dcdac2e8d48c6fd1714a	Bacteria	Proteobacteria	Gammaproteobacteria	Pseudomonadales	Moraxellaceae	Acinetobacter	Acinetobacter_baylyi
7d543628ef4d9b0e4e5456a629f5d715	Bacteria	Proteobacteria	Gammaproteobacteria	Pseudomonadales	Moraxellaceae	Acinetobacter	Acinetobacter_baylyi
c83eb62bc82f55c5f125dd684ab14278	Bacteria	Proteobacteria	Gammaproteobacteria	Pseudomonadales	Moraxellaceae	Acinetobacter	Acinetobacter_baylyi
666c24d5a3a5ed1ab11c15563f11d9c6	Bacteria	Proteobacteria	Gammaproteobacteria	Pseudomonadales	Moraxellaceae	Acinetobacter	Acinetobacter_baylyi
105ac7ad03fa99a9ef0f2309508fd03e	Bacteria	Proteobacteria	Gammaproteobacteria	Enterobacterales	Enterobacteriaceae	Enterobacter	
5112b89cc5a92a7c6ef5565b43fa7543	Bacteria	Proteobacteria	Gammaproteobacteria	Enterobacterales	Erwiniaceae		
775e0480deac3177ec6e7449435632b1	Bacteria	Proteobacteria	Gammaproteobacteria	Enterobacterales	Erwiniaceae		
7ba778a6ec72a0927ed5a2e0de225073	Bacteria	Proteobacteria	Gammaproteobacteria	Enterobacterales	Enterobacteriaceae	Enterobacter	
38b78f42511eaa6d4b8a0b2979a75439	Bacteria	Proteobacteria	Gammaproteobacteria	Pseudomonadales	Pseudomonadaceae	Pseudomonas	
0155cb455b8f4879e69cf849e3f38a6c	Bacteria	Proteobacteria	Gammaproteobacteria	Enterobacterales	Erwiniaceae		
f321b994ec682acfd9ef1d70558b6166	Bacteria	Proteobacteria	Gammaproteobacteria	Enterobacterales	Erwiniaceae		
8d71ff640b0d130894a26218ddfed165	Bacteria	Proteobacteria	Gammaproteobacteria	Enterobacterales	Erwiniaceae		
4ab768980f4412cf1a6516781dd8dfe8	Bacteria	Firmicutes	Bacilli	Bacillales	Bacillaceae	Bacillus	
19c11e432993d9f88f84f3524bd749eb	Bacteria	Proteobacteria	Gammaproteobacteria	Enterobacterales	Erwiniaceae		
f7c14d3f5d8f164f86f28d804c61f5e6	Bacteria	Proteobacteria	Gammaproteobacteria	Enterobacterales	Enterobacteriaceae	Enterobacter	
7bac1ba560c9c6a5ef8a1666049f6e13	Bacteria	Proteobacteria	Gammaproteobacteria	Enterobacterales	Erwiniaceae		
71cb62824446f439ab9703c6bb030d97	Bacteria	Proteobacteria	Gammaproteobacteria	Enterobacterales	Erwiniaceae		
c4fa9da72aa669c920a6aee32e0e4901	Bacteria	Proteobacteria	Gammaproteobacteria	Enterobacterales	Erwiniaceae		
cf2b531081cc679010e94726dd8c7288	Bacteria	Proteobacteria	Gammaproteobacteria	Enterobacterales	Enterobacteriaceae	Kosakonia	
9705b0b60013b5947bdd58245c614000	Bacteria	Proteobacteria	Gammaproteobacteria	Enterobacterales	Enterobacteriaceae	Enterobacter	
86b4081ef432fd73be583b368a41ea36	Bacteria	Proteobacteria	Gammaproteobacteria	Enterobacterales	Erwiniaceae		

a8e48aab432b4501e9ac37a53be002a0	Bacteria	Firmicutes	Bacilli	Bacillales	Bacillaceae	Bacillus		
977e9acbeac3dabb0be39326635cf115	Bacteria	Proteobacteria	Gammaproteobacteria	Enterobacterales				
d1cb8bec59641ca920db8a74a7ca7002	Bacteria	Proteobacteria	Gammaproteobacteria	Enterobacterales	Enterobacteriaceae	Kosakonia		
c8d5ff01240aaf0496fd0bb877a3a02a	Bacteria	Proteobacteria	Gammaproteobacteria	Enterobacterales				
216c0aba29ea0622f595d3a5e9e4d0d5	Bacteria	Proteobacteria	Gammaproteobacteria	Enterobacterales	Erwiniaceae			
64eb022ccaf63f7cc2960d32a1125013	Bacteria	Proteobacteria	Gammaproteobacteria	Enterobacterales	Erwiniaceae			
976951b5d9c2ed0dc3f2d1bd56f881c3	Bacteria	Proteobacteria	Gammaproteobacteria	Enterobacterales	Erwiniaceae			
196c39f8b9fe1b5da3a66a29ec1ac220	Bacteria	Proteobacteria	Gammaproteobacteria	Enterobacterales				
b1df18c794563d5fb3ef14fc506d110e	Bacteria	Proteobacteria	Gammaproteobacteria	Enterobacterales	Erwiniaceae			
08698b783d78dcd5c7ea13a7353ca3ab	Bacteria	Firmicutes	Bacilli	Bacillales	Bacillaceae	Bacillus		
38b4467d8575ccd824ce0aa825b7ceb5	Bacteria	Proteobacteria	Gammaproteobacteria	Enterobacterales	Enterobacteriaceae	Kosakonia		
7e0253210da7e566635c1bbafe63138b	Bacteria	Firmicutes	Bacilli	Bacillales	Bacillaceae	Bacillus		
509cd07c5f0c1a11d0d0d3721abae1e3	Bacteria	Proteobacteria	Gammaproteobacteria	Enterobacterales	Erwiniaceae			
370c09ab2cc713b964d1ee23e6758888	Bacteria	Proteobacteria	Gammaproteobacteria	Enterobacterales				
a75736015426277758ceda9e6b36c7e0	Bacteria	Proteobacteria	Gammaproteobacteria	Enterobacterales				
9f34999b0cadfb8ca181bfaaec05d280	Bacteria	Firmicutes	Bacilli	Paenibacillales	Paenibacillaceae	Paenibacillus	Paenibacillus_wenxiniae	
8c3f329812be2ff82cbede5179c55545	Bacteria	Proteobacteria	Gammaproteobacteria	Enterobacterales	Enterobacteriaceae			
818e96b1ab158054f761dbb410e51190	Bacteria	Proteobacteria	Gammaproteobacteria	Enterobacterales				
6658d6fdc6625d0c8a95d8f4d3d6b988	Bacteria	Proteobacteria	Gammaproteobacteria	Enterobacterales	Erwiniaceae			
092a81eade65ffd4791b9248d3e3edbe	Bacteria	Proteobacteria	Gammaproteobacteria	Enterobacterales				
e78f9b84c9c290b27131084a70c8d9c4	Bacteria	Proteobacteria	Gammaproteobacteria	Enterobacterales				
7a1bc4c1bc0ddb1a6f219019f472c30f	Bacteria	Proteobacteria	Gammaproteobacteria	Enterobacterales	Enterobacteriaceae			
05a6b3fd733303fad30472481062055f	Bacteria	Proteobacteria	Gammaproteobacteria	Enterobacterales	Enterobacteriaceae			
6b28a85fb9dbacc77e7dc7b65e1b5110	Bacteria	Proteobacteria	Gammaproteobacteria	Enterobacterales	Enterobacteriaceae			
17166d4370f241b0140acda9a9262da4	Bacteria	Proteobacteria	Gammaproteobacteria	Enterobacterales	Erwiniaceae	Pantoea	Mixta_gaviniae	
cdf0483f2da17a545a550f53ac4ef916	Bacteria	Firmicutes	Bacilli	Paenibacillales	Paenibacillaceae	Paenibacillus	Paenibacillus_wenxiniae	
fa5812aeb0b839d39564957369a5629f	Bacteria	Firmicutes	Bacilli	Paenibacillales	Paenibacillaceae	Paenibacillus	Paenibacillus_wenxiniae	
670d1f9f18a319e9e2fb6a216f23f7c7	Bacteria	Proteobacteria	Gammaproteobacteria	Pseudomonadales	Moraxellaceae	Acinetobacter	Acinetobacter_baylyi	

3b26416c715b31d84f1662137bf10cf8	Bacteria	Proteobacteria	Gammaproteobacteria	Enterobacterales	Enterobacteriaceae		
8715f46134875805dd8ed69cdd1b14c1	Bacteria	Proteobacteria	Gammaproteobacteria	Enterobacterales	Erwiniaceae	Pantoea	Mixta_gaviniae
1f5e949bb7fc8a29a0843d2ef3b0e6f0	Bacteria	Proteobacteria	Gammaproteobacteria	Enterobacterales	Erwiniaceae	Pantoea	Mixta_gaviniae
97e14252500a8aefd532e5c408adfee2	Bacteria	Proteobacteria	Gammaproteobacteria	Enterobacterales	Erwiniaceae	Pantoea	Mixta_gaviniae
a3161ff2872cc578387f100a8ea43152	Bacteria	Proteobacteria	Gammaproteobacteria	Enterobacterales	Erwiniaceae	Pantoea	Mixta_gaviniae
74ea43a6b1b2e26b4b3c708e8ba06fad	Bacteria	Proteobacteria	Gammaproteobacteria	Pseudomonadales	Moraxellaceae	Acinetobacter	Acinetobacter_baylyi
db4644a80c257964e73c4790816c829c	Bacteria	Proteobacteria	Gammaproteobacteria	Pseudomonadales	Pseudomonadaceae	Pseudomonas	
338b90029f80570fd6ef35bc45e39d80	Bacteria	Proteobacteria	Gammaproteobacteria	Enterobacterales	Enterobacteriaceae		
d479524407c3f6424b2070a7a5502e3f	Bacteria	Firmicutes	Bacilli	Paenibacillales	Paenibacillaceae	Paenibacillus	Paenibacillus_wenxiniae
037010eff5dbd45912c89a3bbaa2e963	Bacteria	Proteobacteria	Gammaproteobacteria	Enterobacterales	Enterobacteriaceae	Kosakonia	
0ef658c8f029923c94290ca24084965e	Bacteria	Proteobacteria	Gammaproteobacteria	Enterobacterales			
d572e1149d36200fd49296b4b5443729	Bacteria	Firmicutes	Bacilli	Paenibacillales	Paenibacillaceae	Paenibacillus	Paenibacillus_wenxiniae
964fc0c233a92fd68d9a0d4430d45c0c	Bacteria	Firmicutes	Bacilli	Paenibacillales	Paenibacillaceae	Paenibacillus	Paenibacillus_wenxiniae
808967b1527e9b8fcb95e758e19209a4	Bacteria	Proteobacteria	Gammaproteobacteria	Pseudomonadales	Pseudomonadaceae	Pseudomonas	
4310a5bffd3758f20b6d83271db25faa	Bacteria	Proteobacteria	Gammaproteobacteria	Pseudomonadales	Moraxellaceae	Acinetobacter	Acinetobacter_baylyi
8e1e924cb95893b047ec45b8cb82944f	Bacteria	Proteobacteria	Gammaproteobacteria	Enterobacterales	Enterobacteriaceae	Cronobacter	Cronobacter_turicensis
8dee20f8caecf22a043d206b852c3a8d	Bacteria	Proteobacteria	Gammaproteobacteria	Enterobacterales	Enterobacteriaceae	Cronobacter	Cronobacter_turicensis
ce4ed31ba1c0ac645a4230910b653ecc	Bacteria	Proteobacteria	Gammaproteobacteria	Enterobacterales	Enterobacteriaceae	Cronobacter	Cronobacter_turicensis
4f1978c875280257c42cf5d2cf5cda63	Bacteria	Proteobacteria	Gammaproteobacteria	Enterobacterales	Enterobacteriaceae	Cronobacter	Cronobacter_turicensis
0bfe76e1f4067a0c1286cd16127b230e	Bacteria	Proteobacteria	Gammaproteobacteria	Enterobacterales	Enterobacteriaceae		
89b299a484146acaea98974a7d86618d	Bacteria	Firmicutes	Bacilli	Lactobacillales	Enterococcaceae	Enterococcus	
fc3272bd3e50b11e011d6ef3dfdea89f	Bacteria	Proteobacteria	Gammaproteobacteria	Enterobacterales	Enterobacteriaceae		
6309ea6ea686a55c86422938eaa4e880	Bacteria	Proteobacteria	Gammaproteobacteria	Pseudomonadales	Moraxellaceae	Acinetobacter	Acinetobacter_baylyi
571a0618945de19ff21e26377b230f6d	Bacteria	Proteobacteria	Gammaproteobacteria	Enterobacterales	Enterobacteriaceae	Cronobacter	Cronobacter_turicensis
8e5ef44521a961498d13c26c1f12e4ce	Bacteria	Firmicutes	Bacilli	Lactobacillales	Enterococcaceae	Enterococcus	
7f4cb7fc77572f4275b9fbcd93cf37c0	Bacteria	Proteobacteria	Gammaproteobacteria	Enterobacterales	Enterobacteriaceae	Cronobacter	Cronobacter_turicensis
1c1134b652171ba500291e0efc03aeb4	Bacteria	Firmicutes	Bacilli	Lactobacillales	Enterococcaceae	Enterococcus	
4f1d0b37a24b8e17c6bbad6401143f31	Bacteria	Proteobacteria	Gammaproteobacteria	Enterobacterales	Erwiniaceae		

06f0c4b99ea8dddb52e00d1c4caf5943	Bacteria	Proteobacteria	Gammaproteobacteria	Pseudomonadales	Pseudomonadaceae	Pseudomonas	
949a08b883cebdf8f17bce1e9880cb85	Bacteria	Firmicutes	Bacilli	Lactobacillales	Enterococcaceae	Enterococcus	
84e4e2970267d093a427258cd1e7fef8	Bacteria	Proteobacteria	Gammaproteobacteria	Enterobacterales	Enterobacteriaceae		
135d60c982d06f6ebd2bb51362dc913e	Bacteria	Proteobacteria	Gammaproteobacteria	Enterobacterales	Enterobacteriaceae		
c7bb36bb6fb78f63187c4cc1851de694	Bacteria	Proteobacteria	Gammaproteobacteria	Enterobacterales	Enterobacteriaceae		
0a77a518f8016939d5ae4e7f18b4325f	Bacteria	Proteobacteria	Gammaproteobacteria	Pseudomonadales	Pseudomonadaceae	Pseudomonas	
aba72de5a1d10273e98bdbcbd82ffeee	Bacteria	Proteobacteria	Gammaproteobacteria	Enterobacterales	Enterobacteriaceae	Cronobacter	Cronobacter_turicensis
d5b4e9d7e187df48a79a03240f638f54	Bacteria	Firmicutes	Bacilli	Lactobacillales	Enterococcaceae	Enterococcus	
ae048cec6a87575d7b2a9db7c2007747	Bacteria	Proteobacteria	Gammaproteobacteria	Pseudomonadales	Pseudomonadaceae	Pseudomonas	
a455a3030ce155aaaba6e7472860f4eb	Bacteria	Firmicutes	Bacilli	Lactobacillales	Enterococcaceae	Enterococcus	
cdf88865d582a1896451f2952427a051	Bacteria	Proteobacteria	Gammaproteobacteria	Enterobacterales	Enterobacteriaceae		
951cc3bdbbc49813299b2b66fee31745	Bacteria	Firmicutes	Bacilli	Lactobacillales	Enterococcaceae	Enterococcus	
1934ff4818858546d8a71aa2e76001d2	Bacteria	Proteobacteria	Gammaproteobacteria	Enterobacterales	Enterobacteriaceae		
dcae9543f0a210242cd839f60082aeea	Bacteria	Proteobacteria	Gammaproteobacteria	Enterobacterales	Enterobacteriaceae		
748c8215487b56e4056a5bc82348d030	Bacteria	Proteobacteria	Gammaproteobacteria	Enterobacterales	Enterobacteriaceae		
87f743c84572c7d4c3ff59d70c7176e8	Bacteria	Proteobacteria	Gammaproteobacteria	Enterobacterales	Enterobacteriaceae	Cronobacter	Cronobacter_turicensis
b1bed57675691df3102647315679919f	Bacteria	Proteobacteria	Gammaproteobacteria	Enterobacterales	Enterobacteriaceae		
1e2d1efc09662df5768670a1d58e96db	Bacteria	Proteobacteria	Gammaproteobacteria	Enterobacterales	Erwiniaceae		
917af0fb7cf8c1b3cb4752637cfdbbe2	Bacteria	Proteobacteria	Gammaproteobacteria	Pseudomonadales	Pseudomonadaceae	Pseudomonas	
ba859bf50c687f8956ecd5068afa05e9	Bacteria	Proteobacteria	Gammaproteobacteria	Enterobacterales	Erwiniaceae		
6f02caa7ef1fb6d2779f918c1decdd8b	Bacteria	Proteobacteria	Gammaproteobacteria	Enterobacterales	Enterobacteriaceae		
99b0c28e7e4a128819dcb423fd8feaf1	Bacteria	Firmicutes	Bacilli	Lactobacillales	Enterococcaceae	Enterococcus	
31fa9877ead18c959fb29b9479edfe37	Bacteria	Firmicutes	Bacilli	Paenibacillales	Paenibacillaceae	Paenibacillus	Paenibacillus_wenxiniae
33111e02daf94b0ed539dcca8d985e8c	Bacteria	Proteobacteria	Alphaproteobacteria	Sphingomonadales	Sphingomonadaceae	Sphingomonas	
89a822178a51db6e53308377cdd1e73a	Bacteria	Proteobacteria	Gammaproteobacteria	Enterobacterales	Enterobacteriaceae		
8cff0bd9d4a1d103010c71a7b85d54e9	Bacteria	Proteobacteria	Alphaproteobacteria	Sphingomonadales	Sphingomonadaceae	Sphingomonas	
5dc7505a4eedef4ddf22d04886f11cc3	Bacteria	Proteobacteria	Gammaproteobacteria	Enterobacterales	Enterobacteriaceae		
ccf1c4a6d14b3d1d5a91661f03dbf282	Bacteria	Proteobacteria	Alphaproteobacteria	Sphingomonadales	Sphingomonadaceae	Sphingomonas	

02b01f8f2b45f8a0cd3e77e0b29c21f7	Bacteria	Proteobacteria	Gammaproteobacteria	Enterobacterales	Erwiniaceae		
c5b47e8abfb27ad18ab69c974dc73255	Bacteria	Proteobacteria	Gammaproteobacteria	Enterobacterales	Enterobacteriaceae		
c8af609765165ad89b8947bc5409d81b	Bacteria	Proteobacteria	Gammaproteobacteria	Enterobacterales	Enterobacteriaceae		
8eb00dde894f5ad02b9088243a03a562	Bacteria	Proteobacteria	Gammaproteobacteria	Enterobacterales	Enterobacteriaceae		
c5a9d83c984029a21ebdc8500b451f96	Bacteria	Proteobacteria	Gammaproteobacteria	Enterobacterales	Enterobacteriaceae		
84f8e84469226b10e61f07e95f0efc08	Bacteria	Proteobacteria	Gammaproteobacteria	Enterobacterales	Enterobacteriaceae		
7183732485f803fc4a6b623025392860	Bacteria	Firmicutes	Bacilli	Bacillales	Bacillaceae	Bacillus	
b72f6ab7ca02ecc176b42613e10da834	Bacteria	Proteobacteria	Gammaproteobacteria	Enterobacterales	Erwiniaceae		
fe0b7320c746b4c91535c1c57f051daf	Bacteria	Proteobacteria	Gammaproteobacteria	Pseudomonadales	Pseudomonadaceae	Pseudomonas	
51701519fc9fc3aed7a8372743bcd515	Bacteria	Proteobacteria	Gammaproteobacteria	Pseudomonadales	Moraxellaceae	Acinetobacter	Acinetobacter_baylyi
1d4fae0415f7d980b460a92ce445096c	Bacteria	Proteobacteria	Gammaproteobacteria	Pseudomonadales	Moraxellaceae	Acinetobacter	
d813774b7efb02fb99b1b58d5ab3b2e4	Bacteria	Proteobacteria	Gammaproteobacteria	Enterobacterales	Erwiniaceae		
5a0b1e4e3822bf5b0da77fc050bbd255	Bacteria	Proteobacteria	Gammaproteobacteria	Enterobacterales	Erwiniaceae		
9050b2c4bf03bd4b8f2f38b8f11c19be	Bacteria	Firmicutes	Bacilli	Bacillales	Bacillaceae	Bacillus	
e0669cb86537c4b0fc07c55a9a58bb94	Bacteria	Proteobacteria	Gammaproteobacteria	Enterobacterales	Erwiniaceae		
379daf2feebd870bc08c1ca1cee2c542	Bacteria	Proteobacteria	Gammaproteobacteria	Enterobacterales	Enterobacteriaceae	Kosakonia	
8ff210ac388f826f381ded44dab88c94	Bacteria	Proteobacteria	Gammaproteobacteria	Enterobacterales	Erwiniaceae		
0bc28d38198cb752d98b9a1a8dac7ed3	Bacteria	Proteobacteria	Gammaproteobacteria	Enterobacterales	Erwiniaceae		
7a975ef700aba1a4f322de78cd97adf5	Bacteria	Proteobacteria	Gammaproteobacteria	Enterobacterales	Erwiniaceae		
24e1266c833ef74593a6d9c461daaa9a	Bacteria	Proteobacteria	Gammaproteobacteria	Pseudomonadales	Moraxellaceae	Acinetobacter	Acinetobacter_baylyi
cdea23f9956fc43963565b01b8b39731	Bacteria	Proteobacteria	Gammaproteobacteria	Enterobacterales	Erwiniaceae		
29b92d2680e49e1ba69adedc38f2009f	Bacteria	Proteobacteria	Alphaproteobacteria	Sphingomonadales	Sphingomonadaceae	Sphingomonas	
bc2a0d1e2d1db80007aaa7a3f74266ae	Bacteria	Firmicutes	Bacilli	Paenibacillales	Paenibacillaceae	Paenibacillus	Paenibacillus_wenxiniae
8acbb82020863dace142addf5ed1c6c5	Bacteria	Proteobacteria	Gammaproteobacteria	Enterobacterales	Erwiniaceae		
33c578e5a9f66bb4d3f9dfa785540e36	Bacteria	Proteobacteria	Gammaproteobacteria	Enterobacterales	Enterobacteriaceae		
c3cac25b433da7813418011e3a6c52f0	Bacteria	Proteobacteria	Gammaproteobacteria	Pseudomonadales	Pseudomonadaceae	Pseudomonas	
cb8591f4937151eb720b611a7d9f9235	Bacteria	Proteobacteria	Alphaproteobacteria	Sphingomonadales	Sphingomonadaceae	Sphingomonas	
ed49180ae59dd94cd3cf4697c6ef9a8c	Bacteria	Proteobacteria	Gammaproteobacteria	Enterobacterales	Erwiniaceae		

dd612aae1c4bdb80ee3255b71f6aa4d2	Bacteria	Proteobacteria	Gammaproteobacteria	Pseudomonadales	Pseudomonadaceae	Pseudomonas	
9ab2c5cc24cd3a2d29b71f07f804cf3e	Bacteria	Proteobacteria	Gammaproteobacteria	Enterobacterales	Enterobacteriaceae		
b6b3f51db0f78adcaec4500b289fc789	Bacteria	Proteobacteria	Gammaproteobacteria	Enterobacterales	Enterobacteriaceae		
8f298864cd39e4c50520a0c16eb66a7b	Bacteria	Proteobacteria	Gammaproteobacteria	Pseudomonadales	Pseudomonadaceae	Pseudomonas	
b6d3aace161ccdb983bc31f0f19fdf1a	Bacteria	Firmicutes	Bacilli	Bacillales	Bacillaceae	Bacillus	Bacillus_clausii
2fff20112e62df3bb60f5724c8de115f	Bacteria	Proteobacteria	Gammaproteobacteria	Enterobacterales	Enterobacteriaceae		
7985656ad5630678033337c7f05ecba00	Bacteria	Proteobacteria	Gammaproteobacteria	Enterobacterales	Enterobacteriaceae		
ea8b47e63e2814101697dec7b7601e0e	Bacteria	Proteobacteria	Gammaproteobacteria	Enterobacterales	Erwiniaceae	Pantoea	
2e3ac109539761fdc7e2cf3190669728	Bacteria	Proteobacteria	Gammaproteobacteria	Enterobacterales	Enterobacteriaceae		
311ea4b66d344848fd7dee02057c6e50	Bacteria	Proteobacteria	Gammaproteobacteria	Enterobacterales	Enterobacteriaceae		
241a5534d1ba6b007915b997ace8dc06	Bacteria	Proteobacteria	Gammaproteobacteria	Enterobacterales	Erwiniaceae		
59f094c853e2992bbf6ca38f229307cc	Bacteria	Proteobacteria	Gammaproteobacteria	Pseudomonadales	Pseudomonadaceae	Pseudomonas	
60a5cc1f83762b6423a9c83dd43ab0d0	Bacteria	Proteobacteria	Gammaproteobacteria	Pseudomonadales	Pseudomonadaceae	Pseudomonas	
d5f53ee124d270289b09967503066682	Bacteria	Proteobacteria	Gammaproteobacteria	Pseudomonadales	Pseudomonadaceae	Pseudomonas	
e4ab0e561a2d2d514d24cb749d0f5420	Bacteria	Proteobacteria	Gammaproteobacteria	Pseudomonadales	Pseudomonadaceae	Pseudomonas	
287a609f17e8691d3a5be8778fc5f4b3	Bacteria	Proteobacteria	Gammaproteobacteria	Oceanospirillales	Halomonadaceae	Halomonas	
ee003db088af5cc1ff1cac3cbd9e75ca	Bacteria	Firmicutes	Bacilli				
16f16fb000e9e050d1895c0a575b2d45	Bacteria	Proteobacteria	Gammaproteobacteria	Enterobacterales	Erwiniaceae		
adb2a38d7250142fe0e337a87a31a9e8	Bacteria	Proteobacteria	Gammaproteobacteria	Enterobacterales	Erwiniaceae		
a09d3b1c89a7a8ded550ade8f6ec2495	Bacteria	Proteobacteria	Gammaproteobacteria	Enterobacterales	Enterobacteriaceae	Kosakonia	
356c66397aa003abbaeb17f0719c95b9	Bacteria	Proteobacteria	Gammaproteobacteria	Pseudomonadales	Moraxellaceae	Acinetobacter	
f5ecf28fad00ffa68c46e69db1f4c31b	Bacteria	Proteobacteria	Gammaproteobacteria	Pseudomonadales	Pseudomonadaceae	Pseudomonas	Pseudomonas_psychrotolerans
2de6a0d760d54a88a5c7aab6ad367207	Bacteria	Proteobacteria	Gammaproteobacteria	Enterobacterales	Enterobacteriaceae		
7a0274b5c49e7ee27477b67f322df568	Bacteria	Proteobacteria	Gammaproteobacteria	Enterobacterales	Enterobacteriaceae		
dd1bd91b3d10900571a4b8349403052d	Bacteria	Proteobacteria	Gammaproteobacteria	Enterobacterales			
0d3b60b5e0150b7b346d78b84ac80ab2	Bacteria	Proteobacteria	Gammaproteobacteria	Enterobacterales	Erwiniaceae		
60dde2c45aeb223b78e29332dc36cb78	Bacteria	Proteobacteria	Gammaproteobacteria	Enterobacterales	Erwiniaceae	Siccibacter	
9685f6a77cf314ccf656bb3bf9cf52c3	Bacteria	Proteobacteria	Gammaproteobacteria	Enterobacterales	Erwiniaceae	Siccibacter	

689a6c996043cedff4120919a5c21e44	Bacteria	Proteobacteria	Gammaproteobacteria	Enterobacterales	Erwiniaceae	Siccibacter	
a585ad71f8405842ef4685fa1464d0a7	Bacteria	Proteobacteria	Gammaproteobacteria	Enterobacterales	Erwiniaceae	Siccibacter	
8073aceecd4f98860ed33db0763e6d8f	Bacteria	Firmicutes	Bacilli	Bacillales	Bacillaceae	Aeribacillus	
63a0c039f10be7e9420883e58c55bf8f	Bacteria	Proteobacteria	Alphaproteobacteria	Sphingomonadales	Sphingomonadaceae	Sphingomonas	
3705dc4aaf47e7e92f42926e64688818	Bacteria	Proteobacteria	Alphaproteobacteria	Rhizobiales	Beijerinckiaceae	Methylobacterium-Methylorubrum	
d2ec1ee0b4134e4f3454376ce3e03f2c	Bacteria	Proteobacteria	Alphaproteobacteria	Rhizobiales	Beijerinckiaceae	Methylobacterium-Methylorubrum	
cbeff48aa4ca321bcbdcc9eb7575a640	Bacteria	Proteobacteria	Alphaproteobacteria	Rhizobiales	Beijerinckiaceae	Methylobacterium-Methylorubrum	
d35e734a10fdca616f7cb0b25b34edb2	Bacteria	Proteobacteria	Alphaproteobacteria	Sphingomonadales	Sphingomonadaceae	Sphingomonas	
8e83f0e513f8d341a783dbc5cb2f8b0c	Bacteria	Proteobacteria	Alphaproteobacteria	Rhizobiales	Beijerinckiaceae	Methylobacterium-Methylorubrum	
9c93259e860265391138ffb7abd41110	Bacteria	Proteobacteria	Alphaproteobacteria	Rhizobiales	Beijerinckiaceae	Methylobacterium-Methylorubrum	
7439f74c07d9cb3da15d289522e1b803	Bacteria	Proteobacteria	Alphaproteobacteria	Rhizobiales	Beijerinckiaceae	Methylobacterium-Methylorubrum	
53b3e344a453ed58401863a52206e09d	Bacteria	Proteobacteria	Alphaproteobacteria	Sphingomonadales	Sphingomonadaceae	Sphingomonas	
79118b9e75537926012784c8241fd455	Bacteria	Proteobacteria	Alphaproteobacteria	Sphingomonadales	Sphingomonadaceae	Sphingomonas	
482f28820454a97e727a4e5fd620ea5a	Bacteria	Proteobacteria	Gammaproteobacteria	Pseudomonadales	Moraxellaceae	Acinetobacter	
6d08186963028a0bb368a76871e48c13	Bacteria	Proteobacteria	Gammaproteobacteria	Enterobacterales	Yersiniaceae	Serratia	
6da307d94a50f6007c685a5045436518	Bacteria	Proteobacteria	Gammaproteobacteria	Enterobacterales	Enterobacteriaceae		
7f9281be8fc7e1150bb545c7750a0023	Bacteria	Firmicutes	Bacilli	Bacillales	Bacillaceae	Bacillus	
41afdbbb88e290a50ac6f0a7e5bf4400	Bacteria	Proteobacteria	Gammaproteobacteria	Enterobacterales	Erwiniaceae		
bbdea7392258fda4949f3d0671753e96	Bacteria	Proteobacteria	Gammaproteobacteria	Enterobacterales	Erwiniaceae		
cbb9092e46578459c3e2eca54a9a16ff	Bacteria	Proteobacteria	Gammaproteobacteria	Enterobacterales	Erwiniaceae		
8a64abf6c8f48a271323cc5b5bf33fd0	Bacteria	Proteobacteria	Gammaproteobacteria	Pseudomonadales	Pseudomonadaceae	Pseudomonas	
c8fdebdad38758ed0b8d20297b554029	Bacteria	Proteobacteria	Alphaproteobacteria	Sphingomonadales	Sphingomonadaceae	Sphingomonas	
e14b2cc9f5b34bdba0e5fff3d62292c2	Bacteria	Proteobacteria	Gammaproteobacteria	Enterobacterales	Erwiniaceae	Pantoea	
6b17e21061b91f9319f4a7ff6e5e4855	Bacteria	Proteobacteria	Alphaproteobacteria	Sphingomonadales	Sphingomonadaceae	Sphingomonas	
8b16d121a3811e1445951818d8b90b01	Bacteria	Firmicutes	Bacilli	Bacillales	Bacillaceae	Bacillus	Bacillus_clausii
c7a1b36304e7cf2ae7cfd2e49b89f42d	Bacteria	Proteobacteria	Gammaproteobacteria	Enterobacterales	Enterobacteriaceae		
0bba615ff27fd3d72dc992ee90d6b81c	Bacteria	Proteobacteria	Gammaproteobacteria	Enterobacterales	Yersiniaceae	Serratia	
156d71ec37b6229eb49747b8f1017e0b	Bacteria	Proteobacteria	Gammaproteobacteria	Enterobacterales			

b6a52b0917a252e110c4cbf7597881b0	Bacteria	Proteobacteria	Gammaproteobacteria	Pseudomonadales	Pseudomonadaceae	Pseudomonas	
a702449cafa4e002c48059d822d14617	Bacteria	Proteobacteria	Gammaproteobacteria	Enterobacterales	Erwiniaceae		
0aac09f6fcd692d6afeabe3ad7989345	Bacteria	Proteobacteria	Gammaproteobacteria	Enterobacterales	Erwiniaceae		
769316b3a036796a6a544c892e3e544c	Bacteria	Proteobacteria	Gammaproteobacteria	Enterobacterales	Erwiniaceae		
a58fb6e3be6f5b4ef34c9f3a5cc22a77	Bacteria	Proteobacteria	Gammaproteobacteria	Enterobacterales	Erwiniaceae		
77a7b90e32c3930d57af108ca5325fc6	Bacteria	Proteobacteria	Gammaproteobacteria	Enterobacterales	Erwiniaceae		
a423140c7cfb08c4f87de40663ce39d2	Bacteria	Proteobacteria	Gammaproteobacteria	Enterobacterales	Erwiniaceae		
cec0ab273138a0f705bfe5810f3aded9	Bacteria	Proteobacteria	Gammaproteobacteria	Enterobacterales	Erwiniaceae	Pantoea	
4c5ddba97e41e071eca1c9c960b7b540	Bacteria	Proteobacteria	Gammaproteobacteria	Enterobacterales	Erwiniaceae		
6766cb541b7f06a91377523f6477e821	Bacteria	Proteobacteria	Alphaproteobacteria	Sphingomonadales	Sphingomonadaceae	Sphingomonas	
da1950148586d64eefc8853b72560b72	Bacteria	Proteobacteria	Gammaproteobacteria	Enterobacterales	Enterobacteriaceae		
cbf39cbb417a2800b949f7623a898982	Bacteria	Proteobacteria	Gammaproteobacteria	Enterobacterales	Enterobacteriaceae		
b1bf2a17358aaab11fadb8f4e2be26d4	Bacteria	Proteobacteria	Gammaproteobacteria	Enterobacterales	Erwiniaceae		
070fe8f226aff30e83b5c007f437c3d5	Bacteria	Firmicutes	Bacilli	Bacillales	Bacillaceae	Bacillus	
f15764c0cba170a3b6013d96d911bc45	Bacteria	Proteobacteria	Gammaproteobacteria	Enterobacterales	Enterobacteriaceae		
715732c4eb5e2fbfcaef0b196c7c78d0	Bacteria	Firmicutes	Bacilli	Bacillales	Bacillaceae	Bacillus	Bacillus_clausii
09d09cc807e553a35ec99359e229468b	Bacteria	Proteobacteria	Gammaproteobacteria	Enterobacterales	Enterobacteriaceae		
705b2da996c9082ba4ea0b8b7012f29b	Bacteria	Firmicutes	Bacilli	Bacillales	Bacillaceae	Bacillus	
e2dc5c1e25ce4dc296eef6fa6a5fd933	Bacteria	Proteobacteria	Gammaproteobacteria	Enterobacterales	Enterobacteriaceae		
8f0fa413ad03cdc1f1134d6968c9c494	Bacteria	Proteobacteria	Gammaproteobacteria	Enterobacterales	Enterobacteriaceae		
4516fabba3e5a091cff9cba6ff8b97c2	Bacteria	Proteobacteria	Gammaproteobacteria	Enterobacterales	Enterobacteriaceae		
e8d1c8c54e9b298d6a049046f227775a	Bacteria	Proteobacteria	Gammaproteobacteria	Enterobacterales	Erwiniaceae	Pantoea	Mixta_gaviniae
d04f307f13a78fadedc0adb2640fb92a	Bacteria	Proteobacteria	Gammaproteobacteria	Enterobacterales	Erwiniaceae	Pantoea	Mixta_gaviniae
95bb7068516e839bb17df763de591ed9	Bacteria	Proteobacteria	Gammaproteobacteria	Enterobacterales	Erwiniaceae	Pantoea	Mixta_gaviniae
4ab92360af3e20ecb382883e73990fed	Bacteria	Proteobacteria	Gammaproteobacteria	Enterobacterales	Yersiniaceae	Serratia	
8e3f25eb2cc8f14240c0fe02e8e854f8	Bacteria	Firmicutes	Bacilli	Bacillales	Bacillaceae	Bacillus	Bacillus_clausii

Appendix Table 3A.4: Negative (beta<0) and positive (beta>0) bacterial and fungal networks obtained through the use of Spiec.Easi R package at pulsar.params parameter with a threshold of = 0.05 for both fungal and bacterial interactions using phyloseq object as an input.

Fungi	Bacteria
Beta pos: 0.2084206	Beta pos: 0.02010776
Beta neg: -0.05823033	Beta pos: 0.01082755
Beta neg: -0.01445401	Beta pos: 0.0161373
Beta pos: 0.1106699	Beta pos: 0.2795667
Beta pos: 0.003274328	Beta pos: 0.03321556
Beta pos: 0.03828365	Beta neg: -0.09724752
Beta pos: 0.09346873	Beta pos: 0.003442199
Beta pos: 0.02354842	Beta pos: 0.08763321
Beta pos: 0.03413234	Beta pos: 0.01104773
Beta neg: -0.01713213	Beta pos: 0.009362029
Beta pos: 0.04900298	Beta pos: 0.03113629
Beta pos: 0.02101023	Beta pos: 0.03378348
Beta neg: -0.006073618	Beta pos: 0.146531
Beta neg: -0.01945691	Beta pos: 0.04878766
Beta pos: 0.05368005	Beta pos: 0.03008837
Beta pos: 0.01318113	Beta pos: 0.1441522
Beta neg: -0.09052923	Beta pos: 0.04185564
Beta pos: 0.03969416	Beta pos: 0.0188025
Beta pos: 0.002713341	Beta pos: 0.09512259
Beta pos: 0.116217	Beta pos: 0.01056139
Beta pos: 0.06062307	Beta pos: 0.01805227
Beta pos: 0.00625432	Beta pos: 0.2219921
Beta pos: 0.04309884	Beta pos: 0.06540517
Beta pos: 0.075521	Beta pos: 0.01398999
Beta pos: 0.03604563	Beta pos: 0.1584741
Beta pos: 0.0135207	Beta pos: 0.02498662
Beta pos: 0.01495913	Beta pos: 0.01211957
Beta pos: 0.00453826	Beta pos: 0.01797876
Beta pos: 0.01391208	Beta pos: 0.06264077
Beta pos: 0.01429931	Beta pos: 0.005378018
Beta neg: -0.0125179	Beta pos: 0.004298648
Beta pos: 0.01404465	Beta pos: 0.06676031
Beta pos: 0.4263608	Beta pos: 0.0219837
Beta pos: 0.07789787	Beta pos: 0.005516022
Beta pos: 0.001700499	Beta pos: 0.01814973

Beta pos: 0.01688363	Beta pos: 0.0005022425
Beta pos: 0.1672016	Beta pos: 0.03033281
Beta pos: 0.2960796	Beta pos: 0.01987516
Beta pos: 0.03844168	Beta pos: 0.06719216
Beta neg: -0.0151504	Beta pos: 0.1241303
Beta pos: 0.02882876	Beta pos: 0.04312465
Beta pos: 0.00659454	Beta pos: 0.001940369
Beta pos: 0.04117517	Beta pos: 0.007852892
Beta neg: -0.007246209	Beta pos: 0.08984784
Beta pos: 0.231926	Beta neg: -0.01447973
Beta neg: -0.002400371	Beta neg: -0.01547501
Beta pos: 0.2864098	Beta pos: 0.1248918
Beta pos: 0.0001691994	Beta pos: 0.001379403
Beta pos: 0.1462748	Beta pos: 0.008192277
Beta pos: 0.02735908	Beta pos: 0.1030053
Beta pos: 0.07461087	Beta pos: 0.05404185
Beta pos: 0.01764517	Beta pos: 0.01771659
Beta pos: 0.02197459	Beta neg: -0.01931538
Beta pos: 0.006813188	Beta neg: -0.0185083
Beta neg: -0.01208062	Beta pos: 0.03494155
Beta neg: -0.002896135	Beta neg: -0.02589847
Beta pos: 0.01894616	Beta pos: 0.06523388
Beta pos: 0.03299004	Beta neg: -0.001168868
Beta pos: 0.01953537	Beta pos: 0.08164874
Beta pos: 0.01282469	Beta pos: 0.06326986
Beta pos: 0.08440643	Beta pos: 0.05758603
Beta pos: 0.2211004	Beta pos: 0.05656681
Beta pos: 0.004107477	Beta pos: 0.004129805
Beta neg: -0.109355	Beta pos: 0.02116159
Beta neg: -0.07453726	Beta neg: -0.05810649
Beta pos: 0.00611471	Beta neg: -0.01365307
Beta neg: -0.01924657	Beta pos: 0.08627817
Beta pos: 0.0008720721	Beta pos: 0.008179342
Beta pos: 0.002445889	Beta neg: -0.02799511
Beta neg: -0.005873165	Beta neg: -0.01729564
Beta pos: 0.0009876699	Beta pos: 0.09558035
Beta pos: 0.02621999	Beta pos: 0.1613647
Beta neg: -0.02323702	Beta pos: 0.04493758
Beta neg: -0.009490852	Beta pos: 0.254411
Beta pos: 0.01530206	Beta neg: -0.03060826

Beta pos: 0.032089	Beta pos: 0.09212213
Beta neg: -0.006458116	Beta pos: 0.002126928
Beta pos: 0.00163966	Beta pos: 0.01631515
Beta pos: 0.03308038	Beta pos: 0.05903305
Beta pos: 0.01049409	Beta neg: -0.02330101
Beta pos: 0.05608028	Beta neg: -0.006074862
Beta neg: -0.005912567	Beta neg: -0.04529589
Beta pos: 0.04758663	Beta pos: 0.01479751
Beta pos: 0.007416193	Beta pos: 0.0335673
Beta pos: 0.009280826	Beta pos: 0.02914753
Beta pos: 0.03048972	Beta pos: 0.02159762
Beta pos: 0.08823739	Beta pos: 0.0161566
Beta pos: 0.06388078	Beta neg: -0.002989995
Beta neg: -0.02037781	Beta pos: 0.04391365
Beta pos: 0.115079	Beta pos: 0.139764
Beta neg: -0.009215079	Beta neg: -0.01538476
Beta pos: 0.04877943	Beta pos: 0.05037587
Beta pos: 0.1195621	Beta pos: 0.0260117
Beta pos: 0.03511786	Beta pos: 0.2773586
Beta pos: 0.03891988	Beta pos: 0.2519579
Beta pos: 0.05942581	Beta neg: -0.006446626
Beta pos: 0.1510716	Beta neg: -0.03253856
Beta pos: 0.05655163	Beta neg: -0.01060275
Beta pos: 0.05389659	Beta pos: 0.05306703
Beta pos: 0.09901307	Beta neg: -0.03936335
Beta pos: 0.177137	Beta neg: -0.01573235
Beta pos: 0.05663429	Beta pos: 0.2040342
Beta pos: 0.1614745	Beta pos: 0.006446684
Beta pos: 0.02299857	Beta pos: 0.009859576
Beta pos: 0.1998938	Beta pos: 0.07455952
Beta pos: 0.1740915	Beta pos: 0.3752768
Beta pos: 0.148913	Beta neg: -0.009640446
Beta pos: 0.01816744	Beta pos: 0.05253584
Beta pos: 0.009773641	Beta pos: 0.01904894
Beta pos: 0.1576708	Beta pos: 0.01668433
Beta pos: 0.4070934	Beta pos: 0.01898901
Beta pos: 0.01891931	Beta neg: -0.002525541
Beta pos: 0.0481905	Beta neg: -0.02953586
Beta pos: 0.1235555	Beta neg: -0.004230954
Beta pos: 0.4076065	Beta pos: 0.01011837

Beta pos: 0.1919895	Beta pos: 0.05312503
Beta pos: 0.1403607	Beta pos: 0.1133011
Beta pos: 0.04319097	Beta neg: -0.01011212
Beta pos: 0.02626567	Beta pos: 0.0374629
Beta pos: 0.2579847	Beta pos: 0.003149456
Beta pos: 0.04675327	Beta pos: 0.05982288
Beta pos: 0.01811205	Beta pos: 0.04025711
Beta pos: 0.05085846	Beta pos: 0.03285699
Beta pos: 0.01397798	Beta pos: 0.08271438
Beta pos: 0.0162798	Beta neg: -0.001733126
Beta pos: 0.006868311	Beta pos: 0.06157116
Beta pos: 0.0371421	Beta pos: 0.0520896
Beta pos: 0.05768306	Beta pos: 0.4749167
Beta neg: -0.01697276	Beta pos: 0.03697932
Beta pos: 0.0795258	Beta pos: 0.03778528
Beta neg: -0.002073095	Beta pos: 0.01858335
Beta neg: -0.006755282	Beta neg: -0.06883909
Beta neg: -0.007614885	Beta neg: -0.005412857
Beta neg: -0.00837097	Beta pos: 0.04933415
Beta neg: -0.04237014	Beta pos: 0.2400116
Beta pos: 0.04410313	Beta neg: -0.01493051
Beta pos: 0.04527763	Beta pos: 0.1482859
Beta pos: 0.03768915	Beta pos: 0.02518306
Beta pos: 0.08858705	Beta pos: 0.2119769
Beta pos: 0.04256871	Beta neg: -0.006708842
Beta pos: 0.03494894	Beta pos: 0.4079761
Beta pos: 0.006689383	Beta pos: 0.00834804
Beta pos: 0.08116889	Beta neg: -0.01351012
Beta pos: 0.1173835	Beta neg: -0.04882402
Beta pos: 0.0008266257	Beta neg: -0.01740275
Beta pos: 0.3065893	Beta neg: -0.01667402
Beta pos: 0.0326471	Beta neg: -0.002289769
Beta pos: 0.2625553	Beta pos: 0.08900694
Beta pos: 0.01146046	Beta pos: 0.00314045
Beta neg: -0.004625842	Beta pos: 0.03545847
Beta pos: 0.07918832	Beta neg: -0.007392456
Beta pos: 0.1060516	Beta pos: 0.1637393
Beta pos: 0.0816632	Beta pos: 0.02267692
Beta pos: 0.1951374	Beta neg: -0.01454777
Beta pos: 0.2466271	Beta pos: 0.1222787

Beta pos: 0.009844214	Beta pos: 0.02963044
Beta pos: 0.08984487	Beta pos: 0.00768875
Beta pos: 0.2467027	Beta pos: 0.1190579
Beta pos: 0.2720057	Beta pos: 0.02149662
Beta pos: 0.1439517	Beta pos: 0.09117979
Beta pos: 0.06472243	Beta neg: -0.002978373
Beta pos: 0.02403322	Beta neg: -0.004405141
Beta pos: 0.1633333	Beta neg: -0.03128361
Beta pos: 0.3378196	Beta pos: 0.001263725
Beta neg: -0.01604711	Beta neg: -0.047138
Beta neg: -0.005598779	Beta pos: 0.05990708
Beta pos: 0.005704786	Beta pos: 0.0243289
Beta pos: 0.1368292	Beta pos: 0.01243714
Beta pos: 0.009459102	Beta pos: 0.02879122
Beta pos: 0.07560839	Beta pos: 0.0266151
Beta pos: 0.0005478119	Beta pos: 0.04748967
Beta pos: 0.006141295	Beta pos: 0.01756589
Beta pos: 0.07535296	Beta pos: 0.1037769
Beta pos: 0.0209336	Beta pos: 0.1766568
Beta pos: 0.07317468	Beta pos: 0.03756068
Beta neg: -0.0009348433	Beta pos: 0.01900062
Beta pos: 0.03876461	Beta pos: 0.01668596
Beta pos: 0.1108516	Beta pos: 0.02590268
Beta pos: 0.0279759	Beta pos: 0.03557416
Beta pos: 0.004869887	Beta pos: 0.01932335
Beta pos: 0.0005764898	Beta pos: 0.03406356
Beta pos: 0.04235634	Beta pos: 0.1202184
Beta pos: 0.04480494	Beta pos: 0.0001795402
Beta pos: 0.1741824	Beta pos: 0.1519247
Beta pos: 0.04608213	Beta pos: 0.02718567
Beta pos: 0.05144063	Beta pos: 0.002940904
Beta pos: 0.0004865187	Beta neg: -0.01160826
Beta pos: 0.07778531	Beta neg: -0.02106661
Beta pos: 0.1007083	Beta pos: 0.229339
Beta pos: 0.1375235	Beta neg: -0.06415643
Beta pos: 0.00816932	Beta pos: 0.03292168
Beta pos: 0.1408185	Beta pos: 0.01958035
Beta pos: 0.001874196	Beta pos: 0.09924431
Beta pos: 0.004552485	Beta pos: 0.01736913
Beta pos: 0.01583896	Beta pos: 0.07700032

Beta pos: 0.04914386	Beta neg: -0.02900708
Beta pos: 0.1693598	Beta neg: -0.01517698
Beta pos: 0.1806618	Beta pos: 0.04450213
Beta pos: 0.1445208	Beta pos: 0.004158167
Beta pos: 0.1043773	Beta pos: 0.07327435
Beta pos: 0.03194093	Beta pos: 0.02149118
Beta pos: 0.05705977	Beta pos: 0.03501555
Beta pos: 0.02547631	Beta pos: 0.2355716
Beta pos: 0.33341	Beta pos: 0.01487826
Beta pos: 0.2721328	Beta pos: 0.06769457
Beta pos: 0.005814046	Beta pos: 0.1144619
Beta pos: 0.04151967	Beta pos: 0.04105015
Beta pos: 0.002705145	Beta pos: 0.007881203
Beta pos: 0.3082167	Beta pos: 0.08853069
Beta pos: 0.01435777	Beta pos: 0.07680213
Beta pos: 0.01212709	Beta pos: 0.04371589
Beta pos: 0.1563934	Beta neg: -0.02375922
Beta pos: 0.007765714	Beta pos: 0.007812781
Beta pos: 0.09992004	Beta pos: 0.2429216
Beta pos: 0.1633184	Beta neg: -0.005808654
Beta pos: 0.04181812	Beta pos: 0.04928584
Beta neg: -0.002370455	Beta pos: 0.03403133
Beta neg: -0.002497242	Beta pos: 0.05846211
Beta pos: 0.05685594	Beta pos: 0.0464937
Beta pos: 0.09474879	Beta neg: -0.001432594
Beta pos: 0.01965246	Beta pos: 0.1444304
Beta pos: 0.01540802	Beta pos: 0.02481039
Beta pos: 0.1000961	Beta pos: 0.06342967
Beta pos: 0.1855215	Beta pos: 0.3055819
Beta pos: 9.818457e-05	Beta pos: 0.0154891
Beta pos: 0.550678	Beta neg: -0.01441621
Beta pos: 0.3530884	Beta pos: 0.005202439
Beta pos: 0.09741614	Beta neg: -0.05853314
Beta pos: 0.02653005	Beta pos: 0.088907
Beta pos: 0.1906336	Beta neg: -0.007320419
Beta neg: -0.01573994	Beta pos: 0.01107401
Beta pos: 0.001092658	Beta pos: 0.01363101
Beta pos: 0.03447629	Beta pos: 0.02873996
Beta pos: 0.1733204	Beta pos: 0.02215287
Beta neg: -0.01686921	Beta pos: 0.03510811

Beta pos: 0.2081176	Beta pos: 0.09689655
Beta pos: 0.2520052	Beta neg: -0.004065837
Beta neg: -0.005438434	Beta pos: 0.2385066
Beta pos: 0.2168608	Beta neg: -0.0393275
Beta pos: 0.006913279	Beta pos: 0.02138881
Beta pos: 0.04037915	Beta pos: 0.288136
Beta pos: 0.02778639	Beta pos: 0.01926151
Beta pos: 0.02029218	Beta pos: 0.03216752
Beta pos: 0.1346237	Beta pos: 0.02736107
Beta pos: 0.0466455	Beta pos: 0.06555359
Beta pos: 0.01349887	Beta pos: 0.01218045
Beta pos: 0.03938963	Beta pos: 0.03395401
Beta pos: 0.1438845	Beta pos: 0.01887299
Beta pos: 0.1035713	Beta pos: 0.09361273
Beta pos: 0.05298868	Beta pos: 0.03680662
Beta pos: 0.009205217	Beta pos: 0.05571089
Beta pos: 0.1490343	Beta pos: 0.01194896
Beta pos: 0.1574003	Beta pos: 0.1041922
Beta pos: 0.01994583	Beta pos: 0.01413704
Beta pos: 0.1255923	Beta pos: 0.05845302
Beta pos: 0.2062887	Beta pos: 0.007729422
Beta pos: 0.04567296	Beta pos: 0.05918778
Beta pos: 0.1669907	Beta pos: 0.01379701
Beta pos: 0.01560095	Beta pos: 0.07185053
Beta pos: 0.0718761	Beta pos: 0.003554775
Beta pos: 0.06376939	Beta pos: 0.1335087
Beta pos: 0.00819117	Beta pos: 0.02091918
Beta pos: 0.1550292	Beta pos: 0.0228852
Beta neg: -0.00140036	Beta neg: -0.004332885
Beta neg: -0.006610298	Beta pos: 0.08173539
Beta pos: 0.02793136	Beta pos: 0.0126093
Beta pos: 0.05866715	Beta pos: 0.1279216
Beta pos: 0.04323269	Beta pos: 0.0028218
Beta pos: 0.02856972	Beta pos: 0.01139998
Beta pos: 0.08679353	Beta pos: 0.0735169
Beta neg: -0.0341073	Beta pos: 0.01489687
Beta pos: 0.2714464	Beta pos: 0.03775274
Beta pos: 0.08597596	Beta pos: 0.006264455
Beta pos: 0.2247947	Beta pos: 0.08733883
Beta pos: 0.0863428	Beta neg: -0.03402777

Beta pos: 0.1639148	Beta pos: 0.1121535
Beta pos: 0.05422282	Beta neg: -0.03471129
Beta pos: 0.05237315	Beta neg: -0.006876616
Beta pos: 0.1296633	Beta neg: -0.002590223
Beta pos: 0.009835391	Beta pos: 0.02401174
Beta pos: 0.03891894	Beta pos: 0.1599381
Beta pos: 0.01298231	Beta pos: 0.003988486
Beta pos: 0.04788261	Beta pos: 0.220237
Beta pos: 0.1743985	Beta neg: -0.004883829
Beta pos: 0.1522613	Beta pos: 0.002515242
Beta pos: 0.0795716	Beta pos: 0.03499185
Beta pos: 0.1308646	Beta pos: 0.0004182746
Beta pos: 0.3123381	Beta pos: 0.01245744
Beta pos: 0.01471474	Beta pos: 0.1266563
Beta pos: 0.05905637	Beta pos: 0.007562605
Beta pos: 0.2981761	Beta pos: 0.003123421
Beta pos: 0.01979976	Beta neg: -0.006350211
Beta pos: 0.01448036	Beta pos: 0.08776805
Beta pos: 0.1594921	Beta neg: -0.01485484
Beta pos: 0.05607579	Beta pos: 0.004470955
Beta pos: 0.02487444	Beta neg: -0.005717209
Beta pos: 0.1146892	Beta pos: 0.01574853
Beta pos: 0.2598008	Beta pos: 0.09614079
Beta pos: 0.02483251	Beta pos: 0.03136428
Beta pos: 0.09919091	Beta pos: 0.01445538
Beta pos: 0.03315945	Beta pos: 0.06577368
Beta pos: 0.02938709	Beta pos: 0.05007801
Beta pos: 0.01489048	Beta pos: 0.003742466
Beta neg: -0.05956698	Beta pos: 0.03902786
Beta pos: 0.1040705	Beta pos: 0.02690974
Beta pos: 0.09010746	Beta neg: -0.004017934
Beta neg: -0.002781681	Beta pos: 0.2093891
Beta pos: 0.1713178	Beta pos: 0.02441257
Beta pos: 0.09292191	Beta pos: 0.000811496
Beta pos: 0.137055	Beta pos: 0.020841
Beta pos: 0.03504069	Beta pos: 0.1155134
Beta pos: 0.01851999	Beta pos: 0.4559885
Beta pos: 0.07022948	Beta pos: 0.08590712
Beta pos: 0.1996368	Beta pos: 0.003144247
Beta pos: 0.07168254	Beta pos: 0.01046816

Beta neg: -0.03574906	Beta pos: 0.01384407
Beta pos: 0.06077202	Beta pos: 0.006248872
Beta pos: 0.01598978	Beta pos: 0.2664575
Beta pos: 0.08622863	Beta pos: 0.03834481
Beta neg: -0.08508109	Beta pos: 0.007558841
Beta pos: 0.3612335	Beta pos: 0.03004318
Beta neg: -0.005373475	Beta pos: 0.0347301
Beta pos: 0.07172594	Beta pos: 0.00859293
Beta pos: 0.1678012	Beta pos: 0.0001015021
Beta pos: 0.08956066	Beta pos: 0.04452173
Beta pos: 0.01048012	Beta pos: 0.03113181
Beta pos: 0.08263323	Beta pos: 0.005947473
Beta pos: 0.1446269	Beta pos: 0.007163614
Beta neg: -0.02246323	Beta pos: 0.03217724
Beta pos: 0.0102848	Beta pos: 0.01757422
Beta pos: 0.02129499	Beta pos: 0.06959494
Beta pos: 0.3749441	Beta pos: 0.005535959
Beta neg: -0.1424845	Beta neg: -0.03524475
Beta pos: 0.002631908	Beta pos: 0.03594528
Beta pos: 0.1228063	Beta neg: -0.03816635
Beta pos: 0.1623633	Beta pos: 0.01818553
Beta pos: 0.03600223	Beta pos: 0.08609402
Beta pos: 0.1015163	Beta pos: 0.13059
Beta pos: 0.08396887	Beta pos: 0.1862348
Beta pos: 0.004715385	Beta pos: 0.01893346
Beta pos: 0.01795981	Beta neg: -0.08255749
Beta pos: 0.06532586	Beta pos: 0.01326653
Beta pos: 0.2633902	Beta pos: 0.09643358
Beta pos: 0.1423226	Beta pos: 0.1459073
Beta pos: 0.1173643	Beta pos: 0.01739456
Beta pos: 0.1208418	Beta pos: 0.07188681
Beta pos: 0.02171156	Beta pos: 0.01938376
Beta pos: 0.004361406	Beta pos: 0.005474469
Beta pos: 0.01142784	Beta pos: 0.01007007
Beta pos: 0.02494914	Beta pos: 0.058403
Beta pos: 0.005639487	Beta pos: 0.04011902
Beta neg: -0.02685646	Beta pos: 0.217783
Beta pos: 0.2433679	Beta pos: 0.2230322
Beta pos: 0.004899774	Beta pos: 0.1157934
Beta pos: 0.3496321	Beta pos: 0.1965622

Beta pos: 2.012465e-05	Beta pos: 0.07917864
Beta pos: 0.023025	Beta pos: 0.3880427
Beta pos: 0.03453933	Beta pos: 0.01614045
Beta pos: 0.03122203	Beta pos: 0.002700764
Beta pos: 0.2871356	Beta neg: -0.03268056
Beta pos: 0.03534461	Beta pos: 0.01766105
Beta pos: 0.002626298	Beta pos: 0.1009105
Beta pos: 0.04848843	Beta pos: 0.002164778
Beta pos: 0.2082793	Beta pos: 0.0113596
Beta neg: -0.04488581	Beta pos: 0.1191921
Beta pos: 0.006823192	Beta pos: 0.02450486
Beta pos: 0.02445322	Beta pos: 0.01525765
Beta pos: 0.02784507	Beta pos: 0.4890461
Beta pos: 0.1272024	Beta pos: 0.02532125
Beta pos: 0.1145015	Beta pos: 0.1610254
Beta pos: 0.02029765	Beta pos: 0.03785539
Beta pos: 0.08179986	Beta pos: 0.02975273
Beta pos: 0.32391	Beta pos: 0.2135615
Beta pos: 0.437877	Beta pos: 0.1061863
Beta pos: 0.03600728	Beta pos: 0.0699238
Beta pos: 0.001055527	Beta pos: 0.04209297
Beta pos: 0.005820494	Beta pos: 0.02445059
Beta pos: 0.1336385	Beta pos: 0.01654452
Beta pos: 0.05658198	Beta pos: 0.0601014
Beta pos: 0.03782121	Beta neg: -0.002480107
Beta pos: 0.2532064	Beta neg: -0.007223342
Beta neg: -0.01312077	Beta pos: 0.1775421
Beta pos: 0.2896939	Beta pos: 0.1541266
Beta pos: 0.008254805	Beta neg: -0.009909238
Beta pos: 0.1457326	Beta pos: 0.08625453
Beta pos: 0.314343	Beta pos: 0.1926392
Beta pos: 0.07529754	Beta pos: 0.130864
Beta pos: 0.11597	Beta pos: 0.03344951
Beta pos: 0.03020843	Beta pos: 0.04585221
Beta pos: 0.4909776	Beta pos: 0.004480002
Beta neg: -0.02596284	Beta pos: 0.1253774
Beta pos: 0.01183653	Beta pos: 0.2600232
Beta pos: 0.01555463	Beta pos: 0.1150214
Beta pos: 0.1053865	Beta pos: 0.0698849
Beta neg: -0.003629526	Beta pos: 0.05834261

Beta neg: -0.03688879	Beta pos: 0.06424372
Beta pos: 0.00564722	Beta pos: 0.04928177
Beta pos: 0.1086809	Beta pos: 0.01959182
Beta pos: 0.03155859	Beta pos: 0.0443991
Beta neg: -0.002056704	Beta pos: 0.2981534
Beta pos: 0.02946814	Beta neg: -0.02612323
Beta pos: 0.368677	Beta neg: -0.03163149
Beta pos: 0.01143094	Beta pos: 0.07281319
Beta neg: -0.04984253	Beta pos: 0.07847189
Beta neg: -0.01202461	Beta neg: -0.01133087
Beta pos: 0.01020093	Beta pos: 0.03340732
Beta neg: -0.03263804	Beta pos: 0.04522245
Beta pos: 0.2243313	Beta pos: 0.1068144
Beta pos: 0.09060726	Beta pos: 0.02003223
Beta pos: 0.05082883	Beta pos: 0.02201674
Beta pos: 0.0377587	Beta pos: 0.04903356
Beta neg: -0.009465822	Beta pos: 0.001111708
Beta pos: 0.4885358	Beta pos: 0.07229717
Beta pos: 0.0982762	Beta pos: 0.0359665
Beta pos: 0.05279608	Beta pos: 0.18721
Beta pos: 0.1149185	Beta pos: 0.03278656
Beta pos: 0.04133584	Beta pos: 0.0322634
Beta pos: 0.003121763	Beta pos: 0.001196175
Beta neg: -0.07934489	Beta neg: -0.009254135
Beta pos: 0.01482826	Beta pos: 0.1822386
Beta pos: 0.03089162	Beta pos: 0.06371941
Beta pos: 0.1644775	Beta pos: 0.1905475
Beta pos: 0.03376198	Beta neg: -0.006245522
Beta pos: 0.1908211	Beta pos: 0.04551156
Beta pos: 0.03256738	Beta pos: 0.005998051
Beta pos: 0.004691962	Beta pos: 0.1303459
Beta pos: 0.003645041	Beta pos: 0.01962046
Beta pos: 0.007203103	Beta pos: 0.00678242
Beta pos: 0.03569803	Beta pos: 0.02559026
Beta pos: 0.04358029	Beta pos: 0.009234993
Beta pos: 0.01577586	Beta pos: 0.01228475
Beta neg: -0.004617434	Beta pos: 0.06270635
Beta pos: 0.03544032	Beta pos: 0.03804014
Beta pos: 0.03272989	Beta neg: -0.007326578
Beta pos: 0.06046426	Beta pos: 0.08610837

Beta pos: 0.3490052	Beta pos: 0.3100759
Beta pos: 0.0481332	Beta pos: 0.02961548
Beta pos: 0.01380861	Beta pos: 0.05180044
Beta neg: -0.033213	Beta pos: 0.06473768
Beta pos: 0.0151972	Beta pos: 0.03255914
Beta pos: 0.08547733	Beta pos: 0.03616795
Beta pos: 0.02064095	Beta pos: 0.08469873
Beta neg: -0.02236999	Beta pos: 0.02479596
Beta pos: 0.04193042	Beta pos: 0.0125613
Beta pos: 0.03057774	Beta pos: 0.09689981
Beta pos: 0.02069739	Beta neg: -0.02595087
Beta pos: 0.2619099	Beta pos: 0.0298373
Beta pos: 0.03580235	Beta pos: 0.08701452
Beta pos: 0.1512684	Beta pos: 0.05147232
Beta pos: 0.02476304	Beta pos: 0.01782444
Beta pos: 0.01541839	Beta pos: 0.00538509
Beta pos: 0.1352263	Beta pos: 0.07286209
Beta pos: 0.03706307	Beta pos: 0.03299009
Beta pos: 0.2369031	Beta pos: 0.01820113
Beta pos: 0.02018975	Beta pos: 0.003075101
Beta pos: 0.1144326	Beta pos: 0.09330694
Beta pos: 0.2026407	Beta pos: 0.0009575095
Beta pos: 0.1903058	Beta pos: 0.03108549
Beta pos: 0.1202639	Beta pos: 0.05430011
Beta pos: 0.2748473	Beta pos: 0.02239993
Beta pos: 0.003313608	Beta pos: 0.1292135
Beta pos: 0.01726654	Beta pos: 0.03128823
Beta pos: 0.01006142	Beta pos: 0.007500622
Beta pos: 0.01546897	Beta pos: 0.01251112
Beta pos: 0.1259056	Beta pos: 0.03612244
Beta pos: 0.06055346	Beta pos: 0.03184447
Beta pos: 0.002473409	Beta pos: 0.06967741
Beta pos: 0.0004307557	Beta pos: 0.2327625
Beta pos: 0.2320783	Beta pos: 0.07356569
Beta pos: 0.09772744	Beta pos: 0.1036939
Beta pos: 0.02809763	Beta pos: 0.01645118
Beta pos: 0.189942	Beta pos: 0.05345019
Beta pos: 0.05365862	Beta pos: 0.06047242
Beta pos: 0.1263595	Beta pos: 0.09880976
Beta pos: 0.03016606	Beta pos: 0.01436603

Beta pos: 0.05627015	Beta pos: 0.001203827
Beta pos: 0.106015	Beta pos: 0.009592233
Beta pos: 0.0310132	Beta pos: 0.04105772
Beta pos: 0.01394172	Beta pos: 0.00283159
Beta pos: 0.09335711	Beta neg: -0.02217948
Beta pos: 0.1440211	Beta pos: 0.103034
Beta pos: 0.0007314455	Beta pos: 0.1050113
Beta pos: 0.05783373	Beta pos: 0.07599991
Beta pos: 0.01381165	Beta pos: 0.007813528
Beta neg: -0.05882315	Beta pos: 0.007126336
Beta pos: 0.0008110475	Beta pos: 0.03624104
Beta pos: 0.05269685	Beta pos: 0.003392606
Beta pos: 0.05994756	Beta neg: -0.002527654
Beta pos: 0.3326819	Beta pos: 0.01912264
Beta pos: 0.02768591	Beta pos: 0.0163744
Beta pos: 0.08103641	Beta pos: 0.2192942
Beta pos: 0.2761657	Beta pos: 0.06538431
Beta pos: 0.1819947	Beta pos: 0.05288744
Beta pos: 0.2458132	Beta pos: 0.01737069
Beta pos: 0.03388904	Beta pos: 0.04297769
Beta pos: 0.0246499	Beta pos: 0.07597211
Beta pos: 0.07677853	Beta pos: 0.0203654
Beta pos: 0.08525026	Beta pos: 0.01817112
Beta pos: 0.007478297	Beta pos: 0.01350929
Beta pos: 0.2678176	Beta pos: 0.007845488
Beta pos: 0.09844695	Beta pos: 0.06310567
Beta pos: 0.1110056	Beta pos: 0.01959926
Beta pos: 0.05341187	Beta pos: 0.08169838
Beta pos: 0.1350192	Beta pos: 0.02200387
Beta pos: 0.2116534	Beta pos: 0.0420378
Beta pos: 0.1376108	Beta pos: 0.003684479
Beta neg: -0.003564441	Beta pos: 0.03039136
Beta pos: 0.0458173	Beta pos: 0.1398081
Beta pos: 0.002977178	Beta pos: 0.1332059
Beta pos: 0.1453836	Beta pos: 0.001507649
Beta pos: 0.06716147	Beta pos: 0.1009621
Beta pos: 0.1255108	Beta pos: 0.01145802
Beta pos: 0.04700041	Beta pos: 0.1560094
Beta pos: 0.1645731	Beta pos: 0.01644134
Beta pos: 0.140186	Beta pos: 0.01831388

Beta pos: 0.06863007	Beta pos: 0.02053858
Beta pos: 0.09218874	Beta pos: 0.01570008
Beta pos: 0.02294336	Beta pos: 0.006104729
Beta pos: 0.03855454	Beta pos: 0.04994077
Beta pos: 0.0899734	Beta pos: 0.01495213
Beta pos: 0.01489583	Beta pos: 0.05789584
Beta neg: -0.01578419	Beta pos: 0.1088277
Beta pos: 0.1775512	Beta pos: 0.004958893
Beta pos: 0.02996296	Beta pos: 0.1105117
Beta pos: 0.08973709	Beta pos: 0.004136217
Beta neg: -0.03148955	Beta pos: 0.07614494
Beta neg: -0.0163256	Beta pos: 0.006531604
Beta pos: 0.067541	Beta pos: 0.006400332
Beta pos: 0.2269425	Beta pos: 0.203358
Beta pos: 0.1640946	Beta pos: 0.1184973
Beta pos: 0.08143224	Beta pos: 0.008529601
Beta pos: 0.05282158	Beta pos: 0.00652179
Beta pos: 0.02621296	Beta pos: 0.02824892
Beta neg: -0.03689559	Beta pos: 0.1348132
Beta pos: 0.0683703	Beta pos: 0.1005029
Beta pos: 0.09334369	Beta pos: 0.01271269
Beta pos: 0.0415791	Beta pos: 0.01520305
Beta pos: 0.06845323	Beta pos: 0.006357729
Beta pos: 0.01282697	Beta neg: -0.01804711
Beta pos: 0.1063163	Beta neg:-0.003003528
Beta pos: 0.05845165	Beta pos: 0.03915335
Beta neg: -0.004949203	Beta pos: 0.01428684
Beta pos: 0.02534017	Beta pos: 0.1469585
Beta pos: 0.02156089	Beta pos: 0.0008186149
Beta pos: 0.06757967	Beta pos: 0.06266182
Beta neg: -0.0283483	Beta pos: 0.01487398
Beta neg: -0.005043979	Beta pos: 0.04203718
Beta pos: 0.08508084	Beta pos: 0.03380865
Beta pos: 0.1529457	Beta pos: 0.02818329
Beta pos: 0.05791672	Beta pos: 0.2718343
Beta pos: 0.07320516	Beta neg: -0.009842282
Beta pos: 0.07418707	Beta pos: 0.037454
Beta pos: 0.05130097	Beta pos: 0.1154866
Beta pos: 0.1045217	Beta pos: 0.06201219
Beta pos: 0.3568756	Beta pos: 0.07169804

Beta pos: 0.003293396	Beta pos: 0.1467754
Beta pos: 0.25233	Beta pos: 0.004576957
Beta pos: 0.2822788	Beta pos: 0.1416255
Beta pos: 0.00495535	Beta pos: 0.0320074
Beta pos: 0.02125876	Beta pos: 0.5181782
Beta pos: 0.1770825	Beta pos: 0.02212176
Beta pos: 0.07669963	Beta neg: -0.001296219
Beta pos: 0.1104745	Beta pos: 0.02032117
Beta pos: 0.09887069	Beta pos: 0.074349
Beta pos: 0.06291472	Beta neg: -0.009564141
Beta pos: 0.3643211	Beta pos: 0.00279409
Beta pos: 0.0143944	Beta pos: 0.07603385
Beta neg: -0.002722826	Beta pos: 0.3129546
Beta pos: 0.1692843	Beta pos: 0.2558341
Beta pos: 0.01889048	Beta pos: 0.02960951
Beta pos: 0.004352034	Beta pos: 0.01507693
Beta neg: -0.06005667	Beta pos: 0.01041256
Beta pos: 0.1320471	Beta pos: 0.1529144
Beta neg: -0.07704249	Beta pos: 0.08871796
Beta pos: 0.3309104	Beta pos: 0.02413441
Beta pos: 0.02390455	Beta pos: 0.01025897
Beta pos: 0.186223	Beta pos: 0.1490129
Beta pos: 0.445236	Beta pos: 0.02836301
Beta pos: 0.180744	Beta pos: 0.009476056
Beta pos: 0.1889331	Beta pos: 0.005393203
Beta pos: 0.2556376	Beta neg: -0.003020767
Beta pos: 0.01803311	Beta pos: 0.0256736
Beta pos: 0.1399776	Beta pos: 0.2271244
Beta pos: 0.2747644	Beta pos: 0.1580529
Beta pos: 0.007099137	Beta neg: -0.009859792
Beta pos: 0.2845962	Beta pos: 0.01560938
Beta pos: 0.2221244	Beta pos: 0.04471075
Beta pos: 0.09298958	Beta pos: 0.1227958
Beta pos: 0.5742366	Beta pos: 0.01056635
Beta pos: 0.07686865	Beta pos: 0.1699192
Beta pos: 0.01834943	Beta pos: 0.03000432
Beta pos: 0.05844924	Beta pos: 0.005441008
Beta pos: 0.3164977	Beta pos: 0.3557938
Beta pos: 0.03151721	Beta pos: 0.09898363
Beta pos: 0.02176503	Beta pos: 0.0005140866

Beta pos: 0.1654377	Beta pos: 0.01493794
Beta pos: 0.04024079	Beta pos: 0.0136726
Beta pos: 0.02383854	Beta pos: 0.0319929
Beta pos: 0.0530479	Beta pos: 0.004206454
Beta pos: 0.03340608	Beta pos: 0.07745174
Beta pos: 0.01710777	Beta pos: 0.0285616
Beta pos: 0.09406337	Beta pos: 0.0006993408
Beta pos: 0.6398222	Beta neg: -0.06048018
Beta pos: 0.008471366	Beta pos: 0.004641464
Beta pos: 0.01336641	Beta pos: 0.07685218
Beta neg: -0.006260787	Beta pos: 0.1502496
Beta pos: 0.09173579	Beta pos: 0.001482801
Beta pos: 0.04990725	Beta pos: 0.01974134
Beta pos: 0.6983151	Beta pos: 0.00215826
Beta pos: 0.1511283	Beta pos: 0.03887664
Beta pos: 0.1263671	Beta neg: -0.004603243
Beta pos: 0.0253649	Beta pos: 0.04577925
Beta neg: -0.01493701	Beta pos: 0.1538063
Beta pos: 0.0343169	Beta pos: 0.005074199
Beta pos: 0.2052107	Beta pos: 0.02276785
Beta pos: 0.04494356	Beta pos: 0.04097197
Beta neg: -0.02929537	Beta pos: 0.03146714
Beta pos: 0.05225398	Beta pos: 0.2640969
Beta pos: 0.421021	Beta pos: 0.02417181
Beta neg: -0.002824245	Beta pos: 0.0371035
Beta pos: 0.07181857	Beta pos: 0.1025453
Beta pos: 0.03353936	Beta pos: 0.1115806
Beta neg: -0.03319913	Beta pos: 0.005919941
Beta neg: -0.05134186	Beta pos: 0.1476896
Beta pos: 0.01665538	Beta pos: 0.0239467
Beta pos: 0.3990017	Beta pos: 0.3100218
Beta pos: 0.1090604	Beta pos: 0.0731703
Beta pos: 0.4011627	Beta pos: 0.02277432
Beta pos: 0.005477463	Beta neg: -0.02358495
Beta neg: -0.02919856	Beta pos: 0.1008372
Beta pos: 0.1317745	Beta pos: 0.03052968
Beta pos: 0.005922602	Beta pos: 0.1868331
Beta pos: 0.05034133	Beta pos: 0.01780755
Beta neg: -0.01362963	Beta pos: 0.01184654
Beta pos: 0.01449684	Beta pos: 0.0008104695

Beta pos: 0.1014538	Beta pos: 0.07630848
Beta pos: 0.173818	Beta pos: 0.2394328
Beta pos: 0.4006615	Beta pos: 0.00165179
Beta pos: 0.2149144	Beta neg: -0.008771806
Beta pos: 0.07459888	Beta neg: -0.003257984
Beta pos: 0.277773	Beta neg: -0.01099216
Beta pos: 0.1093503	Beta pos: 0.142391
Beta pos: 0.1482779	Beta pos: 0.02090683
Beta pos: 0.2906967	Beta pos: 0.1047155
Beta pos: 0.02969221	Beta pos: 0.2542282
Beta pos: 0.0581006	Beta neg: -0.002974904
Beta pos: 0.007193758	Beta pos: 0.0416631
Beta pos: 0.1940647	Beta pos: 0.03093402
Beta pos: 0.01955524	Beta pos: 0.1107842
Beta pos: 0.03600416	Beta pos: 0.04369685
Beta pos: 0.05112221	Beta pos: 0.3005709
Beta neg: -0.02606784	Beta pos: 0.2481263
Beta pos: 0.09505705	Beta pos: 0.009266739
Beta pos: 0.06195247	Beta pos: 0.001906075
Beta pos: 0.07907164	Beta pos: 0.07792778
Beta pos: 0.03924437	Beta pos: 0.02733086
Beta pos: 0.1652111	Beta pos: 0.3063094
Beta pos: 0.05978494	Beta pos: 0.05382352
Beta pos: 0.1904663	Beta pos: 0.02524683
Beta pos: 0.1146605	Beta pos: 0.007818231
Beta pos: 0.05548469	Beta pos: 0.02266416
Beta pos: 0.2496736	Beta pos: 0.267992
Beta pos: 0.0466131	Beta pos: 0.002389784
Beta pos: 0.0395901	Beta pos: 0.05380075
Beta pos: 0.0003859673	Beta pos: 0.2493713
Beta pos: 0.1019751	Beta pos: 0.1951519
Beta neg: -0.07711583	Beta neg: -0.03084099
Beta pos: 0.01276249	Beta pos: 0.01434777
Beta neg: -0.03289213	Beta pos: 0.01231577
Beta pos: 0.05600635	Beta pos: 0.3067419
Beta pos: 0.07950592	Beta pos: 0.2778919
Beta pos: 0.02844498	Beta pos: 0.00212488
Beta pos: 0.1357062	Beta pos: 0.007883167
Beta pos: 0.09861146	Beta pos: 0.001737179
Beta pos: 0.07805319	Beta pos: 0.05476464

Beta pos: 0.2001419	Beta pos: 0.03601491
Beta pos: 0.02416845	Beta pos: 0.03344771
Beta pos: 0.02549857	Beta pos: 0.03591686
Beta neg: -0.009370245	Beta pos: 0.01390342
Beta pos: 0.01399602	Beta pos: 0.02147854
Beta pos: 0.04326757	Beta pos: 0.03040341
Beta pos: 0.6362288	Beta pos: 0.01579757
Beta pos: 0.05314615	Beta pos: 0.05335046
Beta pos: 0.003914682	Beta pos: 0.04831032
Beta neg: -0.03673499	Beta pos: 0.319502
Beta neg: -0.03602409	Beta pos: 0.04325412
Beta pos: 0.02472518	Beta pos: 0.006505126
Beta neg: -0.01754345	Beta pos: 0.01513751
Beta pos: 0.1109493	Beta pos: 0.001078736
Beta pos: 0.2932543	Beta pos: 0.01816388
Beta pos: 0.141977	Beta pos: 0.01922846
Beta pos: 0.4260029	Beta pos: 0.1367625
Beta pos: 0.1196636	Beta pos: 0.2054391
Beta pos: 0.005470041	Beta neg: -0.02300013
Beta pos: 0.03195678	Beta pos: 0.29196
Beta pos: 0.006669706	Beta pos: 0.01930249
Beta pos: 0.01946109	Beta neg: -0.07098677
Beta pos: 0.1962494	Beta neg: -0.05931175
Beta pos: 0.01923232	Beta pos: 0.002922226
Beta pos: 0.1256773	Beta pos: 0.009176275
Beta pos: 0.1914223	Beta pos: 0.03846358
Beta pos: 0.4141771	Beta pos: 0.03990595
Beta pos: 0.01873886	Beta pos: 0.02309492
Beta pos: 0.05573908	Beta neg: -0.02053456
Beta pos: 0.1889605	Beta pos: 0.06020863
Beta pos: 0.1114554	Beta pos: 0.140489
Beta pos: 0.007021936	Beta pos: 0.01111077
Beta neg: -0.02531005	Beta pos: 0.2516062
Beta pos: 0.1277283	Beta neg: -0.0005357824
Beta pos: 0.05516658	Beta neg: -0.01754283
Beta pos: 0.1063632	Beta neg: -0.02802503
Beta pos: 0.103243	Beta pos: 0.03264001
Beta neg: -0.0007756113	Beta pos: 0.1728611
Beta pos: 0.05729168	Beta pos: 0.02656926
Beta pos: 0.004739259	Beta pos: 0.1337862

Beta pos: 0.2489278	Beta pos: 0.003538519
Beta pos: 0.006831846	Beta pos: 0.04162505
Beta neg: -0.003337199	Beta pos: 0.1040276
Beta pos: 0.2041381	Beta pos: 0.2809758
Beta pos: 0.2119347	Beta pos: 0.01868514
Beta pos: 0.3484039	Beta pos: 0.1567097
Beta pos: 0.03008515	Beta pos: 0.2814899
Beta pos: 0.2302488	Beta pos: 0.01654077
Beta pos: 0.09962504	Beta pos: 0.2290961
Beta pos: 0.004545996	Beta pos: 0.04964382
Beta pos: 0.05089232	Beta pos: 0.01245072
Beta pos: 0.4983826	Beta neg: -0.003848163
Beta pos: 0.0006468318	Beta neg: -0.05954595
Beta pos: 0.02863937	Beta neg: -0.003900411
Beta pos: 0.1656475	Beta neg: -0.01785229
Beta pos: 0.110006	Beta neg: -0.002644717
Beta pos: 0.002727255	Beta pos: 0.02838941
Beta pos: 0.02147106	Beta pos: 0.02506201
Beta pos: 0.1917716	Beta pos: 0.02004121
Beta pos: 0.2381137	Beta pos: 0.02322386
Beta pos: 0.0623178	Beta pos: 0.04026598
Beta pos: 0.0004532074	Beta neg: -0.009560056
Beta pos: 0.01197079	Beta neg: -0.02614736
Beta pos: 0.0618144	Beta pos: 0.01902247
Beta pos: 0.06074922	Beta neg: -0.04618608
Beta pos: 0.0210038	Beta neg: -0.01364428
Beta pos: 0.09851786	Beta neg: -0.02895858
Beta pos: 0.03269637	Beta neg: -0.02047009
Beta pos: 0.02601714	Beta neg: -0.008306348
Beta pos: 0.0007798201	Beta neg: -0.002977273
Beta pos: 0.008372112	Beta neg: -0.003291789
Beta pos: 0.02874968	Beta pos: 0.02357043
Beta pos: 0.007294733	Beta pos: 0.1093345
Beta pos: 0.05336571	Beta pos: 0.02385875
Beta pos: 0.07293714	Beta pos: 0.1534499
Beta pos: 0.1483485	Beta pos: 0.004310465
Beta pos: 0.04506233	Beta pos: 0.08481193
Beta pos: 0.0151915	Beta pos: 0.04448816
Beta pos: 0.1804698	Beta pos: 0.001632693
Beta pos: 0.02754227	Beta pos: 0.008787839

Beta pos: 0.08738899	Beta pos: 0.009408251
Beta pos: 0.01020299	Beta neg: -0.02410519
Beta pos: 0.01833259	Beta neg: -0.04707619
Beta pos: 0.08777101	Beta neg: -0.01513648
Beta pos: 0.01574832	Beta pos: 0.1455548
Beta pos: 0.03976496	Beta neg: -0.04522846
Beta pos: 0.008304626	Beta pos: 0.001377385
Beta pos: 0.09294715	Beta pos: 0.03198623
Beta pos: 0.01148529	Beta pos: 0.04770831
Beta neg: -0.007104796	Beta pos: 0.2081129
Beta neg: -0.004480543	Beta pos: 0.03151189
Beta pos: 0.05471096	Beta pos: 0.1231418
Beta pos: 0.2161813	Beta neg: -0.06192816
Beta pos: 0.01537655	Beta pos: 0.2543261
Beta pos: 0.1593133	Beta pos: 0.1913457
Beta pos: 0.197841	Beta pos: 0.2416765
Beta pos: 0.00409791	Beta pos: 0.102045
Beta pos: 0.00402339	Beta pos: 0.108137
Beta pos: 0.1282484	Beta pos: 0.3133019
Beta pos: 0.06018023	Beta pos: 0.02118197
Beta pos: 0.1248065	Beta pos: 0.01721759
Beta pos: 0.120737	Beta pos: 0.05407124
Beta neg: -0.002463889	Beta pos: 0.1585357
Beta neg: -0.01467432	Beta neg: -0.01477209
Beta neg: -0.000162943	Beta pos: 0.00972582
Beta pos: 0.217159	Beta pos: 0.09823862
Beta neg: -0.03779992	Beta pos: 0.05210792
Beta pos: 0.006865905	Beta pos: 0.0006194288
Beta pos: 0.014072	Beta pos: 0.0495592
Beta pos: 0.06589637	Beta pos: 0.001073005
Beta pos: 0.06951129	Beta pos: 0.03945656
Beta pos: 0.04271686	Beta pos: 0.007179606
Beta pos: 0.1234454	Beta neg: -0.03877749
Beta pos: 0.06114349	Beta pos: 0.03910821
Beta pos: 0.07585875	Beta pos: 0.1101367
Beta pos: 0.03469669	Beta pos: 0.002593851
Beta pos: 0.02269676	Beta pos: 0.1762719
Beta pos: 0.05819042	Beta pos: 0.04897106
Beta pos: 0.05554983	Beta pos: 0.1881375
Beta pos: 0.04131735	Beta pos: 0.003232015

Beta pos: 0.1360622	Beta pos: 0.1107294
Beta pos: 0.01379167	Beta pos: 0.001352728
Beta pos: 0.3209719	Beta pos: 0.1137703
Beta pos: 0.08381868	Beta pos: 0.01310087
Beta pos: 0.009800486	Beta pos: 0.03053461
Beta pos: 0.02629055	Beta pos: 0.1582421
Beta pos: 0.1106943	Beta pos: 0.02165649
Beta pos: 0.05735547	Beta pos: 0.07181447
Beta pos: 0.03454315	Beta pos: 0.006812934
Beta pos: 0.03621854	Beta pos: 0.128658
Beta pos: 0.08025517	Beta pos: 0.005881669
Beta pos: 0.001758494	Beta pos: 0.03734653
Beta pos: 0.04689029	Beta pos: 0.02290521
Beta pos: 0.187469	Beta pos: 0.007350946
Beta neg: -0.01253003	Beta pos: 0.06974405
Beta pos: 0.02380448	Beta neg: -0.008875198
Beta pos: 0.01407499	Beta pos: 0.002729497
Beta pos: 0.07649622	Beta pos: 0.1197663
Beta pos: 0.1009627	Beta neg: -0.04562404
Beta pos: 0.03928298	Beta neg: -0.009563883
Beta pos: 0.02027173	Beta neg: -0.03970016
Beta pos: 0.04657305	Beta pos: 0.09416686
Beta pos: 0.01442536	Beta pos: 0.3122596
Beta pos: 0.08494364	Beta pos: 0.02747516
Beta pos: 0.04232559	Beta pos: 0.1424857
Beta pos: 0.4931572	Beta pos: 0.02310875
Beta pos: 0.005370332	Beta pos: 0.05439201
Beta pos: 0.1614692	Beta pos: 0.09576313
Beta pos: 0.02091785	Beta pos: 0.09806903
Beta pos: 0.04837925	Beta pos: 0.009106299
Beta pos: 0.03765276	Beta pos: 0.01898165
Beta pos: 0.02123803	Beta pos: 0.1740927
Beta pos: 0.02158907	Beta pos: 0.1425276
Beta pos: 0.06608973	Beta pos: 0.3139784
Beta pos: 0.0202308	Beta pos: 0.2330345
Beta pos: 0.134366	Beta pos: 0.02218842
Beta pos: 0.01590478	Beta pos: 0.03466231
Beta pos: 0.02130693	Beta pos: 0.008487193
Beta pos: 0.1742298	Beta pos: 0.04898929
Beta pos: 0.03504309	Beta neg: -0.009844219

Beta pos: 0.04320915	Beta pos: 0.01293134
Beta pos: 0.01664857	Beta pos: 0.02580843
Beta pos: 0.01484449	Beta pos: 0.06541744
Beta neg: -0.005128365	Beta pos: 0.01088865
Beta pos: 0.02065022	Beta pos: 0.1127584
Beta pos: 0.02915046	Beta pos: 0.05790533
Beta pos: 0.1401485	Beta pos: 0.02669473
Beta pos: 0.1589029	Beta pos: 0.2229586
Beta pos: 0.1278755	Beta pos: 0.0002972252
Beta pos: 0.09922017	Beta pos: 0.02836424
Beta pos: 0.01785236	Beta pos: 0.02346237
Beta pos: 0.01049968	Beta pos: 0.1413527
Beta pos: 0.04844741	Beta pos: 0.002111967
Beta pos: 0.03773123	Beta pos: 0.009359523
Beta pos: 0.003009584	Beta pos: 0.1213953
Beta pos: 0.04395789	Beta pos: 0.04737665
Beta pos: 0.004056686	Beta pos: 0.08405726
Beta pos: 0.03048257	Beta pos: 0.07504594
Beta pos: 0.04560253	Beta pos: 0.3416845
Beta pos: 0.0815555	Beta pos: 0.179884
Beta pos: 0.4166177	Beta pos: 0.008615126
Beta pos: 0.3081339	Beta pos: 0.436895
Beta pos: 0.0512492	Beta pos: 0.06532782
Beta neg: -0.02521405	Beta pos: 0.02537655
Beta pos: 0.207995	Beta pos: 0.00903157
Beta pos: 0.002590421	Beta pos: 0.02910389
Beta pos: 0.1072454	Beta pos: 0.0368005
Beta pos: 0.02196893	Beta pos: 0.03004357
Beta pos: 0.004608244	Beta pos: 0.07575214
Beta pos: 0.1954878	Beta pos: 0.1357722
Beta pos: 0.03540406	Beta pos: 0.004515319
Beta pos: 0.2337588	Beta pos: 0.006580142
Beta pos: 0.2174493	Beta pos: 0.02935813
Beta pos: 0.02778855	Beta pos: 0.1029001
Beta pos: 0.05154818	Beta neg: -0.01711631
Beta pos: 0.3808783	Beta pos: 0.01145348
Beta pos: 0.1374519	Beta pos: 0.09863426
Beta pos: 0.02709783	Beta pos: 0.1031364
Beta pos: 0.0004909001	Beta pos: 0.1170086
Beta pos: 0.03677524	Beta neg: -0.01078432

Beta pos: 0.2957065	Beta pos: 0.1050201
Beta pos: 0.03166621	Beta pos: 0.08972459
Beta pos: 0.2823364	Beta pos: 0.2302523
Beta pos: 0.1650375	Beta neg: -0.01212163
Beta pos: 0.2920056	Beta neg: -0.01095629
Beta pos: 0.3273004	Beta pos: 0.002734147
Beta pos: 0.005832158	Beta neg: -0.05331358
Beta pos: 0.01939059	Beta pos: 0.08171114
Beta pos: 0.02307367	Beta pos: 0.02878164
Beta pos: 0.01167455	Beta pos: 0.03771408
Beta pos: 0.02069795	Beta pos: 0.08044997
Beta pos: 0.01708783	Beta pos: 0.0269861
Beta pos: 0.1363568	Beta pos: 0.07697141
Beta pos: 0.3424838	Beta pos: 0.004796941
Beta pos: 0.02804493	Beta pos: 0.07962666
Beta pos: 0.2838705	Beta pos: 0.1927574
Beta pos: 0.2317872	Beta pos: 0.04206288
Beta pos: 0.02574327	Beta pos: 0.02542503
Beta pos: 0.02640042	Beta pos: 0.00812753
Beta pos: 0.02943143	Beta pos: 0.01373981
Beta pos: 0.1642571	Beta pos: 0.0386159
Beta pos: 0.2584519	Beta pos: 0.2706407
Beta pos: 0.03411086	Beta pos: 0.02753347
Beta pos: 0.07695229	Beta pos: 0.002329131
Beta pos: 0.07921474	Beta pos: 0.1821019
Beta neg: -0.05374529	Beta pos: 0.02833627
Beta neg: -0.03690326	Beta pos: 0.04345854
Beta neg: -0.001929304	Beta pos: 0.2108666
Beta pos: 0.09451632	Beta neg: -0.01339681
Beta pos: 0.03628281	Beta pos: 0.04030526
Beta neg: -0.0001996825	Beta pos: 0.06987395
Beta pos: 0.07310806	Beta pos: 0.2795943
Beta neg: -0.007617448	Beta pos: 0.1864397
Beta neg: -0.003374689	Beta pos: 0.01138591
Beta pos: 0.3538558	Beta pos: 0.01341046
Beta pos: 0.1835254	Beta pos: 0.1649605
Beta pos: 0.03444426	Beta pos: 0.2627631
Beta pos: 0.180753	Beta pos: 0.1458266
Beta pos: 0.0001724941	Beta pos: 0.2441727
Beta pos: 0.280836	Beta neg: -0.02139823

Beta pos: 0.07935653	Beta pos: 0.005754026
Beta pos: 0.01306576	Beta pos: 0.07983362
Beta pos: 0.09473498	Beta neg: -0.003995899
Beta pos: 0.008330278	Beta pos: 0.1065553
Beta pos: 0.3105513	Beta pos: 0.03236838
Beta pos: 0.02542688	Beta neg: -0.03096932
Beta pos: 0.034863	Beta pos: 0.09614334
Beta pos: 0.03295026	Beta pos: 0.02689111
Beta pos: 0.06973108	Beta pos: 0.1542587
Beta pos: 0.03743927	Beta pos: 0.2949939
Beta pos: 0.205171	Beta pos: 0.02961182
Beta pos: 0.1274761	Beta pos: 0.1349292
Beta pos: 0.2908331	Beta pos: 0.1420634
Beta pos: 0.1705961	Beta neg: -0.007044235
Beta pos: 0.1603281	Beta pos: 0.03082944
Beta pos: 0.009582213	Beta pos: 0.1274967
Beta pos: 0.4167127	Beta pos: 0.001215345
Beta pos: 0.1616951	Beta pos: 0.021315
Beta pos: 0.02102355	Beta pos: 0.01306783
Beta pos: 0.124215	Beta pos: 0.3610372
Beta pos: 0.102118	Beta pos: 0.03760261
Beta pos: 0.1436238	Beta pos: 0.1185609
Beta pos: 0.07839144	Beta pos: 0.1097911
Beta pos: 0.0745817	Beta pos: 0.100075
Beta pos: 0.02869743	Beta pos: 0.03189393
Beta pos: 0.04754446	Beta pos: 0.04081511
Beta neg: -0.007784428	Beta pos: 0.02005984
Beta pos: 0.3276573	Beta pos: 0.01557836
Beta pos: 0.01006362	Beta pos: 0.09393529
Beta pos: 0.3484532	Beta pos: 0.005886366
Beta pos: 0.1697107	Beta pos: 0.02673971
Beta pos: 0.08472431	Beta pos: 0.0045392
Beta pos: 0.02004364	Beta neg: -0.05495144
Beta pos: 0.1446119	Beta pos: 0.02925322
Beta pos: 0.1273054	Beta pos: 0.008294757
Beta pos: 0.03329839	Beta pos: 0.02494902
Beta pos: 0.08542417	Beta pos: 0.04451564
Beta pos: 0.07900811	Beta pos: 0.1428761
Beta pos: 0.03106767	Beta pos: 0.2500272
Beta pos: 0.02318981	Beta pos: 0.2444808

Beta pos: 0.2406282 Beta pos: 0.1464238 Beta pos: 0.1271289 Beta pos: 0.4684185 Beta pos: 0.02378591	Beta pos: 0.02047385 Beta pos: 0.1493421 Beta pos: 0.01303875 Beta pos: 0.1211963 Beta pos: 0.116612 Beta pos: 0.1142885 Beta pos: 0.3273395 Beta pos: 0.09784843

BACTERIAL ALPHA AND BETA DIVERSITY STATISTICS

Appendix Table 3A.5: Fungal alpha and beta diversity statistics

Fungal Simpson diversity between Resistant and Highly susceptible
Call:
lm(formula = Simpson ~ Description, data = alph)
Residuals:
Min 1Q Median 3Q Max
-0.070943 -0.006652 0.003623 0.013946 0.030096
Coefficients:
Estimate Std. Error t value Pr(>|t|)
(Intercept) 0.936590 0.006815 137.428 <2e-16 ***
DescriptionR 0.020515 0.009876 2.077 0.0516.

Residual standard error: 0.0226 on 19 degrees of freedom
Multiple R-squared: 0.1851, Adjusted R-squared: 0.1422
F-statistic: 4.315 on 1 and 19 DF, p-value: 0.05158

Fungal Shannon diversity between Resistant and Highly susceptible

Call:
lm(formula = Shannon ~ Description, data = alph)

Residuals:
Min 1Q Median 3Q Max
-0.65599 -0.11071 -0.02945 0.17370 0.54638

Coefficients:
Estimate Std. Error t value Pr(>|t|)
(Intercept) 3.16185 0.08472 37.321 <2e-16 ***
DescriptionR 0.28054 0.12277 2.285 0.034 *
Residual standard error: 0.281 on 19 degrees of freedom
Multiple R-squared: 0.2156, Adjusted R-squared: 0.1743
F-statistic: 5.221 on 1 and 19 DF, p-value: 0.03398

Fungal Shannon diversity between Resistant and Susceptible
Call:
lm(formula = Shannon ~ Description, data = alph)

Residuals:
Min 1Q Median 3Q Max
-2.64842 -0.63926 0.01723 0.74046 2.36192

Coefficients:
Estimate Std. Error t value Pr(>|t|)
(Intercept) 3.6303 0.3821 9.501 1.95e-08 ***
Description S 1.4787 0.5404 2.736 0.0136 *
Residual standard error: 1.208 on 18 degrees of freedom
Multiple R-squared: 0.2938, Adjusted R-squared: 0.2546
F-statistic: 7.488 on 1 and 18 DF, p-value: 0.01356
BETA DIVERSITY
Fungal Analysis of Variance Table
Response: Distances
Df Sum Sq Mean Sq F value Pr(>F)
Groups 3 0.10763 0.035878 2.1286 0.1148
Residuals 41 0.57308 0.016855

Appendix Table 3A.6: Bacterial alpha and beta diversity statistics

Bacterial Shannon diversity between Resistant and Highly susceptible

Call:
lm(formula = Shannon ~ Description, data = alph)

Residuals:
Min 1Q Median 3Q Max
-0.65599 -0.11071 -0.02945 0.17370 0.54638

Coefficients:
Estimate Std. Error t value Pr(>|t|)
(Intercept) 3.44239 0.08886 38.741 <2e-16 ***
Description HS -0.28054 0.12277 -2.285 0.034 *

Residual standard error: 0.281 on 19 degrees of freedom
Multiple R-squared: 0.2156, Adjusted R-squared: 0.1743
F-statistic: 5.221 on 1 and 19 DF, p-value: 0.03398

Bacterial Simpson diversity between Resistant and Highly susceptible

Call:
lm(formula = Simpson ~ Description, data = alph)

Residuals:
Min 1Q Median 3Q Max
-0.070943 -0.006652 0.003623 0.013946 0.030096

Coefficients:
Estimate Std. Error t value Pr(>|t|)
(Intercept) 0.957105 0.007148 133.902 <2e-16 ***
Description R -0.020515 0.009876 -2.077 0.0516.
Residual standard error: 0.0226 on 19 degrees of freedom
Multiple R-squared: 0.1851, Adjusted R-squared: 0.1422
F-statistic: 4.315 on 1 and 19 DF, p-value: 0.05158

Bacterial Shannon diversity between Resistant and Susceptible

Call:
lm(formula = Shannon ~ Description, data = alph)
Residuals:
Min 1Q Median 3Q Max
-1.00236 -0.11868 -0.00186 0.17308 0.77632

Coefficients:
Estimate Std. Error t value Pr(>|t|)
(Intercept) 3.4424 0.1135 30.339 <2e-16 ***
Description S -0.3902 0.1605 -2.432 0.0257 *
Residual standard error: 0.3588 on 18 degrees of freedom
Multiple R-squared: 0.2473, Adjusted R-squared: 0.2055
F-statistic: 5.914 on 1 and 18 DF, p-value: 0.02569

BETA DIVERSITY

Bacterial Analysis of Variance Table
Response: Distances
Df Sum Sq Mean Sq F value Pr(>F)
Groups 3 0.02200 0.0073343 0.5605 0.6443

CHAPTER 5

Appendix Table 5A.1: List of differentially expressed genes (DEGs) in susceptible leaves in response to *Fusarium graminearum* infection at 24 hpi, 48 hpi, 7 dpi, 14 dpi. DEGs were determined with a log2 fold change ≥ 0 cut-off and an FDR of ≤ 0.05.

Gene symbol	Gene name	Locus name	Sample_1	Sample_2	FPKM 1	FPKM 2	q_value	Gene-regulation FDR ≤0.05 and log2(fold_change)
PUB	U-box domain-containing protein kinase	Sobic.001G305800	24h	48h	21.2658	1.42392	0.0256155	Down-regulated
ATPANK2,PANK2	pantothenate kinase 2	Sobic.010G078100	24h	48h	32.569	8.95639	0.0151516	Down-regulated
NOG	Nucleolar GTP-binding protein	Sobic.010G073200	7d	14d	77.7864	20.8689	0.0151516	Down-regulated
	-	Sobic.001G291200	7d	14d	281.066	72.3329	0.0151516	Down-regulated
	-	Sobic.009G023401	7d	14d	158.217	39.7078	0.0151516	Down-regulated
HAB1	homology to ABI1	Sobic.003G198200	24h	48h	42.6997	9.78897	0.0256155	Down-regulated
RP	Ribosomal protein L1p/L10e family	Sobic.009G228500	7d	14d	25.1895	5.4986	0.0410301	Down-regulated
Rrnad1	Ribosomal RNA adenine dimethylase family protein	Sobic.004G061800	7d	14d	39.9074	8.57089	0.0151516	Down-regulated
	Double Clp-N motif-containing P-loop nucleoside triphosphate hydrolases superfamily protein	Sobic.005G002400	7d	14d	80.3731	17.0949	0.0151516	Down-regulated
LAC12	laccase 12	Sobic.003G357600	48h	7d	152.482	31.9329	0.0410301	Down-regulated
BGLU11	beta glucosidase 11	Sobic.009G114000	24h	48h	32.6917	6.78361	0.0151516	Down-regulated
rRNA processing protein	Ribosomal RiboNucleicAcid processing protein-related	Sobic.002G300300, Sobic.002G300400	7d	14d	40.0239	7.92446	0.0151516	Down-regulated
	-	Sobic.006G051100	7d	14d	101.834	19.7431	0.0256155	Down-regulated

	Protein of unknown function (DUF3741)	Sobic.001G507300	24h	48h	25.0465	4.78342	0.0151516	Down-regulated
IAA26,PAP1	phytochrome-associated protein 1	Sobic.009G203700	24h	48h	24.6424	4.63405	0.0332756	Down-regulated
TPR	Tetratricopeptide repeat (TPR)-like superfamily protein	Sobic.003G223000	7d	14d	8.92096	1.62066	0.0151516	Down-regulated
ENDO4	endonuclease 4	Sobic.003G087200	24h	48h	67.7431	11.934	0.0151516	Down-regulated
ERF1-2	eukaryotic release factor 1-2	Sobic.009G118600	24h	48h	10.4993	1.84687	0.0410301	Down-regulated
GH17	O-Glycosyl hydrolases family 17 protein	Sobic.002G327900	24h	48h	9.46216	1.48633	0.0151516	Down-regulated
Class-II DAHP synthetase family protein	3-deoxy-D-arabino-heptulosonate 7-phosphatase synthetase	Sobic.002G379600	24h	48h	67.2108	10.0367	0.0151516	Down-regulated
BGLU16	beta glucosidase 16	Sobic.008G080400	48h	7d	354.444	52.4899	0.0256155	Down-regulated
	-	XLOC_034160	7d	14d	6107.19	876.707	0.0151516	Down-regulated
SnRK3.16,CIPK1	CBL-interacting protein kinase 1	Sobic.003G139500	24h	48h	183.166	25.9155	0.0151516	Down-regulated
ATMLO1,MLO1	Seven transmembrane MLO family protein	Sobic.004G182300	24h	48h	59.1521	8.01657	0.0151516	Down-regulated
	Plant protein 1589 of unknown function	Sobic.001G415200	48h	7d	12.4371	1.6109	0.0151516	Down-regulated
ACO4,EAT1,EFE	ethylene-forming enzyme	Sobic.004G313100	24h	48h	126.572	16.3721	0.0151516	Down-regulated
BGAL1	beta galactosidase 1	Sobic.010G173800	48h	7d	58.7628	7.51152	0.0151516	Down-regulated
Fe(II)-dependent oxygenase and 2-oxoglutarate (2OG) superfamily protein	Homolog 4,1-aminocyclopropane-1-carboxylate oxidase, putative, expressed	Sobic.003G039700	24h	48h	241.102	29.456	0.0151516	Down-regulated
PSII	photosystem II reaction center protein C	Sobic.001G276500	7d	14d	358.068	43.2717	0.0151516	Down-regulated
CYP71,B34	cytochrome P450, family 71, subfamily B, polypeptide 34	Sobic.002G110200	24h	48h	38.4461	4.44443	0.0151516	Down-regulated
-	XLOC_023654	Sobic.006G225700 Sobic.006G225800	7d	14d	6.9615	0.783715	0.0151516	Down-regulated

LTPL152 - Protease inhibitor/seed storage/LTP family protein precursor, expressed	Bifunctional inhibitor/lipid-transfer protein/seed storage 2S albumin superfamily protein	Sobic.009G221900	24h	48h	44.8862	4.98314	0.0151516	Down-regulated
RuBisCo	ribulose-bisphosphate carboxylases	Sobic.005G194400	7d	14d	184.574	20.2166	0.0151516	Down-regulated
ZIFL1	zinc induced facilitator-like 1	Sobic.005G024900	24h	48h	10.3754	1.11158	0.0151516	Down-regulated
CYP71B37	Polypeptide 37,cytochrome P450, subfamily B, family 71	Sobic.001G235500	7d	14d	23.0842	2.44417	0.0151516	Down-regulated
	myb-like HTH transcriptional regulator family protein	Sobic.004G036500	24h	48h	10.3967	1.06319	0.0151516	Down-regulated
HAM	Heavy metal transport/detoxification superfamily protein	Sobic.006G113900	24h	48h	286.43	28.284	0.0151516	Down-regulated
HAD	Haloacid dehalogenase-like hydrolase (HAD) superfamily protein	Sobic.001G422100	24h	48h	45.0887	4.23981	0.0151516	Down-regulated
AQP1,DELTA-TIP,ATTIP2;1,TIP2;1,DELTA-TIP1,	delta tonoplast integral protein	Sobic.010G146100	48h	7d	185.147	17.2384	0.0151516	Down-regulated
-	XLOC_032216	Sobic.010G206600	7d	14d	138.665	12.7634	0.0410301	Down-regulated
BGLU46	beta glucosidase 46	Sobic.006G146100	24h	48h	95.6714	8.59312	0.0151516	Down-regulated
ATOMT1,OMT1	O-methyltransferase 1	Sobic.007G059100	24h	48h	58.7701	4.98787	0.0151516	Down-regulated
SERK1,ATSERK1	somatic embryogenesis receptor-like kinase 1	Sobic.005G126100	24h	48h	35.0114	2.92951	0.0151516	Down-regulated
AHP4	HPT phosphotransmitter 4	Sobic.009G202900	48h	7d	231.326	18.3273	0.0256155	Down-regulated
	NADH-Ubiqui-/plastoqui-(complex I) protein	Sobic.010G201266	7d	14d	150.867	11.827	0.0256155	Down-regulated
CHI	Chalcone-flava- isomerase family protein	Sobic.008G030100	24h	48h	130.074	9.41738	0.0151516	Down-regulated
ATTERT,TERT	telomerase reverse transcriptase	Sobic.001G366300	7d	14d	3.96392	0.254934	0.0151516	Down-regulated

	nodulin MtN21 /EamA-like transporter family protein	Sobic.009G136100	24h	48h	74.0561	4.63707	0.0151516	Down-regulated
CAS1	cycloartenol synthase 1	Sobic.004G038300	24h	48h	9.18906	0.489617	0.0151516	Down-regulated
CHS,ATCHS,TT4	Stilbene and chalcone synthase family protein	Sobic.005G137200 Sobic.005G137300	24h	48h	36.5141	1.68448	0.0151516	Down-regulated
ARAC8,ATROP10,ATRAC8, ,ROP10	RHO-related protein from plants 10	Sobic.010G096100 Sobic.010G096200	24h	48h	11.0171	0.47096	0.0256155	Down-regulated
	DNAJ heat shock N-terminal domain-containing protein	Sobic.009G207600	24h	48h	48.6042	1.61768	0.0151516	Down-regulated
SIG3,SIGC	RNApolymerase sigma-subunit C	Sobic.009G253000 Sobic.009G253200	24h	48h	28.5358	86.8661	0.0410301	Up-regulated
ATRL6,RL6,RSM3	RAD-like 6	Sobic.009G244300	24h	48h	101.54	345.567	0.0332756	Up-regulated
SnRK3.16,CIPK1	CBL-interacting protein kinase 1	Sobic.003G139500	7d	14d	40.1195	138.531	0.0493234	Up-regulated
ATWRKY74,WRKY74	WRKY DNA-binding protein 74	Sobic.008G153600	7d	14d	12.3247	43.6105	0.0332756	Up-regulated
DiT1	dicarboxylate transporter 1	Sobic.008G112300	24h	48h	117.027	415.067	0.0332756	Up-regulated
PSII	photosystem II reaction center protein C	Sobic.001G276500	48h	7d	100.625	358.068	0.0151516	Up-regulated
RHO termination factor	Rho termination factor	Sobic.004G338300	24h	48h	25.0291	94.0307	0.0410301	Up-regulated
RPL12-C	ribosomal protein L12-C	Sobic.003G246400	24h	48h	190.037	777.551	0.0151516	Up-regulated
ATHX,ATX,THX	thioredoxin X	Sobic.006G265900	24h	48h	54.0312	221.664	0.0493234	Up-regulated
ATRL1,RL1,RSM2	RAD-like 1	Sobic.009G235500	48h	7d	81.4638	340.145	0.0332756	Up-regulated
FKF1,ADO3	flavin-binding, f box 1, kelch repeat,	Sobic.005G145300	24h	48h	7.08507	29.9772	0.0410301	Up-regulated
PSII	photosystem II reaction center protein C	Sobic.001G299900	48h	7d	9.96943	42.2494	0.0332756	Up-regulated
RuBisCo	ribulose-bisphosphate carboxylases	Sobic.005G194400	48h	7d	42.9172	184.574	0.0151516	Up-regulated
GAPA-2	glyceraldehyde 3-phosphate dehydrogenase A subunit 2	Sobic.006G105900	24h	48h	149.209	645.773	0.0332756	Up-regulated

F0F1-ATP	F0 complex, Plant mitochondrial ATPase, subunit 8 protein	Sobic.K031400	48h	7d	8.34911	36.3515	0.0151516	Up-regulated
	XLOC_020090	Sobic.005G050200	24h	48h	56.969	253.52	0.0151516	Up-regulated
TPR	Tetratricopeptide repeat (TPR)-like superfamily protein	Sobic.009G156900	24h	48h	18.4128	82.5653	0.0332756	Up-regulated
ATRL1,RL1,RSM2	RAD-like 1	Sobic.009G235500	24h	48h	18.0027	81.4638	0.0332756	Up-regulated
FMO1	flavin-dependent monooxygenase 1	Sobic.002G287000	24h	48h	6.24571	28.5695	0.0493234	Up-regulated
BGLU46	beta glucosidase 46	Sobic.006G146100	48h	7d	8.59312	40.3056	0.0332756	Up-regulated
PSI	Photosystem II 5 kD protein	Sobic.004G193400	24h	48h	188.075	888.373	0.0151516	Up-regulated
CRK25	cysteine-rich RLK (RECEPTOR-like protein kinase) 25	Sobic.002G327800	7d	14d	8.89424	42.5213	0.0332756	Up-regulated
CPuORF37	conserved peptide upstream open reading frame 37	Sobic.001G349650 Sobic.001G349700	48h	7d	8.38714	40.4851	0.0151516	Up-regulated
LHCB5	light harvesting complex of photosystem II 5	Sobic.005G087000 Sobic.005G087100	24h	48h	53.0995	268.666	0.0332756	Up-regulated
LAC12	laccase 12	Sobic.003G357600	24h	48h	29.1792	152.482	0.0151516	Up-regulated
PSBX	photosystem II subunit X	Sobic.003G055300	24h	48h	39.9299	209.244	0.0151516	Up-regulated
	-	Sobic.003G255100	24h	48h	20.1628	106.245	0.0332756	Up-regulated
	Rhodanese/Cell cycle control phosphatase superfamily protein	Sobic.001G407900	24h	48h	1.4942	7.99007	0.0151516	Up-regulated
	-	Sobic.002G264800	24h	48h	30.3483	162.289	0.0151516	Up-regulated
ATTPS14,TPS14	terpene synthase 14	Sobic.004G019400	7d	14d	3.77595	20.2141	0.0493234	Up-regulated
GH	Glycosyl hydrolase family 38 protein	Sobic.001G268700 ,Sobic.001G268850 ,Sobic.001G269000	7d	14d	8.08501	44.2117	0.0493234	Up-regulated
PB1	Octicosapeptide/Phox/Bem 1p family protein	Sobic.005G111200	24h	48h	18.4682	101.066	0.0151516	Up-regulated

AAP2	amino acid permease 2	Sobic.008G059000	7d	14d	13.5044	74.2336	0.0256155	Up-regulated
C5HC2	Zinc finger (C5HC2 type) family protein/Transcription factor jumonji (jmj) family protein	Sobic.001G284400 ,Sobic.001G284425	7d	14d	3.65062	20.2465	0.0151516	Up-regulated
FT	PEBP (phosphatidylethanolamine-binding protein) family protein	Sobic.003G295300	24h	48h	10.6716	60.149	0.0151516	Up-regulated
BGAL1	beta galactosidase 1	Sobic.010G173800	24h	48h	10.325	58.7628	0.0256155	Up-regulated
LHCA3	photosystem I light harvesting complex gene 3	Sobic.010G189300	24h	48h	186.66	1081.46	0.0151516	Up-regulated
PSBX	photosystem II subunit X	Sobic.002G414400	24h	48h	20.0601	117.224	0.0151516	Up-regulated
JAZ1,TIFY10A	jasmonate-zim-domain protein 1	Sobic.001G482600	7d	14d	41.3244	242.98	0.0332756	Up-regulated
LHCA1	photosystem I light harvesting complex gene 1	Sobic.004G056900	24h	48h	182.082	1076.13	0.0151516	Up-regulated
PTR2,ATPTR2,NTR1,ATPTR2- B,PTR2-B	peptide transporter 2	Sobic.002G367700	24h	48h	5.34699	32.0759	0.0151516	Up-regulated
RGLG2	RING domain ligase2	Sobic.003G396000	7d	14d	7.52775	45.7796	0.0151516	Up-regulated
LHCB6,CP24	light harvesting complex photosystem II subunit 6	Sobic.006G264201	24h	48h	53.862	329.302	0.0151516	Up-regulated
	-	Sobic.004G314800	24h	48h	38.636	240.025	0.0151516	Up-regulated
BGAL1	beta galactosidase 1	Sobic.010G173800	7d	14d	7.51152	46.6724	0.0151516	Up-regulated
bHLH	basic helix-loop-helix DNA-binding superfamily protein	Sobic.007G051800	7d	14d	56.0846	349.728	0.0256155	Up-regulated
CHLM	magnesium-protoporphyrin IX methyltransferase	Sobic.010G022100	24h	48h	6.29858	40.1326	0.0256155	Up-regulated
APAO,ATPAO1,PAO1	polyamine oxidase 1	Sobic.001G472000	7d	14d	38.2889	252.719	0.0151516	Up-regulated
LHCA4,CAB4	light-harvesting chlorophyll-protein complex I subunit A4	Sobic.007G136900 Sobic.007G137000	24h	48h	99.4778	663.807	0.0151516	Up-regulated

IMR1,ALS,AHAS,CSR1,TZP5	Imidazoli- resistant 1/chlorsulfuron	Sobic.004G155800	24h	48h	18.0587	122.632	0.0151516	Up-regulated
Protein of unknown function (DUF1262)	Protein of unknown function (DUF1262)	Sobic.005G220900	24h	48h	3.30011	23.1612	0.0256155	Up-regulated
	-	Sobic.002G064000	24h	48h	15.6543	112.315	0.0256155	Up-regulated
TIP4;1	tonoplast intrinsic protein 4;1	Sobic.009G085900	24h	48h	63.0235	463.438	0.0151516	Up-regulated
	-	Sobic.006G026000	7d	14d	9.54989	70.9045	0.0256155	Up-regulated
HEMA1	Glutamyl-tRNA reductase family protein	Sobic.006G234100	24h	48h	16.6473	124.104	0.0151516	Up-regulated
CCH	copper chaperone	Sobic.004G164200	24h	48h	50.8246	394.726	0.0256155	Up-regulated
	-	Sobic.006G116050	24h	48h	10.3147	82.6737	0.0151516	Up-regulated
	-	Sobic.010G076200	7d	14d	1.1499	9.86447	0.0410301	Up-regulated
Calcium-binding EF-hand family protein	Calcium-binding EF-hand family protein	Sobic.002G376800 Sobic.002G376900	24h	48h	13.5339	117.433	0.0151516	Up-regulated
TIFY10A,JAZ1	jasmonate-zim-domain protein 1	Sobic.001G482600	24h	48h	10.6694	93.2321	0.0493234	Up-regulated
TAT family protein	Tyrosine transaminase family protein	Sobic.002G041100 Sobic.002G041200	48h	7d	30.1095	266.827	0.0151516	Up-regulated
	-	Sobic.003G347200	7d	14d	7.03166	66.5139	0.0256155	Up-regulated
LHCB2.3,LHCB2,LHCB2.4	photosystem II light harvesting complex gene 2.3	Sobic.001G177000	24h	48h	52.586	503.45	0.0151516	Up-regulated
	-	Sobic.006G051100	24h	48h	9.69446	97.0807	0.0410301	Up-regulated
ATRL6,RL6,RSM3	RAD-like 6	Sobic.004G267000	24h	48h	4.77265	49.7879	0.0151516	Up-regulated
LHCB4.2	light harvesting complex photosystem II	Sobic.002G338000	24h	48h	92.0909	1002	0.0151516	Up-regulated
ATKS1,GA2,ATKS,KS1,KS	Proteinprenyl transferases/Terpenoid cyclases/superfamily protein	Sobic.006G211400	7d	14d	0.831267	9.70495	0.0332756	Down-regulated
AQP1,DELTA-TIP,TIP2;1 ATTIP2;1,DELTA-TIP1	delta tonoplast integral protein	Sobic.010G146100	24h	48h	15.829	185.147	0.0410301	Up-regulated

PSB27	photosystem II family protein	Sobic.001G382100	24h	48h	10.4432	130.354	0.0256155	Up-regulated
ATRL6,RL6,RSM3	RAD-like 6	Sobic.003G246900	48h	7d	23.0587	295.307	0.0151516	Up-regulated
GH	Glycosyl hydrolase superfamily protein	Sobic.009G119200	24h	48h	26.6196	343.486	0.0151516	Up-regulated
PSAO	photosystem I subunit O	Sobic.006G073500	24h	48h	42.6582	564.088	0.0151516	Up-regulated
HAD	Subfamily IIIB acid phosphatase,	Sobic.009G070700	7d	14d	4.61606	65.1592	0.0151516	Up-regulated
THI1,TZ,THI4	Thiazole biosynthetic enzyme, (THI1) (ARA6) (THI4)	Sobic.003G191000	24h	48h	67.1094	1113.21	0.0151516	Up-regulated
	-	Sobic.009G010700	24h	48h	7.32268	158.874	0.0151516	Up-regulated
UGT72B3	UDP-glucosyl transferase 72B3	Sobic.002G173900	24h	48h	1.51408	53.8308	0.0256155	Up-regulated
	-	Sobic.001G378550	24h	48h	0	37.7728	0.0151516	Up-regulated
	-	Sobic.001G261577	24h	48h	0	22.0202	0.0151516	Up-regulated
	-	Sobic.002G201200	24h	48h	0	2.40578	0.0151516	Up-regulated
	Phosphorylase superfamily protein	Sobic.003G007800	24h	48h	0	6.71388	0.0151516	Up-regulated
RNA binding	RNA binding	Sobic.010G050750	24h	48h	0	19.8109	0.0151516	Up-regulated
DIR1	Lipid-transfer protein/bifunctional inhibitor/seed storage 2S albumin superfamily protein	Sobic.002G109500	48h	7d	0	7.18481	0.0151516	Up-regulated
	-	Sobic.010G136400	48h	7d	0	20.5148	0.0151516	Up-regulated
LGL	Lactoylglutathione lyase / glyoxalase I family protein	Sobic.003G049700	7d	14d	0	2.79544	0.0151516	Up-regulated
GSTs	Glutathione S-transferase family protein	Sobic.003G164800	7d	14d	0	3.53638	0.0151516	Up-regulated
ANS,LDOX,TDS4,TT18	leucoanthocyanidin dioxygenase	Sobic.004G000700	7d	14d	0	6.91955	0.0332756	Up-regulated
	-	Sobic.006G025700	7d	14d	0	14.3869	0.0151516	Up-regulated

AtOXI1,OXI1,AGC2,AGC2-1	Protein kinase C) kinase and AGC (cAMP-dependent, cGMP-dependent family protein	Sobic.006G128200	7d	14d	0	4.85745	0.0151516	Upregulated
BAN	NAD(P)-binding Rossmann-fold superfamily protein	Sobic.006G227000	7d	14d	0	20.3425	0.0151516	Up-regulated
	RmlC-like cupins superfamily protein	Sobic.006G018100	7d	14d	0	8.69933	0.0151516	Up-regulated
LOX5	LH2/PLAT domain-containing lipoxygenase family protein	Sobic.006G248300	7d	14d	0	2.77189	0.0151516	Up-regulated
ATGSTU19, GSTU19,GST8	glutathione S-transferase TAU 19	Sobic.002G035700	24h	48h	4.12324	0	0.0256155	Down-regulated
BBTI11	Bowman-Birk type bran trypsin inhibitor precursor,	Sobic.003G085300	24h	48h	9.69255	0	0.0332756	Down-regulated
BBTI11	Bowman-Birk type bran trypsin	Sobic.003G088400	24h	48h	39.6896	0	0.0151516	Down-regulated
SAM MTase	S-adenosyl-L-methionine-dependent methyltransferases superfamily protein	Sobic.003G269700	24h	48h	3.74188	0	0.0332756	Down-regulated
ATOSM34,OSM34	osmotin 34	Sobic.008G182300	24h	48h	3.80178	0	0.0410301	Down-regulated
	RmlC-like cupins superfamily protein	Sobic.006G018100	48h	7d	3.22732	0	0.0410301	Down-regulated
	-	Sobic.001G378550	7d	14d	68.796	0	0.0151516	Down-regulated
ATOSM34,OSM34	osmotin 34	Sobic.001G145700	7d	14d	11.7165	0	0.0151516	Down-regulated
	-	Sobic.001G261577	7d	14d	31.1775	0	0.0151516	Down-regulated
FMO	Flavin-binding monooxygenase family protein	Sobic.001G541700	7d	14d	2.19764	0	0.0332756	Down-regulated
RNAP	RNA polymerase subunit beta	Sobic.002G149966	7d	14d	2.98126	0	0.0410301	Down-regulated
GRX	Glutaredoxin family protein	Sobic.003G163500	7d	14d	2.98429	0	0.0151516	Down-regulated
RAV2,EDF2, TEM2,RAP2.8	related to VP1 2/ABI3/	Sobic.003G078100	7d	14d	3.20007	0	0.0151516	Down-regulated

AtGDU4,GDU4	glutamine dumper 4	Sobic.004G075000	7d	14d	2.61893	0	0.0493234	Down-regulated
	-	Sobic.005G208350	7d	14d	2.59703	0	0.0332756	Down-regulated
DIR	Disease resistance-responsive (dirigent-like protein) family protein	Sobic.005G101600	7d	14d	6.5139	0	0.0151516	Down-regulated
DIR	Disease resistance-responsive (dirigent-like protein) family protein	Sobic.005G101800	7d	14d	2.45411	0	0.0151516	Down-regulated
UMAMIT14	EamA-like transporter family protein /Nodulin MtN21	Sobic.007G045900 ,Sobic.007G046000	7d	14d	3.28885	0	0.0151516	Down-regulated
	-	Sobic.008G120450	7d	14d	202.362	0	0.0151516	Down-regulated
PR-2,BG2, PR2,BGL2	beta-1,3-glucanase 2	Sobic.008G146700	7d	14d	6.22761	0	0.0151516	Down-regulated
PAP22,ATPAP22	purple acid phosphatase 22	Sobic.008G036300	7d	14d	3.34854	0	0.0151516	Down-regulated
	Polynucleotidyl transferase, ribonuclease H-like superfamily protein	Sobic.009G126800	7d	14d	2.14048	0	0.0151516	Down-regulated
	-	Sobic.009G014900	7d	14d	7.76843	0	0.0151516	Down-regulated
	-	Sobic.009G093800	7d	14d	4.85901	0	0.0151516	Down-regulated
	-	Sobic.010G136400	7d	14d	20.5148	0	0.0151516	Down-regulated
	-	Sobic.K029400	7d	14d	23.4756	0	0.0256155	Down-regulated

Displays the significant total number of down-and up-regulated through log2 (fold_change) and FDR ≤0.05. DEGs obtained using Cuffdiff (Trapnell et al., 2012) between each experimental group (24 hpi, 48 hpi, 7 dpi and 14 dpi) in susceptible RIL. The log2(fold_change) < 1 was considered down-regulated, and log2 (fold_change) > 1 was considered up-regulated

Appendix Table 5A.2: List of differentially expressed genes (DEGs) in resistant leaves in response to *Fusarium graminearum* infection at 24 hpi, 48 hpi, 7 dpi, 14 dpi (FDR< 0.05). DEGs were determined with a log2 fold change ≥ 0 cut-off and an FDR of ≤ 0.05.

Gene symbol	Gene name	Locus name	Sample_1	Sample_2	FPKM 1	FPKM 2	q_value	Gene-regulation FDR ≤0.05 and log2(fold_change)
NAT	Acyl-CoA N-acyltransferases	Sobic.001G059300,Sobic.001G059400	24h	48h	0	4.77537	0.0525541	Up-regulated
ATPLT5,ATPMT5,PMT5	polyol	Sobic.002G353900	24h	48h	0	21.884	0.0525541	Up-regulated
PER	Peroxidase superfamily protein	Sobic.003G127100	24h	48h	0	5.58996	0.0525541	Up-regulated
CYP94B3	cytochrome P450	Sobic.005G109000	24h	48h	0	13.6748	0.0525541	Up-regulated
	Galactose mutarotase-like superfamily protein	Sobic.006G105200	24h	48h	0	21.8287	0.0525541	Up-regulated
MERI-5,MERI5B,SEN4,XTH24	xyloglucan endotransglucosylase	Sobic.006G205600	24h	48h	0	7.59742	0.0525541	Up-regulated
LHT1	lysine histidine transporter 1	Sobic.007G092400	24h	48h	167.94	14.2845	0.0525541	Down-regulated
ATOSM34,OSM34	osmotin 34	Sobic.008G182900	24h	48h	0	7.61936	0.0525541	Upregulated
CYP79B2	cytochrome P450, family 79 2	Sobic.010G172200	24h	48h	0	7.05804	0.0525541	Up-regulated
ARPN	plantacyanin	Sobic.001G119100	48h	7d	0	12.1125	0.0525541	Up-regulated
XLOC_004270	XLOC_004270	Sobic.001G261577	48h	7d	11.5773	0	0.0525541	Down-regulated
DIR1	Bifunctional inhibitor	Sobic.002G109500	48h	7d	0	24.764	0.0525541	Up-regulated
ATG8C	Ubiquitin-like superfamily protein	Sobic.002G315900	48h	7d	74.9195	0	0.0525541	Down-regulated
GST29,ATGSTU18,GSTU18	glutathione S-transferase TAU 18	Sobic.005G212700	48h	7d	0	6.45983	0.0525541	Up-regulated
ATRD22,RD22	BURP domain-containing protein	Sobic.008G157500	48h	7d	7.90141	0	0.0525541	Down-regulated
	-	Sobic.009G010700	48h	7d	215.94	11.8715	0.0525541	Down-regulated
	-	Sobic.009G014900	48h	7d	3.87669	0	0.0525541	Down-regulated
PR1		Sobic.010G020200	48h	7d	0	20.4022		Up-regulated

ARPN	plantacyanin	Sobic.001G119100	7d	14d	12.1125	0	0.0525541	Down-regulated
XLOC_004270	XLOC_004270	Sobic.001G261577	7d	14d	0	15.3286	0.0525541	Up-regulated
ATG8C	Ubiquitin-like superfamily protein	Sobic.002G315900	7d	14d	0	94.0521	0.0525541	Up-regulated
	-	Sobic.004G007300	7d	14d	0	41.2117	0.0525541	Up-regulated
	-	Sobic.004G016100	7d	14d	0	3.13565	0.0525541	Up-regulated
	-	Sobic.005G213300	7d	14d	6.35218	0	0.0525541	Down-regulated
Lipid-transfer protein/bifunctional inhibitor/seed storage 2S albumin superfamily protein	XLOC_022485	Sobic.006G211701	7d	14d	65.4517	4.29688	0.0525541	Down-regulated
ARPN	plantacyanin	Sobic.006G099900	7d	14d	10.8417	0	0.0525541	Down-regulated
	-	Sobic.010G136400	7d	14d	0	31.4026	0.0525541	Up-regulated
ARPs	Ankyrin repeat family protein	Sobic.001G432500,Sobic.001G432550	24h	48h	0	7.54625	0.0525541	Up-reguated

Displays the significant total number of down-and up regulated through log2 (fold_change) and FDR ≤0.05. DEGs obtained using Cuffdiff (Trapnell et al., 2012) between each experimental group (24 hpi, 48 hpi, 7 dpi and 14 dpi) in resistant RIL. The log2(fold_change) < 1 was considered down-regulated, and log2 (fold_change) > 1 was considered up-regulated

Appendix Table 5A.3: Cluster gene names of statistically significantly susceptible RIL expressed genes using k-means.

Group 1	Group 2	Group 3	Group 4	Group 5 & Group 6
Cluster 1	Cluster 6	Cluster 7	Cluster 3 and 4	Cluster 2 and 5
Sobic.007G051800	Sobic.005G126100	Sobic.001G47200	Sobic.001G415200	Sobic.002G201200
Sobic.008G153600	Sobic.005G024900	Sobic.006G025700	Sobic.003G357600	Sobic.001G378550
Sobic.009G093800	Sobic.006G113900	Sobic.009G202900	Sobic.003G164800	Sobic.001G261577
Sobic.010G136400	Sobic.005G137200	Sobic.001G276500	Sobic.010G146100	Sobic.001G407900
Sobic.010G173800	Sobic.005G137300	Sobic.001G366300	Sobic.001G276500	Sobic.002G173900
Sobic.K031400	Sobic.004G313100	Sobic.001G145700	Sobic.001G349650	Sobic.005G220900
Sobic.001G235500	Sobic.004G038300	Sobic.001G482600	Sobic.001G349700	Sobic.008G030100
Sobic.001G261577	Sobic.004G182300	Sobic.002G327800	Sobic.001G299900	Sobic.009G253000
Sobic.001G284400	Sobic.004G036500	Sobic.003G139500	Sobic.002G041100	Sobic.009G253200
Sobic.001G284425	Sobic.008G112300	Sobic.004G075000	Sobic.002G041200	Sobic.010G022100
Sobic.001G541700	Sobic.010G050750	Sobic.005G002400	Sobic.002G109500	Sobic.010G096100
Sobic.002G149966	Sobic.009G203700	Sobic.005G208350	Sobic.003G246900	Sobic.010G096200
Sobic.003G049700	Sobic.010G078100	Sobic.005G101600	Sobic.003G397300	Sobic.004G267000
Sobic.003G347200	Sobic.009G114000	Sobic.006G248300	Sobic.005G194400	Sobic.008G182300
Sobic.003G396000	Sobic.009G085900	Sobic.008G036300	Sobic.006G018100	Sobic.001G382100
Sobic.004G019400	Sobic.009G156900	Sobic.004G000700	Sobic.006G146100	Sobic.002G367700
Sobic.004G061800	Sobic.009G119200	Sobic.008G146700	Sobic.008G080400	Sobic.006G051100
Sobic.006G025700	Sobic.001G422100	Sobic.006G225700	Sobic.009G235500	Sobic.006G116050
Sobic.006G026000	Sobic.002G035700	Sobic.006G225800	Sobic.009G221900	Sobic.009G244300
Sobic.006G128200	Sobic.001G507300	Sobic.004G000700		Sobic.001G482600
Sobic.006G211400	Sobic.002G379600	Sobic.008G146700		Sobic.002G064000
Sobic.006G227000	Sobic.001G305800	Sobic.006G225700		Sobic.002G287000
Sobic.006G051100	Sobic.007G059100	Sobic.006G225800		Sobic.003G295300
Sobic.007G045900	Sobic.007G136900			Sobic.003G191000
Sobic.007G046000	Sobic.007G137000			Sobic.004G155800
Sobic.008G059000	Sobic.002G327900			Sobic.004G164200
Sobic.008G120450	Sobic.003G087200			Sobic.004G314800
Sobic.009G023401	Sobic.003G198200			Sobic.005G111200
Sobic.009G126800	Sobic.003G269700			Sobic.005G145300
Sobic.010G076200	Sobic.003G088400			Sobic.006G073500
	Sobic.003G039700			Sobic.006G264201
	Sobic.002G110200			Sobic.006G146100
	Sobic.003G139500			Sobic.006G234100
	Sobic.003G085300			Sobic.009G010700
				Sobic.009G235500
				Sobic.009G136100
				Sobic.009G207600

Sobic.010G173800
Sobic.001G177000 Sobic.002G376800 Sobic.002G376900
Sobic.002G264800
Sobic.002G338000
Sobic.002G414400
Sobic.003G055300
Sobic.003G246400 Sobic.003G255100 Sobic.003G357600
Sobic.004G056900
Sobic.004G193400
Sobic.004G338300
Sobic.005G050200 Sobic.005G087000 Sobic.005G087100 Sobic.003G078100 Sobic.005G101800 Sobic.005G194400 Sobic.010G189300
Sobic.006G105900
Sobic.006G265900

Clustering of DEGs expressed in the susceptible RIL relating to expression levels was done using DPGP clustering (McDowell et al., 2018). Differentially expressed genes obtained using cuffdiff (Trapnell et al., 2012) were subjected to DPGP software to identify susceptible RIL significantly expressed transcripts upon *Fusarium graminearum* infection, which were then separated into closely correlated clusters of expression trends. Within the ten clusters, five general expression trends were observed and the clusters were re-grouped into the 6 general trend groups.

Appendix Table 5A.4: Cluster gene names of statistically significantly resistant RIL expressed genes using k-means.

Group 1	**Group 2**	**Group 3**	**Group 4**	**Group 5**
Cluster 2	Cluster 5	Cluster 1	Cluster 3	Cluster 4
Sobic.001G059300	Sobic.009G010700	Sobic.010G136400	Sobic.001G261577	Sobic.006G211701
Sobic.001G059400	Sobic.009G014900	Sobic.004G007300	Sobic.002G315900	Sobic.006G099900
Sobic.001G432500	Sobic.010G020200	Sobic.004G016100		
Sobic.001G432550	Sobic.001G119100			
Sobic.002G353900	Sobic.008G157500			
Sobic.003G127100	Sobic.005G213300			
Sobic.005G109000				
Sobic.006G105200				
Sobic.006G205600				
Sobic.007G092400				
Sobic.008G182900				
Sobic.010G172200				

Clustering of DEGs expressed in the resistant RIL relating to expression levels was done using DPGP clustering (McDowell et al., 2018). Differentially expressed genes obtained using cuffdiff (Trapnell et al., 2012) were subjected to DPGP software to identify susceptible RIL significantly expressed transcripts upon *Fusarium graminearum* infection, which were then separated into closely correlated clusters of expression trends. Within the ten clusters, five general expression trends were observed and the clusters were re-grouped into the 5 general trend groups.

APPENDIX B: Ethics approval letters

UNISA university of south africa

CAES RESEARCH ETHICS REVIEW COMMITTEE

National Health Research Ethics Council Registration no: REC-170616-051

Date: 15/02/2017

Ref #: **2017/CAES/004**
Name of applicant: **Ms K Masenya**
Student #: **56600216**

Dear Ms Masenya,

Decision: Ethics Approval

Proposal: Metagenomic analysis of sorghum using next-generation sequencing

Supervisor: Dr J Rees

Qualification: Postgraduate degree

Thank you for the application for research ethics clearance by the CAES Research Ethics Review Committee for the above mentioned research. Approval is granted for the project.

Please note that the approval is valid for a one year period only. After one year the researcher is required to submit a progress report, upon which the ethics clearance may be renewed for another year.

Due date for progress report: 28 February 2018

The resubmitted application was reviewed in compliance with the Unisa Policy on Research Ethics by the CAES Research Ethics Review Committee on 15 February 2017.

The proposed research may now commence with the proviso that:

1) *The researcher/s will ensure that the research project adheres to the values and principles expressed in the UNISA Policy on Research Ethics.*
2) *Any adverse circumstance arising in the undertaking of the research project that is relevant to the ethicality of the study, as well as changes in the methodology, should*

Af
4 9 4
www.unisa.ac.

University of South Africa
Preller Street, Muckleneuk Ridge, City of Tshwane
PO Box 392 UNISA 0003 South rica
Telephone: +27 12 429 3111 Facsimile: +27 12 2 150
za

be communicated in writing to the CAES Research Ethics Review Committee. An amended application could be requested if there are substantial changes from the existing proposal, especially if those changes affect any of the study-related risks for the research participants.

3) *The researcher will ensure that the research project adheres to any applicable national legislation, professional codes of conduct, institutional guidelines and scientific standards relevant to the specific field of study.*

Note:
The reference number [top right corner of this communiqué] should be clearly indicated on all forms of communication [e.g. Webmail, E-mail messages, letters] with the intended research participants, as well as with the CAES RERC.

Kind regards,

Signature
CAES RERC Chair: Prof EL Kempen

Signature
CAES Executive Dean: Prof MJ Linington

University of South Africa
Preller Street, Muckleneuk Ridge, City of Tshwane
PO Box 392 UNISA 0003 South Africa
Telephone: +27 12 429 3111 Facsimile: +27 12 429 4150
www.unisa.ac.za

APPENDIX C: SCRIPTS AND PACKAGES A
CHAPTER 3

MICROBIOME ANALYSIS

QIIME2 SYSTEM DETAILS AND COMMANDS

System Details

System versions?

Python version: 3.5.4

QIIME 2 release: 2019.10

QIIME 2 version: 2019.10.0

q2cli version: 2019.10.0

QIIME 2 framework, q2cli (a QIIME 2 command-line interface) and the following plugins:

q2-alignment	q2-composition
q2-cutadapt	q2-dada2
q2-deblur	q2-demux
q2-diversity	q2-emperor
q2-feature-classifier	q2-feature-table
q2-gneiss	q2-longitudinal
q2-metadata	q2-phylogeny
q2-quality-control	q2-quality-filter
q2-sample-classifier	q2-taxa
q2-type	q2-vsearch

Commands for Microbiota Analysis Qiime2

qiime tools import --type 'SampleData[PairedEndSequencesWithQuality]' --input-path casava-18-paired-end-demultiplexed --input-format CasavaOneEightSingleLanePerSampleDirFmt --output-path demux-paired-end.qza

qiime demux summarize --i-data demux.qza --o-visualization demux.qzv

qiime deblur denoise-16S --i-demultiplexed-seqs demux-paired-end.qza --p-trim-length 280 --output-dir debluroutput

qiime feature-table summarize --i-table table.qza --o-visualization table.qzv

qiime feature-table tabulate-seqs --i-data rep-seqs.qza --o-visualization rep- seqs.qzv

qiime alignment mafft --i-sequences rep-seqs.qza --o-alignment aligned- rep-seqs.qza

qiime alignment mask --i-alignment aligned-rep-seqs.qza --o-masked- alignment masked-aligned-rep-seqs.qza

qiime phylogeny fasttree --i-alignment masked-aligned-rep-seqs.qza --o- tree unrooted-tree.qza

qiime phylogeny midpoint-root --i-tree unrooted-tree.qza

qiime taxa barplot --i-table table.qza --i-taxonomy taxonomy.qza --m- metadata-file metadata.txt--o-visualization taxa-bar- plots.qzv

qiime feature-classifier classify-sklearn --i-classifier SILVA 138 database --i-reads rep-seqs.qza --o-classification taxonomy.qza

qiime feature-classifier classify-sklearn --i-classifier unite-ver7-99-classifier-20.11.2016.qza --i-reads rep-seqs.qza --o-classification taxonomy.qza

qiime metadata tabulate --m-input-file taxonomy.qza --o-visualization taxonomy.qzv

qiime taxa collapse --i-table table.qza --i-taxonomy taxonomy.qza --p-level 2 --o-collapsed-table TaxaFeatureTable.qza

qiime phylogeny fasttree --i-alignment masked-aligned-rep-seqs.qza --o-tree fasttree-tree.qza –verbose

qiime vsearch dereplicate-sequences --i-sequences demux-joined.qza --o-dereplicated-table table1.qza --o-dereplicated-sequences rep-seqs.qza

qiime vsearch cluster-features-open-reference --i-table table.qza --i-sequences rep-seqs.qza --i-reference-sequences unite-ver7-99-seqs-20.11.2016.qza --p-perc-identity 0.99 --o-clustered-table table-or-99.qza --o-clustered-sequences rep-seqs-or-99.qza --o-new-reference-sequences new-ref-seqs-or-99.qza

biom convert -i table-with-taxonomy.biom -o table-with-taxonomy_json.biom --table-type="OTU table" --to-json

R packages used (R 3.5.2 GUI 1.70 El Capitan build (7612)

library(phyloseq)

library(qiime2R)

library(ggplot2)

library(gridExtra)

library(dunn.test)

library(vegan)

library(randomForest)

library(dplyr)

library(MicrobeR)

library(plotly)

library(tidyverse)

library(magrittr)

```
library(reshape2)
library(vegan)
library(ape)
library(ggpubr)
library(RColorBrewer)
library(UpsetR)
library(venn)
library(microbiomeSeq)
library(intergraph)
library(SpiecEasi)
library(ggnet)
library(Matrix)
library(network)
```

A list of R scripts used for bacteria and fungi

Creating a phyloseq object with qiime2R

```
phy<-qza_to_phyloseq("table.qza", "rooted-tree.qza", "taxonomy.qza","metadata.tsv")
```

Change the colnames to rank_names

```
colnames(tax_table(phy))=c("Domain", "Phylum", "Class", "Order", "Family", "Genus",
"Species")
```

Standardize abundances to median sequence depth

```
total = median(sample_sums(phy))
standf = function(x, t=total) round(t * (x / sum(x))
M.std = transform_sample_counts(phy, standf)
```

Select OTUs where the rowsum for that OTU has at least 20% of samples with a count of 10 each OR where that OTU > 0.001% of the total median count

```
M.f = filter_taxa(M.std,function(x) sum(x 10) (0.02*length(x)) | sum(x) 0.001*total, TRUE)
ntaxa(M.f)
```

Only retain taxa in absolute abundance table with abundance > 0.1%

```
physeqrF = filter_taxa(phy, function(x) mean(x) < 1,TRUE)
rmtaxa = taxa_names(physeqrF)
alltaxa = taxa_names(M.f)
myTaxa = alltaxa[!alltaxa %in% rmtaxa]
physeqaF <- prune_taxa(myTaxa,M.f)
```

Diversity measures

Definition of the most used measures

Simpson diversity index- measures the relative abundance of species, with a higher value indicating high dominance/low biodiversity.

Shannon diversity index-The number of species per sample (measuring richness)

plot_anova_diversity(phy, method = c("richness","simpson", "shannon"),grouping_column = "Description",pValueCutoff=0.05)

UpsetR bar graphs and venn diagrams

```
bac <- read_biom("bacteria-with-taxonomy.biom")
bac <- t(as.matrix(biom_data(bac)))
x <- matrix(NA, nrow=ncol(bac), ncol=nrow(bac))
colnames(x) <- rownames(bac)
for (i in 1:nrow(bac)){
for (j in 1:ncol(bac)){
if(kedibac[i,j]>0){
x[j,i] <- colnames(bac)[j]
}}}
S<-c(x[, 'S1'], x[,'S2'], x[,'S3'], x[,'S4], x[,'S5'], x[,'S6'], x[,'S7'], x[,'S8'], x[, 'S9'], x[, 'S10’], x[, 'S11’], x[, 'S12’])
S <- data.frame(S)
S <- na.omit(S)
S <- unique(S)
```

```
R <-c(x[,'R1'], x[,'R2'], x[,'R3'], x[,'R4'], x[,'R5'], x[,'R6'], x[,'R7'], x[,'R8'], x[,'R9’], x[,'R10’],
x[,'R11’])
R <- data.frame(R)
R <- na.omit(R)
R <- unique(R)

MR <- c(x[,'MR1'], x[,'MR2'], x[,'MR3'], x[,'MR4'], x[,'MR5'], x[,'MR6'], x[,'MR7'],
x[,'MR8’], x[,'MR9’], x[,'MR10’])
MR <- data.frame(MR),
MR <- na.omit(MR)
MR <- unique(MR)

HS <-c(x[,'HS1'], x[,'HS2'], x[,'HS3'], x[,'HS4'], x[,'HS5'], x[,'HS6'], x[,'HS7'], x[,'HS8'],
x[,'HS9], x[,'HS10’], x[,'HS11’], x[,'HS12)
HS <- data.frame(HS)
HS <- na.omit(HS)
HS <- unique(HS)

venn(list(MR, R, S, HS)
venn(MR, R, S, HS)
venn(list(MR, R, S, HS)
input=list(Moderate=MR, Resistant=R, Susceptible=S)
venn(input)
```

```
input=list(Moderate=as.matrix(MR), Resistant=as.matrix(R), Susceptible=as.matrix(S),
Highly=as.matrix(HS))
upset(fromList(input))
par(mfrow(2,1))
venn(input)
upset(fromList(input), order.by = "freq",
sets.bar.color = c("red","purple","blue","green"),
main.bar.color = "black",matrix.color = c("red","purple","blue","green")
```

Bargraph on relative abundance

```
phy<- normalise_data(phy, norm.method = "relative")
p =plot_bar(phy, "Genus", fill="Genus", facet_grid = "Description") +
geom_bar(aes(color=Genus, Genus), stat="identity", position = "stack")
ggsave(“p.pdf”
```

Ordination plots

```
ord.res <- ordination(phy, "bray", method = "PCoA", grouping_column = "Description",
pvalue.cutoff = 0.05)
p <- plot.ordination(ord.res, method="PCoA", pvalue.cutoff=0.05, show.pvalues=T)
```

Statistics on ordination plots

```
zu_45 <- as(sample_data(phy), "data.frame")
groups <- zu_45[["Description"]]
mod<-betadisper(d,groups)
a = anova(mod)
```

Differential abundance

DESeq2 conversion

```
diagdds = phyloseq_to_deseq2(phy, ~ Description)

diagdds = DESeq(diagdds, test="Wald", fitType="parametric")
```

Investigate table results

```
res = results(diagdds, cooksCutoff = FALSE)

alpha = 0.05

sigtab = res[which(res$padj < alpha), ]

sigtab = cbind(as(sigtab, "data.frame"), as(tax_table(kostic)[rownames(sigtab), ], "matrix"))

head(sigtab)

dim(sigtab)
```

Look at the OTUs that were significantly different between the R and HS disease groups

```
library("ggplot2")

theme_set(theme_bw())

scale_fill_discrete <- function(palname = "Set1", ...) {

    scale_fill_brewer(palette = palname, ...)

}

# Phylum order

x = tapply(sigtab$log2FoldChange, sigtab$Phylum, function(x) max(x))

x = sort(x, TRUE)

sigtab$Phylum = factor(as.character(sigtab$Phylum), levels=names(x))

# Genus order

x = tapply(sigtab$log2FoldChange, sigtab$Genus, function(x) max(x))
```

```
x = sort(x, TRUE)
sigtab$Genus = factor(as.character(sigtab$Genus), levels=names(x))
ggplot(sigtab, aes(x=Genus, y=log2FoldChange, color=Phylum)) + geom_point(size=6) +
  theme(axis.text.x = element_text(angle = -90, hjust = 0, vjust=0.5))
```

Co-occurrence network

```
# Col vector up to 74 color samples
col_vector74 =
c("#7FC97F","#BEAED4","#FDC086","#FFFF99","#386CB0","#F0027F","#BF5B17","#666666","#1B9E77","#D95F02","#7570B3","#E7298A","#66A61E","#E6AB02","#A6761D","#666666","#A6CEE3","#1F78B4","#B2DF8A","#33A02C","#FB9A99","#E31A1C","#FDBF6F","#FF7F00","#CAB2D6","#6A3D9A","#FFFF99","#B15928","#FBB4AE","#B3CDE3","#CCEBC5","#DECBE4","#FED9A6","#FFFFCC","#E5D8BD","#FDDAEC","#F2F2F2","#B3E2CD","#FDCDAC","#CBD5E8","#F4CAE4","#E6F5C9","#FFF2AE","#F1E2CC","#CCCCCC","#E41A1C","#377EB8","#4DAF4A","#984EA3","#FF7F00","#FFFF33","#A65628","#F781BF","#999999","#66C2A5","#FC8D62","#8DA0CB","#E78AC3","#A6D854","#FFD92F","#E5C494","#B3B3B3","#8DD3C7","#FFFFB3","#BEBADA","#FB8072","#80B1D3","#FDB462","#B3DE69","#FCCDE5","#D9D9D9","#BC80BD","#CCEBC5","#FFED6F"
## Load the phyloseq object
getrank="Class" ## Note that this could be "Class" or "Genus"...
se.mb.amgut2 <- spiec.easi(phy, method='mb', lambda.min.ratio=1e-2,
nlambda=20, pulsar.params= list(thresh = 0.05))
```

```
ig2.mb <- adj2igraph(getRefit(se.mb.amgut2), rmEmptyNodes=T,
vertex.attr=list(name=taxa_names(phy)))
# Add edged colors based on nodes connected
#The inverse covariance matrix is obtained via a form of regression
betaMat=as.matrix(symBeta(getOptBeta(se.mb.amgut2)))
#otu.ids=colnames(mb$data)
otu.ids <- colnames(se.mb.amgut2[[1]]$data)
edges=E(ig2.mb)
edge.colors=c()
edge.weight=c()
for(e.index in 1:length(edges)){
adj.nodes=ends(ig2.mb,edges[e.index])
xindex=which(otu.ids==adj.nodes[1])
yindex=which(otu.ids==adj.nodes[2])
beta=betaMat[xindex,yindex]
if(beta>0){
edge.colors=append(edge.colors,"forestgreen")
#edge.weight= format(beta*100,digits=3)
weight= format(beta*100,digits=3)
edge.weight=append(edge.weight,weight)
cat("Beta pos:",beta,"\n")
}else if(beta<0){
edge.colors=append(edge.colors,"red")
```

```
weight= format(beta*100,digits=3)
edge.weight=append(edge.weight,weight)
cat("Beta neg:",beta,"\n")
}
}
E(ig2.mb)$color=edge.colors
E(ig2.mb)$weight=edge.weight
#How many nodes connected at specific rank
nb_nodes <- vcount(ig2.mb)
tax_table(physeqaF) <- tax_table(phy)[,getrank]
otu_ids <- V(ig2.mb)$name
idx <- which(row.names(tax_table(phy)) %in% otu_ids)
taxa <- as.character(tax_table(phy)[,getrank])[idx]
ig2 <- asNetwork(ig2.mb)
network.vertex.names(ig2) <- taxa
net <- ig2
net %v% getrank = as.character(taxa)
y= col_vector74[1:nb_nodes]
names(y) <- levels(as.factor(taxa))
#Plot the network
p <- ggnet2(net,
color = getrank,
palette = y,
```

```
alpha = 0.75,
size = 15,
edge.label = "weight",
edge.size=1,
edge.color="color",
edge.alpha = 0.5,
label = FALSE,
label.size = 0.5)
```

Positive network interactions

```
ig2.mb <- adj2igraph(getRefit(se.mb.amgut2), rmEmptyNodes=T,
vertex.attr=list(name=taxa_names(phy)))
# Add edged colors based on nodes connected
#The inverse covariance matrix is obtained via a form of regression
betaMat=as.matrix(symBeta(getOptBeta(se.mb.amgut2)))
#otu.ids=colnames(mb$data)
otu.ids <- colnames(se.mb.amgut2[[1]]$data)
edges=E(ig2.mb)
edge.colors=c()
edge.weight=c()
for(e.index in 1:length(edges)){
adj.nodes=ends(ig2.mb,edges[e.index])
xindex=which(otu.ids==adj.nodes[1])
```

```
yindex=which(otu.ids==adj.nodes[2])
beta=betaMat[xindex,yindex]
if(beta>0){edge.colors=append(edge.colors,"forestgreen")
#edge.weight= format(beta*100,digits=3)
weight= format(beta*100,digits=3)
edge.weight=append(edge.weight,weight)
E(ig2.mb)$color=edge.colors
E(ig2.mb)$weight=edge.weight}
#How many nodes connected at specific rank
nb_nodes <- vcount(ig2.mb)
tax_table(physeqaF) <- tax_table(phy)[,getrank]
otu_ids <- V(ig2.mb)$name
idx <- which(row.names(tax_table(phy)) %in% otu_ids)
taxa <- as.character(tax_table(phy)[,getrank])[idx]
ig2 <- asNetwork(ig2.mb)
network.vertex.names(ig2) <- taxa
net <- ig2
net %v% getrank = as.character(taxa)
y= col_vector74[1:nb_nodes]
names(y) <- levels(as.factor(taxa))
#Plot the network
p <- ggnet2(net,
color = getrank,
```

```
palette = y,
alpha = 0.75,
size = 15,
edge.label = "weight",
edge.size=1,
edge.color="color",
edge.alpha = 0.5,
label = FALSE,
label.size = 0.5)
```

CHAPTER 5

RNA SEQ ANALYSIS

Module used

samtools

hisat2

stringtie

cufflinks

Scripts

hisat2 Sbicolor_454_v3.0.1.idx -1 R1_pe.fastq -2 R2_pe.fastq | samtools sort > bamfile

cufflinks bamfile -p 8 -G Sbicolor_454_v3.1.1.gene.gff3 -o cuff-directory

stringtie bamfile -p 8 -G Sbicolor_454_v3.1.1.gene.gff3 -o gtffile

/scratch/packages/cufflinks/cufflinks-2.2.1/cuffmerge -p 8 -o 103_merged.gtf -g Sbicolor_454_v3.1.1.gene.gff3 -s Sbicolor_454_v3.0.1.fa 103R.txt

samtools sort 131R_7d.bam -o 131R_7d.aligned.out.bam

/scratch/packages/cufflinks/cufflinks-2.2.1/cuffdiff –o 131_diff –b /scratch/sysusers Sbicolor_454_v3.0.1.fa -p 16 --library-type fr-firststrand -T -L 24h,48h,7d,14d –u merged.gtf 131R_14d.aligned.out.bam,131R1_14d.aligned.out.bam,131R2_14d.aligned.out.bam 131R_48h.aligned.out.bam,131R1_48h.aligned.out.bam,131R2_48h.aligned.out.bam 131R_7d.aligned.out.bam,131R1_7d.aligned.out.bam,131R2_7d.aligned.out.bam 131R_24h.aligned.out.bam,131R1_24h.aligned.out.bam,131R2_24h.aligned.out.bam

/scratch/packages/cufflinks/cufflinks-2.2.1/cuffdiff –o 103_diff –b /scratch/sysusers/Sbicolor_454_v3.0.1.fa -p 16 --library-type fr-firststrand -T -L 24h,48h,7d,14d –u merged.gtf 103R_14d.aligned.out.bam,103R1_14d.aligned.out.bam,103R2_14d.aligned.out.bam 103R_48h.aligned.out.bam,103R1_48h.aligned.out.bam,103R2_48h.aligned.out.bam 103R_7d.aligned.out.bam,103R1_7d.aligned.out.bam,103R2_7d.aligned.out.bam 103R_24h.aligned.out.bam,103R1_24h.aligned.out.bam,103R2_24h.aligned.out.bam

R Packages:

RSQLite
ggplot2 v0.9.2 reshape2
plyr
fastcluster
rtracklayer
Gviz
BiocGenerics (>=0.3.2)
Hmisc
cummerbund

R Scripts

```
cuff<-readCufflinks("cuffdiffoutput")
cuff
annot<-read.table("gene_annotation.tab",sep="\t",header=T,na.string="-")
disp<-dispersionPlot(genes(cuff))
disp
genes.scv<-fpkmSCVPlot(genes(cuff))
isoforms.scv<-fpkmSCVPlot(isoforms(cuff))
dens<-csDensity(genes(cuff))
dens
densRep<-csDensity(genes(cuff),replicates=T)
densRep
brep<-csBoxplot(genes(cuff),replicates=T)
brep
v<-csVolcanoMatrix(genes("X24h"))
v<-csVolcano(genes(cuff),"X14d","X24h")
s<-csScatterMatrix(genes(cuff))
s<-csScatter(genes(cuff),"X24h","X14d",smooth=T)
dend<-csDendro(genes(cuff))
dend.rep<-csDendro(genes(cuff),replicates=T)
data(sampleData)
myGeneIds<-sampleIDs
```

```
myGeneIds
myGenes<-getGenes(cuff,myGeneIds)
myGenes
head(fpkm(myGenes))
head(fpkm(isoforms(myGenes)))
head(repFpkm(TSS(myGenes)))
h<-csHeatmap(myGenes,cluster='both')
h.rep<-csHeatmap(myGenes,cluster='both',replicates=T)
h.rep
b<-expressionBarplot(myGenes)
v<-csVolcano(myGenes,"X48h","X24h","X14d", "X7d")
den<-csDendro(myGenes)
getwd()
mySigMat<-sigMatrix(cuff,level='genes',alpha=0.05)
mySigMat
data(sampleData)
runInfo(cuff)
b<-expressionBarplot(sigGenes)
sigGenes <- getGenes(cuff,sig)
csHeatmap(sig, cluster='both')
sig <- getSig(cuff, alpha=0.05, level='genes')
sig
sigGenes <- getGenes(cuff,sig)
csHeatmap(sigGenes, cluster='both')
png(filename = 'thin_heatmap.png', width = 400, height = 1000, units = 'px')
csHeatmap(sigGenes, cluster='both')
dev.off()
list.files()
getwd()
b<-expressionBarplot(sigGenes)
sigGenes <- getGenes(cuff,tail(sig,100))
```

```
csHeatmap(sigGenes, cluster='both')
png(filename = 'thin_heatmap.png', width = 400, height = 1000, units = 'px')
csHeatmap(sigGenes, cluster='both')
b<-expressionBarplot(sigGenes)
sig <- getSig(cuff, alpha=0.05, level='genes')
length(sig)
resSig <- sig[ which(res$padj < 0.1 ), ]
resSig <- sig[ which(sig$padj < 0.1 ), ]
sum( sig$pvalue < 0.01, na.rm=TRUE )
sig
```

Gene clustering

```
DP_GP_cluster.py -i _gene.txt -o k2 -p png n 1000 –plot
```